UNIVERSITE D'ABOMEY - CALAVI (UAC)

INSTITUT NATIONAL DE L'EAU

Federal Ministry of Education and Research

WASCAL
West African Science Service Center on Climate Change and Adapted Land Use

Registered under N°: 3732-17 */UAC/VR-AARU/SA*

A DISSERTATION

Submitted

In partial fulfillment of the requirements for the degree of

DOCTOR of Philosophy (PhD) of the University of Abomey-Calavi (Benin Republic)

In the framework of the

Graduate Research Program on Climate Change and Water Resources (GRP-CCWR)

By

Moussa IBRAHIM

Public defense on: 08/04/2017

======

ANALYSIS OF CLIMATE CHANGE IMPACT ON THE AVAILABILITY OF WATER RESOURCES IN THE NIGER RIVER BASIN, WITH FOCUS THE NIGER INLAND DELTA (NID)

======

Supervisors:

Prof. Abel Afouda, Professor, University of Abomey Calavi, Benin
Dr. Dominik Wisser, Associate Professor, University of Bonn, Germany

======

Reviewers:

Benjamin N. NGATCHA, Professor University of Ngaoundere (Cameroun)
Julien G. ADOUNKPE, Professor University of Abomey-Calavi (Benin)
Zoubeida BARGAOUI, Professor University of Tunis El Manar (Tunis)

======

JURY

Euloge AGBOSSOU	Professor, University of Abomey-Calavi (Benin)	President
Benjamin N. NGATCHA	Professor, University of Ngaoundere (Cameroun)	Reporter
Julien G. ADOUNKPE	Professor, University of Abomey-Calavi (Benin)	Reporter
Albert GOULA BI TIE	Professor, University of Abobo-Adjamé (Cote d'Ivoire)	Examiner
Emmanuel A. LAWIN	Professor, University of Abomey-Calavi (Benin)	Examiner
Abel AFOUDA	Professor, University of Abomey-Calavi (Benin)	Thesis Director

Advisors:

Dr. Abdou Ali, Senior Hydrologist, AGRHYMET Regional Center, Niamey – Niger.
Prof. Adama Mariko, Professor, Ecole Nationale d'Ingénieurs Abderhamane Baba Touré (ENI-ABT), Bamako – Mali.
Prof. Ousmane Seidou, Associate Professor, United Nations University Institute for Water, Environment and Health (UNU-INWEH).

Dedication

This thesis is dedicated to the loving memory of my uncle.

Acknowledgment

This PhD work is realized in the framework of the West African Science Service Center on Climate Change and AAdapted Land use (WASCAL) and funded by the **German Ministry of Education and Research (BMBF) in collaboration with the Benin Ministry of High Education and Scientific Research** (MESRS).

During this thesis, I received support and help of many people that I want to thank here.

First, my two directors of thesis Abel AFOUDA, Director of the Graduated Research Program (GRP) Climate Change and Water Resources and Associate Professor at UAC and Dominik WISSER, Assistant Professor at the University of University of New Hampshire, NH, USA for their excellent guidance, enthusiasm, and intellectual support. I wish to thank Mr. AFOUDA, my director for his patience, availability, understanding, encouragement and calm so relaxing. You excitedly worked to establish the cooperative supervision agreement and greatly facilitated my mobility at the Center of Development research ZEF, University of Bonn. I also thank my co-director, Mr. WISSER for directing this thesis. You pressed me to my limits, gradually, always with a perfect dose. I am aware that if I am stronger and more confident today, you are largely responsible. My PhD experience has been so enriched by the presence of both of you. I sincerely hope one day to return this favor to you AFOUDA and WISSER. I especially want to thank my PhD advisor Dr. Ali ABDOU for providing me with interesting discussions, which have clearly improved my scientific approach.

I would also like to thank the jury, Prof. Euloge AGBOSSOU, Prof. Benjamin N. NGATCHA, Prof. Julien G. ADOUNKPE, Prof. Albert GOULA BI TIE, Prof. Emmanuel A. LAWIN, and Prof. Abel AFOUDA; for having accepted and taken the time to evaluate my thesis, and have made comments that have greatly improved the quality.

Also, I would like to thank Prof. Abel AFOUDA, Prof. Bernd DIEKKRÜGER, Dr. Dominik WISSER, Dr. Ali ABDOU, Dr. Adama MARIKO, and Prof. Ousmane SEIDOU, for agreeing to supervise this research.

Special thanks to UAC in collaboration with the German Federal Ministry of Education (BMWF) for giving me a doctoral scholarship through the WASCAL program. I am also very grateful to the West African Science Service Center on Climate Change and

Adapted Land Use (WASCAL) program for coordinating this research. Also, thanks the AGRHYMET Regional Centre, and the Center for Development research ZEF for hosting me during my data processing in this thesis. Also, the Niger Authority Basin in Niamey, the National Directorate of Meteorology of Mali, the National department of Water resources of Mali, for providing me the meteorological and hydrological data.

I am also grateful to several people to Arthur E MYNETT, Moussa BOUKARI, Stephen E. SILLIMAN, Gil MAHÉ, Biljana RADOJEVIC, Leonard K. AMEKUDZI, Jerome A. OMOTOSHO, Amadou Thierno GAYE, Hubert ONIBON, Jacques-André NDIONE, Goula Bi Tié ALBERT, Mahamadou SYLLA, Corentin SOMÉ and Julien ADOUNPKE for their lectures, the exchanges and advice on hydrological modeling, statistics, water balance, climate change and land cover mapping issues.

My sincere gratefulness goes to Dominik WISSER, for his help, and who gave me a lot of Satellite remote sensing weather data, and CORDEX data that help me to assess the water availability under changing conditions, and who has been an excellent mentor over the years since the start of this program. You helped me to acquire my first knowledge in R programming, and you accompanied me by your availability and wise suggestions till the end of this thesis.

Thanks to Dr. Ali ABDOU for his ongoing support from the beginning to the end of this thesis.

I want to thank all colleagues met during my PhD mobility in Germany for their interest, questions and encouragements. I think especially to Christian BORGEMEISTER, Bernhard TISCHBEIN, Henning and his family, Frederik HÄFKER, Papa SOW, Fazallah, Sabine, Jelana, late Niclas, and Minnatha BOUTROS, who supported me a lot during my stay in Germany.

My Colleagues in WASCAL and away, Felicien BADU, Adama TOURE, Fati AZIZ, Kossi KOME, Valentin KOFFI, Vincent AZUKA, Djibi SAMBOU, Jean HOUNPKE, Mamounata KABORE, Abdourahamane GADO, Diafarou MOUMOUNI, Kabirou RABE, Sanoussi RABE, Salifou ABDOU, Abdou IBRAHIM, Nassirou LAWALI, Mansour NASSIROU, Maman INOUSSA, Zakari IBRAHIM, Mamane, Abdoulkarim LAWALI, and Seidou MAMADOU for their kindness and encouragement.

Finally, I would like to thank my family, especially my parents for their unconditional support, love, patience, care, and all the support they have given me throughout my studies. My brothers Habibou, Chapiou, my sisters Rakia, Hadiza, Roumantou, Jamila, Aichatou, Charifa and my lovely wife Ramatou for your moral support and advice in the most difficult periods and always present to celebrate my successes.

Abstract

The Niger river basin is characterized by hydro-climatic changes induced by land use and climate change that have significant impacts on local populations. The Niger Inland Delta (NID) wetland comprises a large flooded area that plays an important role in the ecosystem services. A significant fraction of the river flow is lost through evaporation and water use in the NID and the conditions are likely to change with increasing population and changing inflow conditions. In this study, we evaluate the recent hydro-climatic trends in the upper basin and Niger inland delta of the Niger River basin in order to assess the potential climate change. Trend of Niger inland delta pan-evaporation were also analyzed. An overall decrease of precipitation (1950-2010) and runoff (1950-2010); and an increase of temperature (1980-2010) and pan-evaporation (1970-2009), were observed. However, when a long study period is considered, all the trends are not statistically significant. In the same way, when IPCC standard period (1981-2010) is considered; all the climatic data show a significantly increasing trend in the NID except the evaporation whose trend is not significantly decreasing over the area. In this period, significant decreasing trends are found for mean annual discharge at a 0.05 significance level. A comprehensive understanding of the NID's hydro-climatological functioning is therefore crucial for assessing the water resources in the basin under changing conditions in the future. This study focuses on a comprehensive understanding of the NID's hydro-climatological functioning using water balance model approach to develop NIDWat. After a clear description of the water budget's elements specific to the NID catchment, a spatial and temporal dynamics of the annual flood across the NID over the period 2000-2009 was performed using data from satellite QuickSCAT and its associated sensor SeaWinds. The estimated areas were used along with observed discharge and remotely-sensed climatic data to quantitatively evaluate each water balance component. The results indicate: (i) a clear spatiotemporal of the flooded areas varied between 25,000 km^2 in wet periods and 2000 km^2 in dry periods; (ii) an average evapotranspiration loss of 17.31 km^3 (43% of the total inflow) was assessed in the catchment; (iii) precipitation's contribution to the NID's budget totals 5.16 km^3 (12.8% of the total inflow); and (iv) the contribution of return flow from irrigated fields totals 1.8 km^3 (4.5% of the total inflow, among which 1.2 km^3 are from "Office du Niger") to the flooded areas, refined the NID's water balance estimates. The NIDWat model

was validated against observed river discharge and water abstractions and shows a good performance. We then implemented the model as a module in a hydrological model to assess the water balance in the NID and the downstream water availability under changing conditions. We use a multi model approach using regional climate data from the CORDEX initiative. Results suggest, despite decreasing runoff, an increase in ET losses and changes in the temporal dynamics of flooding that impact water resources availability downstream. Knowledge gained on NID's water balance analysis will be used to develop and calibrate hydrological models in the Niger Inland Delta of the basin.

Keywords: Niger Inland Delta, trend analysis, flooded area extent, water balance, hydrological model, Climate Change & water availability.

Synthèse

Résumé

Le bassin du fleuve Niger se caractérise par des variations hydro-climatiques induites par l'occupation des sols et le changement climatique qui ont un impact important sur les populations locales. La zone humide du Delta intérieur du Niger (DIN) comprend une grande zone inondée qui joue un rôle important dans la provision des services écosystémiques. Une grande partie du débit du fleuve Niger entrant est perdue par l'évaporation et les usages de l'eau dans le DIN ; et ces conditions sont susceptibles de s'intensifier avec l'augmentation de la population et la modification du regime hydrologique des affluents. Dans cette étude, nous analyserons les récentes tendances hydro-climatiques sur le bassin supérieur et le DIN dans le bassin du fleuve Niger afin d'évaluer un potentiel changement du climat. La tendance des données de bac d'évaporation dans le DIN, a également été analysée. Une baisse globale des précipitations (1950-2010), et du débit (1950-2010) ; et une augmentation de la température (1980-2010) et d'évaporation (1970-2009) ont été observées. Cependant, lorsqu'une longue période d'étude est considérée, toutes les tendances ne sont pas statistiquement significatives. De la même manière, lorsque la période standard du GIEC (1981-2010) est considérée ; toutes les données climatiques montrent une tendance significativement croissante dans le DIN, à l'exception de l'évaporation dont la tendance ne décroît pas de manière significative sur la zone. Au cours de cette période, des tendances significatives décroissantes sont constatées pour les débits moyens annuels à un niveau de signification de 0,05. Une bonne connaissance du fonctionnement hydrologique du DIN est donc cruciale pour évaluer les ressources en eau dans le bassin avec l'évolution des conditions à l'avenir. Cette thèse se concentre sur une compréhension globale du fonctionnement hydrologique du DIN afin développer NIDWat, un modèle de bilan hydrique pour le DIN. Après une description claire des éléments du bilan hydrique pour le bassin versant du DIN, une caractérisation spatiale et temporelle de l'inondation annuelle dans le DIN sur la période 2000-2009 a été effectuée à l'aide des données « SeaWinds » produit par le satellite « QuickSCAT ». Les superficies inondées estimées ont été utilisées avec les données hydro-climatiques observées afin d'évaluer quantitativement

chaque composante du bilan hydrique. Les résultats indiquent: (i) une variation spatio-temporelle des zones inondées variant entre 25 000 km^2 en périodes humides et 2000 km^2 en période sèche; (ii) une perte moyenne d'évapotranspiration de 17,31 km^3 (43% de volume total) a été évaluée dans le bassin versant; (iii) la contribution de la précipitation au bilan hydrique de DIN s'élève à 5,16 km^3 (12,8% de volume total); et (iv) la contribution des eaux de drainages des champs irrigués s'élève à 1,8 km^3 (4,5% de volume, dont 1,2 km^3 provenant de «l'Office du Niger») vers les zones inondées, a amélioré les estimations du bilan hydrique du DIN. Le modèle NIDWat a été validé avec les données observées des débits et celles es prélèvements d'eau, et montre une bonne performance. Pour évaluer la disponibilité de l'eau en aval dans des conditions variables, nous avons incorporé NIDWat comme un module dans un modèle hydrologique calé sur le bassin du Niger. Ensuite, nous avons utilisés une approche à plusieurs modèles en utilisant les données climatiques régionales issues de l'initiative CORDEX. Les résultats suggèrent, malgré une baisse des débits dans le future, une augmentation des pertes en eau due à l'évapotranspiration sera observée, ainsi le changement dans la dynamique temporelle des inondations ; qui auront une incidence sur la disponibilité des ressources en eau en aval du DIN. Les connaissances acquises sur l'analyse du bilan hydrique de DIN peuvent être utilisées pour développer et étalonner des modèles hydrologiques dans le bassin du fleuve Niger.

Mots-clés : Delta intérieur du Niger, analyse des tendances, zones inondées, bilan hydrique, modèle hydrologique, changement climatique & disponibilité en eau.

Introduction

Problématique

Le bien-être de la société humaine sur la terre est étroitement lié au climat. Cela est particulièrement vrai dans les régions où l'économie repose sur l'agriculture. Le climat, cependant, est en train de changer au fil du temps, due à des causes naturelles et anthropiques. Depuis une soixantaine d'année, la zone soudano-sahélienne, soumise aux aléas climatiques, est marquée par un déficit pluviométrique qui a entraîné une diminution des ressources en eau et une modification de la végétation. En outre, la disponibilité de l'eau est un défi persistant pour les pays d'Afrique de l'Ouest en général et dans le bassin du fleuve Niger en particulier. Les changements observés dans le courant de flux menacent directement les activités socio-économiques tels que le secteur de l'agriculture qui constitue l'un des principaux supports de subsistance des populations du bassin du Niger. L'exploitation inappropriée de ces

ressources naturelles déjà peu abondantes, pour satisfaire des besoins variés et accrus des populations, pose le réel problème de leur pérennisation. L'amélioration des méthodes de gestion habituelles, en vue de parvenir à un développement durable indispensable à la satisfaction des besoins spécifiques des populations et à l'équilibre environnemental de la zone, reste une préoccupation fondamentale partagée par les instances dirigeantes et le monde de la recherche scientifique internationale. La gestion intégrée des ressources naturelles, en vue d'améliorer les conditions de vie des populations et d'assurer la préservation des écosystèmes environnementaux, impose a priori la compréhension de leur dynamique naturelle. Dans un contexte d'exploitation raisonnée des ressources naturelles, pour réussir le développement durable notamment des milieux sahéliens très sensibles aux effets dévastateurs de la variabilité climatique, une des préoccupations scientifiques actuelles est de contribuer à mettre en place des outils d'aide à la gestion permettant de pallier la surexploitation et minimiser l'impact des changements de la disponibilité des ressources naturelles.

Ce travail de thèse mené sur le bassin du Niger avec un focus sur le Delta intérieur du Niger au Mali s'inscrit dans cette logique. Le delta intérieur du fleuve Niger au Mali est un vaste ensemble inondable au centre du Sahel où régime hydrologique, dynamique de l'environnement et activités humaines (pêche, agriculture, élevage) sont étroitement associés. La durabilité des modes d'exploitation par l'homme d'un tel milieu, question fondamentale aussi bien pour l'économie du pays que pour la conservation de la biodiversité, est liée à la disponibilité et à la dynamique de l'eau. Le delta intérieur du fleuve Niger couvre une superficie d'environ 30 000 à 40 000 km^2. Plusieurs études récentes ont montré l'importance de l'étendue annuelle de l'inondation sur la productivité du milieu (Olivry 1994 ; Orange et al., 2002 ; Mariko, 2003 ; Kuper et al., 2003 ; Zwarts et al., 2005 ; Seiler et al., 2009, Mahé et al., 2009). Or depuis les années 1970, le continent africain est soumis à une sécheresse sans précédent (Olivry, 1994 ; Paturel et al., 1997), qui a occasionné une baisse importante du niveau des eaux de surface et souterraines, notamment au Mali (Mahé et al., 2000). Cette baisse des écoulements a provoqué une réduction des surfaces inondées dans le delta intérieur du Niger, entraînant des problèmes graves d'exploitation pour les populations de la zone qui vivent au rythme de son remplissage et de sa vidange (Marie, 2002). Devant cette situation de crise induite par vingt ans de déficit hydrologique, Il est donc intéressant d'évaluer les ressources en eau disponibles. Cependant, Au cours des 4 dernières décennies, certaines études ont tenté d'analyser la disponibilité des ressources en eau et ont développé des modèles hydrologiques

et / ou réservoirs, modèles hydrauliques et agroécologiques pour aider les parties prenantes à prendre de meilleures décisions. Malheureusement, les modèles hydrologiques simulent encore mal le débit sur le fleuve Niger en aval du delta intérieur du Niger ; et ces simulations ont une valeur limitée pour la prise de décision. La non performance des modèles hydrologiques dans la simulation de débit de la rivière est due à l'absence d'une bonne représentation du processus et fonctionnement hydrologique du Delta Intérieur du Niger DIN et dans l'approche méthodologique du bilan hydrique pour cette région. La connaissance de la dynamique spatio-temporelle du cycle de l'eau dans le delta intérieur du Niger apparaît donc comme une nécessité pour un développement durable de la région.

Objectifs de l'étude

Les travaux présentés dans cette étude ont pour objectif principal une meilleure connaissance sur la disponibilité en eau dans le bassin du fleuve Niger en relation avec la variabilité climatique. Ils se basent sur l'étude de la dynamique de l'inondation et de l'estimation des pertes en eau dans le delta intérieur du Niger au Mali. De manière spécifique, l'objectif de cette étude est d'analyser les tendances hydro-climatiques dans le bassin ; de caractériser, à partir des données de l'imagerie satellitaire radar (SeaWinds/QuikSCAT) les surfaces inondées qui se distinguent en surfaces en eau libre et en végétation inondée ; de définir les éléments du paysage expliquant le fonctionnement du régime hydrologique du Delta intérieur du Niger au Mali en de développer un modèle conceptuel du bilan hydrique des processus hydrologiques dans le DIN ; et d'analyser le bilan hydrologique en rapport avec la variabilité climatique dans le but d'évaluer les impacts du changement climatique sur la ressource dans le future pour une meilleure prise de décision en matière de gestion des ressources en eau.

Zone d'étude

Le fleuve Niger est le troisième du monde par sa longueur (4 200 km) après le Nil et le Congo et le second par le débit après le Congo. Il s'écoule de la dorsale guinéenne jusqu'au Sahara suivant un axe Nord-Est en décrivant dans sa traversée des régions sahéliennes et subdésertiques une grande boucle où il perd une part importante de ses apports hydriques, en particulier dans le delta intérieur (Brunet-Moret et al., 1986).

Le Delta intérieur du fleuve Niger au Mali est une vaste plaine d'épandage des eaux du Niger et du Bani, situé entre 13° et 17°N et 2° et 6,5°W, qui s'étend sur une superficie d'environ 50 000 km2. Il s'étire suivant un rectangle orienté SW-NE sur plus de 350 km entre

Ké-Macina et Douna au Sud et Tombouctou au Nord (Figure 1). Composé d'un réseau d'affluents et de défluents, de lacs et de plaines d'inondation (Brunet-Moret et al, 1986) son fonctionnement hydrologique (Olivry, 1994) dépend essentiellement d'une part des régimes hydro climatiques des bassins supérieurs des fleuves Niger et du Bani, dont les sources sont situées en Guinée et en Côte d'Ivoire, et d'autre part des conditions morphologiques et climatologiques propres au Delta intérieur, régissant les écoulements et le bilan hydrologique.

Sur la station de Mopti située au centre du Delta la pluviométrie moyenne annuelle sur la période sèche est de 450 mm contre 550 mm en année humide. Le Delta intérieur malien est un écosystème où régime hydrologique, dynamique de l'environnement naturel et activités humaines (pêche, agriculture, élevage) sont étroitement associés. Une gestion rationnelle de cette vaste zone humide soumise à un climat sec est indispensable pour un développement durable de la région. Le Delta compte plus d'un million d'habitants recensés en 1998 sur une étendue de 40 000 km² environ. Les prédictions des modèles montrent que la population dans le bassin du Niger va augmenter de 8 millions en 1999 a plus de 20 millions d'habitants en 2049 avec un taux moyen de croissance entre 2.6% et 3.7% per an (KFW, 2010).

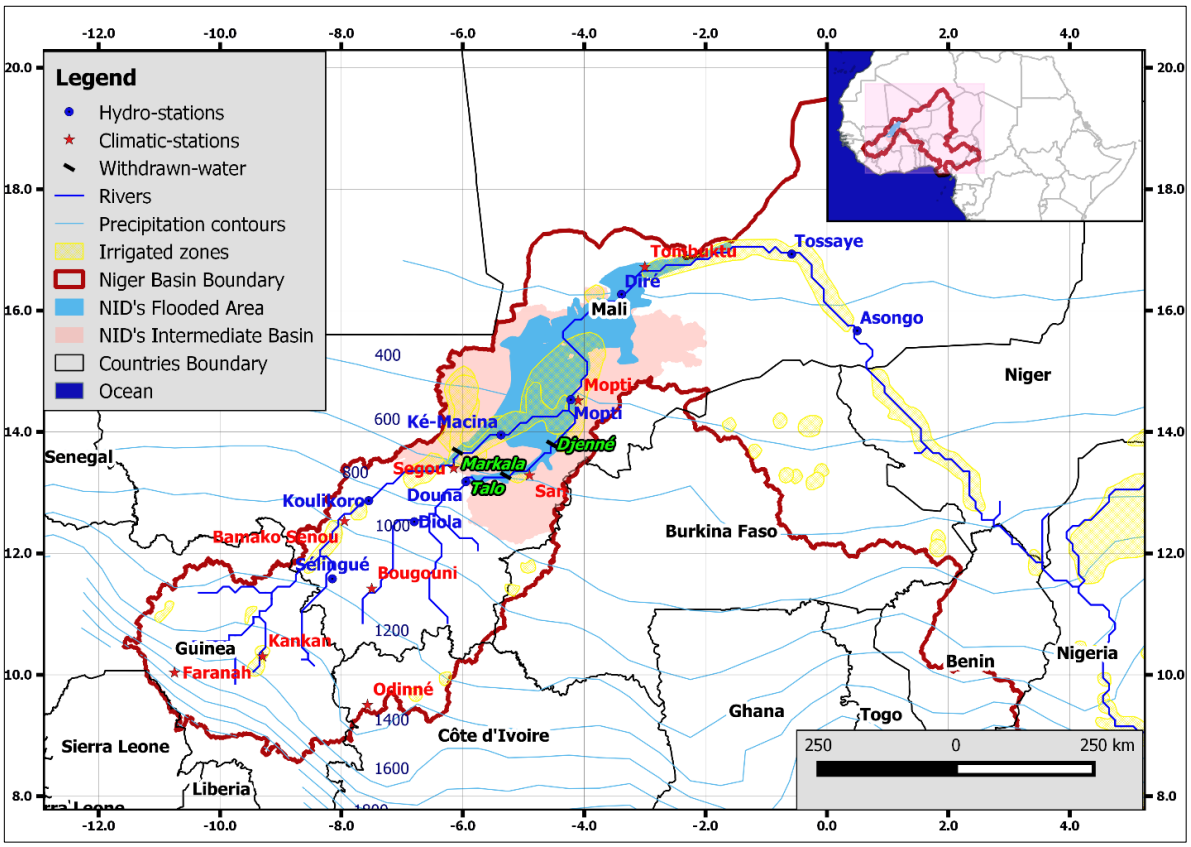

Figure1 : Situation de la zone d'étude

Approche méthodologique

Analyse des tendances

Les méthodes non stationnaires basées sur la détection de point de changement ont été effectués sur les données historiques en hydrologie et climat dans la partie supérieure et à l'intérieur du delta intérieur. Ces données ont été qualitativement contrôlées et ensuite homogénéisées. Les tendances possibles, et les ruptures ont été explorées dans les données hydro-climatiques au sein de la zone d'étude.

Fonctionnement hydrologique du Delta

Il est axé sur la description des éléments du paysage expliquant le fonctionnement du régime hydrologique du DIN au Mali (figure 2). Il porte également sur l'analyse du bilan hydrologique en rapport avec le développement d'un modèle conceptuel spécifique au DIN. Une caractérisation spatiotemporelle des surfaces inondées a été faite à partir des données de télédétection optique et microondes (SeaWinds/QuikSCAT) afin d'estimer les pertes d'eau observées à partir de la différence de débit de l'écoulement de surface. Le modèle non-linéaire a été implémenté et testé pour prédire la surface inondée en utilisant le débit maximum entrant. Les simulations ont été comparées en utilisant les résultats des études antérieures dans la même région. En outre, les modèles d'évaporation potentiels ont été évalués pour représenter les pertes d'eau par évaporation potentiels en utilisant les données climatiques nécessaires. Les résultats des modèles sur l'evaporation potentielle ont été comparés à aux données de « l'évaporation piche » enregistrée dans la même région ; en utilisant comme critère le pourcentage des Biais, le coefficient Nash-Sutcliffe, la corrélation, l'erreur moyenne quadratique -rapport de l'écart type. L'équation de Penman-Monteith a été le modèle le mieux indiqué pour calculer le potentiel ET sur la zone d'étude. Les approches développées ont ensuite été utilisées pour estimer les pertes en eau potentielles saisonnières et annuelles de la zone humide du DIN.

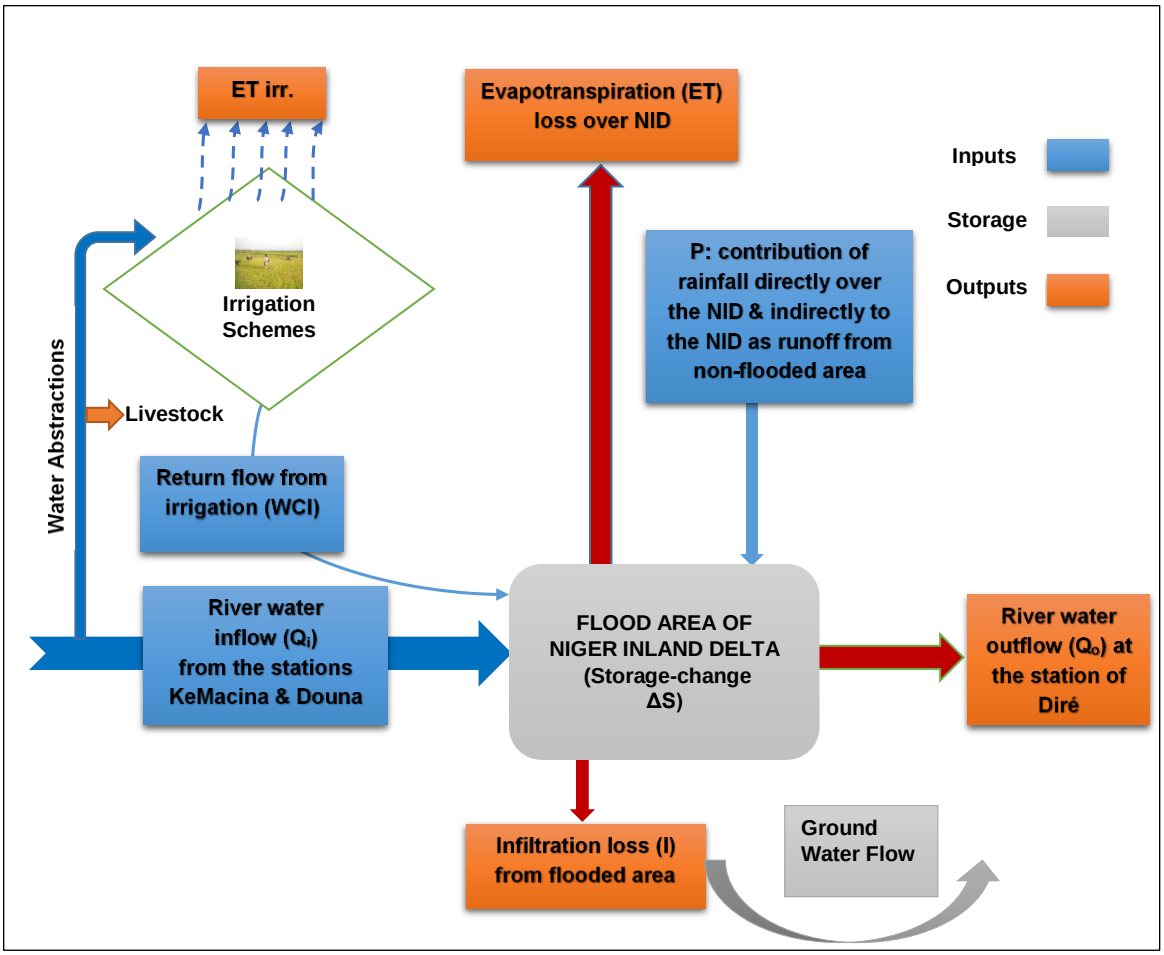

Figure 2 : description schématique du fonctionnement hydrologique du DIN

Evaluation de l'impact du changement climatique sur la ressource

Enfin, il est proposé une intégration du modèle pour le DIN comme un module dans un modèle hydrologique existant afin d'évaluer le bilan hydrique dans le DIN, et la disponibilité de l'eau en aval sous des conditions variables. Nous avons utilisé l'approche multi modèles utilisant des données climatiques régionaux de l'initiative CORDEX. Le modèle hydrologique WBMplus sur le bassin du fleuve Niger (NRB) a été développé pour la période 1944-2013 ; et simuler le débit du fleuve à la station de Mopti donnant l'écoulement entrant dans la plaine inondable du DIN.

Résultats

Une baisse globale des précipitations (1950-2010), et du débit (1950-2010) (figure 3); et une augmentation de la température (1980-2010) et d'évaporation (1970-2009) ont été observées. Cependant, lorsqu'une longue période d'étude est considérée, toutes les tendances ne sont pas statistiquement significatives. De la même manière, lorsque la période standard du

GIEC (1981-2010) est considérée ; toutes les données climatiques montrent une tendance significativement croissante dans le DIN, à l'exception de l'évaporation dont la tendance ne décroît pas de manière significative sur la zone.

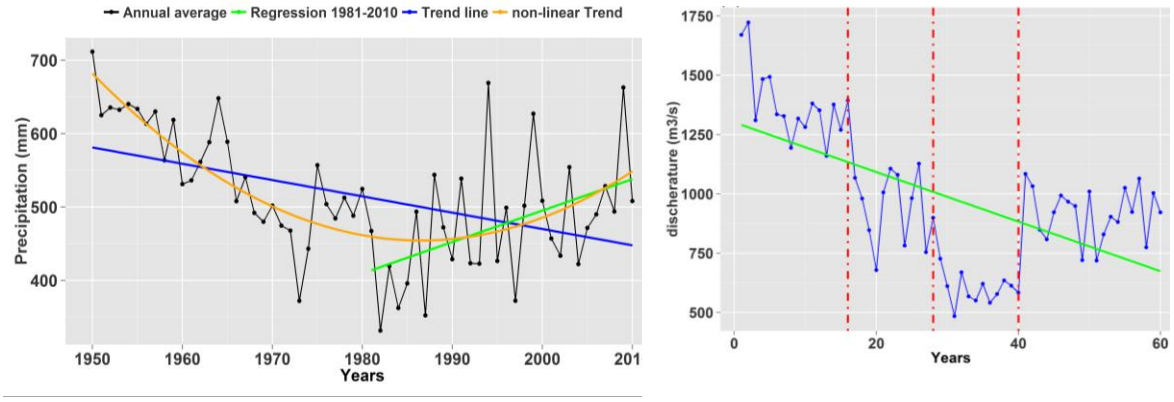

(**a**) (**b**)

Figure 3 : Illustration : **(a)**des tendances possibles sur les précipitations dans le DIN, et **(b)** les ruptures sur les débits dans le DIN.

Seule l'étude des images satellitales permet d'avoir un aperçu de la dynamique spatio-temporelle de l'inondation (figure 4). L'imagerie radar from « SeaWinds/QuikSCAT » assure une grande répétitivité temporelle et est donc préférée aux autres produits disponibles (Landsat).

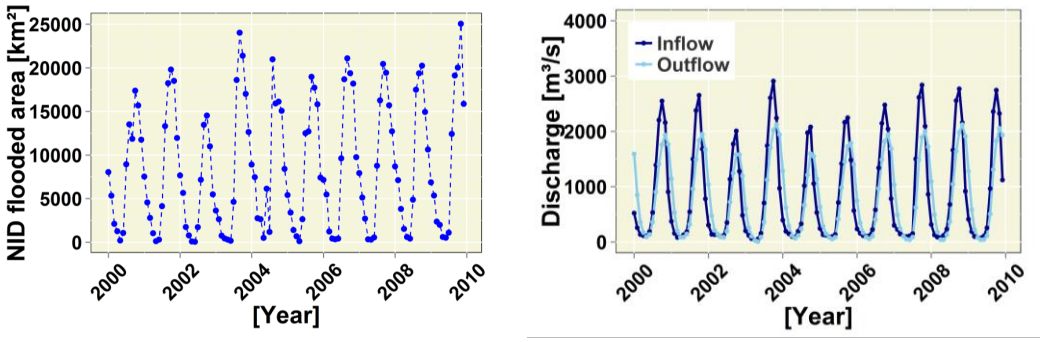

(**a**) (**b**)

Figure 4 : (a) Estimation des surfaces mensuelles inondées du DIN avec les données « SeaWinds/QuikSCAT » pour la période 2000-2009 ; **(b)** Débits entrant et sortant dans le DIN sur la période 2000-2009.

Les superficies inondées estimées ont été utilisées avec les données hydro-climatiques observées afin d'évaluer quantitativement chaque composante du bilan hydrique. Les résultats indiquent: (i) une variation spatio-temporelle des zones inondées variant entre 25 000 km^2 en périodes humides et 2000 km^2 en période sèche (figure 4); (ii) une perte moyenne d'évapotranspiration de 17,31 km^3 (43% de volume total) a été évaluée dans le bassin versant;

(iii) la contribution de la précipitation au bilan hydrique de DIN s'élève à 5,16 km^3 (12,8% de volume total); et (iv) la contribution des eaux de drainages des champs irrigués s'élève à 1,8 km^3 (4,5% de volume, dont 1,2 km^3 provenant de «l'Office du Niger») vers les zones inondées, a amélioré les estimations du bilan hydrique du DIN (figure 5).

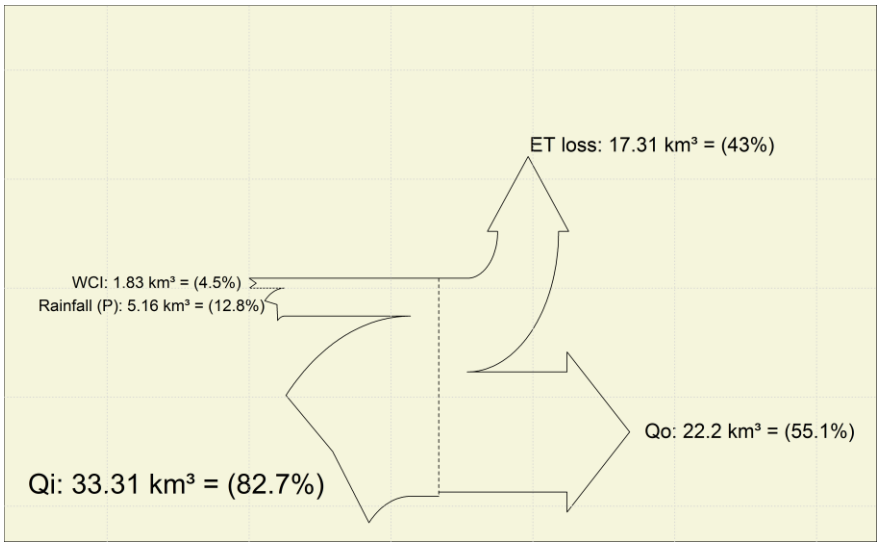

Figure 5 : diagramme de « Sankey » montrant le bilan hydrologique dans le Delta intérieur du Niger qui est établi par différence entre les débits entrant aux stations hydrologiques de Ké-Macina et Douna pour la période de 1980-2004.

L'évaluation des impacts du changement climatique sur la disponibilité des ressources en eau dans la zone d'étude à partir de plusieurs modèles utilisant les données climatiques régionales issues de l'initiative CORDEX, montre une augmentation des pertes en eau due à l'évapotranspiration, mais aussi une baisse des débits dans le futur (figure 6); qui auront bien évidement un impact dans la dynamique temporelle des inondations et de ce fait une incidence sur la disponibilité des ressources en eau en aval du DIN.

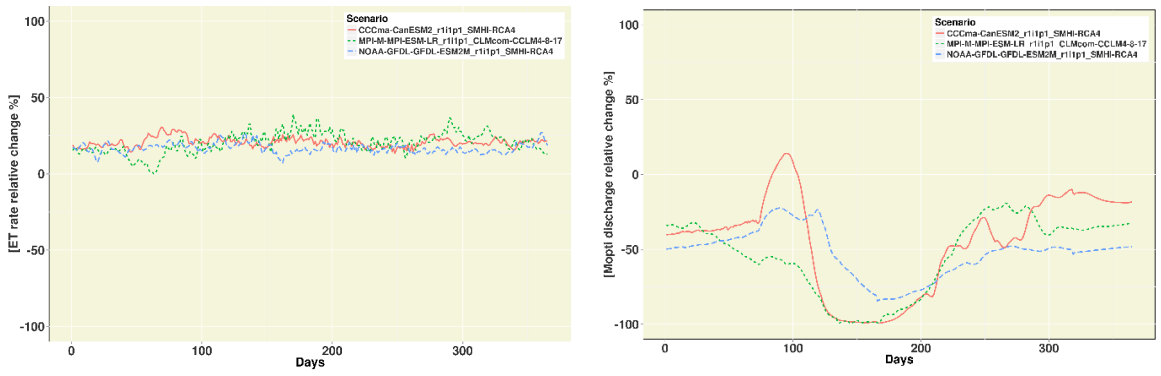

(**a**) (**b**)

Figure 6 : (a) une augmentation des pertes en eau due à l'évapotranspiration ; (b) une baisse des débits dans le futur à la vue de ces trois scenarios.

Conclusion

La télédétection apparaît, à la suite de cette recherche, un complément incontournable de toute étude hydrologique du Delta intérieur du Niger. Elle offre la possibilité d'un suivi spatio-temporel de zones inondées, sols exondés, et aussi la connaissance du régime de l'inondation annuelle du DIN sur la seule base des données existantes et de l'analyse hydrologique utilisable à des fins de gestion des ressources de la région. Les valeurs de surface inondées trouvées sont dans la limite de celles précédemment données dans la littérature, du fait d'une plus grande précision, même avec des images « SeaWinds/QuikSCAT » dont la résolution maximale n'est que de 25 km. Les surfaces inondées varient selon l'hydraulicité des années. Sur l'ensemble du Delta la surface totale inondée peut atteindre de 14 000 à 25 000 km², selon les images étudiées. On prévoit d'utiliser les relations de régression non linéaire pour connaître les surfaces maximales inondées à partir des débits maximaux aux stations hydrologiques. Les résultats suggèrent également que les débits à l'entrée du Delta peuvent être utilisées avec une précision acceptable pour prévoir l'expansion spatio-temporelle de l'inondation dans le DIN. Les estimations des pertes en eau issue de l'évaluation des méthodes de calcul d'évapotranspiration potentielle ont permis de retenir la meilleure représentation de l'évapotranspiration dans notre zone d'étude. Les approches développées ont ensuite été utilisées pour estimer les pertes en eau potentielles saisonnières et annuelles de la zone humide du DIN. Le résultat des pertes annuelles moyennes d'évapotranspiration est 17.31 km^3 (43% de l'apport total). Les performances de NIDwat ont été évaluées à l'aide du diagramme de « Sankey ». Les résultats issus de ce modèle non linéaire sont satisfaisants. La limite de ce modèle pourrait résider sur la courte série de données utilisées car ce modèle nécessite une longue série de données. En outre, les résultats obtenus ont démontré que d'autres composants potentiels du bilan hydrique tels que les précipitations indirectes et directes et les flux de retour provenant de l'irrigation pourraient affiner le budget de l'eau sur le DIN. Ainsi, on peut conclure que cette approche du modèle « NIDWat » pourrait être un bon moyen de représenter les processus hydrologiques du DIN dans les modèles hydrologiques. L'ensemble des paramètres hydro-climatiques étudiés (pluviométrie, température de l'air, évaporation potentielle et débit) montre un gradient, positif ou négatif selon le paramètre envisagé. Selon les

scénarios de changement climatique et les résultats de la modélisation, le débit du fleuve Niger à la station de Mopti à l'intérieur du DIN baissera au 21ème siècle. Ainsi, de nombreux facteurs tels que le changement climatique et les impacts de la variabilité ont induit des changements dans le flux de courant qui affectent directement la disponibilité de l'eau pour toutes les activités, en particulier l'agriculture, qui est la principale question de survie de la population du DIN. L'étude a permis de comprendre les processus hydrologiques sur le NID et d'évaluer la disponibilité des ressources en eau sur le NID sous condition changeante. Par conséquent, tout modèle hydrologique pour le bassin du fleuve Niger devrait tenir compte des processus hydrologiques du DIN afin de faire de bonnes prédictions pour mieux informer les acteurs du développement.

Table of Contents

List of Acronyms

Acronym	Definition
AGRHYMET	Agriculture, Hydrology and Meteorology Research Center
CC	Climate Change
CORDEX	COordinated Regional climate Downscaling EXperiment
DEM	Digital Elevation Model
CRU	Climatic Research Unit
ERA-IN-TERIM	European Centre for Medium-Range Weather Forecasts (ECMWF) Re-Analyses ERA-Interim program data
ETP	Evapotranspiration
GCM	Global Circulation Model
GDP	Gross Domestic Product
GIS	Geographic Information System
GLOWA	Global Change and the Hydrological Cycle
HydroSHEDS	Hydrological data and maps based on SHuttle Elevation Derivatives at multiple Scales
IDW	Inverse distance weighted
IMPETUS	Integrated Approach to the Efficient Management of Scarce Water Resources in West Africa
IPCC	Intergovernmental Panel on Climate Change
IWRM	Integrated Water Resources Management
LBC	Lateral Boundary Condition
MERRA	Modern-Era Retrospective Analysis for Research and Applications
NBA	Niger Basin Authority

NASA	United States National Aeronautics and Space Administration
NASH	Nash-Sutcliffe coefficient
NID	Niger Inland Delta
NIDWat	Niger Inland Water Balance
NRB	Niger River Basin
NOAA	National Oceanic and Atmospheric Administration
OK	Ordinary Kriging
RCM	Regional Climate Model
RMSE	Root Mean Square Error
RSR	Ratio of RMSE to the standard deviation of the observations
SRTM	Shuttle Radar Topography Mission
SSTs	Sea Surface Temperatures
TRMM	Tropical Rainfall Measuring Mission
UNICEF	United Nations Children's Fund
WB	Water Balance
WBMplus	Water Balance Model plus
WCRP	World Climate Research Project
WHO	World Health Organization
WHYMAP	World-wide Hydrogeological Mapping and Assessment Programme

List of Figures

List of Tables

Chapter 1. General Introduction

This chapter gives a general background that reviews the literature on the subject, explains the context of the thesis work, states the problem and justifies the present study. The objectives of the work which include both the global objective and the specific objectives are also provide here. It explained the research questions and hypothesis, afterward, the findings of the research were discussed. Lastly, it presents an introduction of the study area and then the organization of the thesis.

1.1. Context and problem statement

Climate change has substantial impact on hydrological, biological, and ecological systems such as water availability and quality, floods, and droughts (Vegas, 2002).The impact of climate change on water availability in river basins depends on two factors: the changes in climatic variables that drive the hydrological processes, such as precipitation, solar radiation and temperature; and the sensitivity of the basin to these changes (Fung et al., 2009). Nevertheless, we should always keep in mind that climate variability and change may not be the most significant driver of long-term water insecurity.

The essential elements of life for people around the world, access to water, food production, health, and use of land and the environment; are threatened by the climate change (Brouwer and Hofkes, 2008). Human society is vulnerable both to climate change and climate variability, and the greater part of this vulnerability is related to water resources.

Climatic changes or climatic variability may have major impacts on the hydrological regime, for example increases in floods, dry seasons and erosion, and deterioration of the water quality and diversity of ecosystems. Socioeconomic impacts related to alterations in the availability of water resources for domestic and industrial use, production of food, generation of energy, among others, can occur.

The Niger River basin is a significant source of water and food for West Africa which, as an agricultural region, is highly dependent on the water availability and management practices.

The basic analysis of in situ discharges confirms the impact of the Niger inland delta area on the river flow, characterized by a strong reduction of the streamflow at the downstream compared to the upstream flow of the delta. In the simulations, the flooding scheme leads to a non-negligible increase of evaporation over large flooded areas, which decreases the Niger River flow by 15% to 50% in the locations situated after the inland delta as a function of the input rainfall dataset used as forcing (Pedinotti et al., 2012). However, the analysis of total water storage has shown that its contribution is not negligible and must be taken into account to reproduce the evolution of the water budget (Pedinotti et al., 2012).

Thus, there is a clear need for assessing the effect of possible climate changes on the hydrological and hydrogeological regime. Hydrological assessment for water availability must pay particular attention to low flow and drought hydrology. Hence water supply operators need to be sure that they understand how their system will respond to all aspects of the climate of the supply area over long periods of time. To withstand the stresses caused by the global change and to produce enough information about the hydrological processes of the Niger Inland Delta, an improved modeling representation of the delta in a basin model for the entire catchment has to be done more accurately.

Most hydrological models do not adequately consider the impact of the Niger Inland Delta on river flow in the basin. However, it is essential to establish how climatic changes and direct human activities (primarily irrigation and reservoir operations) affect the hydrological cycle in the Inland Niger Delta and how the Delta itself impacts river flow.

Although adaptation can take many forms, most practical measures (e.g. low regret water sector adaptations) are implemented in the face of deep uncertainty and/or incomplete climate risk information (Sarr, 2012). Because of the large uncertainties in climate modeling and climate change projections, the interpretation of climate risk in formation and its use for adaptation decision-making should be carried out with extreme caution. In as much as modeling tools can be of great help in providing information for adaptation to climate, over interpretation of their projections could lead to maladaptation (Lopez, 2011).

This thesis seeks to make an important contribution to understanding the hydro-climatology of the entire Niger basin by exploring strategies for improving knowledge on the Niger inland delta in terms of its hydrological functioning. The approaches to be used include

analysis of recent trends in hydro-meteorological data, water balance model and assessment of climate change impacts on water resources. WBMplus model is already set up for the region, and it runs for the entire basin (Wisser et al., 2010) and will be used in our research.

Spatial detail climate trend analysis that provides scientific sound information for long term water management was not yet performed for the region of the Niger Basin in general and for the Inland Delta in particular, therefore is subject of this study.

1.2. Literature review

The whole of West Africa has been faced with extreme climate variations over the past 5 decades with extended extreme drought conditions during the 70s and 80s (Lebel and Ali, 2009). In this region, precipitation is closely linked with the monsoon, and a better understanding and prediction method are needed for improved water resource management. Spatial and temporal variability of rainfall over Africa offers considerable challenges for assessing and understanding climate change over the continent. This is because of the complexity of African regional climates and the influence of regional geographic features, such as deserts, land cover variations, mountain chains, large lakes, land-sea contrasts and the sea surface temperatures (SSTs) of the surrounding Indian and Atlantic oceans (Sylla et al., 2013).

Sahelian regions are characterized by a mosaic of semi-arid grasslands and permanently, periodically or temporary flooded areas. The vegetation structure of the grasslands is determined by a south-north gradient of increasing aridity on the one hand and by varying forms of human impact on land on the other. The Niger Inland Delta (NID) like most sahelian regions is characterized by a mosaic of semi-arid grasslands and permanently, periodically or temporary flooded areas. This permanent and/or periodical availability of water throughout the year makes the region one of the most important agro-pastoral centers in the African Sahel. The vegetation structure of the grasslands is determined by a south-north gradient of increasing aridity on the one hand and by varying forms of human impact on land on the other. These have contributed in making the Niger Inland Delta one of the most threatened ecosystems of Sub-Saharan Africa (Csaplovics, 1996).

Groundwater helps in maintaining a balance in the ecosystem and is the primary source of potable water in most part of the study area but also an important lever of development. Faced with ever-increasing anthropogenic pressures (population growth & pollution), the sustainable management of groundwater in both a quantitative and qualitative is mandatory. In the context of sustainable management and foresight, knowledge and monitoring of the status of groundwater in those aquifers are fundamental. Characterization and control of groundwater circulation is a major hydrogeological issue. However, the relatively small amount of information complicates this characterization, and the complexity is increased further by the diversity of geological structures encountered.

The increasing demand for water resources in the upper and middle Niger basin as a result of rapid population growth has resulted in tremendous pressure on the already stressed natural resource. While the direction and magnitude of the hydrologic regime remain highly uncertain, there is greater certainty concerning environmental trends caused directly by human activity in the basin. A 50-year period considered by climate models showed that the population of the basin will increase to more than 20 million in 2049 from 8 million in 1999 even if birth rates were slowed down. Currently the population growth rate (Table1.1) ranges from 2.6% to 3.7% per year (KFW, 2010).

Table1. 1: *Population, population growth, urbanization and GDP: CIA 2010; connection rates: WHO/UNICEF 2008*

	Burkina Faso	**Guinea**	**Mali**	**Niger**
Population (in million)	15.8	10	13.5	15.3
Population growth	3.1%	2.6%	2.6%	3.7%
Population in the Niger River Basin (in million)	2.1	1.6	7.8	8.3
Annual rate of urbanization (average: 2005-2010)	5%	3.5%	4.8%	4%
GDP per Capita (USD) (2009)	1,200	1,100	1,100	700

The relationship between Africa's highly variable hydro-climatology and groundwater resources is unclear. Although there has been an improved understanding of this relationship, the availability of very limited observational data sets remains a constraint (Carter and Parker, 2009; Howard and Griffith, 2009; MacDonald et al., 2012). Strong relationships are observed between negative rainfall anomalies and declining groundwater recharge in the

River Niger Basin (Mahé et al., 2009) and reduced baseflow discharges in the Central Kenyan Rift (Olago et al., 2009).

The variability on the temporal distribution of water resources (rainfall and flow) is a major cause of vulnerability in West Africa. Indeed, the ignorance of the short-and medium-term rainfall and flows resulting most often by poor people preparing to cope with climate extremes becoming more frequent: scarcity of rains, floods and direct corollaries that are lower yields or even total loss of agricultural production or the destruction of infrastructure with high economic value such as roads and dams. In such a context, any scientific information on the trend in the short and medium-term rainfall and runoff becomes a crucial tool of decision making in operating and managing water resources (rainfall, surface water, groundwater ...). Agriculture, the first socio-economic activity in the Sahelian zone could therefore know better prospects if, locally, a seasonal reliable information providing information used in the decision making was critical agricultural provisions of the farmers.

Instead of attempts to increase the accuracy and precision of climate predictions, resources should be channeled in the direction of understanding of the vulnerability of climate influenced decisions to irreducible uncertainties as this will be more beneficial to society (Commission of the European Communities, 2009; Termeer et al., 2012).

Studies of regional and global climatic changes and variabilities and their impacts on the water resources have received considerable attention in recent years. Intergovernmental Panel on Climate Change (IPCC) revealed that, the historical climate record for Africa shows warming of approximately 0.7°C over most of the continent during the 20th century, and a decrease in rainfall over large portions of the Sahel (IPCC, 2007). The surface water resources of the major river basins of West Africa in general and in particular the Sahel region show very sensitive inter-annual fluctuations due to climate changes facing this vast region for over thirty years (Le Lay et al., 2007; Lebel & Ali, 2009). The identification and characterization of the variability of water resources in order to better guide the mitigation approaches of potential impacts have generated much more interest among the scientific world.

Water resource management is a major issue in Niger Inland Delta (Mariko 2003; Zwarts et al., 2005). The past and current trend of the Hydro-climatic data is of very high importance for a more sustainable evaluation and characterization of the past and present status of water

resource (Descroix et al., 2009). Therefore, the hydro-climatic data can be the major source of information for the analysis of the water resource availability. In arid and semi-arid areas of West Africa rainfall is a concern for both people and the scientific world; with its important role in the successful development of the agriculture, irrigation, water supply, reservoir operation and hydro-power generation. These latter, are strongly penalized by declining resources (Mariko et al., 2013). Therefore, to improve understanding about the water budget for developing strategies on water resources management over the Niger River Basin (NBR); identification of the temporal and spatial patterns of rainfall that influence the hydrological processes is a must (Oguntunde and Abiodun, 2012) . To know the recent status of water resources downstream the NID in the future and to develop water balance model for satisfying hydrological functioning; understanding the spatial assessment of rainfall volume upstream is a key factor. Assessment of the overall quality of the climate information from the available data particularly precipitation trend analysis showing the degree of temporal and spatial variability which is key tools impacting on a number of concerns such as population growth, economy, society, environment and water resources (Hiernaux et al., 2009; Frappart et al., 2009; Mahé et al., 2013).

Many studies related to rainfall time series fluctuations were done across West Africa that include the NID or different parts in NRB; and show a noticeable decline trend from the 70 particularly in the Sahel region (L. Descroix et al., 2009; Druyan, 2011; Hubert P., Carbonnel, 1987; Le Barbé & Lebel, 1997; Li, Coe, & Ramankutty, 2005; Mahé et al., 2001; Sharon E. Nicholson, 2000; Sharon E. Nicholson & Palao, 1993; Sircoulon, 1987). The study done by Oguntunde et al. (2012) has included the whole NRB but the study was related to climate change. They used the climate models to assess the potential change of different climatic feature within NRB using meteorological data. The average seasonal temperature of NRB was studied using data from 6-hourly sea surface temperature data for present-day and future; and the temperature changes were plotted (Oguntunde & Abiodun, 2012). Generally, the mean baseline and future mean surface temperatures for this region show increases over a 20-year period.

New approaches to improve the estimate of one-time parameters at different time steps (decadal, yearly, etc.) were tested (Le Barbé & Lebel, 1997; T. Lebel et al., 1996; Taupin, Amani, & Lebel, 1998) to improve visualization of rainfall variability in the Sahel.

Similarly in the past, some authors have studied the evolution of rainfall in the Sahel (L'Hôte, Mahé, Somé, & Triboulet, 2002; J. E. Paturel et al., 1997; J.-E. Paturel et al., 2003; Servat et al., 1997). According to their results, since the beginning of the century, four periods of droughts 1907-1916, 1940-1949, 1968-1974 and 1980-1984 affected the Sahelian zone with transboundary rigorousness (Sircoulon, 1976). Among which it has been noticed some dramatic drought's years like the 1973-1974 and 1983-1984 ones; for their considerable extension beyond the Sahel and their persistence over several years.

Many authors have studied the rainfall variability in the Sahel which has strongly affected the discharge evolutions over the past decades in West Africa (WA) (L'Hôte et al., 2002; J.-E. Paturel et al., 2003). However, after the wet periods 1950s and 1960s, and the strong rainfall deficit since 1970; some studies have highlighted that the rainy seasons are becoming wetter and wetter in some parts of WA (Thierry Lebel & Ali, 2009; Ozer, Erpicum, Demaree, & Vandiepenbeeck, 2003). Therefore, it is important to assess this affirmation from those authors in the NID's local condition. Recently, Descroix et al., (2015), based on the variation of rainfall, pointed out a strong fluctuations in river discharge with a generally decreased trend from 1960 to 2010. While (Mahé et al., 2013) emphasized on the nonlinear effect of the negative rainfall variation over WA resulting in a decrease runoff. Therefore, this study seeks to analyze the spatiotemporal variability of annual rainfall in the Niger river basin in general and the NID in particular during 1981 - 2010; including analysis of discharge trends by using Man-Kendall test as non-parametric approach and a simple linear regression method, known as a parametric approach.

The annual flooding of large alluvial plains is a vital resource for many ecosystem services, including agriculture, livestock, groundwater recharge and biodiversity. It plays an important role in sustaining the livelihood of one (1) million people, and is an important component affecting the water availability of the basin downstream (Zwarts et al., 2005). The food production is very important; as example yields, can go up to 6-7 tons/ha for rice under irrigated agriculture practices in the large-scale "Office du Niger" irrigation scheme (97,000 ha), diverting water at the Markala dam upstream of the Delta. In addition, fisheries constitute an important source of revenue for the inhabitants of the NID with annual production varies between 70,000 to 120,000 tons.

Changing climate conditions are expected to modify the availability of water resources in the NID and the timing and availability of water resources downstream of the NID (Orange et al., 2002; Kuper et al., 2003; Zwarts et al., 2005; Mahé et al., 2009; Mahé, et al., 2013; Descroix et al., 2009). Therefore, a sound understanding of the processes that control NID's role in the hydrological cycle of the basin is essential for ensuring rational management of water resources under current and future climate and environmental conditions (Wolski et al., 2006).

Several models of the NID have been developed previously (Olivry,1994; Orange et al., 2002; Kuper et al., 2003; Zwarts et al., 2005). These were hydrological and/or reservoir versions, hydraulic and agro-ecological models that simulated either a part of or the entire system.

The dynamics of the inland delta have been largely neglected in basin scale hydrological models. The hydrological models are mostly used as tools for quantitative description of hydrological processes in wetlands, due to their ability to simulate the hydrological effects of various management alternatives. However, wetland modelling approaches differ in complexity, physical basis and data requirements, so the choice of a model depends on the specific purpose of the modelling exercise (Wolski et al., 2006). Past studies revealed difficulties in estimate the various components of hydrological processes, or to create hydrologic simulations over extended time periods (Dadson et al., 2010; Hughes et al., 2014), arising from the complexity of these processes in the NID.

Starting with the Gallais study 1967 (cited by Olivry, 1994), a number of studies have been conducted regarding the water balance of NID and its flood extent. In Olivry, (1994); Olivry conducted a thorough evaluation of the water losses of NID system based on 38 years of the available data by that time. The surface of the flooded area was deduced from the hydrological balance. The model was designed to simulate surface flood area extent; but failed to model the natural physical flood processes in terms of duration and flood frequency.

Further studies on the water balance of the NID by Orange et al., (2002) revealed information on the maximum flooded area extent that can occur over the NID at maximum surface water levels. Orange's approach was quite different to that of Olivry,1994. Surface flood area analysis of the behavior of the NID by Orange et al., (2002) has revealed that there is high

variability of the inundated area based on the discharge inflow from the upstream. Similar studies on water balance by Zwarts et al., (2005) attempted to represent the effects of up-stream abstractions on an inundation area, by estimating average reduction in outflow and flooded area. Similar indices were used by Mahé, et al., (2011) in their spatial-temporal model, and was aimed at forecasting surface flood areas using water balance. On the other hand, Dadson et al., (2010) model consistently overestimated outflows from the NID by 40%, though it performed well for reproduction of the timing of observed flows. Dadson's study seriously underestimate the influence of key regions, and has revealed that the model's over-prediction of discharge in the system could have been caused by losses due to the abstraction of water from the river, groundwater recharge in the NID, or underestimating evaporation from the land surface or river channel. This reasoning was plausible, since all the three processes could possibly affect the distribution of flow in the NID that could be attributed to one or several of the following (Zwarts et al., 2006).

The most recent work on the water balance of NID is the study done by Ogilvie et al., (2015) who studied the remotely sensed flooded areas at high temporal and spatial resolution, and refined evaporation estimates as well as precipitation across the NID wetland using a water balance model. This result is consistent with the previously explored correlation between the NID flood area extent and surface water inflow. However, the model's simulated evaporation losses were underestimated by 12% for the period 2001 – 2011, when compared to the previous study of Olivry,(1994) or in situ pan evaporation measurements. Ogilvie et al., (2015) have recognized that the lower evaporation losses could have been caused either by evapotranspiration (ET) from non-flooded areas of the wetland (soil moisture, vegetation) which was not assessed; and would have increased the overall evaporation losses, or by remote sensing flooded areas uncertainties. Since all these processes are recognized as possibly affecting the evaporation losses estimates in the NID this explanation of the inconsistency in the conceptual model was plausible. Most previous studies have underestimated water losses in the basin resulting from evaporation, the main component of water loss in wetlands (Schwerdtfeger et al., 2014); very few studies have considered additional water losses through water withdrawal, that are estimated to amount to 0.4 km^3 of water per year (Zwarts et al., 2005).

Water losses from most wetlands, particularly tropical wetlands, were mainly caused by evaporation (Schwerdtfeger et al., 2014). However, the hydrological changes of NID throughout the year is controlled by the extension of the flooded area. A large area is inundated during the pluvial season because of the very flat plain, where the wetland is located. This means with a hot climate that if a larger area is flooded, ET increases too. The consequence is an increasing amount of evaporative water loss which has major impacts on stream flow and on water storage (Zwarts et al., 2005). Therefore, in order to improve the water budgets, the quantification of evaporative water loss is crucial for a better understanding of the hydrological regimes (Drexler et al., 2004). Several studies have addressed the measurement and estimation of NID's ET or evaporation, however, most of these papers were focused on particular average quantity numbers, which differ from year to year as well as the water loss. Besides of the natural flooding and the connected evaporation, there are some irrigation schemes which can be hold accountable for 0.4 km^3 of water withdrawal per year (Zwarts et al., 2005).

Zwarts et al., (2005) highlighted that from August to December the potential ET of rice changes from 9 mm per day to 5.7 mm per day in the end. The water used by the plants shows more variation if regarded in more detail, but is generally in the order between 5.5 and 7 mm per day. Evaporation varies between 160 and 240 mm per month depending on the temperature and sunshine with an average of 200 mm per month (Zwarts et al., 2005). Another estimation of evaporation was conducted by Mahé et al., (2009), which presumed a total evaporation from the delta as an averages of approximately 800 mm per year. However, from 1984 to 1985 the value was only around 400 mm, whereas from 1924 to 1925 it went up to 1300 mm. While, Dadson et al., (2010) stated that after an isotopic composition analysis of river water in the NID region, there were indications that evaporation is responsible for a reduction of water volume by 25% across the total Niger Inland Delta region. Most of the calculation gave a rough estimate of evaporation as each ET calculated in the cited publication uses different inundated areas and or approaches. However, the following table 1.2 will give a broad overview of some assumptions made in the past studies:

Table1. 2: *Water balance equation used; and Evaporation method used; Estimate of Losses*

Studies	**Evaporation / Evapotranspiration/ Flooded Area**	**Illustrations**

Olivry, (1994)	Water losses, due to the intense E, vary from 40 km^3 to 6 km^3.	Losses = E + I + ΔS - P by hypothesis I = P ΔS is negligible Then, Losses = E with Losses= Inflow - Outflow S = V/E
Orange et al., (2002)	Results have shown high variability of flooded areas (between 6,000 km^2 in 1984 and 25,000 km^2 in 1955)	Model Agro-ecology: water losses max. water level of 610 cm at Mopti to simulate the inundated area. Volume entrant (KéMacina + Douna (km^3)) - Volume sortant (Dire (km^3)) = Pertes en eau (km^3)
Mariko, (2003)	Max. Flooded areas for the regional approach (22360), and for the local approach (26 301), in km^2	Estimate the inundated area by means of low resolution NOAA/AVHRR data (four NOAA-images from 1999) The water balance method: V-Vv –E+P – I = dSt With V: (Ké-Macina+Douna), Vv: (Diré) By hypothesis, P = I: (precip. compensate infiltration), ΔS was neglected.
Zwarts, (2005)	11.4 km^3 per year	Inflow minus Outflow
	160 to 240 mm per month,	Calculated from climatic data (temperature and sunshine hours)
Mahé et al., (2009)	15 km^3 per year	Estimated by assuming 800 mm of evaporation per year
	8 km^3 per year	Calculated according to rainy season
	540 mm per year	Using NID's area of about 40000 km^2 for the wet year 1955
	61 mm per year	With surface water area of 9000 km^2 for the dry year 1984
	29.5 km^3 (combination of Southern and Northern Delta)	Annual average cumulated ET for the period of 1972 to 1996
	11.4 km^3 (combination of Southern and Northern Delta)	Annual average cumulated ET for the period of 1972 to 1996
Dadson et al., (2010)	25% of water volume (no value given in the paper)	Isotopic composition analysis

	Annual evaporation exceeds 2200 mm	From 15000 km² of NID's inundated area
Ogilvie, et al., (2015)	Losses ranged between 9.5 km^3/year and 19 km^3/year over 2001– 2010. Direct precipitation over the flooded areas varied between 2.6 km^3/year 8.5 km^3/year; residual term of the WB varied between -0.7 and 5 km^3/year	Water balance equation: ΔS = Inflows into the wetland (KéMacina + Douna) + direct Rainfall - PET - Outflow from the wetland (Koryoumé) + Residual

Climate change is associated with global warming that is induced by the increase in atmospheric carbon dioxide and radiatively active trace gases. Hence, this fact would have possibly altered land and water resources, their spatial and temporal distribution, the hydrologic cycle of water bodies, water quality, and water supply systems and water demand in different regions (IPCC, 2007). This is the focus of scientific investigations due to the fact that climate change has significant effects on the environment, ecosystems, water resources and almost every aspect of human life (IPCC, 2014). The most essential and immediate impacts of global warming can be expected to lead to the changes in local and regional water availability, since the climate system is interactive with hydrologic cycle (Eastham et al., 2008). In semi-arid lands, water resources are very sensitive to minor changes in precipitation and evapotranspiration by vegetation, because the fraction of precipitation that runs off or percolates to groundwater is small (Nicholson, 2001).

The whole of West Africa has been faced with extreme climate variations over the past 5 decades with extended extreme drought conditions during the 70s and 80s (Lebel and Ali, 2009). In this region, precipitation is closely linked with the monsoon, and a better understanding and prediction method are needed for improved water resource management. Spatial and temporal variability of rainfall over Africa offers considerable challenges for assessing and understanding climate change over the continent. This is because of the complexity of African regional climates and the influence of regional geographic features, such as deserts, land cover variations, mountain chains, large lakes, land-sea contrasts and the sea surface temperatures (SSTs) of the surrounding Indian and Atlantic oceans (Sylla et al., 2013).

Niger basin is vulnerable to climate change since the population of the sharing basin countries largely depends on agriculture, which is very sensitive to climate change. In Niger Inland Delta catchment area, the rise in population growth is expected to cause an increase of water demand in different sectors. Hence, water and its availability, would be the highest concern, with regards to climate change issues for societies and the environment. Climate change also increase the vulnerability of ecosystems due to temperature increases, changes in precipitation patterns, frequent severe weather events such as flooding and prolonged droughts (IPCC, 2007).

With regard to the rapid growth in population, the need for the optimum development of water resources has become more urgent than ever. Though, Nicholson (2001) highlighted that the most significant climatic change that has occurred has been a long-term reduction (20 to 40%) in rainfall over the semi-arid regions of West Africa. While, increased heat will lead to more evapotranspiration, but the increase is expected to be partly offset by reduction in plant water use. Higher temperatures may also have an impact in the resources availability. Therefore, climate variables, population growth, irrigated agriculture, urban and industrial water use are major factors deriving water availability issues (Fung, et al., 2009). The impact of climate change on water availability of NID wetland is not well studied. This study was conducted to evaluate impacts of climate change on water availability of the NID by developing temporal climate change scenarios (precipitation and temperature) for the future periods of 2006-2099 and to quantify the possible impacts of the climate change on the available water for the period of 2006 - 2099 using WBMplus hydrological model.

It may be summarized that one of the major challenges facing the sustainability of water resources is climate change. Therefore, studies of water balance model over the NID combine with studies of climate change effects on the water resources appears to be suitable technology to address the sustainability of water resources at downstream of the Niger Inland Delta.

1.3. Thesis Objectives

This includes global and specific objectives.

1.3.1 Main objective

The aim of this research work is a better knowledge of water resources availability in the Niger river basin taking into account the impact of climate change and variability. The thesis make focus on the Niger Inland Delta with a better understanding of the hydrological systems and processes.

1.3.2 Specific objectives

Four specific objectives are formulated to guide in the effective achievement of the main purpose. These are as follows:

(1) Conduct trend analysis of the hydro-climatic data in the upper and NID of the Niger basin, and perform their spatial data interpolation;
(2) Characterize the extent of NID flooded area using monthly-scale inflow data; and to quantify the water losses throughout the Niger Inland Delta;
(3) Develop a conceptual module specifically suited for Niger inland delta which can be potentially integrated into hydrological models to improve the NID representation in models;
(4) Assess the potential impacts of future climate change over the NID.

1.4. Research Questions

The broad question is: how could we improve the assessment of Climate Change (CC) impacts in the NID resources?

Some of the critical questions to be answered include the following:

- What are the recent hydroclimatic trends (temperature, rainfall, and discharge) in the study area?
- How can we improve hydrological model simulation over the NID using estimated flooded area based on spatial and temporal remote sensing data?
- How to enhance the estimation of water losses over the NID which is critical for water resources availability over the Niger Basin?
- How could we better translate changes from climate to changes in water resources over the NID?

1.5. Hypothesis

The following hypotheses are verified:

Hypothesis 1: The trend analysis of the hydro-climatic data in the upper and NID of the Niger basin, and their spatial data interpolation gives less realistic result;

Hypothesis 2: The extent of the flooded area of the NID resources responds to the trends and patterns of hydrological behaviour in the NID catchment;

Hypothesis 3: Known hydrological functioning of the NID, improved hydrological models, as well as reducing some of the uncertainties in the quantification of some hydrological model parameters; are important factors for enhancing the generated basin outflow;

Hypothesis 4: Climate and hydrological changes in the upper Niger basin have significant effects on the river discharge, water losses and water balance in the Niger Inland Delta.

1.6. Novelty

The innovations of this thesis are threefold:

- This study demonstrated how remote sensing data can be used to help conducting hydrological process analysis at high temporal and spatial resolution across large wetlands. Understanding surface flooded area processes for the Niger Inland Delta are crucial for water balance purposes. The use and possibility of effectively mapping wetland using microwave SeaWinds data have been illustrated; and it allowed us to describe the phenomenon of flooding in the delta in terms of water extent. We have shown that inter-annual variability of flood patterns dominates the NID. We have determined the link between spatial patterns of water with Mopti maximum discharge over the NID. The results are in good agreements and they are further used to monitor the water losses over the Niger Inland delta.
- In Niger Inland Delta, the water balance approaches developed by researchers was not standard in the descriptions of water balance equation used; and evaporation method used; and estimate of losses. Likewise, the method selection is done subjectively. In this thesis, we compared several evaporation methods and selected the best. The developed water balance approach is based on a comprehensive method

for representing the fundamental hydrological processes over the NID. Additionally, the developed approach considered the precipitation contribution and the return flow from large irrigated schemes.

Consequently, this thesis contributed to highlight the importance to consider the selection of method in water losses estimates while balancing the water over the NID's flooded area. Furthermore, it has improved the understanding of the hydrological functioning of the NID; and hence the assessment of the downstream water availability under changing conditions.

1.7. Scope of the thesis

The hydrological functioning of the NID has to be carefully addressed. In this study, we incorporate downstream interests into our analysis regarding the water availability. NID downstream flow outcomes are inherently difficult to quantify, and are therefore often omitted in hydrological model simulation. The aim of this study is to develop a decision-support system for effective wetland management in the NID, in which surface flow, losses and hydrological impacts of dams and irrigation systems can be analysed in relation to water balance approach. Multidisciplinary in nature, this study draws on the fields of hydrology, remote sensing and climate change.

To assess the overall quality of the climate information it is necessary to analyse trends in the hydro-climatic data. So, statistical approach is proposed to investigate consistency in the recent trends on climate with observations of hydro-climatic variables. Furthermore, the main discharge stations on the Niger basin are used to assess the runoff trend. This allows an assessment of the overall quality of the climate information from the available data in the Niger River Basin. we focus on the hydro-climatology of the upper Niger River and the Niger Inland Delta (NID). The upper Niger is defined as the Niger basin up to and not including the NID.

For the spatiotemporal dynamics of the flooded area estimate, we use optical and microwave remote sensing data. Then, we calculate the water losses over the inland delta, taking into account the impact of water abstraction for irrigation, return flows, and the flooded area. An evaluation of methods to calculate potential was also performed. In addition, we assess return flows from irrigated areas that were ignored in previous studies.

These information's are used to evaluate impacts of climate change on water availability of the NID by developing temporal climate change scenarios (precipitation and temperature) for the future periods of 2006-2099 and to quantify the possible impacts of the climate change on the available water for the period of 2006 - 2099 using WBMplus hydrological model.

1.8. Expected results and benefits

- Assessment of the overall quality of the climate information from the available data, completed trend analysis for all stations with figure and table (draft of a manuscript for peer review paper);
- Detailed characterization of the NID with regard to hydrological impacts, wet vs. dry years, area, sub-annual time steps for the last ~10years.
- Analysis of the water balance of the delta on monthly time steps, taking into account remote sensing area estimates, special attention should be paid on the evapotranspiration estimate;
- Fully tested and validated model implemented in R that simulates losses (ET) in the NID and outflow over time, taking the discharge at Mopti and temperature as input data, (draft of a manuscript for peer review paper);
- Analysis of hydrological components of the hydrological cycle in the NID and the entire basin, computed with a hydrological model, driven with > 10 regional climate models. (draft of a manuscript for peer review paper);

The proposed research focuses on the climate change impact assessment in order to increase the resilience of wetland communities. A sustainability assessment will help to gain a comprehensive understanding of hydrological status and gain an understanding of the specific needs for management options. An improvement of existing tools such as the hydrological models set for water availability assessment and its applicability in a Niger basin context will provide insights that will be suggested to cope with the future impacts on the water availability. They will provide solutions to ecosystem services related engineering problems in order to keep up with a sustainable development and a long-term adaptation to the risk of climate change. These beneficiaries include fishermen, cattle breeders, shipping companies and farmers, as well as the biodiversity of the river and connected floodplains.

1.9. Outline of the thesis

This thesis is organized in five (5) chapters:

Chapter 1: General introduction that reviews the literature on the subject, states the problem and justifies the present study. The key results are also summarized and discussed in Chapter 1

Chapter 2: It presents the study area with the characteristics of the NID wetland and upper Niger basin. This second chapter of the work focuses on the Hydrological functioning of the NID (relief, vegetation, climate, hydrology, soil and land use, and demography).

Chapter 3: This chapter gives details on the several data used in this study are presented in this section. These data include climate data (precipitation, and atmospheric data), hydrological data, irrigation data and topographical data. It shows the materials involve in this work. And presents methodology developed for the trend analysis of hydroclimatic data and spatial interpolation; for the water balance over delta at monthly basis; and for the assessment of the impacts of climate change on the hydrological functioning of the NID and water availability in the basin.

Chapter 4: This chapter presents the results of the trend analysis of the available hydrological information on seasonal and annual variation in river discharge and rainfall patterns. It draws an assessment of the overall quality of the climate information from the available data.

Chapter 5: This chapter describes the results on detailed characterization of the NI's flooded area. This chapter also includes the analysis of the water balance of the delta on monthly time steps, taking into account remote sensing area estimates with special attention paid on the evapotranspiration estimate.

Chapter 6: The chapter six presents the results on the Assessment of the impacts of climate change on the hydrological functioning of the NID and water availability in the basin using the water balance model developed in chapter 5, driven with output from regional climate models.

Chapter 7: draws the global conclusion on all the entire work carried out in this study. This conclusion concerns the performance of the developed water balance model.

The contributions of the present thesis to the knowledge of the scientific community are presented in this chapter. The perspectives resulting from the study are presented also in this section.

Chapter 2. Study Area

This chapter presents the study area by giving a brief description of the Niger river Basin and then focusing on the Niger Inland Delta of Mali. Aspects such as climate, hydrographic network, and vegetation which could have an impact on the water resources availability of the study region. The Niger Inland Delta, on which the research work mainly focus on, is entirely described in all aspects in order to have a good understanding of the local characteristics in terms of hydrology functioning.

2.1. Localization

Niger River Basin (NRB) is located in the West Africa and it extends between 5°N and 24°N of latitude, and 12°W and 17°E of longitude. It includes 10 ten countries, namely Algeria, Benin, Burkina Faso, Cameroon, Chad, Côte d'Ivoire, Guinea, Mali, Niger and Nigeria. West Africa's largest river basin covering ~ $2.2x10^6$ $km^{2.}$; however, it has an active drainage area (Figure 2.1) of the basin of about $1.5x10^6$ km^2. The Niger River is the third longest river in Africa after the Nile and the Congo River; and has a total length of 4,200 km (Zwarts et al., 2005). Its population of more than 100 million with a growth rate over 3% per year; mostly rely on rain-fed agriculture and livestock rearing, which are sensitive to droughts and floods. This population is mainly agricultural. This part of West Africa is divided into three climatic zones: (1) the savanna zone located over Guinea highlands, known as the Upper Niger catchment; (2) the Sahel zone, namely the Middle Niger catchment; (3) and the Savanna and Guinea zones located between Cameroon and Nigeria highlands, known as the Benue sub-basin (Oguntunde and Abiodun, 2012). The most important rivers that flow through this part of Africa are Niger, Gambia and the Senegal. More details on the West African relief and vegetation are provided in the next paragraphs. The river flows Northeast through the Upper Niger basin and enters the Niger Inland Delta (NID) in Mali; an active wetland area, which is the focus of this study.

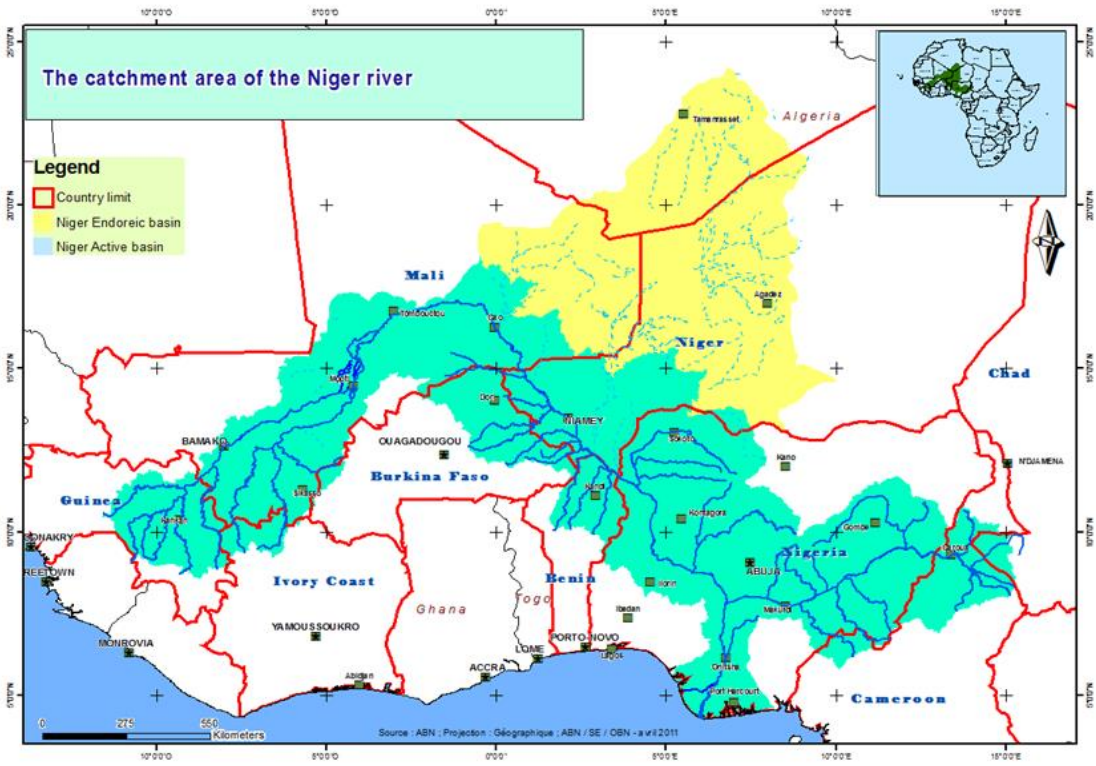

Figure2. 1: *Catchment area of the Niger River (Source: ABN)*

The source of the Niger is located close to the Fouta Djallon Mountains in the South of Guinea at an altitude about 800 m. Due to the topographical and hydrological characteristics, the river is often divided into four sub basins: the Upper Niger Basin, the Central Delta, the Middle Niger Basin and the Lower Niger Basin (see Figure 2.2). It supports large-scale irrigation, fisheries and livestock herding, provides drinking water, generates hydropower and allows navigation. A large part of the river basin is located in the Sahel, a semiarid area between the Sahara Desert and the Sudanian savannas is limited to the four countries of the upper and middle Niger Basin countries (Burkina Faso, Guinea, Mali and Niger). The upper and middle Niger basin has about 20 million inhabitants, of which about 8 million each live in Mali and Niger (KFW, 2010) .

The size of the flooded area is subject to strong annual variations, depending on the discharge of the Upper basin. A large part of the water is lost in the delta due to evaporation and seepage. Its main tributary, the Benue River, flows from highlands of Cameroon and joins the Niger at Lokoja, Nigeria, before reaching the Atlantic Ocean at the Gulf of Guinea (Oguntunde and Abiodun, 2012).

With a rainfall in the region varying between 356 and 682 mm, the inland delta of the Niger river receives runoff from both the River Niger and the River Bani (249 000 km^2). It is divided into a northern part (15 000 km^2) and a southern part (58 000 km^2). The average input and output discharges are approximately 1490 and 900 m^3s^{-1} (1955/1996), respectively. The annual average water loss is approximately 40% (24 - 48%). The losses are greater in the northern (10.5 km^3) than in the southern delta (8.2 km^3), but this situation was reversed in 1984 (Mahé et al., 2009).

The Niger Basin Authority (NBA)/Autorité du Bassin du Niger (ABN) is headquartered in Niamey and is mandated to coordinate the basin-related water policies of the member states in order to facilitate a sustainable integrated water resources management (IWRM).

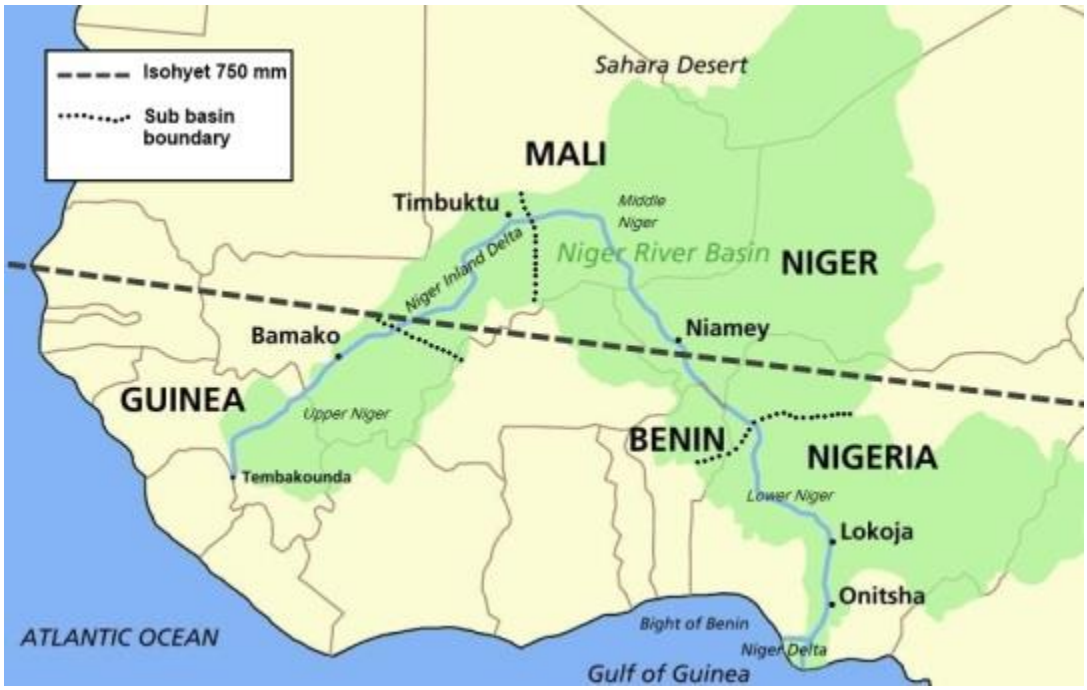

Figure2. 2**:** *Map of the Niger River Basin, showing the four sub basins (source: River Basin KFW, 2010)*

2.2. Relief

The West African relief is relatively simple compared to other parts of the continent. It is mainly characterized by large tabular spaces, plateaus or low-lying plains about 200m on average. The plains occupy the coastal border and are larger in scope in Senegal, Gambia and the Niger valley. Aside, from the Senegal River, Volta and Niger River, these plains are drained by small watercourses; however, they have much higher than regular flows and reaches irrigating the coastal plains of East Africa. The two major water features associated with these plateaus are Niger basin and lake Tchad. The lake Tchad and the Niger inland delta, and the southern marshes provide the atmosphere large amounts of water vapor (Carrington et al., 2001). Medium altitude plateaus and mountains characterize the southern margins and northeast of West African space. The uplands of "l'Air", Tibesti and Cameroon are the three major topographical items. Semazzi & Sun (1997) quoted by Philippon (2002) showed the important role played by the Atlas-Hoggar for the Sahelian precipitations during northern summer; it causes the appearance of a quasi-stationary wave in the northeast flow associated with anticyclonic circulation northeast to the uplands and cyclonic southeast. A second group of plateaus and uplands includes the mountains of Fouta Djalon and the Guinean Mountains (Nimba Mountains) to the west, the Bauchi plateaus to the east.

2.3. Vegetation

In Niger river basin, the vegetation formations are very arranged by zonal bands. The homogeneity of the NRB is only relative because most vegetations are being moth-eaten by cultivated areas, or comprises different facies. In NRB, three main types of vegetation are identified: dense forest, savannah, and shrubland (Fig. 2.3). The dense forest is predominantly localized along the coast of the Guinea Gulf. While for the savanna, it is wooded, bushy or grassy; and shrublands are deprived of herbaceous stratum.

Therefore, Mali can be divided into two predominant forms of vegetation, the humid tropical forest at the southern coast and the semi-arid grassland and shurbs in the north. Vegetation within the Niger Inland Delta has enough specific training influenced by the seasonal regime of flood from Niger and Bani. It has been the subject of numerous studies (Hiernaux & Diarra, 1986; Marie, 2002; Hiernaux et al., 2009). The area is mostly covered with grasslands, wooded grasslands, and a combination of swamp and river adjacent forests structures

like gallery forest. The typical vegetation is mostly presented by various types of grasslands and woodlands. In all of the three described ecoregions cultivation takes place in different level of intensity, but is mostly represented in the Sudanian Savanna type (Marie, 2002).

Naturally the water availability represents the main restricting factor for vegetation growth in the Sahel. Due to its location the Niger Inland Delta is thus very important for the local biodiversity. With the spatial and temporal water variability, there is three major vegetation cycles which are occurring with a certain temporal delay compared to the water cycle. This delay may vary from few days, like the death of grasses, up to several months, withering of trees. Many trees and/or shrubs dominated by Acacia kirkii, nilotica of shallow depressions and human induced vegetation are temporarily flooded. Acacia areas are likely coveted for growing cereals. While the shrubs layer reaches height values between 50 cm to 3 m, the few trees do not exceed an average height of 3 to 5 meters (Mariko, 2003).

Flood plains of the inner Delta, dominated by grasslands, especially bourgou offer outstanding productivities up to between twenty and thirty tones of dry substances per hectare (Marie, 2002). The annual flooding of Delta by the floodwater of Niger and Bani allows to maintain an entire ecosystem with abundant biotic abilities providing a variety of foods to fish and livestock whose management and exploitation constitutes a major challenge for socio-economic development of the region.

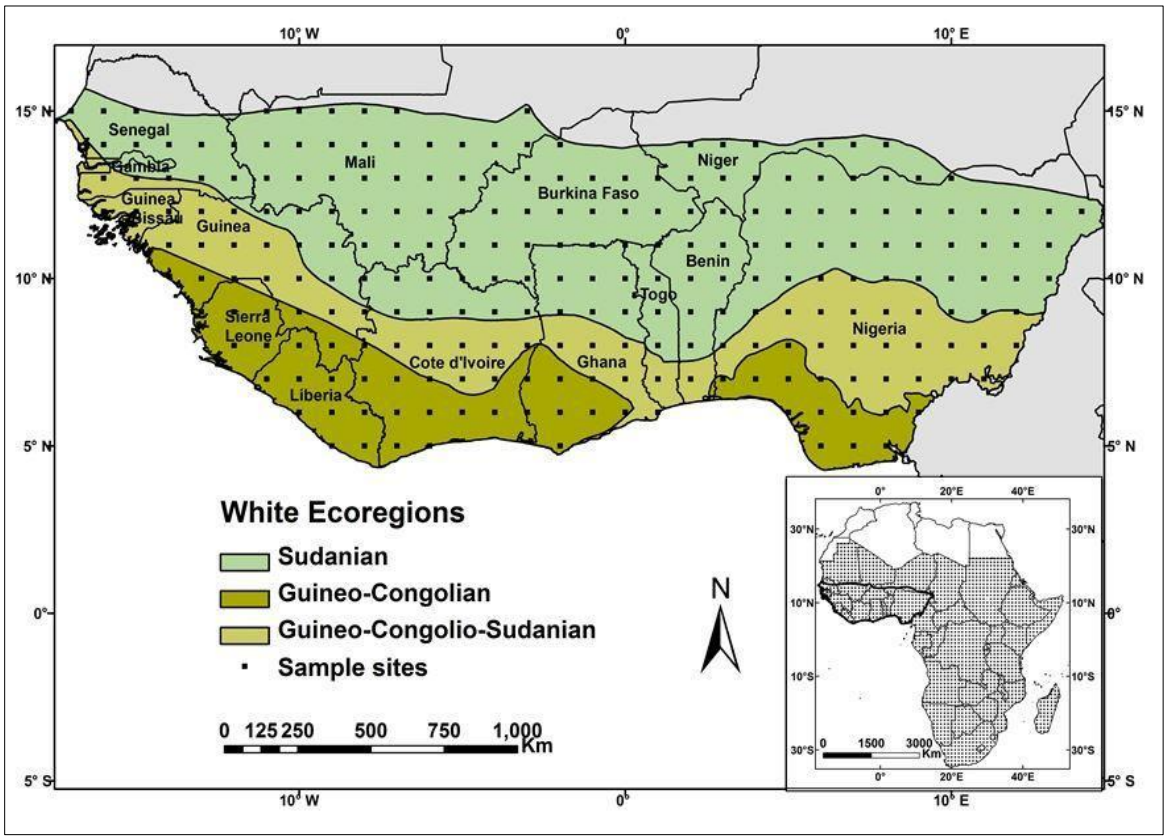

Figure2. 3: *The three main ecoregions in West Africa (adapted from* Vittek et al., 2013)

2.4. Climate

The climate of the Niger basin is tropical and Sudano-Sahelian. In general, the NRB is influenced by three sub-climate zones based on the amount of precipitation decreasing from south to north: a savanna zone with mean annual rainfall between 1000 and 2000mm, a Soudanian zone with mean annual rainfall ranging from 600 to 950 mm, and a Sahelian zone with mean annual rainfall of 200-550 mm (Zwarts et al., 2005). The natural resources are changing and adapting at the rhythm of climate. The combined study of hydrology and climate enables us to understand and measure the impact of these variations on the availability of natural resources particularly in surface water.

The Niger basin climate is relatively governed by compared wind activities. The division of the year into seasons is conditioned by the movement of two large subtropical anticyclones: (1) the Sahara anticyclone of direction North-East/South-West which gives rise to a dry, hot wind, called "harmattan", (2) and “Saint Helena” anticyclone, responsible for the

"monsoon" carried by a cool and very humid sea wind direction Southwest/Northeast (Fig. 2.4). The dynamic contact of these two warm dry air masses from the North (harmattan) and wet from the South (monsoon) is the intertropical convergence zone (ITCZ), (Leroux, 1997). Regarding to the ground, this is called the Intertropical Zone (ITZ) in the portion of which are linked rainfall.

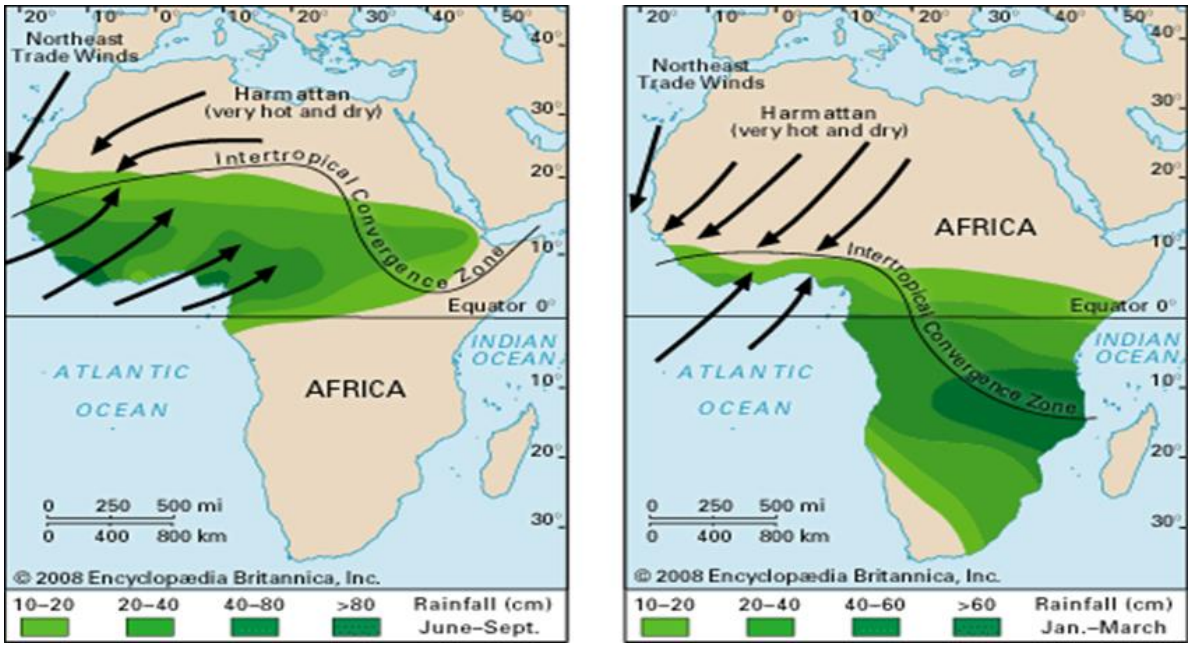

Figure2.4: *West African monsoon cycle*

With large part of the river basin located in the Sahel zones, its climate is a semiarid area between the Sahara desert and the Sudanian savannas .However, the climate of Niger Inland Delta can be described as semi-arid to arid with a sharp distinction between dry season and rainy once (Mahé et al., 2001). This distinction between the seasons is not as precisely defined as one is expecting. Most of the scientists refer to a three months rainy season from July to September (Seiler and Csaplovics, 2005) or four month until October (Mariko, 2003) and according to this a nine (or eight) months dry season. Zwarts,et al., (2005) used a three-month enduring pluvial season as well, however, for his hydrologic year, the dry season covers about 4 months (December - March) and the rainy period extended over about 8 months from April to November." This work will refer to the hydrological year period starting from May. Referring in line to Seiler (2005) whose work defined the seasons as follows: "During a hydrologic year, the dry season covers about 4 months (December - March) and the rainy period extends over about 8 months from April to November."

The annual amount of rainfall in the Upper Niger region varied from less than 250 mm in the northeastern region and over 1750 mm in the south west (Zwarts et al., 2005). The Sahel-Sudan zone is known as region of great rainfall variability (Lebel and Ali, 2009), that why Mahé (2009) used different values, in particular for the period from 1955 till 1996 values which varied between 356 and 682 mm, with an average of 545 mm, for the NID's region. The peak of rainfall in the upper Niger region is observed in August (Zwarts et al., 2005). For this region, there are two main wind directions, which are transporting the precipitation, one from the northeast and the other from the southwest. While the major strong northeasterly winds occur mostly in the late dry season (Seiler and Csaplovics, 2005). Nygaard (2010)states that modeling as well as observations both indicates that the northeasterly winds are more frequent than the southwesterly ones. There are very few indications for winds from either the northwest or the southeast. In most cases the average wind speed is substantially higher in the north than in the south (Nicholson, 1981).

After the great drought (since 1973), the Sahel suffered an ongoing decline of rainfall and consequentially a reduction of water resources. The average discharge in one year proportionally to the average discharge over the entire considered period for the Niger River has declined in a much higher aspect compared to the precipitation over the same time. Hydrologists suppose that the strong water depletion through human activities regarding the groundwater reserves in the upper catchment areas, is attributed to this non-linear relationship (Kuper et al., 2003).

The yearly amount of all solar radiation ranges from 1650 to 2000 kW per m² per hour, with a tendency to higher outcome in the south and southeastern areas of Mali compared to significant smaller results in the north and Northeastern areas. This is a logical function of both the position of the sun and the cloud cover. In the north, corresponding to the wetland, the radiation values ranging from approximately 4000 Wh per m² per day in the dry season to 7000 Wh per m² per day in the rainy period. Looking southwards, the annual variation in solar radiation becomes less variable, with an almost constant level of 5000 - 6000 Wh per m² per day. Whereby it is interesting that the radiation in the north and south are not congruent, as in the south the value being highest in October to April, but in the north in May to September (Nygaard et al., 2010). This shift is important while calculating the evaporation for the Niger Inland Delta.

2.5. Hydrography

The hydrographic network of the Niger basin is relatively dense, as it consists of main tributaries (Niger, Bani, and Benue), as well as a some dam water reservoirs (Mahé et al., 2013) (Fig. 2.5). Based on the precipitation pattern, the hydrological regime in the NRB is sudano-sahelian type, as it is characterized by low flow variability over the Bani river in Mali (Descroix et al., 2009). At the middle bed of the NRB there are many depressions forming the Niger Inland Delta (NID) unit influencing the flow regime locally. Though, during the wettest years some units of the NID have water constantly. Locally, the NID plays an important role in the hydrological regime of the Niger River at Mali (Mahé et al., 2001). The two major tributaries, the Niger and the Bani, join the NID's wetland nearby the region of Mopti in Mali.

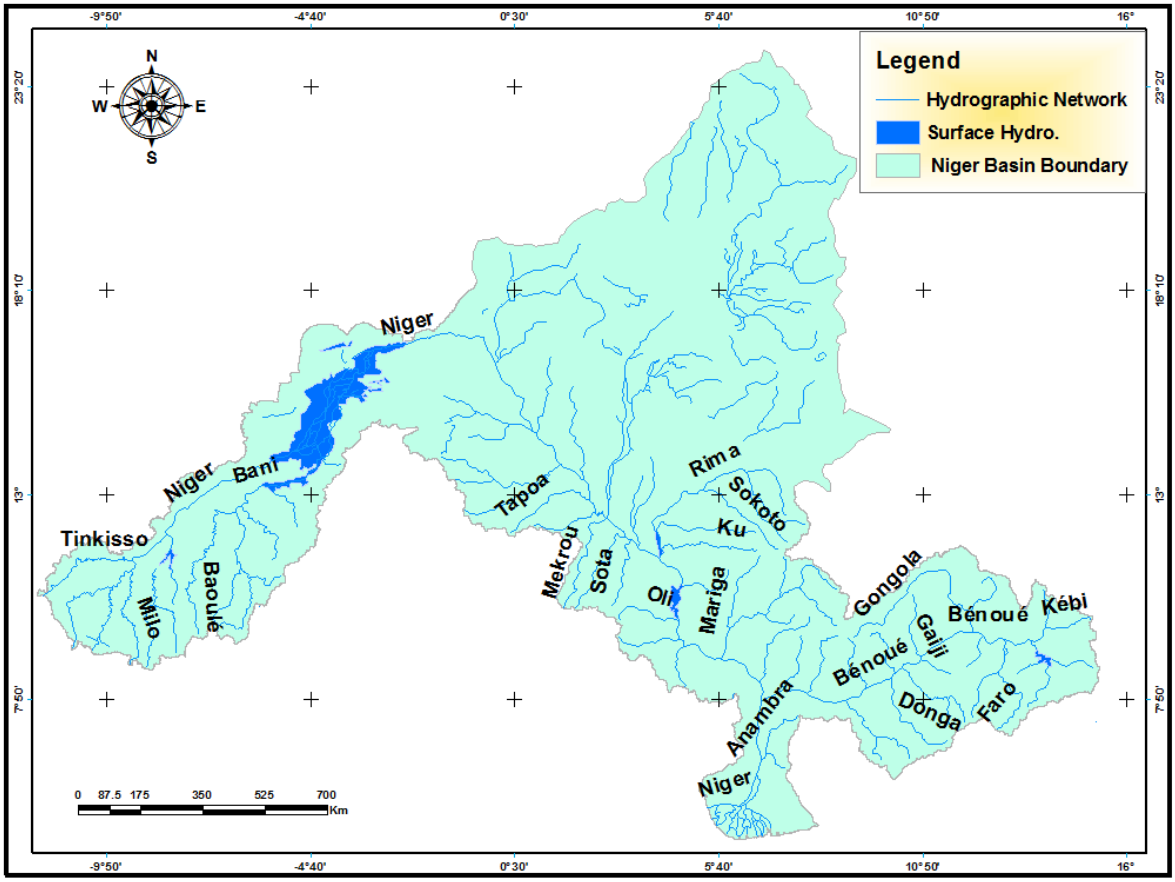

Figure2. 5: *Hydrographic Network of the Niger Basin (Source: NBA)*

The upstream basin located in highland of Guinea with an area of 69690.4 km² is drained by almost 5 tributaries, with the Niger River as the main river originate from the Nimba Mountains at an altitude of about 800m above sea level. The upper Niger hydrographic network constitutes a wide range whose main tributaries are Tinkissu, upper-Niger, Niandan, Milo and Sankarani (Moret - Brunet et al., 1986). The Bani river is formed by the convergence of the "Baoulé" and "Bagoé". The "Baoulé" does not have large tributaries, while "Bagoé" receives on its left bank and the Banifing and Kankelaba, and on its right bank the Banifing. The Bani river receives on its right bank Banifing.

From the highland of Guinea after a distance of about 500 km, the river flows down-stream to the northeast and enters in Mali (Dadson et al., 2010). The upper basin of the Niger river and Bani river is the catchment area until the outlet of KéMacina and Douna respectively (Fig 2.6) and covers an area of about 249 000 km² (Mahé et al., 2009). This is in contrast with the definition of Zwarts et al., (2005) who consider in his study the Niger Inland Delta as part of the Upper Niger basin. This study focuses on the hydrology of the Niger Inland Delta, and therefore the upper basin is defined as the Niger basin up to t entrance of the NID.

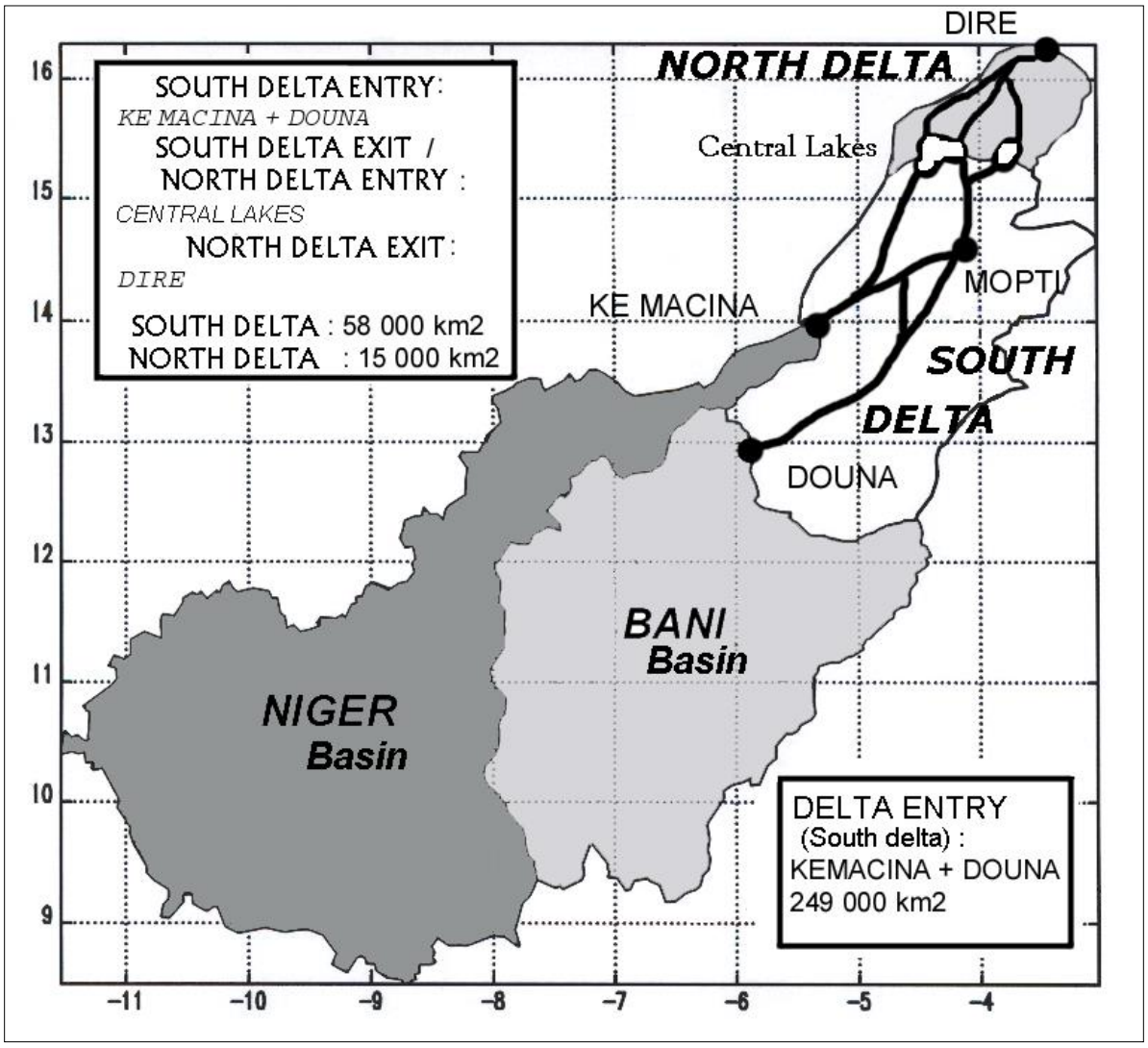

Figure2. 6: *The Upper Niger Basin with the Niger Inland Delta subdivisions (Source: adapted from Mahé et al., 2009).*

Starting from the inputs KéMacina + Douna, the NID (fig. 2.7) is characterized by a very dense and complex network of tributaries, distributary channels, floodplain significantly expanded on the major bed and a chain of lakes on the right bank and left of the Niger river. With a rectangle of SW-NE 450 km long and 125 km wide (Olivry, 1994), the Inland Delta covers an area of more than 50,000 km^2 with variable extension of hydrographic links according to the progress of the flood wave and hydraulic river's feature in the year. The NID comprises two large hydrographic features: the upstream Delta and the Delta downstream. We describe below by presenting the main flow axis (Moret-Brunet et al., 1986; Olivry, 1994; Csaplovics, 1996).

The upstream Delta at downstream of KéMacina for the Niger and, Douna for Bani constituting two major channels Diaka and Issa Ber, is extending to the Lake Debo. The In-land Delta is extending downstream towards outputs of Lake Debo with three main flow axes (Issa Ber West Barra Issa center, Koli-Koli smallest in the East) to Dire. It is characterized by a wide spread river system within a sandy region that limits flooded areas. From KéMacina to Dire, the Niger river flows over about 500 km away and just lost 12 m altitude, i.e. an average gradient of 2.2 cm per kilometer. The gradient of Niger River during humid period is about 2 cm km^{-1} between Mopti and Niafunke, but drops to 1 cm km^{-1} Niafounke to Dire. It reaches 3 cm km^{-1} at upstream of Lake Debo, (Moret et al., 1986; Zwarts et al., 2005; Mahé et al., 2009).

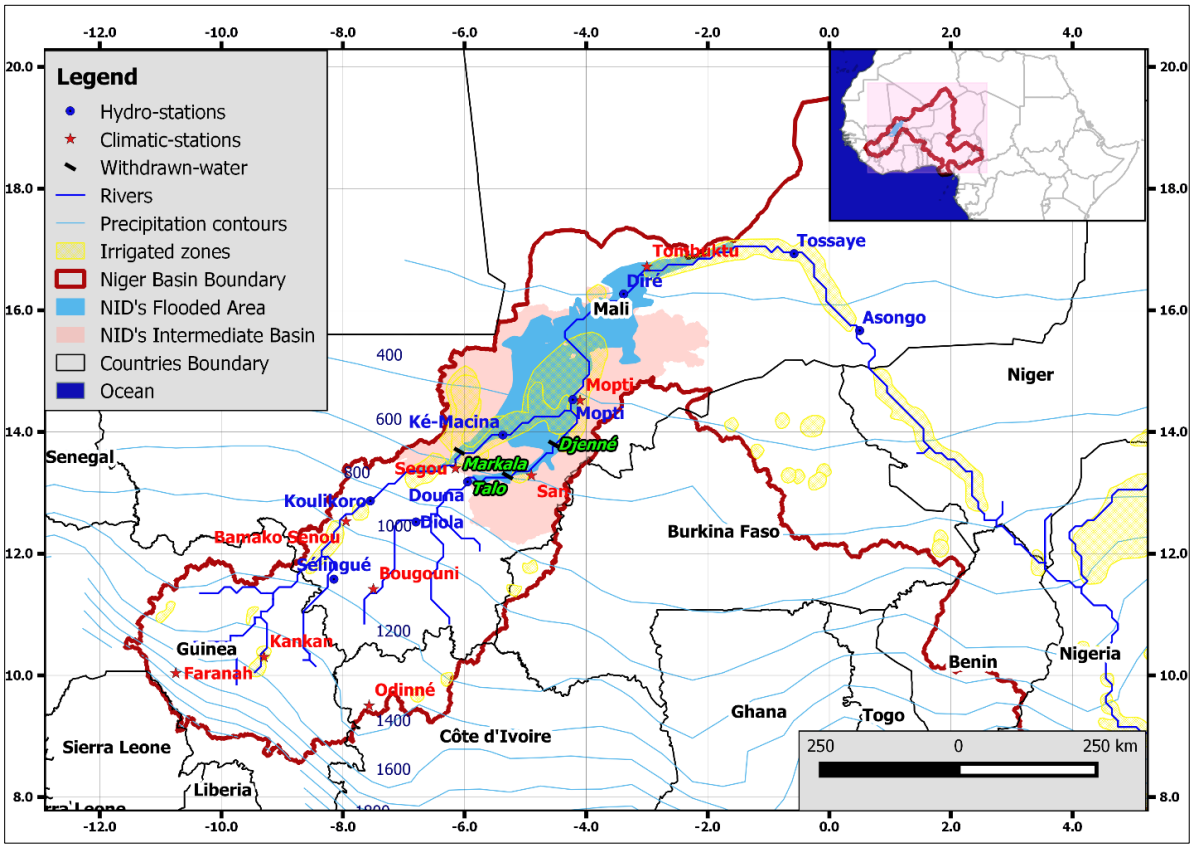

Figure2. 7: *Location of the NID within the Niger river basin and hydro-meteorological stations (source: ABN)*

2.5.1. Hydrological regime

The Niger river has an annual mean observed discharge of 885 m^3 per second (Dadson et al., 2010) and is characterized by strongly seasonal flows, with high peaks causing slightly delayed floods in the pluvial period (Mahé et al., 2013). This huge variation in the

river discharge within a year follows from the large seasonal variation in rainfall; while during the dry period, the flow of the Niger river is only a fraction of its maximum (Zwarts et al., 2005). Mariko (2003) highlighted that described climatic oscillations leading to very high annual runoff variability. Meaning that in all Niger river basins the relative standard deviation is much larger for the river discharge than for the rainfall. For the Bani, the main tributary connects to the Niger river inside of the Niger Inland Delta close to the city of Mopti where the disparity between river discharge and rainfall is especially large (Zwarts et al., 2005).

These flow variations are especially interesting as the Niger river shows a secular tendency of an evolution towards an aridity influenced river (Mariko et al., 2013). Regarding the aridity, the discharge is strongly reduced between the city of Ségou, at 900 km from the Niger river source, and Toumbuktou, at 1500 km, slightly downstream of the Niger Inland Delta (Fig. 2 8). This reduction is due to evaporative water loss caused by the hot climate in the Sahel zone (Zwarts et al., 2005). However, the observation of the total runoff since 1907 shows that there are strong alternation between decades of dryer character and other more humid periods (Mariko, 2003).

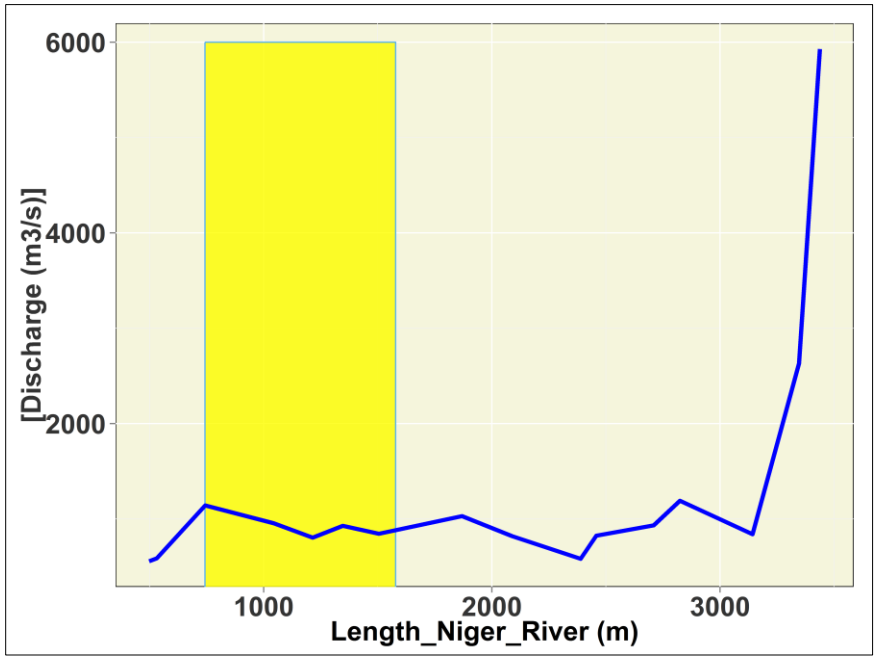

Figure2. 8: *Discharge profile for mean annual river flow of the Niger as a function of the distance from its origin. The Niger Inland Delta (point out with yellow band) is situated between Ségou (900 km) and Tombuktou (1500 km).*

2.5.2. Climatic and anthropogenic factors (Dam reservoirs and Irrigation)

The annual rainfall in the catchment area of the Upper Niger, mainly focuses on the three-month July till September, varies between 1100 and 1900 mm per month with an average value of 1500 mm. Although the river discharge is determined by precipitation, its variation is not directly linked to the annual rainfall, but reaches values between 600 m³/s and 2300 m³/s and is by this much more distinct in its characteristics. This can be explained due to the fact that the peak river flow is not only dependent on the preceding precipitation, but it is also connected to the groundwater aquifers (Fig. 2.9). The level of groundwater is mainly controlled by rainfall during the previous years (Zwarts et al., 2005). Thereby the river flow may decline even in a wet year if the preceding time was a series of dry years. That is why the great drought in the 1970, during which the flow of the Niger river declined to unprecedented low levels, still influences the present discharge (Seiler & Csaplovics, 2005).

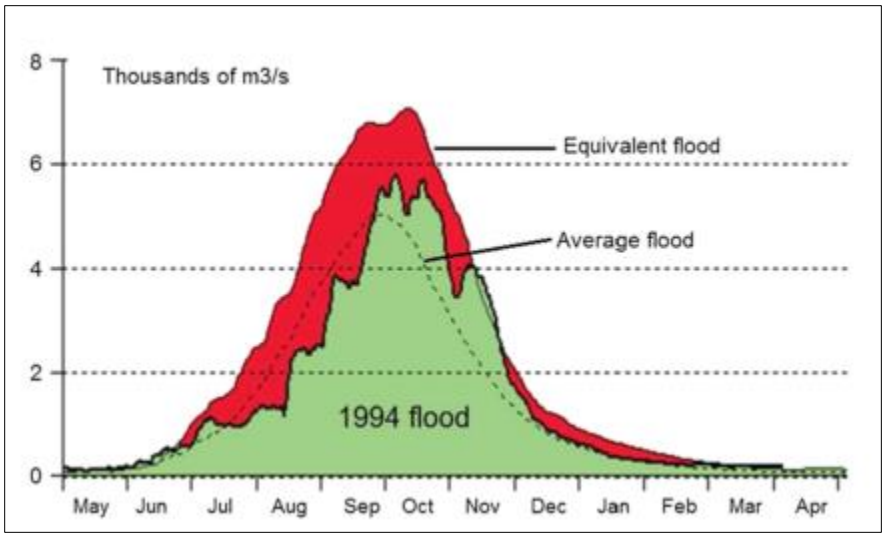

Figure2. 9: *Niger river station of Koulikor, evaluation between the 1994 flood and the equivalent flood before the drought (average of 5 years of same rainfall amount as 1994). The dotted line is the average flood (1907-1996). After the drought, the flood peak is lower, and the baseflow appears more rapidly (adapted from Mahé, et al., 2013)*

Whereas the Niger Inland Delta influences the Lower Niger Basin, the Upper Niger Basin is responsible for the amount of water reaching the wetland and thus accountable for the maintenance of the ecological function. Confronted with severe droughts in the seventies and eighties and a fast-growing population combined with increasing food insecurity some large irrigation schemes, dams for irrigation and hydropower facilities have been constructed in the upper basin. As a result flood intensity and peak flows have been reduced, while low

flows in the dry season have increased (Rebelo et al., 2012). Thus, the impact from these structures and the situation in the Upper Niger has to be discussed to understand certain processes in the Niger Inland Delta.

The basin area close to the source of the Niger River in Guinea and Ivory Coast accumulated is only 5.3% of the total area of the whole Niger River basin. However, because the springs are located in these countries this part of the basin is actually very important for the whole river. The quantity of water entering Mali from Guinea and Ivory Coast is around the value of 40 km^3 per year. This is a greater value than the amount of water, which flows about 1800 km further downstream from Niger towards Nigeria, and is calculated for 36 km^3 per year in that section. This reduction is resulting from processes taking effects inside the Inner Niger Delta, mainly through evaporation, as well as owing to absence of tributaries on the left bank in Mali and Niger, meaning from the Sahara desert region (Zwarts et al., 2005). The main tributary, the Bani, originates in the Ivory Coast and in the highlands of the Futa Djallon respectively by Zwarts (2005) and Seiler (2005); and has a total catchment area of 129000 km^2 and is by this as large as the rest of the Upper Niger basin upstream of the NID, which shows the importance of the Bani for the NID wetland (Zwarts et al., 2005). However, the total flow of the Bani is around a quarter of the discharge of the Niger before entering the Inner Delta (Tardy et al., 2004).

The water requirements for upstream irrigation and hydropower still receive a higher priority in the management plans then for the maintenance of Niger Inland Delta functions is recommendable. Even though the management plan does include an impact assessment for the wetland regarding planned upstream land and water development. This includes a list of upkeep priorities for the wetland, mainly quantitative targets like minimum acceptable environmental flow and flooded area, and maximum fish and rice production adjusted with an activity to adapt to the upstream demand. The influence of such management activities is not assessed by now (Rebelo et al., 2012).

There are three existing dams in the Upper Niger region, and four more under consideration for construction. The Sélingué Dam on the Sankarani River, not far from the border of Guinea, is the biggest and is in use for hydro-power since 1981 (Kuper et al., 2003). The Sotuba dam, operational since 1929, is another hydropower plant, located directly down-

stream from Bamako. The storage capacity is quite small and by this does not have a significant hydrological impact on the Inner Niger Delta. The Markala Dam, is a diversion dam for irrigation purpose of the Office du Niger just downstream of Ségou and in function since 1947 (Mahé et al., 2009; Zwarts et al., 2005). In general all three dams lead to a restrain of water during the flood season and water releases during the dry season with the main impact in form of a flattening of the flood crest and a decrease of the flooded area in the flood plains and river reaches (Kuper et al., 2003) (Fig. 2.10).

Besides the influence of the dams, there is only one large water user in the Upper Niger basin (Zwarts et al., 2006). The "Office du Niger" (ON) operates an agricultural area, called Delta mort, with about 67000 ha just upstream of the delta (Kuper et al., 2003). Therefore, about 100 m^3 per second is taken from the river in the time from August to November and about 60 m^3 per second from December to April. In the flood period, this is equivalent to only a few percent, around 6%, regarding to the high-water level. But in the dry period the withdrawal accounts for 50-60% of the total discharge and thus largely dependent on the additional water released from the Sélingué reservoir (Zwarts et al., 2005).

It has seen over the year around 2.7 km^3 water volume are used to irrigate the ON irrigation scheme (Kuper et al., 2003). Zwarts (2005) states this equals to 8.3% of the total annual river flow, and Zwarts (2005) is quoted with this values by Dadson (2010), whereas Kuper (2003) specify this amount to more than 10% of the yearly Niger supplies. Even though the influence depends strongly on the discharge in the specific year, meaning during times with huge discharge, the effect declines to around 4% of the total discharge, but increases to 15% in a year with a low flood (Zwarts et al., 2005). Currently, there are some project planning to extend the ON irrigated area by about 100000 ha. Furthermore, the master plan of this agricultural zone will ultimately reaches an irrigation infrastructure for over 250000 ha (Kuper et al., 2003). Rebelo (2012) actually stated a planned increase of the agricultural area of the Office du Niger by 4 - 5 times to approximately 500000 ha.

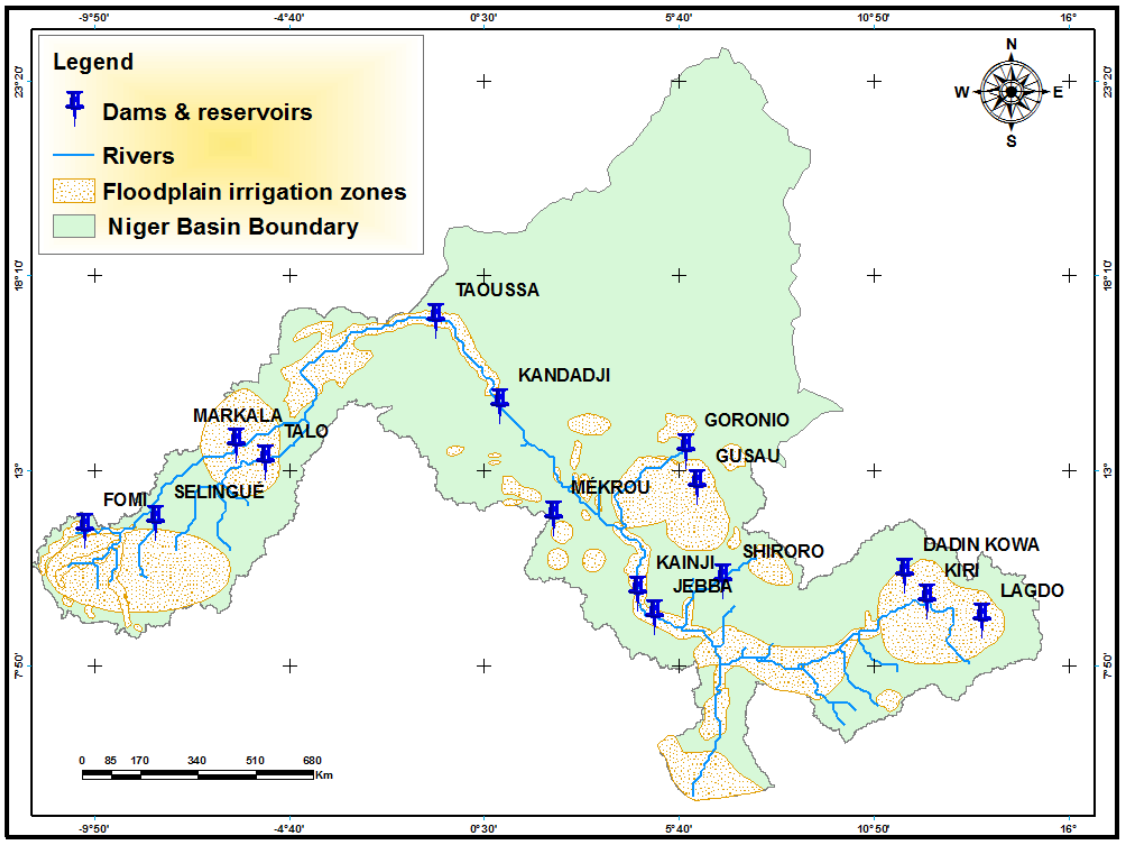

Figure2. 10: *The Niger Basin with four existing dams (Fomi, Selingé, Markala, Talo,kaindji, Jebba, Shiroro, Goronio, kiri, Dadin kowa, and lagdo), the remainings are under construction or project study. (Source:ABN)*

2.5.3. Description of the flood Process in the Niger Inland Delta

The Niger Inland Delta (NID) in Mali is one of the largest and most important wetlands in Africa (Landmann et al., 2010) and has a huge influence of the Lower Niger River, the climate in the surrounding and the inhabitants depending on the ecological services provided by the wetland. The semi-arid environment influences the ecology of inland deltas strongly and characterized it by a mosaic of permanently, periodically and not-periodically flooded areas. The flood extent varies both in scale and in time due to not regularly occurrence of annual rainfall in the catchment areas and the resulting floods contributed by the specific river systems (Seiler and Csaplovics, 2005).

The Niger Inland Delta is a large floodplain located in Mali centered in various extensions around 14°50′16.80″N and 4°20′17.02″W (Landmann et al., 2010) or describable as a rectangle between the upper left corner at 15°37'N; 4°40'W and lower right corner at

13°38'N; 3°26'W. (Seiler and Csaplovics, 2005). The area has a median elevation between 250 and 330 meters above mean sea level (Mahé et al., 2009). As expected from a wetland hydric soils, equivalent to the FAO soil classification, are the most dominant soil type (Landmann et al., 2010). However, the lands outside of the regularly flooded wetland and not occupied by pools largely comprise of very sandy soils and even sandhills (Mahé et al., 2009).

Since 2004 it is part of the RAMSAR convention and stated as a wetland (1ML001) of the area of 41,195 km² (Rebelo et al.,2012). It is exposed to a semi-arid climate with local rainfall generally below 600 millimeters per year, which mainly occurs during the wet season from September till November (Landmann et al., 2010).

However, the knowledge about the area is tenuous and not coherent. For example, even something as obvious as the actual size of the NID varies from publication to publication. According to Mahé (2009) the flooded areas vary in the proportions between 1 and 5 according to dry or wet years, as shown in the following table 2.1.

Table2. 1: *NID Wetland areas from different publications*

Publication	**Total wetland area (km^2)**	**Flooded area (Km^2)**
(Kuper et al., 2003)	36000	10000 - 20000
(Zwarts et al., 2005)	34970	44000 (1957) 9500 (1984) 18500 (average) 17600 (without Lakes)
(Seiler et al., 2009)	40000	10000 - 40000
(Mahé et al., 2009)	73000	40000 (1955) 9000 (1984)
(Landmann et al., 2010)	41195	5209 (RAMSAR site area)
(Dadson et al., 2010)		15000
(Rebelo et al., 2012)	41195	16000 (average) (RAMSAR site area)
(Ogilvie et al., 2015)	20000	10300 - 20000 (Peak) (2000-2011) 3000 - 4000 (Minimum) (200-2011)

	16000 (average)

2.5.4. Hydrological functioning of the Niger Inland Delta

Due to its location in the middle of the Sahel, the Niger Inland Delta in Mali constitutes a hydrological singularity. It is characterized by very gentle slopes leading to surface water velocities not exceeding 0.3 to 0.6 m/s (Mariko, 2003) in the main channel by a group of central lakes (from west to east: the Wallado, Debo, and Korientzé lakes) where all the upstream flows from the south converge to a single exit point at Diré on the Niger River. According to (Olivry, 1994) the hydrological functioning of NID is largely dependent on flow conditions, and most of the water resources from the much watered upstream regions of the Delta; and hence from hydro-climatic regimes of Niger and Bani upper basins, morphological conditions of NID governing runoff (topography, micro-relief, shape and plains altitude, lakes, reservoirs) and finally the weather conditions (rain, evaporation, infiltration) that come into account in the water balance inside NID in a ratio of 5 to 10% of upstream inputs (Mahé, et al., 2009).

Thus, NID acts as a temporary storage of large amounts of water lost by the discharge, which are driven mainly by evaporation, and in a small proportion (unknown) by infiltration. The storage of water in the NID governed by the longitudinal (from upstream to downstream) and transversal (towards the plains) flood propagation results in the reduction of the annual flood (Olivry, 1994) observed on the hydrograph at gauge station Dire (output of the NID).

As stated above regarding the Upper Niger River basin, there are mostly two large scaled structures influencing the discharge in NID. Namely the Selingué reservoir with a water loss of approximately 0.83 km³ per year and the water intake by “Office du Niger” for the irrigation scheme at 'Delta mort' with estimated water losses of the value of 2.7 km³ per year. However, the hydrological regime of the NID is controlled by the extension of the flooded area. Because of the very flat plain, where the wetland is located, a large area is flooded during the rainy season. However, this means in a hot climate that if a larger area is flooded, evaporation increases too. The consequence is an increasing amount of water loss going in line with a rising flood level (Zwarts et al., 2005). The effect is greatest between

September and November, when the peak extent of the flooded region coincides with high temperatures (Dadson et al., 2010).

From the two rivers, Niger and Bani, a total volume of 3.7 km³ (which is less than 10% of the total annual discharge 39.1 km³); would have reached the Niger Inland Delta if there would be neither dams nor irrigation upstream (Zwarts et al., 2005). Thus the input to the NID from the rivers Niger and Bani accounts for an average of 1490 m³ per second form 1955 to 1996 (Mahé et al., 2009). This is equal to a combined total average accumulated volume inflow of 35.4 km³ per year (Zwarts et al., 2005). The outflow at Diré adds up to an average of 900 m³/s (Mahé et al., 2009), or is equal to 23.1 km³ per year (Zwarts et al., 2005). Due to the easy equation of subtracting the annual values the assumption can be made that the water loss inside of the wetland must be 11.4 km³, which accounts for 33% of the inflow (Dadson et al., 2010; Zwarts et al., 2005). By subtracting the daily average value the annual average water loss accounts for approximately 40% (Mahé et al., 2009). These are average quantity numbers, which differ from year to year as well as the water loss Besides of the natural flooding and the connected evaporation, there are some irrigation schemes which can be hold accountable for 0.43 km³ of water withdrawal per year (Zwarts et al., 2005).

Yet, Dadson (2010) stated that besides being well documented as a source of water vapor and a sink of latent heat, very few quantitative constraints have been offered. A further investigation is to be needed. Although a doubling of the total land-atmosphere water flux exists due to significant evaporative loss from the inundated region (Dadson et al., 2010). As described before, there is a delay between pluvial period in the catchment of the rivers leading into the Inner Niger Delta and the effect of the flood. Because of that an increase of the water levels arrives at the western to southern fringes of the delta as late as in early to mid-October and fade away at the beginning of January along the northern boundary of the delta. In consequence, large areas of the extremely flat delta are inundated during the period of extremely hot climate at the early dry season (Seiler and Csaplovics, 2005). Thus, the combination of flooding and hot climate has major influence of the loss due to evapotranspiration.

The evaporation describes the vaporization of water in case of open water surfaces caused by higher temperatures, wind and sun radiation. There is a differentiation between potential and real evaporation. In the first case, the maximal possible transfer from liquid

water to water vapor is given as a function of the air water content and air temperature in relation to the energy supply. The real evaporation is the value which is actually vaporized and is always smaller or at best equal to the potential evaporation. Evapotranspiration is the aggregated value of evaporation and the transpiration from animals and plants. The evapotranspiration is a ratio of soil moisture, biomass, the type of the transpiration used by the plants, the density of the plant canopy and ground cover, the intensity of the sun radiation, the water content of the air, the soil temperature, temperature of water & air, and of the wind speed.

From August to December the potential evapotranspiration of rice changes from 9 mm per day to 5.7 mm per day in the end. The water used by the plants shows more variation if regarded in more detail, but is generally in the order between 5.5 and 7 mm per day. By accumulating the rice paddies needs with the evaporation of the area in the region of around Mopti, it leads to the value of water demand for irrigated agriculture in the range of 13 to 14.7 mm per day. Based on a daily intake of fresh water by considering pumping over a time period of 11-12 hours, the discharge per hectare is 3 to 3.8 liter per second (Zwarts et al., 2005). "Taking into account losses in the system, it is reasonable to assume an irrigation value of 4 l/s/ha or for all 100 km^2 together 40 m^3/s. Given an irrigation period of four months, this would correspond with an annual water intake of 0.21 km^3. Note that this number may even be smaller since the calculation ignores the rainfall in August" (Zwarts et al., 2005). The consequence of the 0.21 km^3 water use is an increase of water surface and by this an increase of evaporation, leaving the unanswered question, up to which amount water is lost by evaporation?

2.6. Soils and Land use

The pedology of the Niger inland delta watershed is related to its geomorphological evolution and the climate of the region. The "Delta Mort" is a rather flat alluvial plain with heterogeneous soil conditions, ranging from sandy elevations and dunes to argillaceous soils in the former basin and silty soils in between (Zwarts et al., 2005), and most soils in the watershed are highly weathered, friable and of low structure and high density. They are tropical ferruginous soils with sandy surface textures and surface crusts, and they

generally lack nutrients, exhibit poor structure, and have low organic matter content (Dadson et al., 2010). The soils are poorly developed due to the nature of the parent rock and their thinness. Thus, the geomorphology is general because the Niger River is a sequence of:

- flood basins favorable to rice development;
- different levels of mostly sandy alluvial terraces with discontinuous bands of clay depression areas;
- colluvium-alluvial glacis with low ramps (less than 3%) and long slopes;
- glacis of denudation with steep ramps; and,
- continental shelf battleship.

To summarize, two types of soil are predominant in the basin: crystalline rock composed of former kaolinitic materials, and soil from the alteration of montmorillonite materials. The former has low fertility and the second has relatively high fertility, and both have significant drainage. These hydromorphic and ferruginous soils are found mostly in the farmlands. As in all irrigation systems in the world there is always a serious risk for soil depletion/degradation and processes such as salinisation, alkalinisation and sodification. In the case of the "Office du Niger" irrigation zone several studies on these problems were carried out (e.g. Zwarts et al., 2005). Soil degradation is a common phenomenon in the "Office du Niger" irrigation zone.

However, despite the thinness of these soils the vegetation still grows, due to the high influence of rainfall. The vegetation evolves from south to north: savannah dotted with clear sparse forest, to steppe shrubs and bushes. The vegetation formation in the watershed is thorny and lightly wooded savannah (Marie et al., 2002). They are either widely dispersed, or form thickets in more or less parallel bands alternating with bare patches (striped bush). The following species are found in different areas of the basin:

- Gum trees (*dacryodes hexandra*) that form real wooded belts around permanent and semi-permanent ponds and along the *thalwegs*;
- Balanitis (*balanites aegyptiaca*) that are scattered throughout the basin, as well as jujube trees (*zizyphus vulgaris*);
- Baobab trees (*Adansonia digita*) that are sometimes near important settlements, particularly in the Aribinda, Bouroum, and Liptougou regions;

- Grass (*Andropogon gayanus, penissetum*) that generally forms a discontinuous carpet, except in depressions with clay soils, where meadows of wild fonio (*Parricum Lactum*) are dominant; and,
- Shea trees (*Vitellaria paradox*) and "néré" trees (*Parkia biglobosa*) in the extreme south of the watershed.

2.7. Demography, environmental, social and economic activities

All over the world, floodplains are extremely productive biological systems. This is one of the reasons why floodplains in the Sahel attract so many people. The Niger Inland Delta of Mali forms no exception. The Delta accommodates more than one million people at present, most of which fully depend on its natural resources. With approximately 25 inhabitants per km^2, the population density of the NID is much higher than in its dry surroundings.

The major characteristic of the NID is the large variation in natural conditions between seasons and between years. This is due to changes in flood level and the large seasonal and annual variation in rainfall. As a consequence of variable rainfall and flood level, the productivity of resources also varies from year to year. Many people living in the Delta, such as herders and fishermen, move with the flood to make optimal use of the variation in productivity in different ecological zones. Herders have to migrate with their cattle while fishermen follow the shifting waterfront. Indeed, the population of the region is largely composed of six social groups. In the NID section, they are mainly Bambaras, Peuls, Bozos, Somonos, Sonrhaïs and Tamasheq. Their main activities are irrigation, farm livestock & breeders by tradition, fishering and also practice agriculture.

The agricultural sector in and around the NID can be subdivided into irrigated agriculture and flood-related agriculture. As in other Sahel countries, the annual rainfall has a dominant effect on the rural economy of Mali, especially in the drier part of the country. The production of millet, sorghum and rice decreases sharply if the annual rainfall in the Sahel zone decreases to below the 400 mm. The rice farmers in the NID are also dependent on rain in the weeks before the flood covers their rice fields, but the production is mainly determined by the flooding. The rice variety being used on the floodplains grows with the rising water and needs coverage by water for 3 months. Most rice is cultivated in areas being inundated by 1 - 2 meters. The rice production in the area of "Office Riz Ségou", "Office Riz Mopti"

and on the floodplains of the NID varied from year to year. This variation could be attributed to flood level and to a lesser degree to rainfall. In total, the average production amounted to 83,000 tones, but at a low flood this reduced to 10,000 and if the flood is high to 80,000 to 120,000 tones.

The fishery sector is one of the leading economic activities in the NID. The economic value of the fishery industry varies due to fluctuations in catch levels as well as variations in the fish price. The estimate of total auto-consumption by the 300,000 fishermen and the 555,000 non-fishermen in the NID is based on the measured daily fish consumption per family, assumed to be constant over time. The validity of this implicit assumption is uncertain, because it is plausible that the daily consumption by local people likely varies in relation to the total annual catch and thus to the flood level.

Although livestock is mobile and can one way or another mitigate damage from reduced water availability, livestock migration is unable to avoid significant losses during droughts. Despite statistical uncertainties, several conclusions can be drawn. • The number of livestock increases with river height in the NID. Nomadic pastoralists increase the size of their herds when water is available. This implies that the maximum sustainable population of livestock is limited by the availability of bourgou in the NID and thus, by the flow of Niger and Bani Rivers into the Niger Inland Delta.

Since time immemorial livestock dominates the floodplain of the Inner Niger Delta. Wild grazers like antelopes have virtually disappeared together with lions and elephants. The intensive human exploitation through fishing, grazing and the use of other natural resources leaves no room for these wild animals, though some hippos and manatees are still dwelling in the deeper parts of the Niger. Notwithstanding this loss of African wildlife and transformation of a natural floodplain, the Niger Inland Delta still can be considered as a hotspot of biodiversity in the Sahel. Its large concentrations of waterbirds and breeding colonies of herons and cormorants have been one of the main reasons for the Malian government to assign the entire Niger Inland Delta as International Important Wetland under the Ramsar Convention (on February 1st, 2004). The few floodplains in the Sahel are renowned for their ecological values. These values are strongly related to the hydrological regime (Welcomme 1986, as cited in Zwarts et al., 2005) and between floodplains show many similarities.

The Niger river plays an important role in the trans- port of goods and people. Particularly during the wet season, boats are the most popular means of transport in the Delta. Not only does river transport allow people and goods to reach remote places, transport by boat is also relatively inexpensive compared to road transport.

2.8. Partial Conclusion

The description of NID wetland showed that the region is of high significance in influencing the Niger river hydrological flow regime. Also, it is demonstrated from literature review that the climate, human activities and land cover of this zone play an important role in the water balance over the region. The choice of the inlet (KéMacina and Douna) and the outlet (Dire) of the NID basin is also thoughtful because this gages stations have a good data recording and are primarily situated on the main tributaries (Niger and Bani). The study area being vital in the Niger Basin makes it to be a zone in which a lot of the land is exploited for rainfed agriculture and irrigation. Additionally, many studies were conducted in this NID due to the data availability over a long period at fine scale and the importance of the area. It is particularly found that hydrological functioning and water losses estimate efficiency are the most concerned aspects who shows huge gaps knowledge as regards the water balance over the NID.

Chapter 3. Data, materials and methods

This chapter presents data used in this thesis work. These data include climate data (precipitation, and atmospheric data), hydrological data, irrigation data and topographical data. Different statistical methods for trend analysis used in this study, such as the moving-average method, linear regression method and Mann-Kendall method for seasonal forecasting are presented. Methodology for the water balance over delta at monthly basis; and for the assessment of the impacts of climate change on the hydrological functioning of the NID and water availability in the basin. The materials involved in this thesis work are presented here.

3.1. Data

The data used in this thesis include climate, hydrological, topographical data, irrigation data, and microwave remote sensing data. The microwave remote sensing data were used to evaluate the flooded area extent, whereas the topographic, climate and hydrological data are used to develop the NID water balance model and the assessment of impact of climate change on the Niger Inland Delta with the WBMplus hydrological model output at Mopti. All the data have undergone data quality control. Most of the data are trust data because, they are collected from high institutions where the data are critically control before uploading in the data base.

3.1.1. Topographical Data

The intermediate NID catchment is delineated using a 1 arc-second resolution digital elevation of Niger River Basin, downloaded from SRTM Water Body Data files (SWBD) (Lehner et al., 2005). Next the used of GIS method for watershed delimitation with respect to the topography, in order to carry out the parameterization of the model.

3.1.2. Hydrological Data

The hydrological data are also used in this thesis to develop NID water balance model. The data are daily mean discharge collected from the best available NID stations (Fig 3.1).

The data five stations (Table 3.1) are collected from “la Direction National de l’Hydraulique (DNH) du Mali”.

Table3. 1:*Hydrological stations of the NID intermediate Basin*

Station Name	Longitude	Latitude	River	Observation period	Country
Ké-Macina	-5.39	13.96	Niger	1954-2013	Mali
Douna	-5.9	13.21	Bani	1923-2004	Mali
Diré	-3.38	16.28	Niger	1950-2013	Mali
Mopti	-4.22	14.53	Niger	1952-2013	Mali

3.1.3 Climate Data

The climate data comprises precipitation (In-situ daily data and satellite data), atmospheric data (In-situ daily data), and COordinated Regional Climate Downscaling Experiment (CORDEX) data. The In-situ daily precipitation and atmospheric data (observed stations data) were used to develop the water balance model. The CORDEX data were to simulate potential responses of the NID to climate change.

The precipitation data including the observed data from rain gages, and precipitation data from the Modern-Era Retrospective Analysis for Research and Applications (MERRA) were used. The In-situ daily precipitation data is from the stations in Mali. These daily data were obtained from the “Division de la Climatologie” at the “Bureau d’Alerte Précoce, Agence Nationale de la Météo, Bamako, Mali.” for the period of 1950-2010; and from “le centre regional d’AGRHYMET, Niamey, Niger” for the stations in Guinea (period 1950-2006).

Four of these stations are located within the watershed while the remaining stations are located in the upstream of the Niger basin (Fig 3.1). The arithmetic mean method is a typical method generally used to calculate average areal precipitation (Adams et al., 2014). It was applied to estimate average precipitation over the NID watershed from the observed rainfall time series (Table 3.2).

Table3. 2: *Details of climate stations*

Station name	Latitude (°decimal)	Longitude (°decimal)	Elevation (m)	Climatic Data	Range
Faranah	10.03	-10.75	463	Precipitation	1950-2006
				Temperature	-
Kankan	10.30	-9.30	376	Precipitation	1950-2006
				Temperature	-
Sikasso	11.35	-5.68	375	Precipitation	1950-2010
				Temperature	-
Bamako-Senou	12.53	-7.95	381	Precipitation	1950-2010
				Temperature	1980-2010
Bougouni	11.42	-7.50	351	Precipitation	1950-2010
				Temperature	1980-2010
Ségou	13.40	-6.15	289	Precipitation	1950-2010
				Temperature	1980-2010
				RH	1980-2010
				Wind Speed	1980-2010
Mopti	14.52	-4.10	272	Precipitation	1950-2009
				Temperature	1980-2010
				RH	1980-2010
				Wind Speed	1980-2010
				Pan ET	1970-2009
Tombuktu	16.72	-3.00	264	Precipitation	1950-2010
				Temperature	-
San	13.28	-4.90	284	Precipitation	1950-2010
				Temperature	-

The other type of precipitation data specifically the satellite rainfall data is derived from the historical available remote sensing precipitation: Modern-Era Retrospective Analysis for Research and Applications (MERRA), MERRA precipitation with the observation-based Global Precipitation Climatology Project (GPCP) pentad product 1-degree daily data set were used. The data cells that cover the study area were sorted out from the daily climate

data of the world. The range of the spatial coverage was taken between 10°W to 10°E and 5°N to ~20°N. The average and the average of the cells were calculated for year 1996 to 2013. There is a free access to the different versions of MERRA data, which is updated on a regular basis. They are preferred for their quality, as well as the ability to compare variations in climate.

Atmospheric data include Relative Humidity (RH), Air Temperature (Ta), and Wind Speed (v). These variables are daily data for the period of 1980-2010 obtained from the National Meteorology Services in Mali.

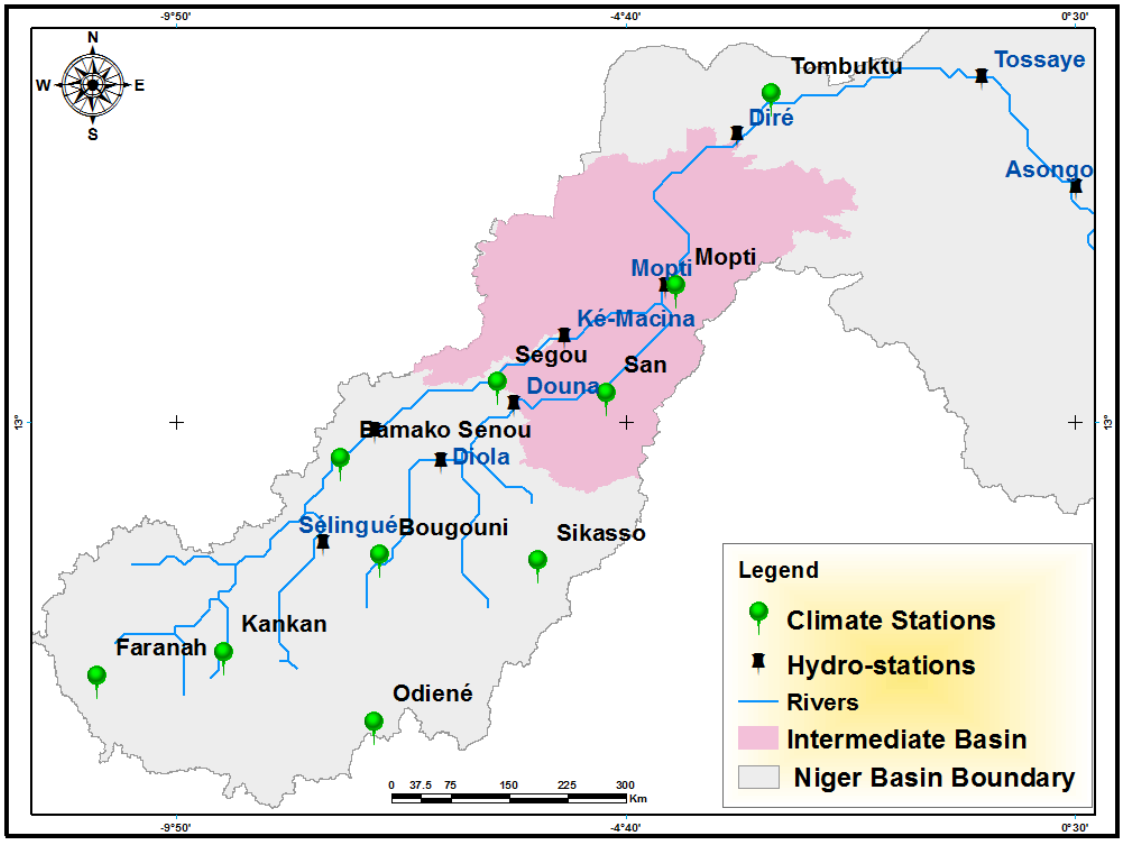

Figure3. 1: *Observed rainfall and flow-discharge measure stations*

3.1.4. Microwave remote sensing data

To analyze the spatial and temporal variations of the floodplain extent, we used optical and microwave remote sensing data received from the SeaWinds instrument onboard of QuikSCAT in combination the ETM+ sensor onboard Landsat 7 for the period 1999 - 2009.

The data source for this study was the National Aeronautics and Space Administration's database, which was supplemented with image data from the United States Geological Survey (USGS) Landsat archives (http://earthexplorer.usgs.gov); and SeaWinds scatterometter form the National Space Development Agency (NASDA) of Japan (http://podaac.jpl.nasa.gov/QuikSCAT).

For this research, the dataset "Landsat 7 8-Day Raw Composite" was used. ETM + images are acquired in six spectral bands with a spatial resolution of 30 m (and a thermal band at 60 m and a panchromatic band received in a 15 meters' dimension) with an approximate size of each scene around 170 km in north-south expansion and 183 km in east-west dimension, with a temporal resolution of a 16-day repeat cycle.

a.) SeaWinds on-board Quick Scatterometer from NASA

The satellite QuikSCAT, which is an acronym for Quick Scatterometer, is a slightly disregarded Earth observation vessel operated by the NASA solely carrying the active radar Scatterometer SeaWinds as the main instrument (http://podaac.jpl.nasa.gov/QuikSCAT). There is a possible mix-up with the SeaWinds Scatterometer flown on the ADEOS-2 satellite, mainly maintained by the NASDA, the National Space Development Agency of Japan, in cooperation with the NASA and the CNES (Frolking et al., 2011). However, in this thesis a mentioning of data from SeaWinds will always be in reference to the QuikSCAT instruments. SeaWinds is an active radar scatterometer with the primary mission to measure the surface wind speed and directions (http://podaac.jpl.nasa.gov/QuikSCAT). The focal point of SeaWinds was to be able to get high-resolution measurements of near-surface winds over ice-free global oceans.

SeaWinds data have spatial resolution of 25 km under all weather and cloud conditions for day & night. A 12.5km resolution is possible through special processing, but has significantly more measurement speckle (http://winds.jpl.nasa.gov/missions/QuikSCAT/). However, no wind information can be measured within a distance of 15 to 30km close to coastlines or in presence of sea ice (http://podaac.jpl.nasa.gov/QuikSCAT). SeaWinds data is collect over ocean, land, and ice in a continuous, 1,800-kilometer-wide band (about approximately 400,000 measurements and covering 90% of Earth's surface in one day). SeaWinds instrument onboard QuikSCAT is a microwave radar that infers surface wind stress by meas-

uring radar backscatter from capillary waves at the ocean surface in Ku-Band of 13.4 gigahertz by 110-watt pulse and at 189-hertz pulse repetition frequency (Chelton & Freilich, 2005). Wind speed and direction are calculated through the process of receiving a backscatter signal reported as the wind (relative to surface ocean currents) that would exist at 10-m height if the atmospheric static stability were neutral. This backscatter is the measured reflected radiation emitted by the active scatterometers as a pulse of low-power microwave radiation. Microwave backscatter value is highly dependent of an objects moisture reflecting the radiation and by the roughness of the surface of this object due to its influence on the direction of the bounce back. This is used by SeaWinds in the form that the wind roughened up sea surface and thus influences the backsactter. Waves caused by the wind are reflecting the scatterometer radar signal primarily by means of a Bragg resonance condition. Because of the Bragg resonance condition and the relative short wavelenght of SeaWinds; a high correlation between the reflected satellite emitted microwave signal and the surface wind speed and its direction exists over water surface. We chose the SeaWinds dataset for NID's wetland mapping because of its longer duration than the NASA scatterometer (NSCAT; which lasted only for about 9 months).

For the thesis, the SeaWinds data were delivered as egg images in netCDF (Network Common Data Format) files for the years 2000 to 2009 and a coverage of whole northern part of Africa in HH as well as VV polarization.

b.) ETM+ on-board Landsat7 from NASA

Landsat products are probably the most used satellite datasets in scientific remote sensing applicate at all. This is not only due to the fact that the program is the world's longest continuously acquired collection of satellite-borne remote sensing data (http://landsat.usgs.gov/about_project_descriptions.php) but as well as thanks to the easy access of the datasets. Compared to the user-unfriendly, unnecessary complicated and bureaucratically overloaded application request of the ESA for Envisat datasets, it is just the effort of a few mouse clicks to get Landsat images.

The first satellite of the Landsat program was launched in 1972. Back then it was referred to as "Earth Resources Technology Satellite-1 (ERTS-1)", however it was renamed in Landsat 1 in 1975 (http://geo.arc.nasa.gov/sge/landsat/l7.html). Since then a total of 8

satellites were launched, from which only one, Landsat 6, was not functional due to its destruction during the start. The images were produced by a multispectral scanner and are used for civilian research referring to topics of agriculture, industrial, geology, forestry, regional planning, education, mapping and global change (http://landsat.usgs.gov/about_project_descriptions.php). At the date of this thesis the satellite Landsat 7 and Landsat 8 are the only one operating. Landsat 8 was launched in February 2013 and is designed to operate around 5 years with the possibility to expand its working time up to 10 years (http://landsat.usgs.gov/about_landsat7.php). By now Landsat 7 is in Orbit since more than 15 years. The Landsat program is a cooperation between the NASA and USGS (United States Geological Survey) (http://landsat.usgs.gov/about_project_descriptions.php).

For this thesis, only images acquired by Landsat 7 are used. This is because thus no compatibility problems arrive from different sensors and due to the overlapping with the time-series of QuikSCAT SeaWinds. Landsat 7 was launched in April 1999 on a Delta II vehicle from California (http://landsat.usgs.gov/about_landsat7.php) and operates with the instrument suit called Enhanced Thematic Mapper Plus (ETM+). The created images consist of eight spectral bands, three in the visible spectrum of light, three in the near- to mid-thermal wavelength, one thermal band and one is a panchromatic band (http://geo.arc.nasa.gov/sge/landsat/l7.html). Panchromatic is the simultaneous measurements of the broad spectral range from ultraviolet over visible light to infrared. The loss of distinction between separated areas of the electromagnetic spectrum is compensated by an increase in the resolution (Wu, et al., 2011). The bands 1 to 7 are recorded in a spatial resolution of 30 meters. According to Landmann et al., (2010) the Landsat WRS-2 path 175 and row 050 should cover most of the Inner Niger Delta wetland, but in detail this is not sufficient. AS Zwarts et al., (2005) stated, to cover the entire Inner Niger Delta, one needs images from the area between the city of Djenné and the lake Lac Débo, which would correspond to the Landsat 7 scene of path 197 and row 50 and additionally of path 197 and row 49. Actually, it would be necessary to get even a third image from path 196 to cover the southwestern part of the Inner Niger Delta near Ké-Macina (Zwarts et al., 2005). However, the path 196 is recorded by the satellite at another date then the main path 197 and furthermore, it is comparable much more effort to cover the whole delta by means of the single Landsat 7 scene from EarthExplorer then to achieve the same effect by using the Google Earth Engine (https://earthengine.google.org).

3.1.5. Field irrigation data

These data were sourced from two irrigations schemes namely "Office-Riz-Mopti" (ORM), and "Office du Niger" (ON) that have approximately irrigated areas of 36 000 ha and 100 000 ha respectively. We collected the monthly data on water withdrawals from the Bani river at Mopti from ORM (Djenné & Talo zones) and on the Niger river at Markala dam for irrigation of "Office du Niger" at Ségou.

3.1.6. Data source and quality control

The data used in this thesis include climate, hydrological, and topographical data. To analysis the long-term hydroclimatic trends in the NRB the following available hydro-meteorological datasets were used. Daily precipitation and temperature data (1950 - 2010) from 9 National Meteorological Observatory (NMO) stations were provided by the countries National Meteorology Agency and the AGHRYMET regional Centre of Niamey. The monthly and annual precipitation & temperature used in this study were compiled from the 9 rain gauge stations, whose records started from 1950s, 1960s, and 1980s and ended in 2006 & 2010 (each station having a 30-year long record at least). The location of the stations in the basin is shown in Fig. 3.2, and their longitudes latitudes are listed in Table 3.2 & Table3.3. Also, the daily discharges (Table 3.3) of the NRB used in this study, was provided by the Bureau of Niger Authority Basin (NBA) of the Niger river.

Besides, to view the long-term climatic trends in the NID the historical available remote sensing precipitation: Modern-Era Retrospective Analysis for Research and Applications (MERRA), MERRA precipitation with the observation-based Global Precipitation Climatology Project (GPCP) pentad product 1-degree daily data set were used. The data cells that cover the study area were sorted out from the daily climate data of the world. The range of the spatial coverage was taken between 10°W to 10°E and 5°N to ~20°N. The annual average and the average of the cells were calculated for year 1996 to 2013.

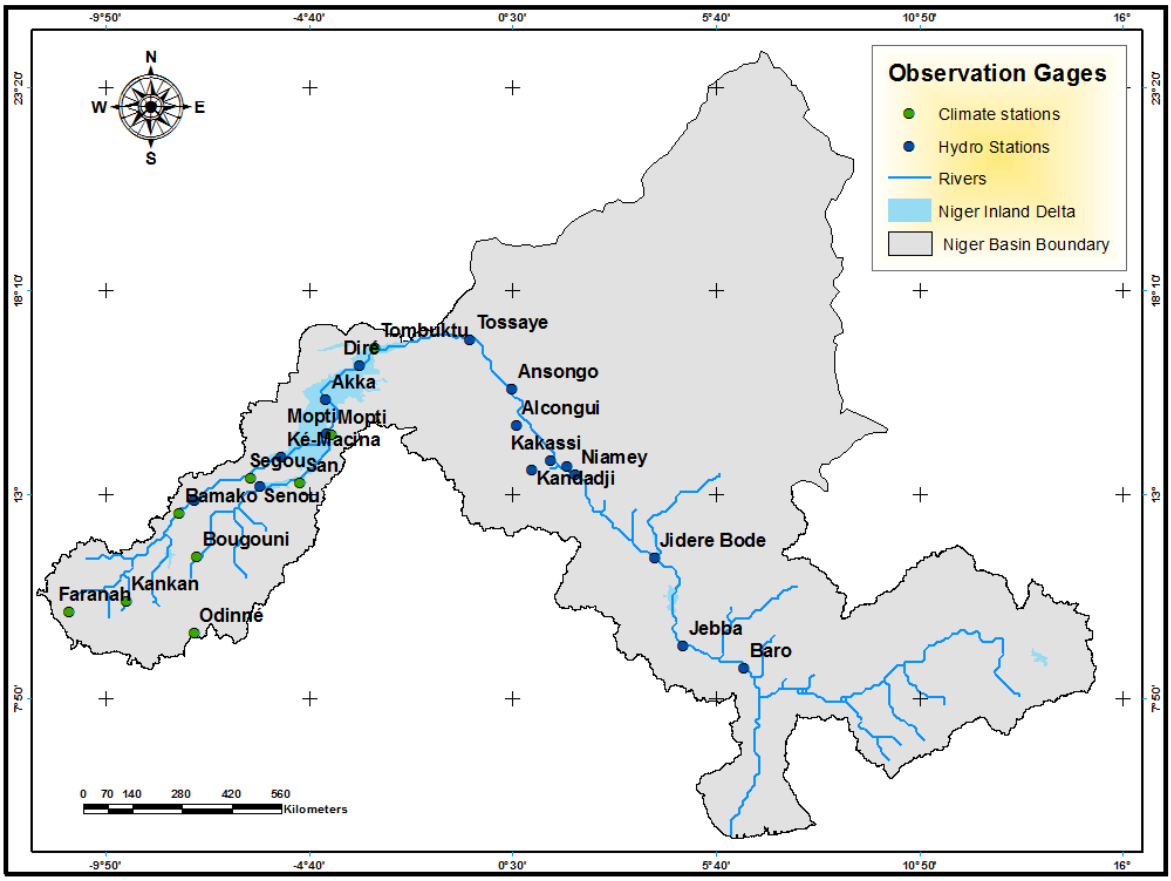

Figure3. 2: *Observed rainfall and streamflow measure stations (Source: ABN)*

Table3. 3: *Hydrometric stations on the Niger Basin and available data*

Serial N	Longitude	Latitude	River	Station Name	Observation period	Country
1	-7.56	12.86	Niger	Koulikoro	1921-2013	Mali
2	-5.39	13.96	Niger	Ké-Macina	1954-2013	Mali
3	-5.9	13.21	Bani	Douna	1923-2004	Mali
4	-3.38	16.28	Niger	Diré	1950-2013	Mali
5	-4.23	15.39	Niger	Akka	1961-2007	Mali
6	-4.22	14.53	Niger	Mopti	1952-2013	Mali
7	0.49	15.67	Niger	Ansongo	1951-2012	Mali
8	-059	16.93	Niger	Taoussa (Tossaye)	1951-2012	Mali
9	-3.65	16.41	Niger	Goundam	1961-2013	Mali

10	0.59	14.75	Gorouol	Alcongui	1980-2012	Niger
11	-8.66	11.68	Niger	Banankoro	1968-2013	Niger
12	1.89	13.73	Sirba	Garbé-Kou-rou	1980-2012	Niger
13	1.47	13.86	Dargol	Kakassi	1989-2012	Niger
14	0.99	13.61	Niger	Kandadji	1980-2012	Niger
15	2.10	13.50	Niger	Niamey	1980-2012	Niger
16	3.39	11.88	Niger	Malanville	1953-2013	Benin
17	6.34	8.58	Niger	Baro	1980-2012	Nigeria
18	4.12	11.38	Niger	Jidere Bode	1980 -2012	Nigeria
19	67.5	7.8	Niger	Lokoja	1980-2012	Nigeria

Data quality control was conducted for all variables since there is a lack of good climate data throughout African Sahel. For each station, rain gauges' time series have less than 10% missing data as this ratio varies from 0 to 6% for all 9 stations over the period. Also, only a few gaps were found in the other climate data records, and they do not alter the quality. For the Mopti pan evaporation records, figure 3.3 shows that the annual missing data ratios are significant (>10%) at the beginning of the series, and more pronounced in 1997 (75%). We have an average rate of missing data of 9% per year for the period 1970-2009. Interpolation process was used to approximately fill the gaps. Then, annual values were by summing up for a year all the monthly values.

For runoff, the data are characterized by missing data ratios of 0 to 46% over the period. Runoff analyses were done with the raw data and periods of non-negligible discharge flow found. Mean runoff of a given month is considered insignificant if it is less than 25% of the mean monthly discharge of the entire period. Time series with more than one month of missing data within the hydrological year of non-negligible discharge were omitted.

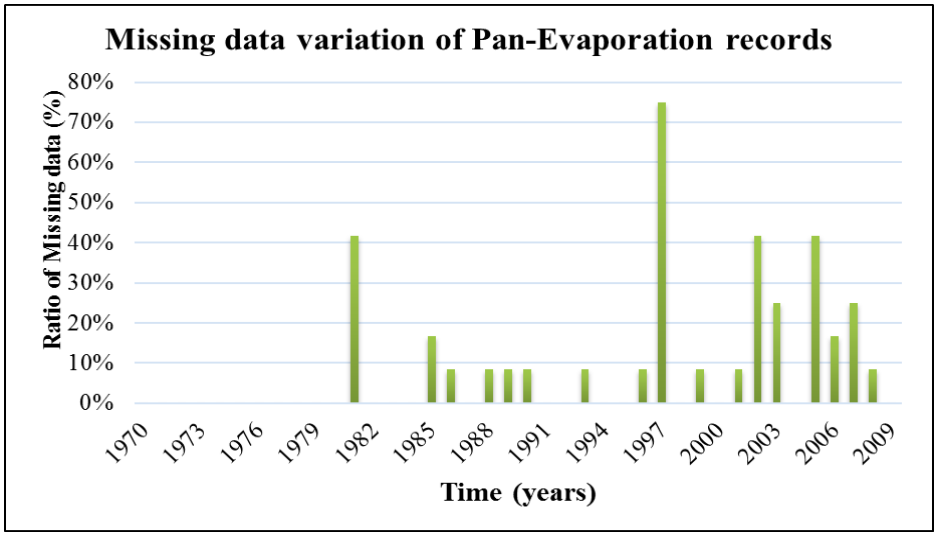

Figure3. 3*: Gap ratios in monthly Pan evaporation records at Mopti (1970-2009)*

3.2. Materials

For the purposes of this research work, we used the following materials:

- Laptop Computer (Lenovo Hardware system)
- GPS (Global Positioning System) / Bathymetry apparatus
- Digital Camera
- Consumables

Software:

- A GIS software (ArcGIS 10.2, QGIS 2.6.1);
- A data processing software;
- R pro to tune WBMplus parameters;
- Ubuntu Linux;
- WBMplus model; and,
- Microsoft office 2010 professional for text treatment.

WBMplus is a fully coupled water balance and transport model that simulates the vertical water exchange between the land surface and the atmosphere and the horizontal water transport along a prescribed river network. It is a spatially explicit model describing varying components of global hydrological cycle. WBMplus extends WBM by explicitly accounting for the effects of irrigation and reservoirs on the hydrological cycle (Wisser et al., 2010).

WBMplus represents a major upgrade to previous WBM implementations by incorporating irrigational water uptake and reservoir operations in a single modeling framework.

3.3. Methods

3.3.1. Trend analysis

From literature review, moving average method is not a relevant test for trend analysis. We have two types of trend: a linear and nonlinear. Classically in literature we can find the linear trend as linear regression that fits data with straight lines in selected time intervals (e.g., linear test, Mann-Kendal, etc.). Such a trend is frequently sensitive to the selected time series intervals. Therefore, based on our data, to evaluate the trend and variability of hydroclimatic elements including precipitation, temperature, Pan-evaporation and river discharge in the basin during the recent years, we employed some trend analysis methods, such as the moving-average method, non-linear regression method and Mann-Kendall method. A trend is considered to be present if it has been detected by at least 2 tests. The trend analysis tests were applied on stations for available climatic data on the upper and Niger Inland Delta regions. Using Thiessen polygon method, mean annual catchment temperature and precipitation were calculated for the upper Niger and NID for the year 1950 - 2006 and 1950 - 2010 respectively, from the stations where data was available (Table 3.2). Stations that do not have data of temperature during the period of collection were not considered (Table 3.2).

3.3.1.1. Mann-Kendall test

One of the most important statistical methods commonly used to test a non-linear trend in hydroclimatic time series is the Mann-Kendall (MK) test (Ding et al., 2011). This trend analysis method has been widely used in long-term hydrologic and climatic time series (Chen, Guo, Xu, & Singh, 2007; Ding et al., 2011; Knowles, Dettinger, & Cayan, 2006; Neumann, Jung, Laux, Kunstmann, & Karlsruhe, 2007; Oguntunde et al., 2006; Yue, Pilon, & Cavadias, 2002; Zhang, Xu, Tao, Jiang, & Chen, 2010) . The mathematical equations for calculating MannKendall Statistics S, with the mean, variance (Var(S)) and the standardized test statistics Z are as follows:

$$S = \sum_{k=1}^{n-1} \sum_{j=k+1}^{n} \operatorname{sign}(x_j - x_k) \qquad \text{(Eq. 3.1)}$$

where: n is the length of the time series $x_i, \ldots\ldots, x_n$;

$\mathrm{sign}(.)$ is a sign function; and

x_j and x_k are values in years j and k respectively.

$$\text{With, } \mathrm{sign}(x_j - x_k) = \begin{cases} +1 \text{ if } (x_j - x_k) > 0 \\ 0 \text{ if } (x_j - x_k) = 0 \\ -1 \text{ if } (x_j - x_k) < 0 \end{cases} \qquad \text{(Eq. 3.2)}$$

The variance is computed as:

$$\mathrm{Var}(S) = \frac{1}{18}\left[n(n-1)(2n+5) - \sum_{p=1}^{q} t_p\,(t_p - 1)(2t_p + 5)\right] \qquad \text{(Eq. 3.3)}$$

where: q is the number of groups; and

t_p is the number of data values in the pth group.

The test statistic Z approximately follows a standard normal distribution and is then given as:

$$Z = \begin{cases} \dfrac{S-1}{\sqrt{\mathrm{Var}(S)}} \text{ if } S > 0 \\ 0 \text{ if } S > 0 \\ \dfrac{S+1}{\sqrt{\mathrm{Var}(S)}} \text{ if } S < 0 \end{cases} \qquad \text{(Eq. 3.4)}$$

No assumptions as to the underlying distribution of the data were necessary since it is a non-parametric test. A positive value of Z indicates an increasing trend and a negative value indicate a decreasing trend (hypothesis H_1). The Z statistic is used to test the null hypothesis, H_0, that the data is randomly ordered in time, against the alternative hypothesis H_1. H_0 is rejected at a particular level of significance (5 %) if the absolute value of Z is greater than 1.96 ($|Z| > 1.96$).

The true slope estimates of an existing trend were done using the Sen's non-parametric method. The trend magnitude is estimated as follows:

$$\beta = \mathrm{median}\,\frac{x_j - x_i}{t_j - t_i} \qquad \text{(Eq. 3.5)}$$

where: x_j and x_i are the values at t_j and t_i respectively.

Hence the relative change (R_C) is computed as follows:

$$R_C = \frac{n * \beta}{|x|} \qquad \text{(Eq. 3.6)}$$

where: n is the length of trend period;

β is the magnitude of the trend slope of the time series (Sen's slope); and

$|x|$is the absolute average value of the time series.

3.3.1.2. Spatial Interpolation

In this study, two different methods; namely Inverse Distance Weighted (IDW) (Shepard, 1968) and Ordinary Kriging (OK) were employed to determine the spatial pattern of annual rainfall over the Niger river basin. These interpolation techniques are methods that determine cell values for locations where no information have been taken, reproducing the spatial continuity of rainfall fields predicated rain gauge measurements (Fathian & Aliyari, 2016).

a.) inverse distance weighted

This interpolation technique is based on the functions of the inverse distances in which the weights are characterized by the inverse of the distance and normalized, so their aggregate equivalents one. The general equation of IDW is expressed as:

$$\hat{Z}(S_0) = \sum_{i=1}^{N} \lambda_i Z(S_i) \qquad \text{(Eq. 3.7)}$$

where: $\hat{Z}(S_0)$ is the estimated value of prediction for point S_0;

N is the number of measured sample sites surrounding the prediction location;

λ_i are the weights assigned to each measured point; and

$Z(S_i)$ is the observed value at the site S_i .

The weight is inversely proportional to the distance between the observations and the inter-polated location. The weights decrease as the distance increases. The weight equation is as follows:

$$\lambda_i = \frac{d_{io}^{-p}}{\sum_{i=1}^{N} d_{io}^{-p}} \qquad (Eq. 3.8)$$

where: d is the opposite of the distance; and

p is a mathematical power parameter which controls the significance of measured sites on the interpolated values based on their distance from the output site.

b.) Ordinary Kriging (OK)

The OK is a stochastic model that incorporate autocorrelation, referring to the statistical connections among the measured sites in order to provide estimates for accuracy in predictions (Ali, Lebel, and Amani, 2005). Kriging approach is based on two main steps: i) the structural analysis based on the variogram and ii) the estimation of a value at an unknown point.

The distance or direction between sample sites reflects a spatial correlation used to explain variations in the surface by applying variogram. This spatially correlated components are measures by using the semivariogram; which is dependent on the both distance and direction factors. Hence, it can represent the direction-dependent variability and looks at variance between pairs of data points over a range of separation scales. However, the experimental semivariogram has to be fitted with a mathematical function/model. An example of a mathematical function is the exponential model as presented below:

$$\mathrm{Y(h)} = \begin{cases} 0 & \text{if } \mathrm{h} = 0 \\ \mathrm{C_0} + \mathrm{C_1}\left(1 - \exp\left(-3\frac{\mathrm{h}}{\mathrm{a}}\right)\right) & \text{if } \mathrm{h} > 0 \end{cases} \qquad \text{(Eq. 3.9)}$$

where: $C_0, C_1, and\ a$ are extract model parameters for the dataset under consideration

from the semivariogram; and

h, is the distance separating any two points.

Then after using the model parameters to estimate semivariance values for any point, the value of the unknown point is calculated from the following mathematical expression:

$$\mathrm{Z(S)} = \mu(\mathrm{S}) + \varepsilon(\mathrm{S}) \qquad \text{(Eq. 3.10)}$$

where: Z is the value at point S;

μ is the trend component value at point S; and

ε is the random, autocorrolated component.

3.3.2. Flooded area characterization and water balance analysis

3.3.2.1. Pre-Processing of Data

Based on the acquired RS dataset over NID, a series of pre-processing steps were necessary prior to the classification procedures and flooded area estimates. Landsat images were in orthorectified and geometrically corrected, with default of WGS-84 datum and UTM projection system, and are of Level1 of the Product Generation System (more information http://landsat.usgs.gov/Landsat_Processing_Details.php). Enhanced resolution images from SeaWinds use two different forms of Scatterometer Image Reconstruction algorithm to reduce speckle and improve quality. The results are two products, one called egg the other one slice. For egg measurements, the full antenna response is used and the resolution is of 4.5 km pixel grid, while a simplified spatial algorithm function is used for slice measurements, with a 2.225 km pixel spacing. The provided egg product of SeaWinds is already an orthophotography, where some algorithms have produced a relief displacement correction from the stereophotography. Hence, no orthorectification or georeferenciation was needed for the both satellite data. The other result is slice product which has much noisier than egg product.

The Landsat 7 scenes from October of every year between 2000 and 2009 were examined. If more than one scene exists in the month, then the one with less cloud cover was taken. Therefore, the prepossessing steps include (1) enhancing the ETM+ data resolution; (2) creating masks of clouds, and applying those masks to the Landsat bands in order to exclude pixels belonging to clouds from land cover classification; (3) converting the multispectral bands (1, 2, 3, 4, 5 and 7) from DN to reflectance, applying atmospheric and noise correction; and (4) mosaicking temporally different images, in order to obtain a cloud-free.

However, in order to achieve the spatial resolution of the spectral bands to 15 m, a Brovey pan sharpening algorithm of the I.pansharpen tool (http://grass.osgeo.org/grass70/-manuals/i.pansharpen.html) was performed. Thus, the 3 bands with lower resolution are combined in a virtual raster and the panchromatic band is used to calculate 3 new bands at the higher

resolution. As in an example for the band 1 combined with band 2 and band 3 of the Landsat 7 images; the following formula is used:

$$\text{New Band1} = \frac{\text{Band1}}{\text{Band1+Band2+Band3}} * \text{panBand} \qquad \text{(Eq.3.11)}$$

To adjust the geographic references introduced by the difference in projection of SeaWinds and Landsat 7 were applied; we geo-referenced the both satellite data to UTM 29 (EPSG 32629).

3.3.2.2. Land Cover Mapping (Flooded areas assessment)

To characterize the landscape and to account for these flooded areas extents, we used an unsupervised and supervised classification method to identify major land cover classes. Our approach relied on the assessment of flood areas using a combination of SeaWinds and Landsat 7 images, offered below an opportunity to measure directly the inundated area. Their optimal thresholds were assessed by means of selecting Landsat TM pixel values that exceed the band 5 and band 7. We combined areas detected for the images over the period 2000 – 2009, and provided spatial and quantitative assessments of the flooded areas for both Landsat 7 image and SeaWinds. To validate the results, the produced land-cover maps were first compared to the available MODIS NDVI datasets for the same time period. Later, results were compared with past studies and known relationship between Mopti discharge data and flooded areas were conducted.

a.) Supervised Classification of Landsat 7 images

To achieve the classification of the satellite-borne measurements of the ETM+ sensor onboard of Landsat 7, we used the pre-processed Landsat 7 images dataset. The process for this classification requires the following steps:

1. Creating training areas, by locating and circumscribing them with polygonal boundaries, in order to classify the origin image calculated from all the pixels enclosed in the training area site by using mean values and variances for each band;
2. Classifying the image mosaic in order to create natural groupings of the spectral properties of the pixels and to get a brief overview of the conventional classes by using the findings of an ISODATA unsupervised algorithm;

3. Classifying the image mosaic with Maximum Likelihood (ML) and sequential maximum a posteriori (SMAP) algorithm;
4. Elaborating threshold and kappa values, which was useful for classifying particularly vegetation and water;

Classifying the SMAP classification and the normal distribution and the continuous uniform distribution as representatives of the a-posteriori distribution.

Initially, unsupervised classification was used to determine homogeneous areas or regions of potential interest for an area selection by combining it with a segregation of the spectral class before conducting more detailed analyses. In this research, a method of land cover classification for water detection has been developed using a combination of all bands for Landsat 7 expect the band 8. Other methods using Landsat images were published for similar studies (Zwarts et al., 2005; Vittek et al., 2013). Many other remote sensing instruments had already been used in the literature for flood areas assessment over NID (Mariko et al., 2013; Ogilvie et al., 2015; Mahé et al., 2011), but with different techniques. The most commonly used supervised classification is the maximum likelihood classification (MLC), which assumes that each spectral class and its distinct features can be described by a multivariate normal distribution. But, for the classification of the selected Landsat 7 scenes of each October between 2000 and 2009 the sequential maximum a posteriori estimation(SMAP) (GRASS GIS toolbox & Google Earth Engine) was used because of its similarity to MLC.

Following the land cover mapping of the Landsat the images, the representation of each pixel as vector inside a vector area created by the classification borders using thresholding was carried out. The highest Kappa accuracy of 80.37 % and 64.36 % was achieved from all 7 bands both SMAP and ML classifications algorithm respectively. Hence, to improve the obtained classes, the creation of training areas was done with the help of unsupervised classification, and existing knowledge on land-cover classification features of the area (Land use map of the west Africa version 2000, previous studies). Therefore, flooded area extent over the NID have been mapped and we have produced a time series of the variable water from 2000 to 2009.

b.) Threshold based Landsat 7 images

With selecting Landsat TM band 5 and band 7, land and water were distinguished. Zwarts et al., (2005) highlighted that water implies an algorithm of band 5 between 100 and 135, and band 7 between 70 and 90. For this study, a threshold technique is used to select every pixel if the logical conjunction was true for a value of equal or less than 80 for band 5 and equal or less than 70 for. Thus, for every month from January 2000 until December 2009, a threshold selection from band 5 and band 7 of the Landsat 7 images was performed. However, the SMAP tool from the GRASS GIS toolbox was used to perform operations with help of Javascript. The produced area was calculated and compared to the area received from the threshold selection of band 5 and band 7 from the same Landsat 7 scenes.

The threshold technique for classification is used to select high pixel values and to detect area from the extracted band 5 and band 7. Hence, using the threshold approach, a selection of every pixel if the logical conjunction was true for a value of equal or less than 80 for band 5 and equal or less than 70 for band 7. The difference to the approach of Zwarts et al., (2005) may be due to the varying reflection unit of measurement for Landsat 7 ETM+ scene. The threshold between classes is more important than the interior of an area itself. This was done by representing each pixel as vector inside a vector area created by the classification borders. The borders are created in such way, that only the surrounding classes close to the regarded border are of influence. In cases, where more than one neighbor in influencing the threshold generation a voting based on the dimensions of the vector gave a weighted influence on some classes.

c.) SeaWinds classification

A land cover classification by SeaWinds is not a typical conducted way and the publications mostly do not state how to create the best classification. Actually, SeaWinds time-series were used for land cover mapping in various publications, like from Ashcraft, (2003); Weissman et al., (2003). However, in this research, a new approach is developed for a land cover classification by SeaWinds. The approach to classifying the SeaWinds backscatter measurements is:

1. to create the boundary box in order to get dataset into an area of interest which is a common way for land cover classification;

2. to segment the image in order to identify spatially contiguous regions within an image that are homogeneous in some way, by this the residual classification errors are reduced through image processing techniques;
3. to perform an unsupervised classification with the "I.maxlik" module of the GRASS toolbox in order to find sensible thresholds most important for the classification by comparison to NDVI maps created from MODIS satellite data and Landsat data;
4. to develop a new array for value of the backscatter with a focus on operation regarding N-dimensional array object, then classify by the thresholds received during the processing with GRASS GIS.

To get an outcome able to be processed, the area of the wetland was calculated. With the geo-projection of the file in longitude and latitude (given by EPSG 4326) and the original Sea-Winds file dimensions (0.05 x 0.05 degree), the true area grid was performed by means of Quantum GIS plugin MMQGIS. Then, to derive the flooded areas over the NID for every month between January 2000 and December 2009, the area grid was multiplied with the counted pixel representing the wetland in the classified SeaWinds array. However, the results seemed to be marginally overestimating the real extent of the wetland. Thus, a weighting of the classes was used to acknowledge the fact, that inside of one pixel with the size of 0.05x0.05 degrees are probably more than just one land cover. Hence the marginally overes-timated extent of the wetland was softened by a decrease of 25% and the outer fringe by 50%.

3.3.2.3. Flooded areas relationship with flow discharge

In order to detect the presence of relationship between the inflow and the extent of flooded area relative to the gauge of Mopti, a water extent as a function of river flow in the preceding month, a non-linear regression model was conducted, where discharge inflow is the inde-pendent variable and flooded area is the dependent variable.

3.3.2.4. Water balance of the NID

We conceptualized the hydrological system of the NID as a set of storage terms, and in-flow and outflow terms (Fig. 3.4).

The surface water inflow component into the NID is a combination of the discharge records from all the major catchments in the upstream basins of the Niger and Bani rivers, as shown in Fig. 3.4, and surface runoff generated within the NID and rainfall over the flooded areas.

The water balance of the NID can be expressed as:

$$\Delta S = Q_i(t) + P(t) - ET(t) - I(t) + WCI(t) - Q_o(t) \qquad \text{(Eq.3.12)}$$

where: ΔS = change of storage,

Q_i = river water inflow, calculated as the sum of discharge measured at the stations KeMacina and Douna,

P = contribution (direct and indirect) of rainfall over the NID,

ET = evapotranspiration loss over the NID,

I = infiltration loss from flooded area,

WCI = return flow from irrigation to the NID's water balance,

Q_o = river water outflow at the station of Diré, and

t = time.

All units are in (km^3 $month^{-1}$).

Although there is some evidence of groundwater movement in parts of the wetland, there is a highly impermeable clay layer under much of the system (Dadson et al., 2010) which minimizes the influences of infiltration loss. We therefore did not consider infiltration.

The applied methods were able to make a clear contribution to the estimation of a flooded area for developing water balance model over the area of the Niger Inland Delta. The period that produced the maximum flood extent (month of October at Mopti gage station) is selected for each image, namely Landsat 7, and SeaWinds data. The results from this process show that These microwave remote sensing data are best- represented the flood area extent over the NID with good correlation as compare to previous estimates.

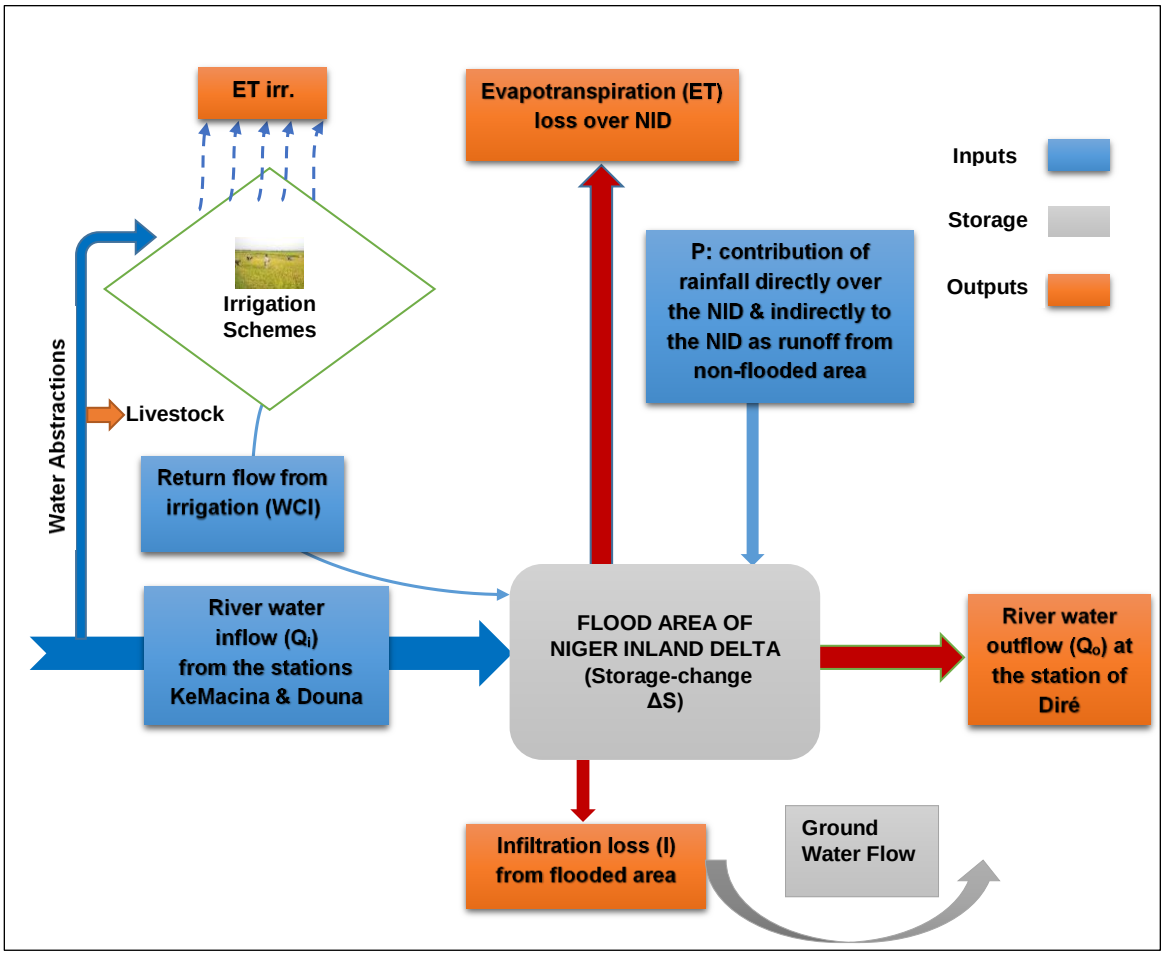

Figure3. 4: *Schematic diagram showing stores and fluxes of water over the NID*

3.3.2.5. Estimation of water balance terms

a.) Evaporation (ET) loss computation

Radiation is the principal weather parameters that determines evapotranspiration in the tropics (De Bruin & Holtslag, 1982); we tested 8 different methods to calculate potential evapotranspiration PET (supplementary information appendix A) models that differ with respect to complexity and input data requirements.

We computed PET for each of those methods for the climate data available for the station Mopti and compared those results with measured pan evaporation at Mopti.

To obtain PET from the Class A pan evaporation data obtained from the "Division de la Climatologie" at the "Bureau Alerte Précoce, Agence Nationale de la Météo, Bamako, Mali", we multiplied pan observations with a pan coefficient of 0.75, the mean of reported pan coefficients in the Sahel that typically range 0.70 to 0.80 (Alazard, et al., 2015).

The statistical approach is used here to select the best potential evaporative model from existing ET methods (Appendix B) with changing parameters, and those with constant parameters. In the statically ET method selection, the following indicators were processed in this work.

- Coefficient of determination

The coefficient of determination (R^2) is the square value of the correlation coefficient (CC) according to Bravais-Pearson. R^2 can also be expressed as the square ratio between the covariance and the multiplied standard deviations of the observed and simulated values. Indeed, the CC is a widely-used measure in model comparison because it possesses the invariance properties.

$$R^2 = \frac{\sum_{i=1}^{n}(OB_i-\overline{OB})(PR_i-\overline{PR})}{\sqrt{\sum_{i=1}^{n}(OB_i-\overline{OB})^2}\times\sqrt{\sum_{i=1}^{n}(PR_i-\overline{PR})^2}} \qquad \text{(Eq.3.13)}$$

Where, OB and PR are respectively the observed and simulated values; n is the number of data.

The CC lies within the limits of -1 and 1. A correlation of +1 or −1 denotes a perfect linear association between observed and simulated data, while a correlation of zero means that there is no linear relationship between the variables.

- Nash-Sutcliffe coefficient

The Nash-Sutcliffe statistic (NSC) can be defined as a measure on how the observed variance is simulated. The efficiency proposed by Nash & Sutcliffe (1970) is computed as one minus the sum of the absolute squared differences between the simulated and observed values normalized by the variance of the observed values during the period under investigation (see Equation 4.1).

$$NSC = 1 - \frac{\sum_{i=1}^{n}(OB_i-PR_i)^2}{\sum_{i=1}^{n}(OB_i-\overline{OB})^2} \qquad \text{(Eq.3.14)}$$

The range of NSC lies between 1 and -∞. A value of 1 indicates a perfect match of modeled data to observed data; NSC = 0 means that the model predictions are as accurate as the mean

of the observed data. Whereas, an efficiency NSC < 0 indicates that the mean value of observed time series would have been a better predictor than the model.

- Percent Bias

Percent bias (PBIAS) measures the average tendency of the simulated values to be larger or smaller than their observed ones.

$$\text{PBIAS} = 100 * [\frac{\text{sum(sim}-\text{obs)}}{\text{sum(obs)}}] \qquad \text{(Eq.3.15)}$$

The optimal value of PBIAS is 0.0, with low-magnitude values indicating accurate model simulation. Positive values indicate overestimation bias, whereas negative values indicate model underestimation bias.

- Mean square error

The mean squared error (MSE) is one of the most widely used simulation scores. It is expressed and estimated using Equation 3.16.

$$\text{MSE} = \frac{1}{n}\sum_{i=1}^{n}\left(\widehat{X}_i - X_i\right)^2 \qquad \text{(Eq.3.16)}$$

Selection of the best represented potential evaporation model required analyzing the statiscal indicators for all 8 models, with the observed pan evaporation records in the study region.

b.) Precipitation (P) Contribution to the NID

Rainfall contributes to the water balance of the NID as direct rainfall over the flooded area and indirectly as runoff that is generated on non-flooded areas that drain in the NID. We assumed a runoff coefficient of 5% for this rainfall (Mahé et al., 2009). The In situ daily rainfall data (i.e. from observed station) was used to evaluate the rainfall contribution. The Thiessen polygon method widely used to calculate average areal precipitation (Ball & Luk, 1998) was implemented to estimate average rainfall over the watershed from the rainfall time series.

c.) Return flow from irrigated fields (WCI)

To estimate the amount of water returning to the NID from irrigated areas as return flow, we subtracted estimated consumptive water use in irrigation schemes (Vandersypen et al., 2007) from the reported water abstraction data from the Bani and Niger rivers. Consumptive use was calculated as potential crop evapotranspiration, ETirr, by multiplying a crop coefficient, kc with the reference potential evapotranspiration (ET0) computed with the Penman-Monteith equation according to FAO (Allen, et al., 1998).

Net Irrigation water requirement is expressed as (derived from Allen et al., 1998):

$$I_{net} = ET_{irr} + S + I_n + P_e \qquad \text{(Eq.3.17)}$$

Where: I_{net}= net irrigation water requirement;

ET_{irr}= water requirement ($ET_{irr} = K_c \times ET_0$, with ET_0 as Evapotranspiration of reference K_c as crop coefficient);

S = depth of water for soil condition (data collected from the "Office du Niger");

I_n = Infiltration rate within the irrigation scheme (Data collected at "Office du Niger); and

P_e = effective rainfall ($P_e = P \times e_r$, with P as rainfall over the area and e_r as coefficient for effective rainfall).

Gross water requirement (consumptive water use (CW)):

$$CW = I_{gross} = I_{net}/e_p \qquad \text{(Eq.3.18)}$$

where: e_p is the irrigation scheme efficiency coefficient (0.65, this efficiency is not already considered in the percolation losses), taken from available "Office du Niger" statistics (Frenken, 2005).

d.) Change of storage (∆S) assessment

Data surface water level (h) collected from the National Hydraulic Headquarters of Mali, were used for assessment of the storage changes.

$$S = \int A_f \times \Delta h \qquad \text{(Eq.3.19)}$$

where: S = volume of storage (km^3);

A_f = flooded area (km^2);

Δh = variation of surface water level (in km), with h as the mean hydrological records water height at the gauging stations (Mopti, Dire & KeMacina).

Thus,

$$S_{t+1} = S_t + A_f \times \Delta h \qquad \text{(Eq.3.20)}$$

where: S_{t+1} = volume of storage (km^3) for the next month;

S_t = volume of storage (km^3) for the actual month;

Δh = variation of surface water level (in km).

Hence the Change in storage was estimated as:

$$\Delta S = \overline{A_f} \times \overline{\Delta h} \qquad \text{(Eq.3.21)}$$

where: ΔS = Change of storage (km^3 per month) for the considered time;

$\overline{A_f}$ = Average flooded area (km^2) between the actual month and the past one;

$\overline{\Delta h}$ = average variation of surface water level (in km) between the actual month and the past one.

3.3.2.6. Analyzing the water balance

The closing of the water balance over the NID (NIDWat) at monthly time steps was carried out in two steps. First, we assessed the water budget terms over the NID described above independently of the terms of the water balance equation (Equation 3.12) using input datasets derived from the observed and satellite data time series. Then, simulated water losses were compared to discharge differences obtained from the inflow-outflow for annual time steps.

3.3.3. Potential climate change impact assessment approach

Numerous methodologies for assessing the potential impacts of climate change on water have been developed and reported. Nearly all these have used climate model data and water resources models. The complex climate models for projections of the global climate for the next century generate large amounts of data but it is often very difficult to identify reliable data within them (Lopez, 2011). Many methods have been generally used in assessing change impacts on water. It starts with discussion about climate models, followed by description of downscaling techniques that bring climate model data to the local scale, then the use of water resource models.

The classical methodology consists of using climatic output data from general Circulation models (GCMs) to retrieve climate scenarios. The weather generator was then used

to produce daily temperature and precipitation data to serve as an input data for the hydrological model to simulate stream flow. However, this study used a distributed hydrological model in assessing the impact of possible climate change scenarios on water resources in the basin. Therefore, we separated the climate change impact assessment into two parts. The first was a sensitivity analysis of the river discharge due to hypothetical changes in the annual mean precipitation and temperature. The second analysis was based on climate change scenarios from the CORDEX data. The future simulated results were compared with the base line period as a means of obtaining the change caused by climate change. The procedure is obviously detailed below.

3.3.3.1. COordinated Regional climate Downscaling EXperiment

Many downscaled regional climate projections have confirmed or refined the IPCC assessment over diverse regions of Africa. Statistical downscaling uses statistical relationships between the regional or local climate and selected large-scale parameters (Schmidli et al., 2007). These relationships are empirical and are applied using the predictor fields from GCM in order to construct scenarios (Schmidli et al., 2007). Examples of statistical downscaling methods are weather generators (Wilby et al., 2004). The dynamical and statistical downscaling techniques are both based on certain assumptions that are very difficult to verify and are, therefore, associated with some uncertainty (Schmidli et al., 2007). GCMs that represent in detail the atmospheric dynamics and physical processes that take place, have shown great effectiveness in representing large-scale phenomena. However, GCMs are limited when taking into account the micro-scale and mesoscale features, hence the use of RMs to try to improve some aspects of GCMs (Steve, 2012). As part of international efforts to provide future climate data for impact studies, many data sets are becoming available. This fact leads in the used of the COordinated Regional climate Downscaling Experiment (CORDEX) output data for this study.

CORDEX is an initiative of the World Climate Research Project (WCRP) of the United Nations. It aims to improve coordination of international efforts in regional climate downscaling, both by dynamical and statistical methods. The recent Coordinated Regional Climate Downscaling Experiment (CORDEX) initiative from the World Climate Research Program promotes running multiple RCM simulations at 50 km resolution for multiple regions (Kim

et al., 2013). New multi-year simulation experiments focused on Africa, using common lateral Boundary Condition (LBC) for driving each model were performed.

The climate change scenarios used for this study were based on the outputs of CORDEX. The outputs of 16 regional models from AR5 climate change scenarios, designated representative concentration pathways RCP8.5 for two intervals, 1951-2005 (historical), and 2006-2100 (future) was considered. The near future was defined as the period (2035-2065), while the far future is taken as the period 2065-2100.

3.3.3.2. Hydrological Water Balance Model plus (WBMplus)

Various hydrological models exist and there is no strict guideline on the selection of the model. An exhaustive literature review on models used on large catchment area that incorporated land- use changes, runoff and soil characteristics of watersheds and basins was done. Hydrological models are naturally inadequate in many ways because they abstract and simplify existent hydrological patterns and processes (Brown and Heuvelink, 2005). Previous application of the process-based distributed model WBMplus for various environments and the proven capabilities were essential for the selection of this model for this study. One major successful use of the model was by (Wisser et al., 2010) in a global-scale analysis of the significance of local water resources captured in small reservoirs for crop production. Additionally, Cohen et al., (2013), Wada, et al., (2011), Wei et al., (2013) and Hoogeveen et al., (2015) have used WBMplus during their research. But in this context, it is worth using a low cost or free model which West African National Hydrological services could afford due to economic constraints. Another advantage of WBMplus model is that it allows a number of different physical processes to be simulated in a watershed; it was developed specifically for watershed-scale analyses and incorporates urban land features that are less important at larger spatial scales.

WBMplus is a fully coupled water balance and transport model that simulates the vertical water exchange between the land surface and the atmosphere and the horizontal water transport along a prescribed river network. It is a spatially explicit model describing varying components of global hydrological cycle. WBMplus extends WBM by explicitly accounting for the effects of irrigation and reservoirs on the hydrological cycle (Wisser et al., 2010).

WBMplus represents a major upgrade to previous WBM implementations by incorporating irrigational water uptake and reservoir operations in a single modeling framework. The extended version of WBMplus model combines the previous functionality of water withdrawals and reservoir routing with hydrological processes that are related to wetland storage, lawns and impervious surfaces (Pellerin et al., 2007) . It also well simulates total runoff from each grid cell which is the sum of storm, surface, and groundwater release in a watershed; and should be suited for application in the present study.

3.3.3.3. Sensitivity, Calibration and Validation

The sensitivity analysis in this study was undertaken. The analysis involved the entire parameters. Model simulations were evaluated by using regression coefficient (R^2). A combination of both manual and automatic calibration method was used for the model simulation. First manual calibration has been used mainly for annual water balance and it was followed by automatic calibration. The calibration was done using part of historical records. The WBMplus hydrological model on the Niger River Basin (NRB) was developed for the period 1944-2013. The remaining dataset was used for the model validation.

3.3.3.4. Model Simulation

WBMplus was applied to simulate the impacts of climate change on river flow by considering multi model approach, using regional climate data model output (RCP 8.5) from CORDEX. The procedure is as follows (Fig. 5.1). For instance, potential evaporation calculation alone as evaporative water losses, was performed using the Penman Monteith function.

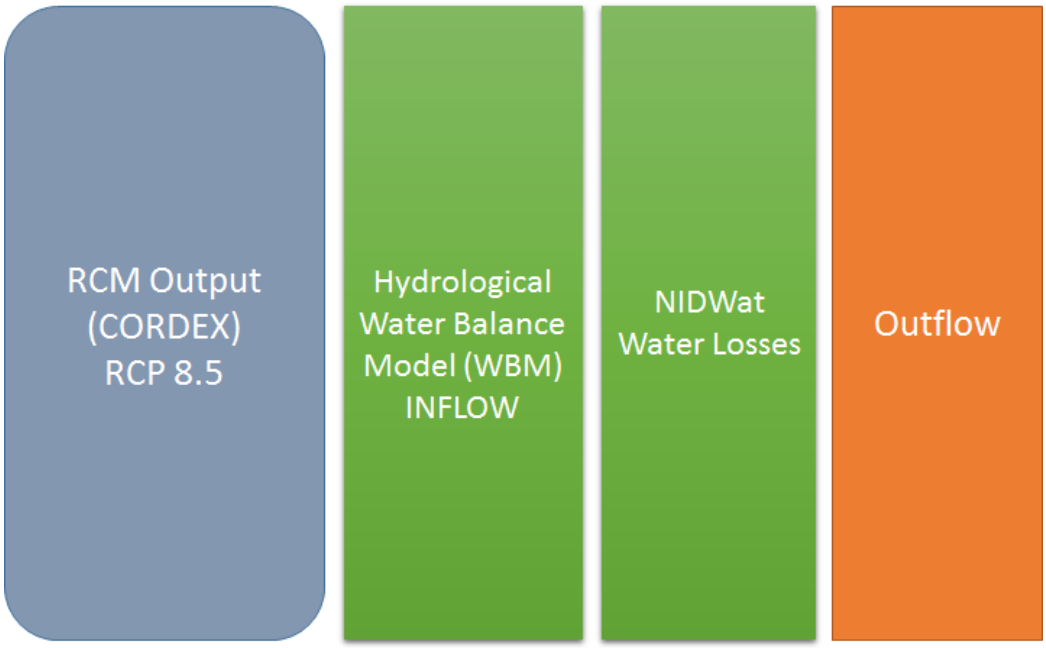

Figure3. 5: *Schematics of the water balance model using the existing CORDEX output and WBMplus functions; and NIDWat for assessing the Evaporative water losses*

3.4. Partial Conclusion

Many studies were conducted in this area due to the data availability over a long period at fine scale. The daily rainfall data and hydrological data are of good quality despite of the presence of some gaps. The remaining described atmospheric data were easily accessible from international research centers websites and they do not have missing data that could alter the forecasting process. It is particularly found that hydrological data are the data having more missing data compared to other climate and atmospheric data. All these data combined to the good choice of the area would make easier the different model development.

In this study, the potential temporal and spatial trends of hydro-climatic data are considered for the upper and middle basins of the Niger river. Using the available meteorological data and the statistical methods, the major components of the water resource namely, temperature, evapotranspiration and the precipitation are analyzed. To assess the overall quality of the climate information it is necessary to analyze trends in the hydro-climatic data. So, statistical approach is proposed to investigate consistency in the recent trends on climate with observations of hydro-climatic variables. Furthermore, the main discharge stations on the Niger basin are used to assess the runoff trend. This allows an assessment of the overall quality of

the climate information from the available data in the Niger River Basin. This study demonstrates how remote sensing data can be used to help conducting hydrological process analysis at high temporal and spatial resolution across large wetlands. Understanding surface flooded area processes for the Niger Inland Delta are crucial for water balance purposes. We use optical and microwave remote sensing data to characterize the temporal flooding, and observations of river flow and spatially explicit information on water abstractions to develop NID-Wat, a water balance model for the NID. The model was validated against observed river discharge and water abstractions and shows a good performance. We then implemented the model as a module in a hydrological model to assess the water balance in the NID and the downstream water availability under changing conditions. We use a multi model approach using regional climate data from the CORDEX initiative. Results suggest, despite increasing runoff an increase in ET losses and changes in the temporal dynamics of flooding that impact water resources availability downstream.

Chapter 4. Trend Analysis of Hydro-climatic Data and Spatial Interpolation

This chapter presents the results on hydroclimatic trends over the study area. The recent trend in climate and hydrology is investigated. It appears that the water resource availability is affected due to the occurrence of frequent and uneven extreme events such as drought. Different statistical method's results for trend analysis used in this study, such as the moving-average method, linear regression method and Mann-Kendall method for seasonal forecasting are presented. Hydro-climatic trend of data (Temperature, precipitation, evapotranspiration and discharge) with its different is discussed here. All the trends are shown in comparing statistically its significance with IPCC standard period (1981-2010).

4.1. Climatic and hydrologic data trend

4.1.1. Temperature

The meteorological station data shows a general increasing trend of the temperature in the Niger basin. The increase is not significant for the period of the IPCC standard period (1981-2010). On the other hand, the trend seen over the NID and at upstream NID for the study period of 1980 to 2010, the rise is slightly less and not statistically significant as compared to IPCC standard period (Fig. 4.1a & 4.1b). The average temperature for IPCC standard period for the upper and inside the NID is respectively 27.9°C & 29.4°C. However, the 10 years moving average over the NID shows that the temperature decreased by 0.2°C by the year 1990 and increased by 0.3°C up to 2005. While, the 10 years moving average at NID's upstream shows that the temperature decreased by 0.1°C by the year 1994 and increased by 0.1°C at 2003 (Fig. 4.1c & 4.1d.). Then, the temperature showed an increasing trend by 0.5°C by the year 2010 with reference to the average temperature at IPCC standard period (Fig. 4.1c).

(a)

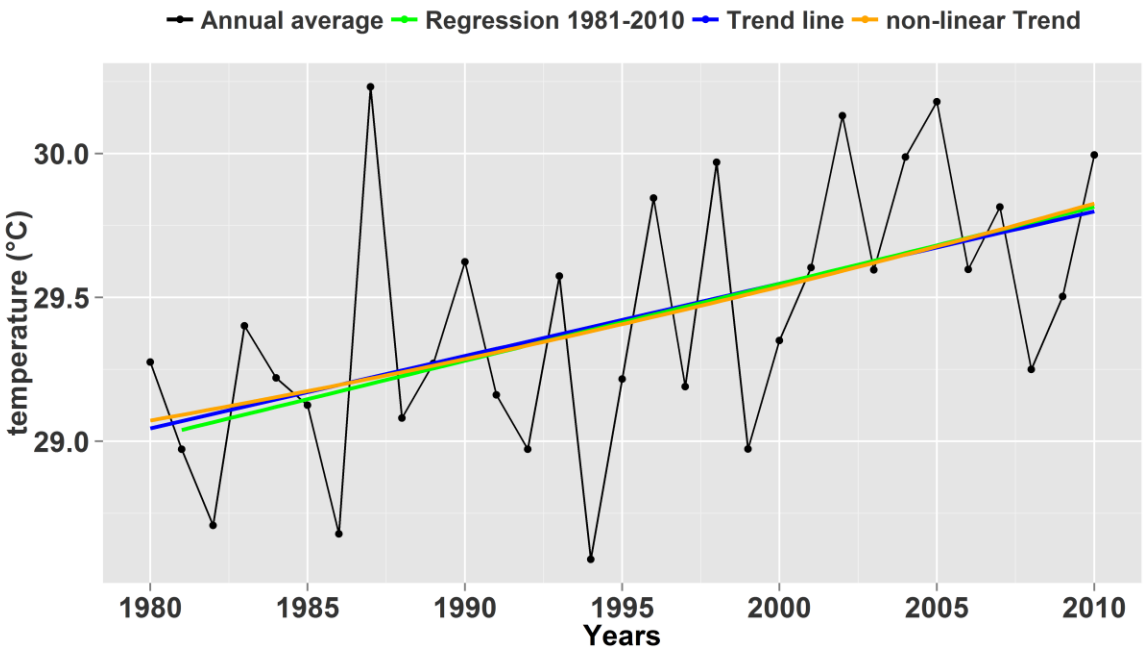
Annual average
Regression 1981-2010
Trend line
non-linear Trend
temperature (°C)
30.0
29.5
29.0
1980
1985
1990
1995
2000
2005
2010
Years

(c)

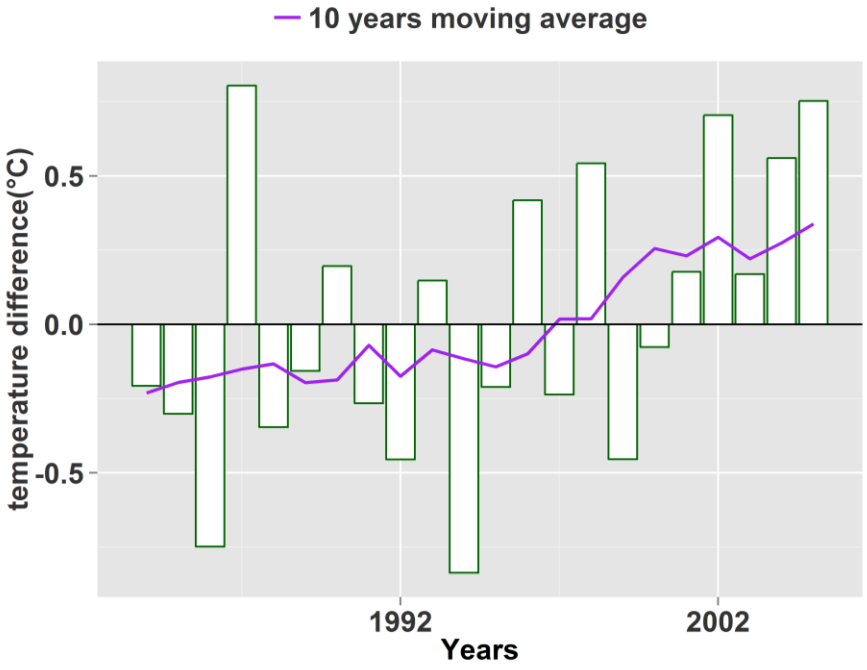
10 years moving average
temperature difference(°C)
0.5
0.0
-0.5
1992
2002
Years

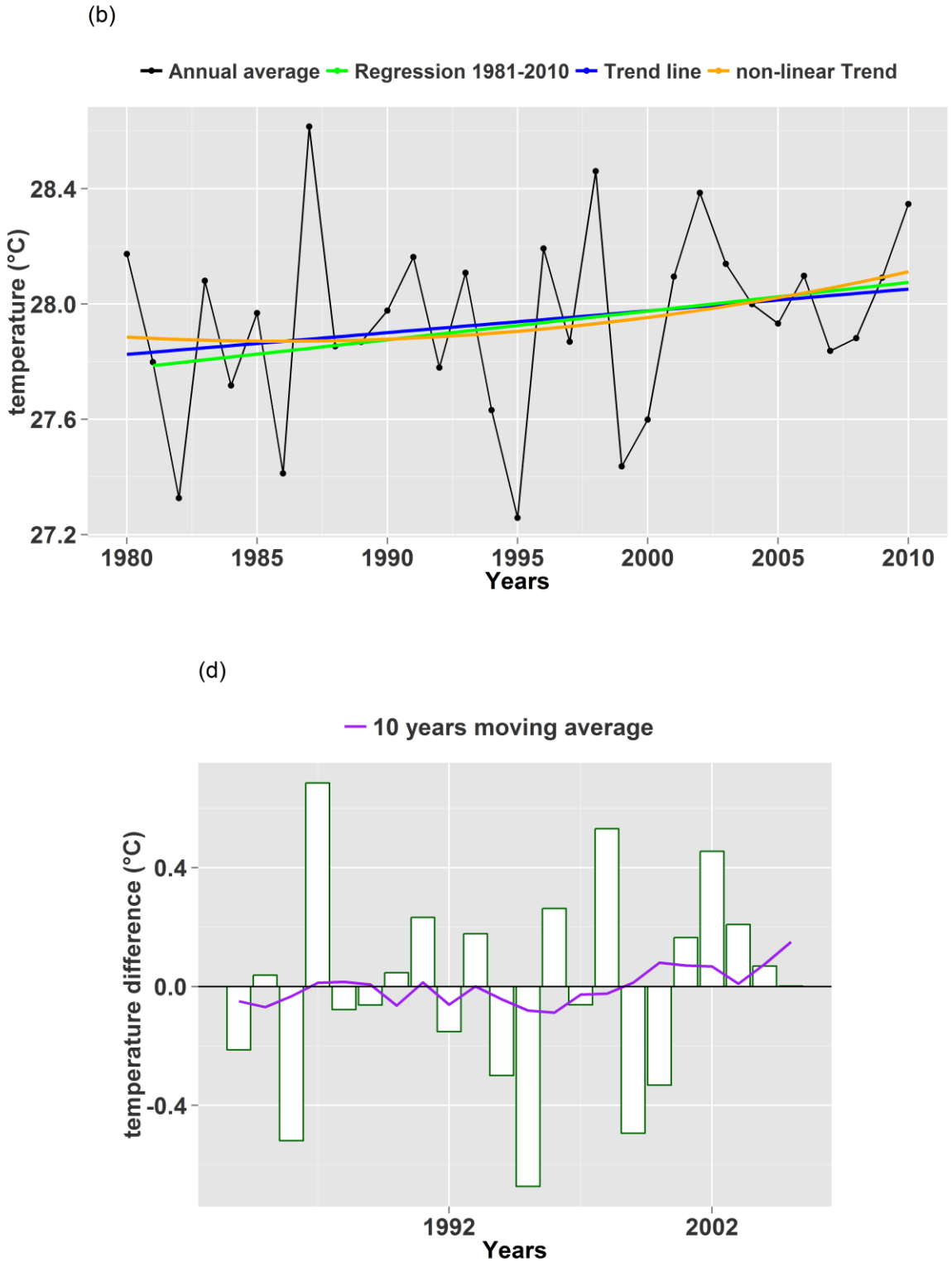

Figure4. 1: *The average temperature trend*

(a.) annual average temperature trend of the meteorological stations (Ségou & Mopti) data over the NID, (b.) annual average temperature trend of the meteorological stations (Bougouni & Bamako Senou) data at upper the NID, (c.) Annual average temperature trend over

the NID minus the mean IPCC standard period average temperature for meteorological stations data, (d.) Annual average temperature trend upstream the NID minus the mean IPCC standard period average temperature for meteorological stations data

4.1.2. Precipitation

In case of precipitation, the trend is opposite to the temperature. For the period of 1950 2010, it is decreasing. In contrast, during the IPCC standard period it is increasing and is statistically significant. The average precipitation over the NID, Mali-upstream NID, and Guinea-upstream NID, for the IPCC standard period according to the meteorological stations records is 475, 1051, and 1481 mm/year respectively (Fig. 4.2a, Fig. 4.2b, & Fig. 4.2c). The 10 years moving average for the period of 1950-2010 show a decreasing trend of precipitation in the NID wetland. The precipitation was lowest from 1981 to 1985. The precipitation decreased by 125mm compared to the average precipitation at IPCC standard period. If the 10 years moving average is considered there is a slight increase not significant in the precipitation over the NID in the year 1990 to 2010 whereas, there is a decreasing trend in the periods 1950-1970 (Fig. 4.2d).

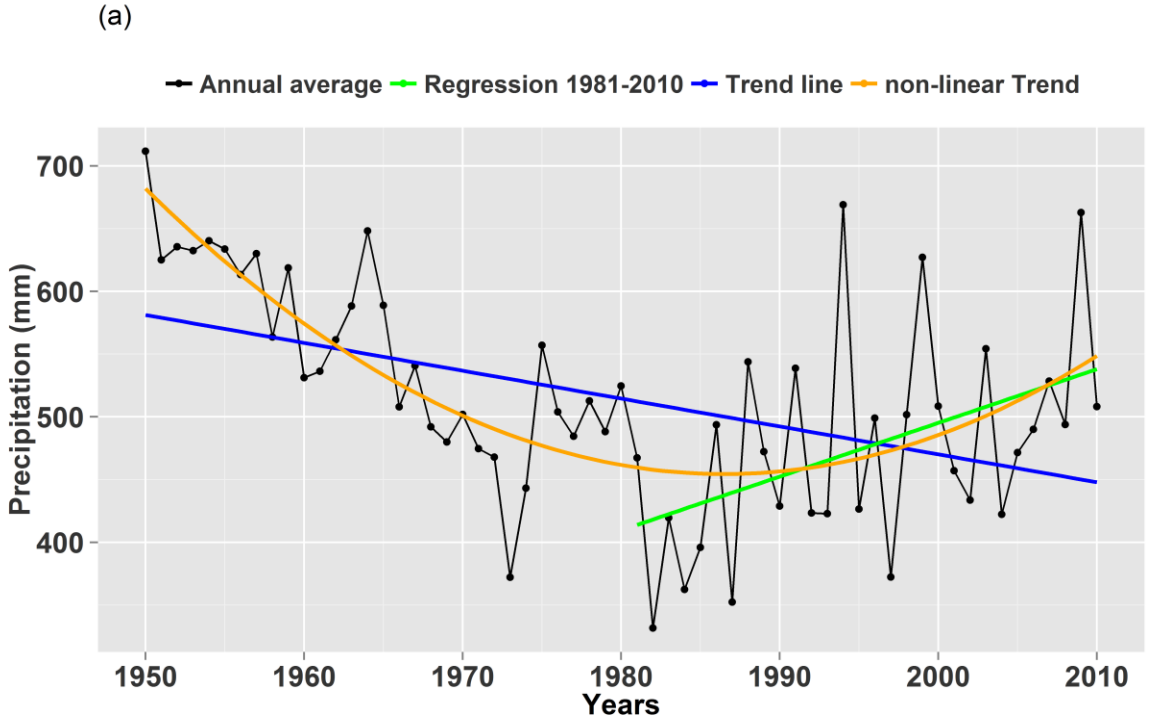

(d)

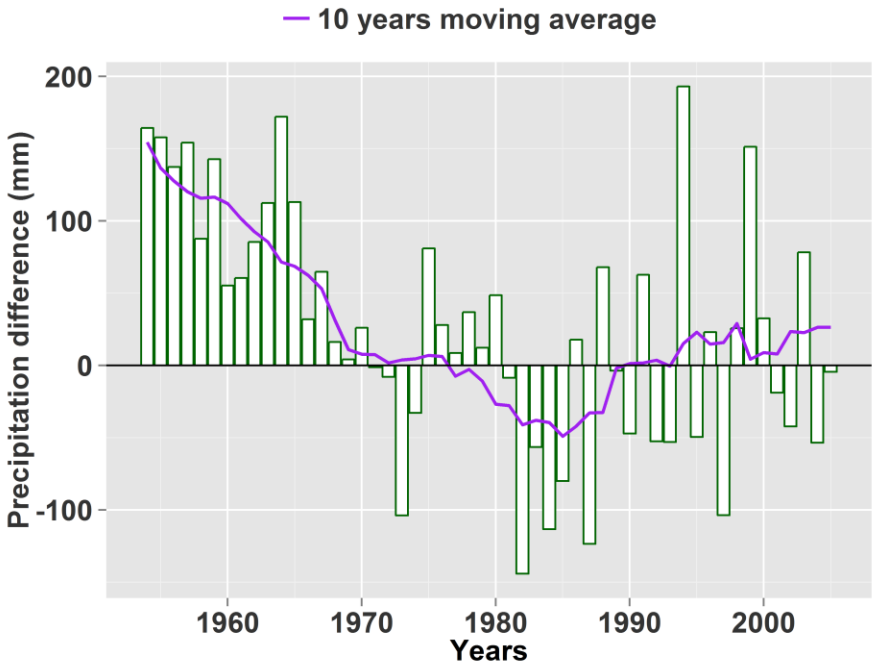
10 years moving average
200
100
0
-100
Precipitation difference (mm)
1960
1970
1980
1990
2000
Years

(b)

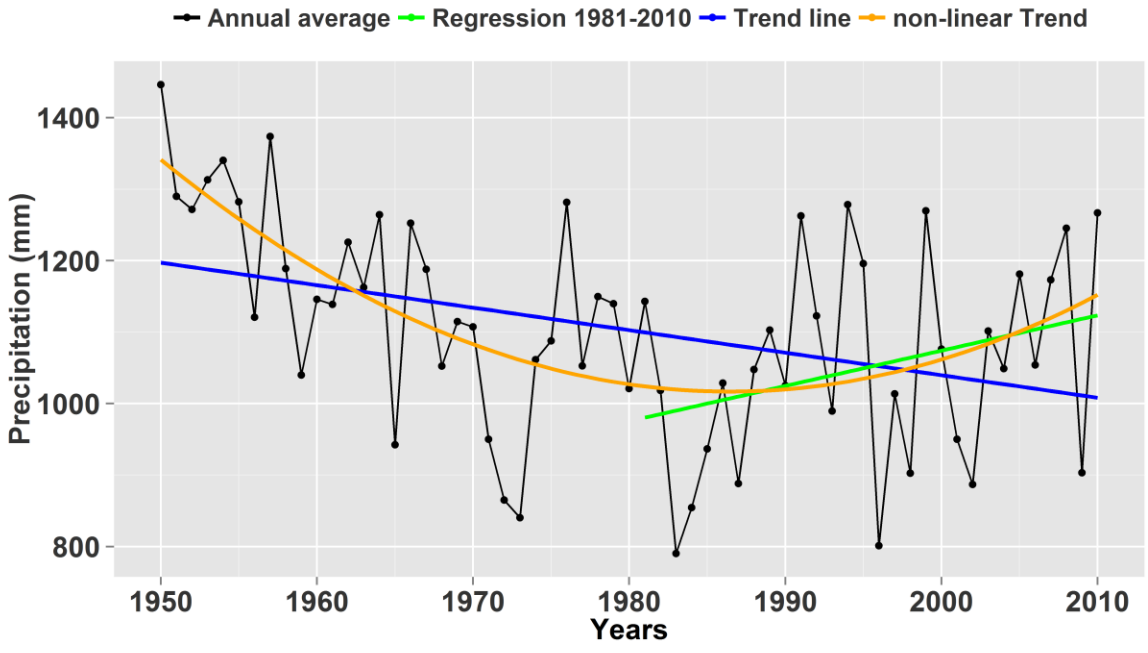
Annual average
Regression 1981-2010
Trend line
non-linear Trend
1400
1200
1000
800
Precipitation (mm)
1950
1960
1970
1980
1990
2000
2010
Years

(e)

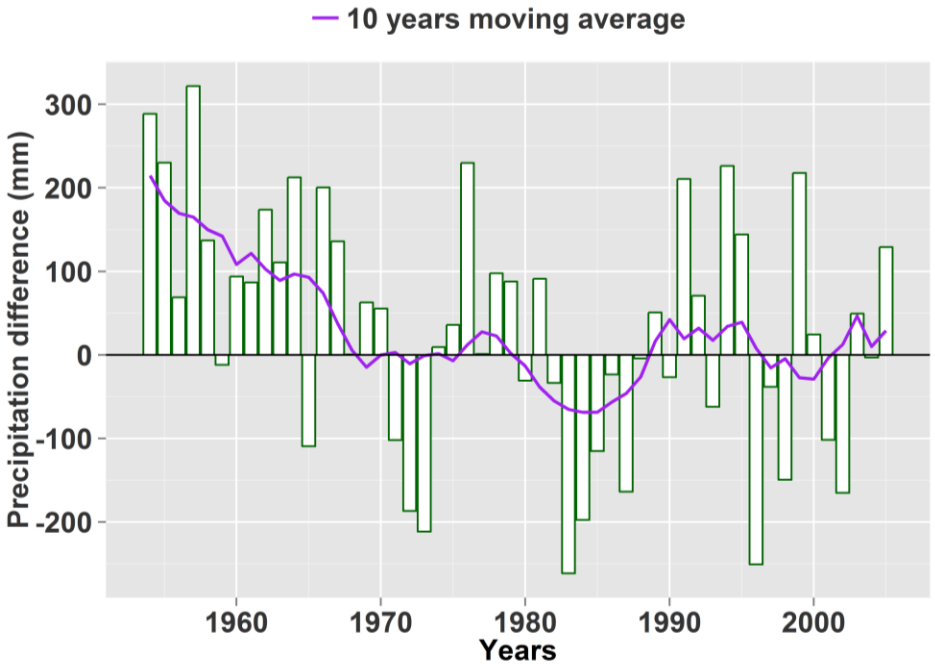
10 years moving average
Precipitation difference (mm)
300
200
100
0
-100
-200
1960
1970
1980
1990
2000
Years

(c)

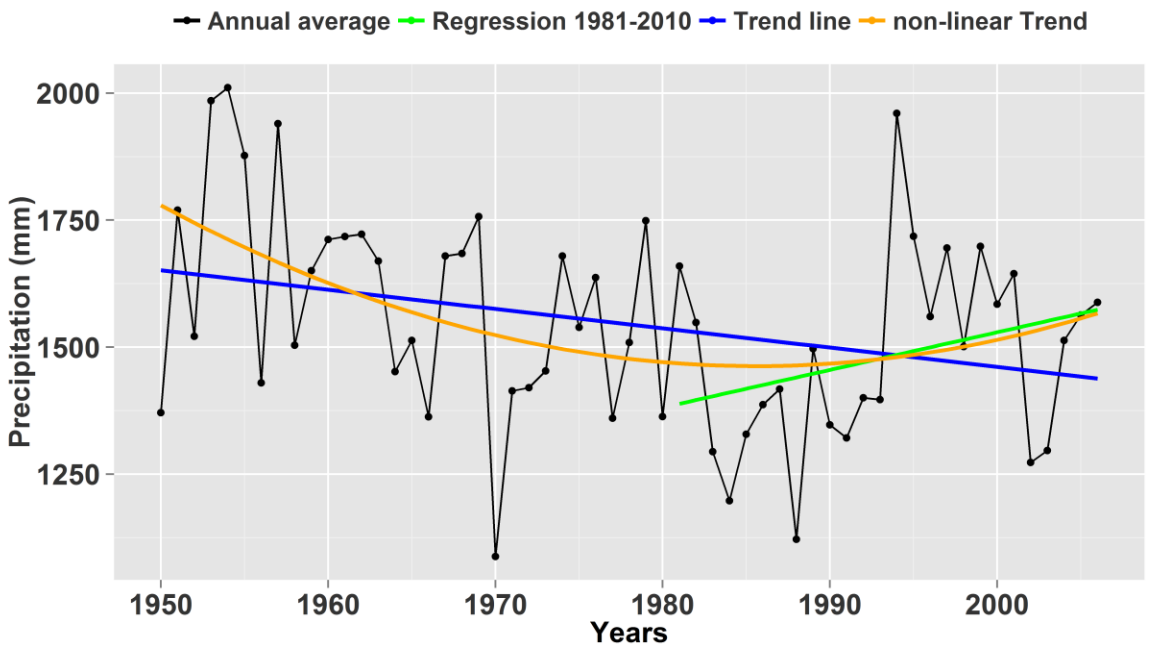
Annual average
Regression 1981-2010
Trend line
non-linear Trend
Precipitation (mm)
2000
1750
1500
1250
1950
1960
1970
1980
1990
2000
Years

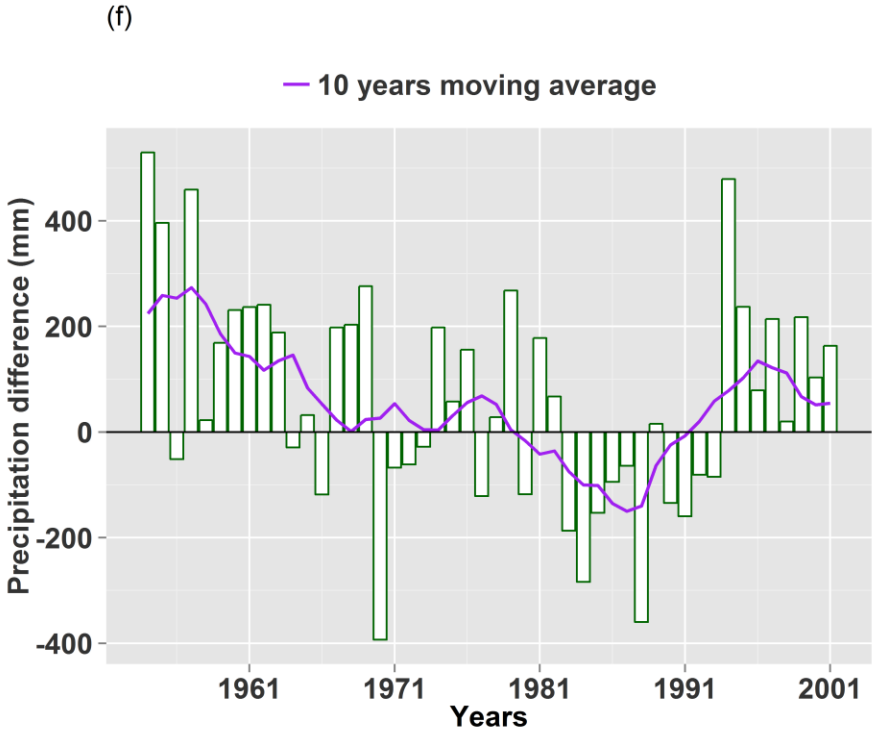

Figure4. 2: *The average preciptation trend*
(a.) annual average precipitation trend of the meteorological stations (Ségou, San, Mopti & TombuKtu) data over the NID, (b.) annual average precipitation trend of the meteorological stations (Sikasso, Bougouni & Bamako Senou) data at upper the NID in Mali, (c.) annual average precipitation trend of the meteorological stations (Kankan & Faranah) data at upper the Niger Basin in Guinea, (d.) Annual average precipitation trend over the NID minus the mean IPCC standard period average precipitation for meteorological stations data, (e.) Annual average precipitation trend at Mali upstream the NID minus the mean IPCC standard period average precipitation for meteorological stations data, (f.) Annual average precipitation trend at Guinea upstream the NID minus the mean IPCC standard period average precipitation for meteorological stations data.

4.1.3. Evaporation trend

The Mopti pan evaporation data show a slightly increasing trend in the NID. The evapotranspiration is increasing at the rate of 5 mm per year and the trend is not statistically significant. However, the decrease is at higher rate and not statistically significant at the IPCC standard period (Fig. 4.3a). The average Mopti pan evaporation is 2499.2 mm/year considering the study period 1970-2009; and the average pan evaporation is 2482.80 mm/year if IPCC standard period is only considered. Similarly, the 10 years moving average of Mopti Pan evaporation has slightly increasing trend for 10 mm per year considering the period of 1981-2000 (Fig. 4.3b).

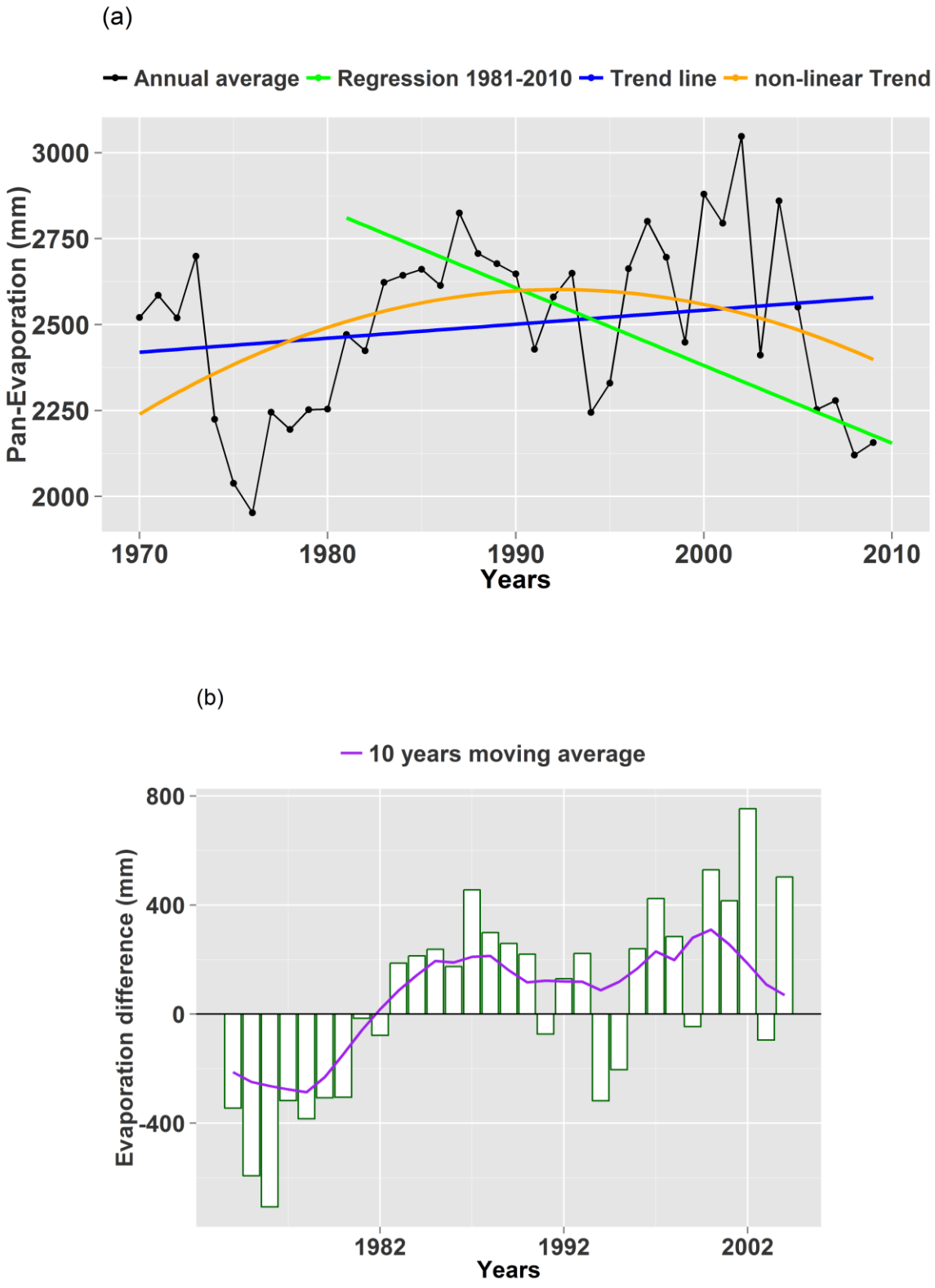

Figure4. 3: *The average evaporation trend*
(a.) annual average evaporation trend of the Mopti pan recorded data over the NID, (b.)

Annual average evaporation trend over the NID minus the mean IPCC standard period average evaporation for Mopti Pan Evaporation data records.

4.1.4. Streamflow trend

These results were plotted in Fig. 4.4. It observes that: (1) For the upper basin a wet period (1920-1930; 1945-1970) and a dry (1971-2010) period are clearly seen which have a mean annual discharge of 700 m^3/s (450 m^3/s) higher (lower) and for the NID a mean annual discharge of 450 m^3/s higher (350 m^3/s) higher (lower) than the long-term mean, respectively. This variation in the discharge shows the idea of how dry or wet the part of Niger Basin are in the upstream of NID and the wetland. The discharge runoff is higher in the upper basin at the Niger basin part of Mali (for e.g. Koulikoro); whereas, the streamflow values are lower in the NID cathment at the outlet of the delta. The changepoints (breaks red dotted lines) plot for runoff timeseries (Fig. 4.4 (a.) & (c.) shows that there are 3 distinct changes of the specific runoff with regards test statistic for the analysis of the data. The linear fit (Fig. 4.4 (a.) & (c)) shows that the flow discharge decreases with the increase in area but it is not statistically significant. Furthermore, the streamflow varies according to moving average plot rather than the trend line.

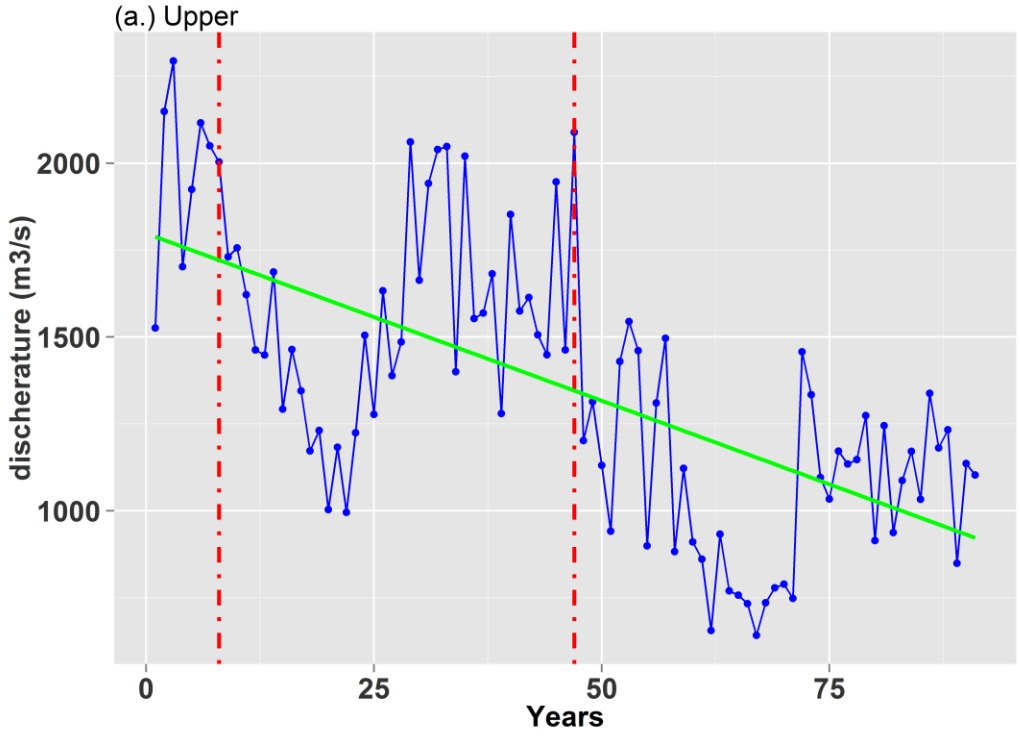

(b.) Upper

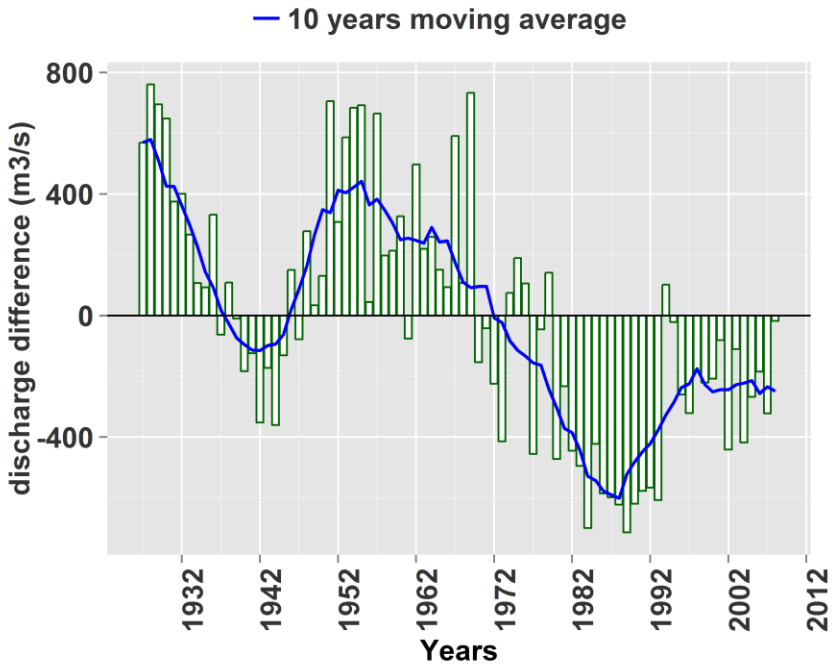
10 years moving average
800
400
0
-400
discharge difference (m3/s)
1932
1942
1952
1962
1972
1982
1992
2002
2012
Years

(c.) NID

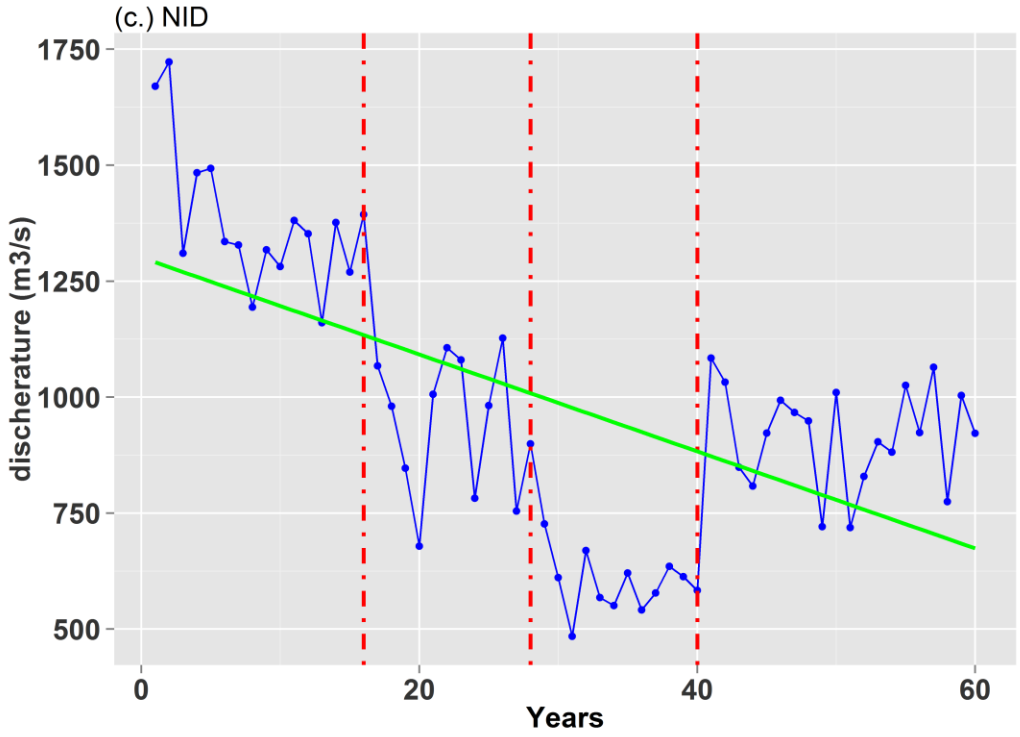
1750
1500
1250
1000
750
500
discherature (m3/s)
0
20
40
60
Years

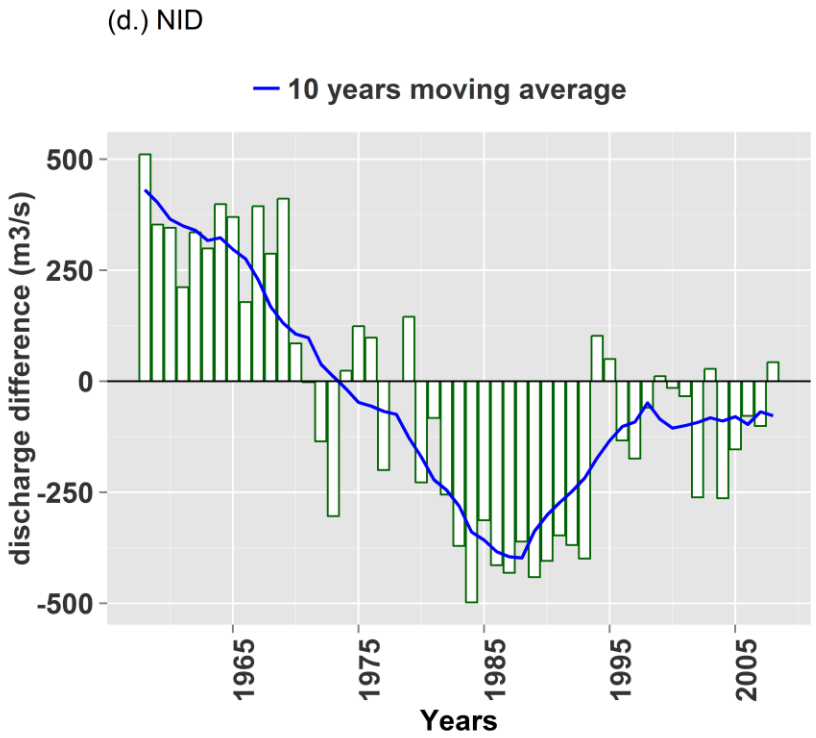

Figure4. 4: *The average discharge trend*
(a.) annual average streamflow of the upper gage stations of Mali with green line = trend line and red dotted lines= changepoints for the timeseries; (b.) Annual average discharge difference trend minus the long term mean period of discharge data over the upper stations of Mali; (c.) annual average streamflow of gage stations inside the NID of Mali with green line = trend line and red dotted lines= changepoints for the timeseries; (d.) Annual average discharge difference trend minus the long term mean period of discharge data over the NID stations of Mali.

4.2. Spatial analysis

The GCPC data which is the average calculated from 1996 - 2013 shows that the precipitation varies from 200 to 1400mm/year in the study region (Fig. 4.5 a). The statistical analysis for the region shows that the mean precipitation is 773mm. The precipitation value is alike to the satellite climate data (Fig. 4.5b & 4.5.c).

(a)

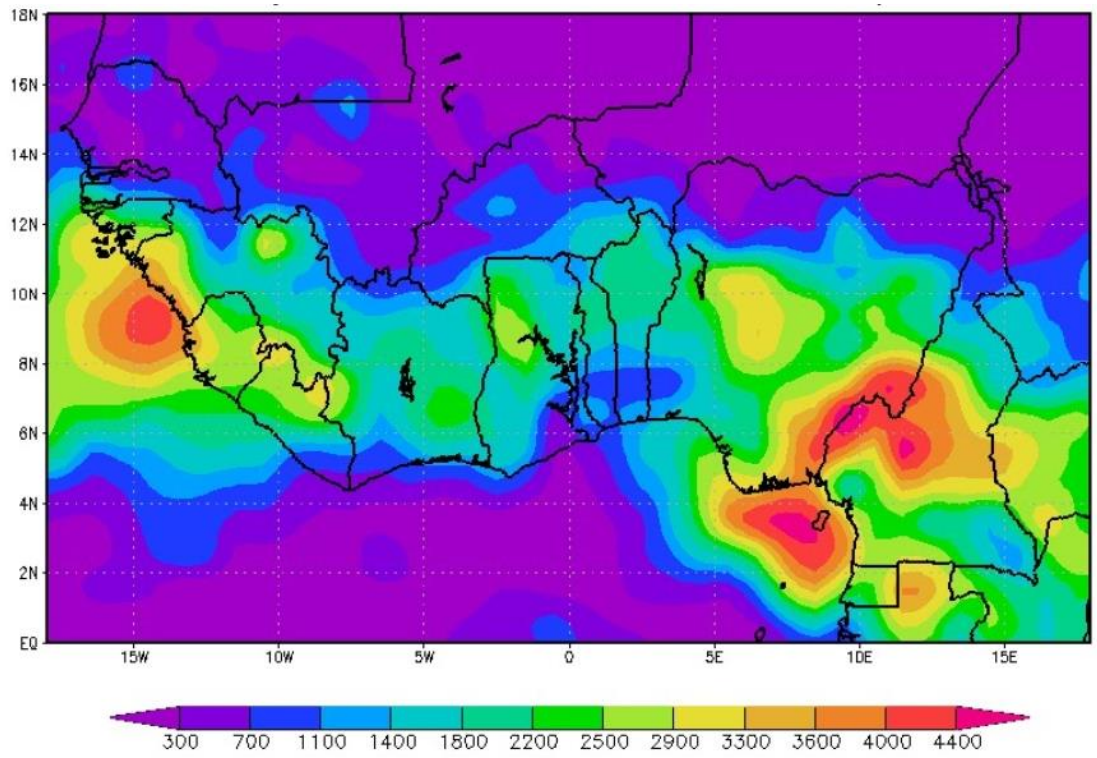

(b.)

Annual average Precip.for the study area (mm)

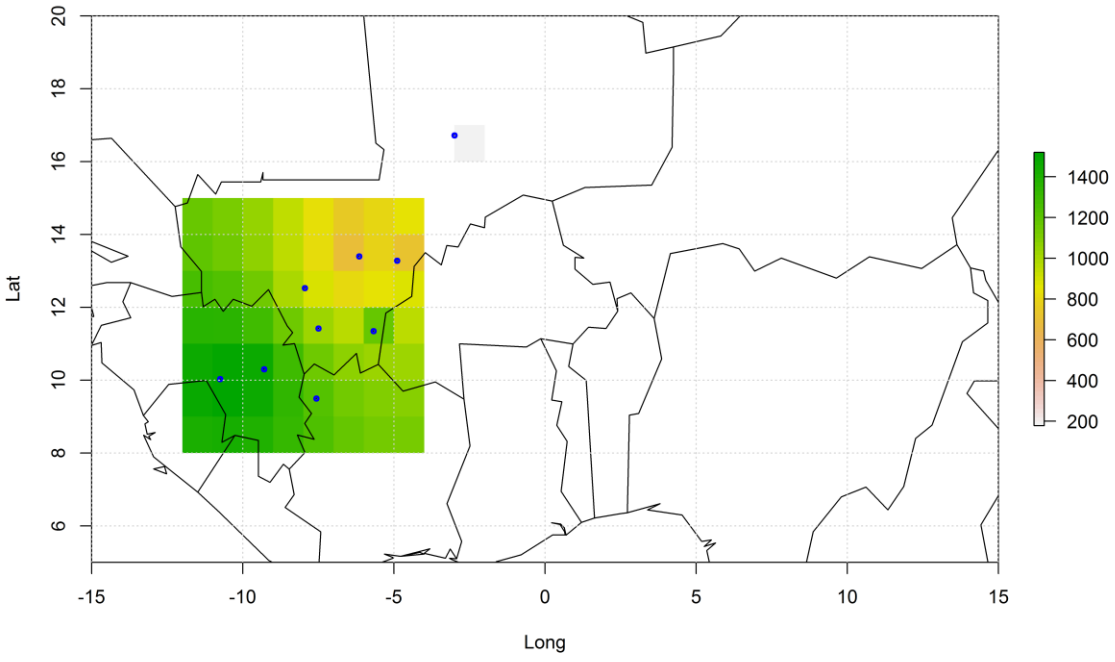

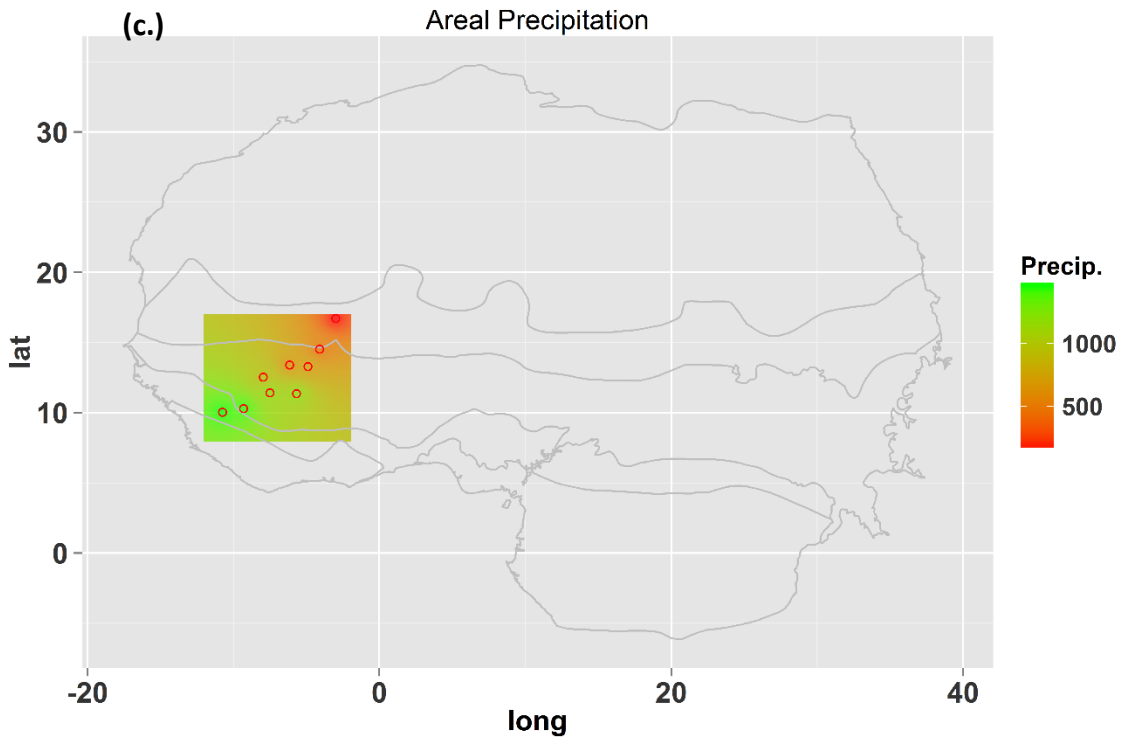

Figure4. 5: *The spatial distribution of precipitation*
(a.) Long term annual average precipitation for GCPC dataset of study area stations of; (b.) the OK spatial variation of the of the recorded data of gage stations within the basin; (c.) the IDW spatial variation of the precipitation of the recorded data of gage stations within the basin.

In this study, we use the two interpolated techniques, explicitly, OK and IDW to spatial analysis of annual precipitation trends in the basin. This is in view applying various spatial interpolation methods in the GIS model in order to show the existence of spatial patterns in the trends. In this section, the interpolated trend results are shown in Figure 4.6 using both methods at significance levels between minimum and maximum range of Mann-Kendall statistics.

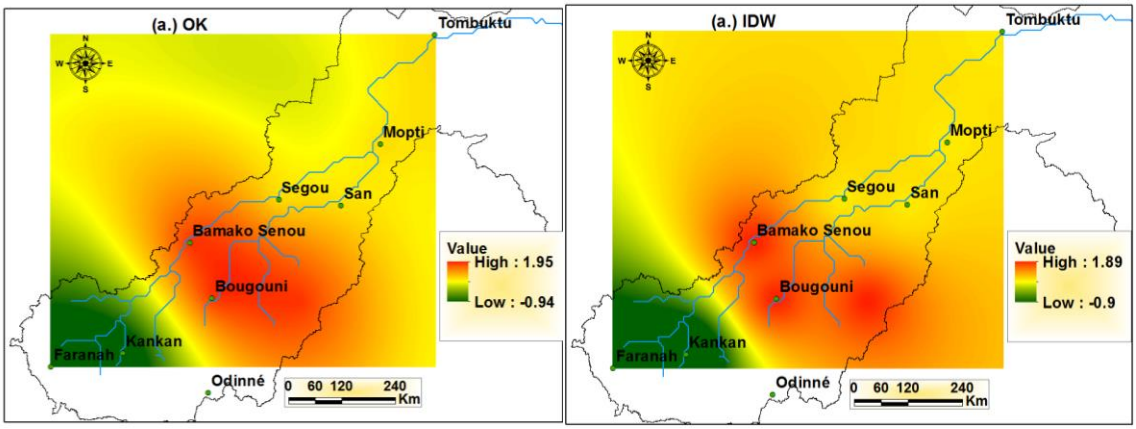

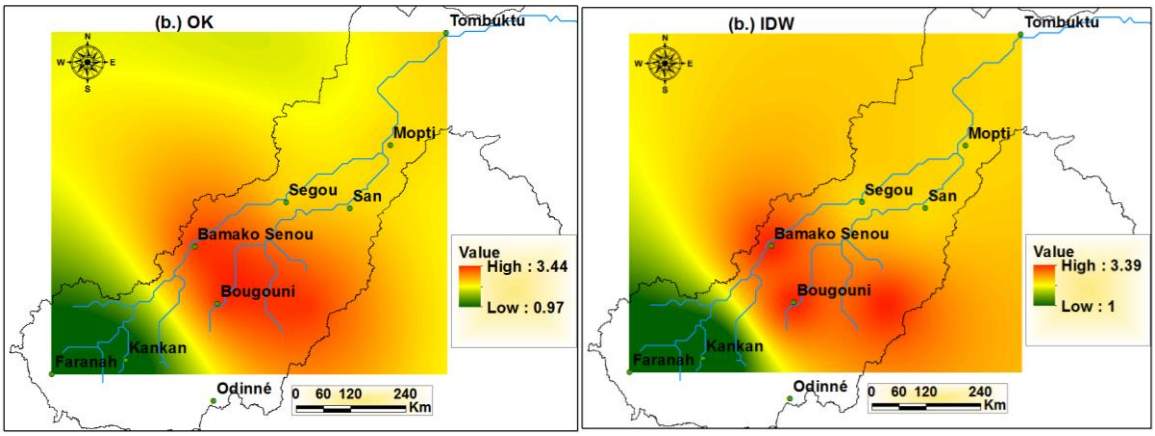

Figure4. 6: *Spatial distribution of the statistics Z of the Mann–Kendall test for the annual rainfall (a) Period 1950-2010 (b) Period 1981 - 2010*

4.3. Discussion

4.3.1. Hydro-climatic data trend analysis

To study the variation of historical annual and seasonal precipitation, temperature, evaporation, and discharge, the mean annual and seasonal values for the entire study period (1950 – 2010, and 1980 -2010) and for each the IPCC period (1981 - 2010) are assessed and compared. During these periods, the climate variables in the region as regards the temperature and precipitation, show variation similar for the upper region and the NID wetland zone. The general trend of the temperature is increasing and the precipitation shows decrease in line with the previous studies in West Africa (Paturel et al., 1997; Servat et al., 1997; Paturel et al., 2003; L'Hôte et al., 2002). The period (1981-2010) is slightly warmer than the long-term average. The results demonstrate that the seasonal variations of the 10 years moving values are much larger than those of mean annual differences, especially for temperature. The climatic trend in NID's floodplain is in line with this fact (Fig. 4.1 & 4.2). The temperature and precipitation are increasing in the IPCC standard analysis (from 1981-2010). The precipitation trend is not in line with these facts for the overall study period of 1950-2010; however, the trend is not statistically significant. Henceforward, in summary the long-term trend analysis demonstrate that the temperature and precipitation has increasing and decreasing trend respectively in the study area. Although it should also be noted that the current trend (after 1990s) of the precipitation is increasing but it is not statistically significant. Subsequently, the increasing trend might be linked randomly to that of the temperature for some decades.

According to many studies (L. Descroix et al., 2009; Druyan, 2011; Hubert P., Carbonnel, 1987; Le Barbé & Lebel, 1997; Li et al., 2005; Mahé et al., 2001; Sharon E. Nicholson, 2000; Sharon E. Nicholson & Palao, 1993; Sircoulon, 1987) there was a decline in rainfall from the 70 in the Sahel region. In similarity, to this study, the lowest rainfall occurred within that period (331 mm/year in 1982 for NID, 840 mm/year in 1984 for upper NID in Mali, and 1087 mm/year in 1970) and showed likely return period of some 15 to 20 years (Fig. 4.2.d, 4.2.e, and 4.2.f).

The effect of increasing temperature and decreasing precipitation can be seen over the evaporation trend of the NID. In general, an increasing trend of the evaporation is seen in the NID (Fig. 4.3a & 4.3b). However, the trend is decreasing and not statistically significant considering the period 1981-2009 (Fig. 4.3a). This result can be justified with the overall decreasing trend of precipitation. Nevertheless, the evaporation is increasing with temperature for the study period, the decrease in the precipitation decreases the discharge runoff. The observed streamflow based analyses shows decrease of river runoff in their long-term average for the study region. Therefore, the decreasing trend in the discharge runoff may be a major problem in the water resource management. Since

The above discussion shows that when entering the 1970s there is a very dry period in the Niger basin. More essentially, this decrease in streamflow will have a direct impact on the very sustainability of the ecosystem's services in the NID. Though, some authors (Ozer et al., 2003; Pedinotti et al., 2012; Descroix et al., 2015) suggested a return of a wetted period meanwhile the 1990s. If this situation does not change in this 21st century it will have positive impact for water availability in the Niger basin region.

The trend analysis illustrates that the long-term trend is not statistically significant as compared to IPCC standard period trend (Ibrahim, et al., 2016). This result suggests that hydro-climatic data trend is decreasing except temperature and evaporation trend. Yet, it might not be concluded that the climate has changed in the study region, because all variables are not statistically significant for the same study period. In addition, the trend analysis also shows the importance of considering the region in three features (upper Guinea, Upper Mali, and NID) of the catchment and two parts of the study period. The schematic representation of the hydro-climatic data shows that, with regards to the length of the study period, the trends look to be significant or else not significant. The decrease or increase seems to be regular for

a certain period whereas, it appears to be affected by some random variation of the extreme values within the study period when range of the analysis period is changed. This fact is in accordance with Druyan, (2011) who stated that, no clear trend for either decreasing or increasing precipitation from global climate model (GCM) products. With such context, while, it could not be assumed that the climate has not changed in the Niger Basin whereas looking at the trends of the climatic data, it must be noted that there will be decrease in the water resource availability in the future if the trends in the hydro-climatic data remains. This is highlighted in (Ibrahim, et al., 2016).With this regards, the water resource management should be done considering the plausible decrease of the water resource availability in the Niger basin.

4.3.2. Spatial interpolation of precipitation

We used two spatial interpolations techniques not as to compare their performance technique, but a cross-validation, as a way in evaluating he performance of the interpolation, the accuracy of the interpolation process. It should be noted that for assessing the interpolation accuracy for the entire study area, the cross-validation method considers the uniformly. Both the OK and IDW methods show different variation of change in annual rainfall regarding the spatial analysis. Decreasing change in mean annual rainfall is not significant for the period 1950 - 2010. For the IPCC standard (recent years 1981-2010), the increasing change in mean annual rainfall is seen to be positively significant. This fact is in line with the study by Oyebande and Odunuga, (2010) that for the past 4 decades, 10 to 30% drop in mean annual rainfall was observed in the region. This decrease can be related to changes in the sea surface temperature afterward 1960s (Lebel and Ali, 2009). For the period 1981-2010, the maximum positive significant change is observed in the regions showing lower yearly rainfall (Fig. 4.6(b.)). Therefore, the precipitation excess for the period 1981-2010 is increased compared to overall trend values in the basin. The potential evapotranspiration is high in the Niger Inland Delta area; this variation can be justified by the variation of the temperature and precipitation. In this context, a special focus is required to the NID zones because they are the zones with high water use. This has pointed out that evapotranspiration is most important factor compared to the precipitation.

The dominant trend in precipitation is clearly positive in southern and northern NID, while there is an apparent negative trend in western part of NID. The interpolated maps exhibit that

negative trends are few and located in the west region of NID's wetland and upper region of the basin in Guinea (Fig. 4.6(a.)).

4.4. Partial Conclusion

Hydroclimatic data trend analysis is found to be with high importance for the study region. The assessment of the water resource availability from past and the probable future condition is a paramount tool for management of the water resource. For the evaluation of the water resource condition, the hydroclimatic data trend can be a reliable skill. This fact made the statistical approach of the hydroclimatic data trend to be widely used to show whether the climate change has happened in the area or if the tendency seen is just climate variation. In this research, the hydroclimatic data trend does not exhibited a consistent trend when considered overall period of the data for the study. The trend and its statistical significance differ according to the range of the study period considered. Regarding this trend analysis, it cannot be concluded that, the climate change has occurred in the upstream and NID's wetland areas. However, considering the period 1981-2010, it would be noted that all the climatic data show an increasing trend in the NID except the evaporation whose trend is not significantly decreasing over the area. The temporal trends of stream flow discharge are the result of the combined effect of precipitation and temperature. Significant decreasing trends are found for mean annual discharge at a 0.05 significance level.

The spatial variation of the hydroclimatic data shows that the precipitation is higher at the inland part of the study region. Historical data show no trend for precipitation in considering the study period while, the trend for the 1981-2010 has positive significant trend especially for the NID areas of the Niger basin at the 0.05 significance level. Hence, results in this study from the trend analysis can provide a general idea about the water resource availability in the basin.

The key findings of the study can be summarized in following points:

- The general trend of the hydroclimatic data analysis shows a decreasing trend in the basin except for the evaporation; however, all trends are not statistically significant when considering the full study period. Hence, it cannot be concluded that climate has changed in the basin.

- The long-term trend shows decreasing water resource availability in the NID.
- Spatially, the increase in precipitation is higher in the western part of the NID compared to eastern and inland part of the wetland.

The results presented here shows a general idea about the water resource conditions in time and space, this should be taken a basic skill for water resource management instead of models in order to reduce uncertainties.

Chapter 5. Assessment of water losses in the NID and their impacts on water availability in the Niger river basin

The assessment of flood area extent is the most important step in water balance analysis particularly in the NID, where water losses is dependent on the flood propagation which in turn is influenced by some aspects. The resulting products from the methodology developed to estimate the flooded area extent and are presented in this chapter. The results are in good agreements between the estimated flooded area data and the remotely observed surface flooded area from past studies. Furthermore, in this chapter, the water balance model's result developed for Niger Inland Delta is presented with a particular focus on water losses estimates. Result of ET model's evaluation on selecting the best represented method is presented here. Additionally, results of actions from irrigation schemes on a large scale (e.g., ON & ORM) whom have implications for water balance in the system are presented in this chapter. The water balance analysis is well explained and the conditions used to estimate the identified hydrological terms are clearly discussed. Finally, the chapter is closed with validation of the model with other estimates, remote sensing area estimates, and water balance.

5.1. Land cover classification over the NID

The land cover classification results have allowed the monitoring of land cover changes for different classes, from surface water to agricultural & vegetation on dry land. However, the already finalized maps for every October from 2000 till 2009 are used principally as indicators to monitor floods over the NID (Fig. 5.1).

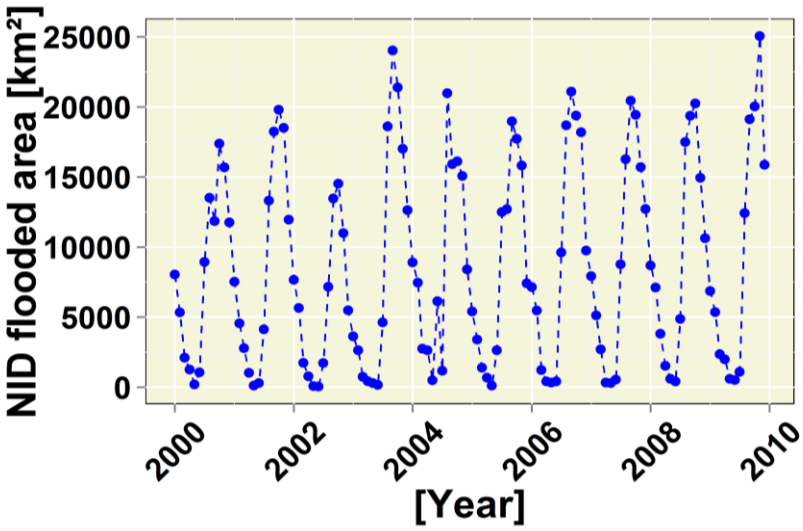

Figure5. 1: *Monthly Flooded surface area estimates with RS SeaWinds data in the NID over the period 2000-2009.*

5.1.1. Inter-Annual Variability of Floods over the NID

The finalized classification of the wetland area using remote sensing data (SeaWinds data from QuikSCAT) from 2000 to 2009 provides estimates of the variation in flooded area in the NID (Fig. 5.2). Over the ten hydrological years studied, the peak flooded surface area varies between a maximum of 25054 km² in autumn 2009, and a minimum of 7162 km² in autumn 2002. The 2000 to 2009 mean of the maximum flooded surface area was 14977 km² with a standard deviation of 7227 km², which highlight the significant inter-annual variability in the extent of flooding.

During the dry season, the flooded surface area receded progressively to a minimum of 317 km² (2000 to 2009 inter-annual mean) then following April, then increased in June and rose rapidly in August. Minimum values, measured between March and April, vary between 300 km² and 4000 km².

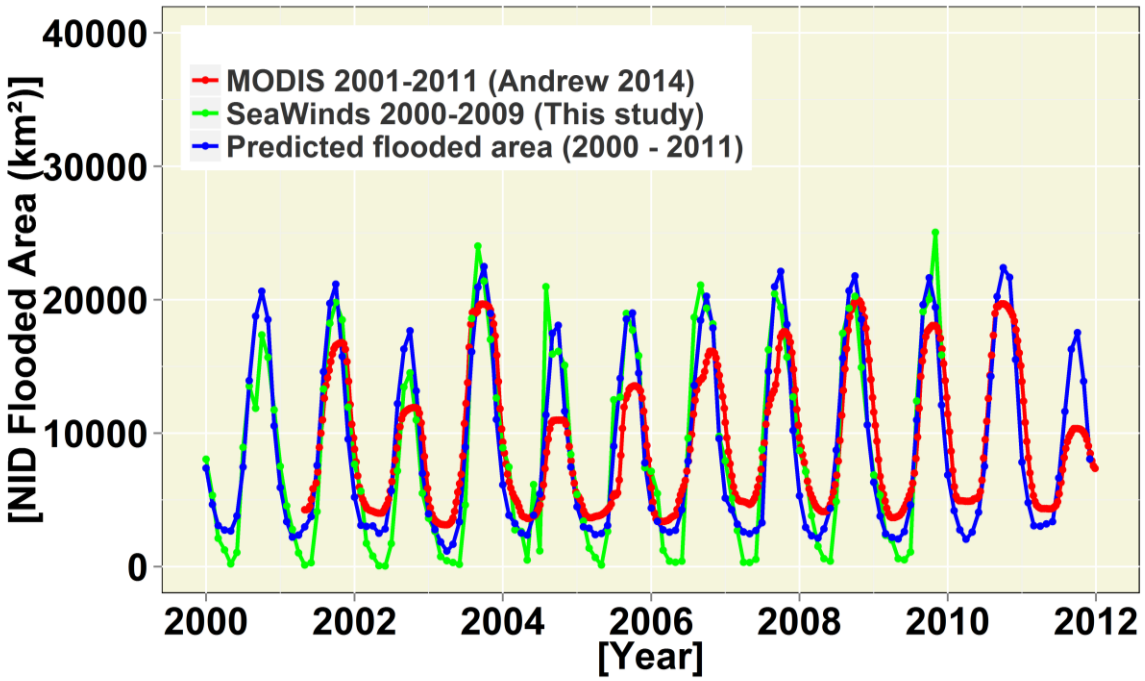

Figure5. 2: *Monthly flooded surface area estimated using SeaWinds data in the NID over the period 2000-2011 compared to observed flooded area using MODIS and Sea-Winds satellites.*

5.1.2. Remotely sensed flooded area comparison - Discharge and area relationship

The extent of the flooded area is related to the maximum river flow at Mopti (Fig.5.3) and can best be expressed with a non-linear regression model:

$$A_f = 126 * (Q_i)^{0.65} \quad \text{(Eq.5.1)}$$

($\sim R^2 = 0.92$)

Where: A_f is the flooded area in km^2; and Q_i is the mean October inflow data in m^3s^{-1} at Mopti gauging station.

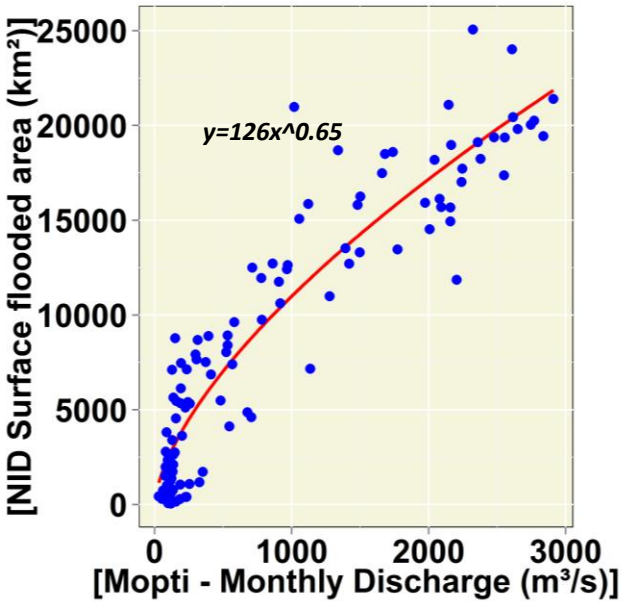

Figure5. 3: *Non-linear regression relationship between inflow discharge and remote sensing area estimates (SeaWinds data), relative to the gauge of Mopti (Monthly discharge m^3/s).*

Over the NID, the most recent decade (2000s) display higher flooded area pattern compared to decades 1990s and 2000s. Figure 5.4 (Fig. 5.4) illustrates the 2000 - 2009 of relative mean area change at NID over sample period of our analysis of maximum in the extent of flood with maximum peak flow. Observed percentage change in flooded area trends highlights slightly its response with increase in flow (Fig.5.4).

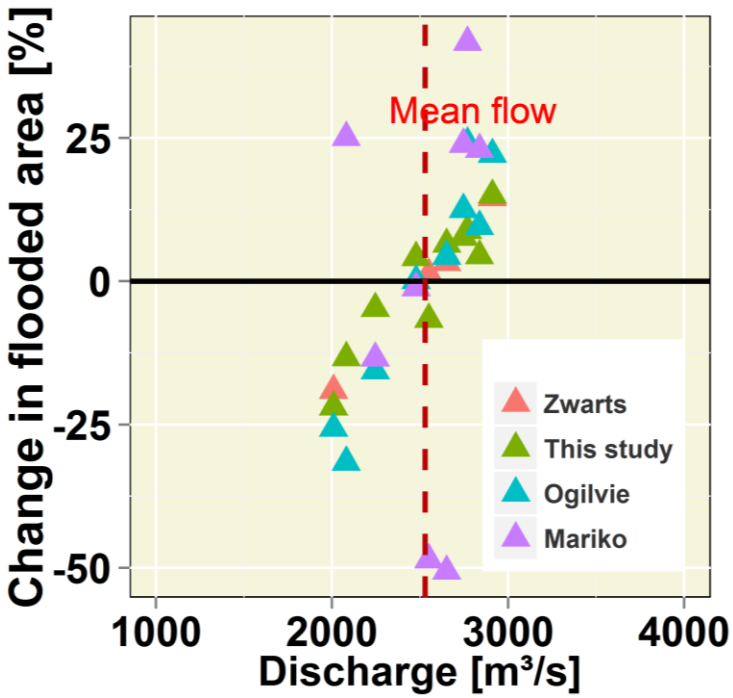

Figure5. 4: *Estimated RS flooded surface areas and Peak flow discharge at Mopti perceptions of relative mean area change at NID; Points show percentage of response with increase in flow*

5.2. Water balance hydrological variables estimations

5.2.1. Water losses (Evaporation (ET)) estimations over the NID

Comparing the results from the eight PET models with the Mopti class A pan records over 360 months (January 1980 to December 2009), we found that the modeled data adequately represented the dynamics observed (Fig. 5.5a). The simulated mean annual evapotranspiration rate computed using the eight PET models showed significant differences ranging from -500 and 500 mm per year (Fig. 5.5b). Comparing the recorded pan evaporation data at Mopti and using performance criteria recommended by Moriasi & Arnold (200), we found that the Penman-Monteith model is best suited to calculate PET in the NID. The comparisons of the methods are first made on an annual basis. The observed yearly evapotranspiration and the relative errors of the calculated evapotranspiration to the observed pan values are presented in Table 5.1. It is seen that on a mean annual basis the Modified Turc model (2549 mm) gives the smallest error & the lowest bias compared with measured pan evaporation (2558 mm), followed by the Hamon (2409 mm), and Penman-Monteith (2370 mm) models.

Regarding the Pearson coefficient of correlation, it is seen that the PMO (Penman-Monteith) model and the Priestley-Taylor model have the highest coefficient's values, with r =

0.73 and r = 0.72, respectively. The Modified Turc method has the lowest value, with r = 0.01 as shown in Table 5.1.

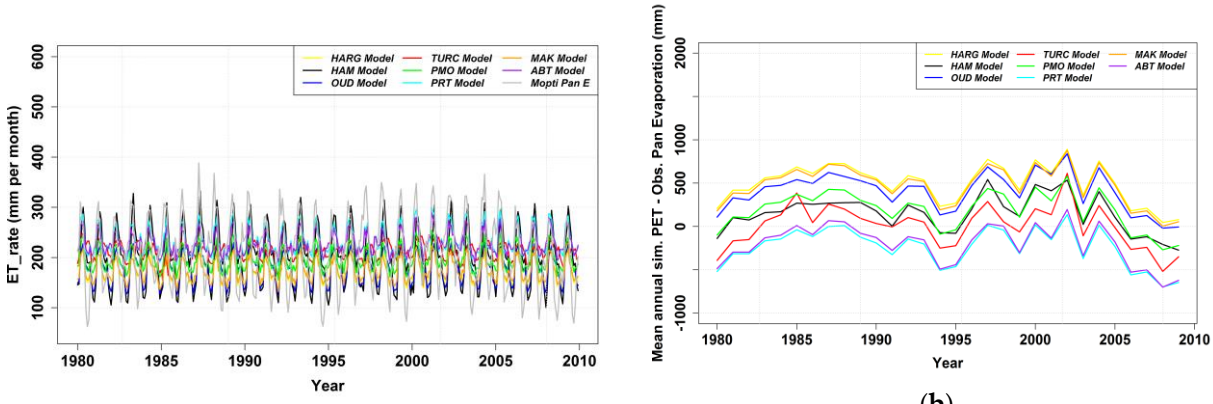

(**a**) (**b**)

Figure5. 5: *(a) comparison of PET models with Mopti observed pan evaporation on a monthly mean basis, (b) ET Models comparison with difference for each Model against measured values at Mopti station over the period of 1980 to 2009.*

Table5. 1: *Evapotranspiration Models comparison results from based on the statistical indicators*

(Where: OUD = Oudin evapotranspiration equation, HAM = Hamon method; TUR = Modified Turc method; HARG = Hargreaves method; PMO = Penman-Monteith combination equation; ABT = Simple Abtew equation; PRT = Priestley-Taylor method; MAK = Modified Makkink equation).

Model Performance Tools	**OUD**	**HAM**	**TUR**	**HARG**	**PMO**	**ABT**	**PRT**	**MAK**
ET Mean values estimates (mm)	2153	2409	2549	2059	2370	2760	2795	2087
Percent Bias (%)	-15.8	-5.8	-0.4	-19.5	-7.4	7.9	9.3	-18.4
RMSE-RSR	1.98	1.11	1.04	2.34	1.23	1.30	1.38	2.24
Pearson coefficient of correlation with observation	0.30	0.27	0.01	0.60	0.73	0.68	0.72	0.64
Average rank	6	3.25	2.75	7.25	2.5	3.75	4.25	6.25
Rank	6	3	2	8	1	4	5	7

The calculated water loss due to evapotranspiration is shown in Figure 5.6. The percentage of ET loss calculated for each annual inflow in selected hydrological years (Figure 5.7a) was compared with corresponding available discharge data inflow (KeMacina + Douna). Time series of input water volumes in the Niger Inland delta and of the water losses through the NID show that the average percentage of water losses, due to the high evapotranspiration,

is approximately 50% (Figure 5.7b). Observations reveal that the Niger River at NID experienced a downward shift in discharge in 1982 and 1992 is proportional to the decrease in ET loss; and is also coherent as observed rise from 1994 till 2004 (Figure 5.7a). However, a large volume of inflow in the NID at Mopti led to greater floods in the area and hence larger ET loss (Figure 5.7b).

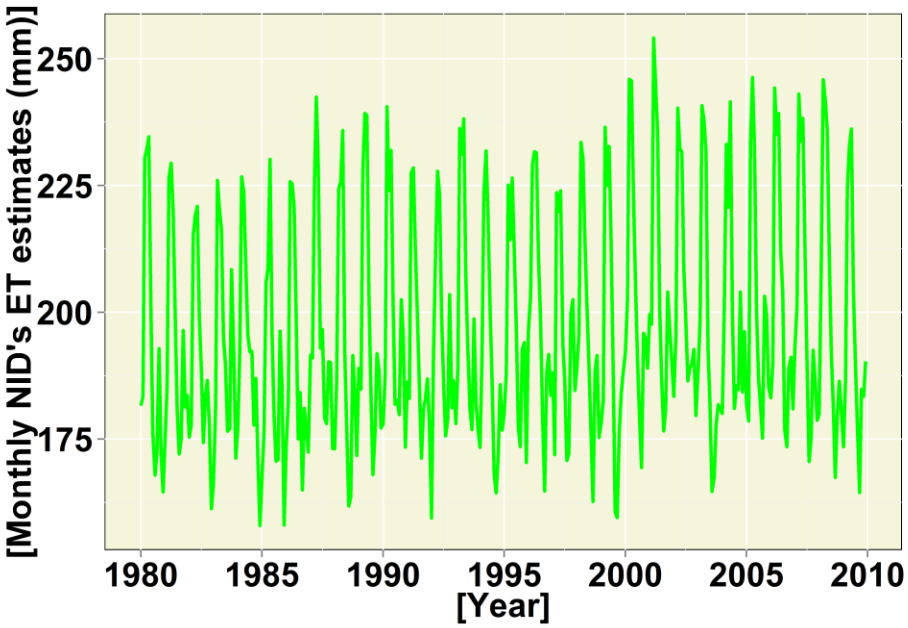

Figure5. 6: *PET computed times series for the period of 1980 to 2010 in the NID*

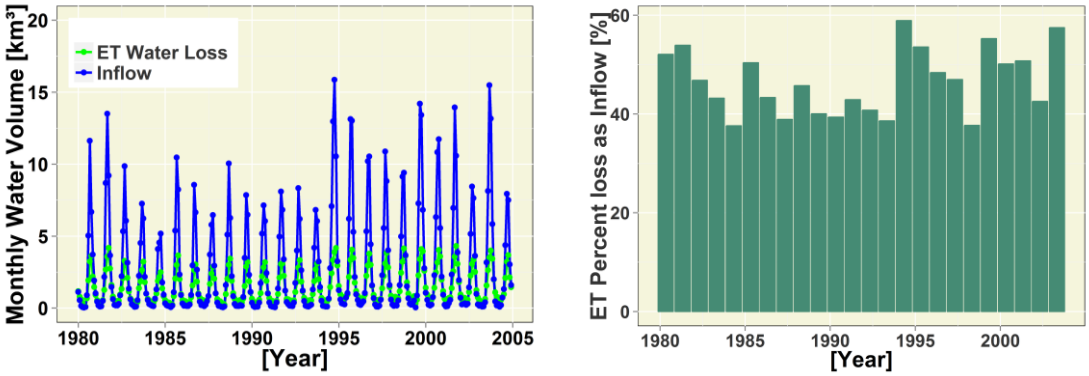

(**a**) (**b**)

Figure5. 7: *(a) Calculated evaporation (ET) losses in the Niger Inner Delta and combined river flows in KeMacina + Douna with values over the period 1980–2004; (b) Annual ET loss as a percent of the inflow in the NID*

5.2.2. Accounting for rainfall contribution

Precipitation contribution over the wetland, calculated from the observed average rainfall data over the estimated flooded areas and runoff from intermediate NID's watershed, varies from 3.10 to 9.12 km³/year. This is explaining the minor contribution of indirect runoff from the reduced surface to the overall water balance of the wetland.

5.2.3. Estimates of return flow from irrigation

Based on the available irrigation details from the ON, we estimate the volume of the abstracted water needed for irrigation to average 0.223 km^3 per month. Owing to the water abstractions on the Niger River for ON irrigation, we consider data on the Bani River only. The Djenné dam is designed to counteract the water loss caused by the Talo Dam in the Bani River downstream. The combined impact of existing and planned infrastructures on NID flow is assessed on the basis of information provided by the "Office Riz Mopti" (ORM). Due to the Djenné and Talo dams, an average flow reduction of 0.291 km^3 per month (Table 5.2) from Bani River to the NID at Mopti is expected. Then, the result for the water contribution from irrigated fields in terms of water depth to the water balance within the NID is shown in the Table 5.3.

Table5. 2: *Average monthly amount of water abstraction (km3/month) over the Niger Inland Delta for irrigation (Where ON is "Office du Niger" irrigation schemes, Djenné & Talo are reservoirs for the ORM's ("Office-Riz-Mopti") irrigation schemes).*

	J	F	M	A	M	J	J	A	S	O	N	D	Sum
ON	0.150	0.168	0.181	0.207	0.226	0.254	0.264	0.264	0.314	0.337	0.194	0.117	2.677
Djenné	0.000	0.000	0.000	0.000	0.000	0.000	0.039	0.156	0.236	0.290	0.218	0.000	0.938
Talo	0.000	0.000	0.000	0.000	0.000	0.000	0.008	0.129	0.040	0.077	0.155	0.000	0.408
Total	0.150	0.168	0.181	0.207	0.226	0.254	0.311	0.549	0.589	0.704	0.567	0.117	4.024

Table5. 3: *Monthly water contribution from irrigated fields (WCI) (km^3 $month^{-1}$) (WU is defined as the total withdrawn water, CW is the consumptive water used and WCI is water contribution from irrigation refers to return flow from irrigated fields).*

Months	WU (10^{-3} km^3 $month^{-1}$)	CW (10^{-3} km^3 $month^{-1}$)	WCI (10^{-3} km^3 $month^{-1}$)
January	151	138	13
February	168	153	15

March	182	163	19
April	207	184	23
May	225	206	19
June	254	224	30
July	312	260	52
August	512	226	286
September	566	236	330
October	833	273	560
November	605	141	464
December	118	102	16

5.3. Water balance over the NID (NIDWat)

To enhance the water budget of the NID to distinguish the water availability, it is important to look beyond abstracted water from rivers (Niger and Bani) for irrigation. The return flow which referred to the non-consumptive water used drained to the NID and generated by the irrigation schemes, was computed. The average water volume of return flow from irrigation dataset (Table 5.3) is ranging from 0.013 km^3 to 0.559 km^3 per month. This is lower than the values between 2.50 km^3 in 1994 to 2.85 km^3 in 1999, with an average of 2.69 km^3 per year of the total annual intake for irrigation (at ON). It is important to highlight that this is before the KéMacina station, and therefore the abstraction is not relevant in the water balance, it is indeed the WCI which is of interest here, and this totals 1.8 km^3. Some of this is from Office Riz Mopti and the total balance of these may be null (as withdrawals, PET and return occur within the NID), hence it's really the return flow from Office du Niger, which was not previously estimated, and this is in the order of 1.2 km^3 per year in line with previous findings (Zwarts et al., 2005). Zwarts et al. (2005) also noted the importance of inter-annual variability in irrigation water use impacting on the NID's flood area extent. Our computed relative average annual return flow from irrigation is lowest (about 4.5%) over the NID, but significant for the water balance and on downstream wetland benefits (Figure 5.9). The range of values obtained were consistent with previous value of 3.7 km^3 estimated by Zwarts et al. (2005) (less than 10% of total inflow) of annual water intake for irrigation, though the value was moderately superior and met our expectation. Figure 5.8 highlights, in annual mean, that

evapotranspiration annual losses are overestimated as compared to the discharge differences between inflow and outflow over the NID. This implies that other contribution over the wet-land must be accounted for.

The water balance cannot be closed by the data available. Figure 5.9 shows the Sankey diagram of the water budget over the NID's surface flooded area which shows an error of 1.9%. Our simulated mean annual evaporation loss of 17.31 km^3 is superior to that of the discharge differences (11.18 km^3). The average of evaporation losses is in accordance with the previous result based on the hydrological balance.

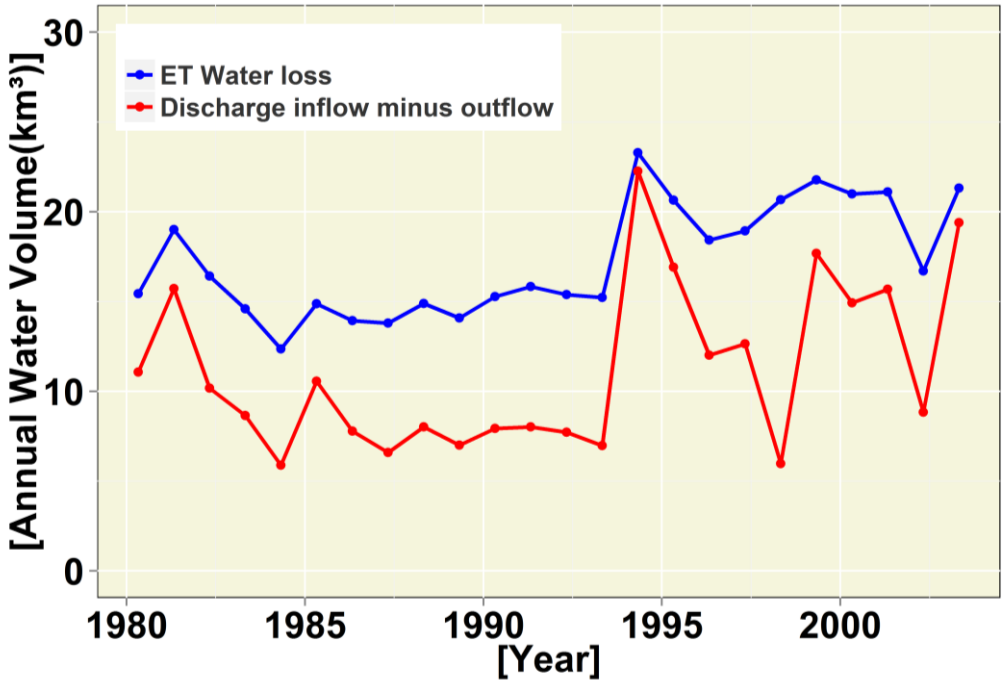

Figure5. 8: *Correlation between mean annual ET loss (water balance term) and the annual volume discharge difference over the NID's flooded area for the hydrological year 1980 – 2004*

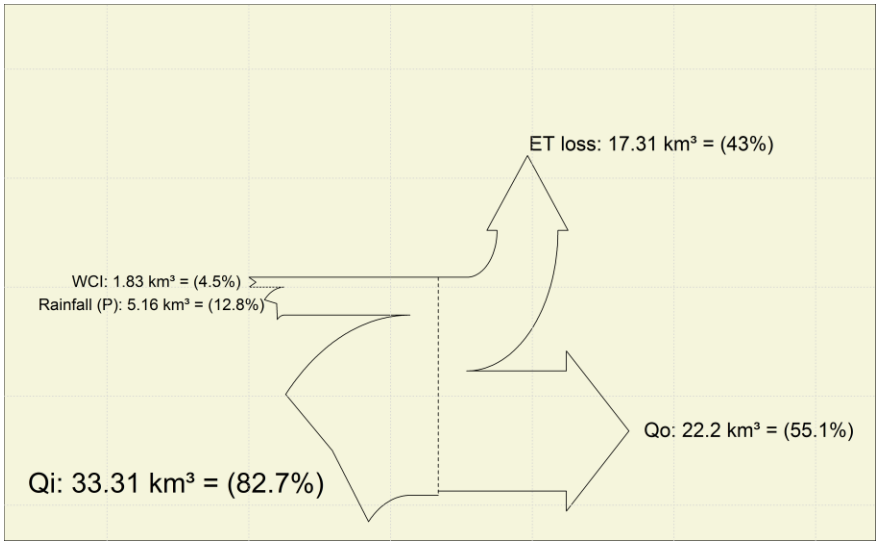

Figure5. 9: *Sankey plot showing the annual average water fluxes of the water balance terms over the NID's floodplain for the period 1980 - 2004.*
(With: Q_i = river water inflow, calculated as the sum of discharge measured at the stations KeMacina and Douna, P = contribution (direct and indirect) of rainfall over the NID, ET = evapotranspiration loss over the NID, WCI = return flow from irrigation to the NID's water balance, Q_o = river water outflow at the station of Diré, and % refer to the percent of the total annual flux).

5.4. Discussion

5.4.1. Comparing remotely sensed flooded areas with previous estimates

Remotely sensed areas comparisons of this study flooded areas previous estimates were conducted by comparing time series of monthly (over a 10-year period) wetland extent estimates from each flooded areas dataset over selected existing wetland mapping (Mariko, 2003; Zwarts et al., 2005; Ogilvie et al., 2015) with respect to corresponding estimates of water extent. Comparison of inundated surfaces from this study to previous estimates is well illustrated in Figure 5.10. The accordance between this study surface flooded area in comparison to past flood extent estimates, which is good enough to confirm the method for the SeaWinds classification (Fig 5.10). Inter seasonal relationship between Mopti maximum monthly flows (October) and patterns of peak flooded areas are shown in Fig.5.3.

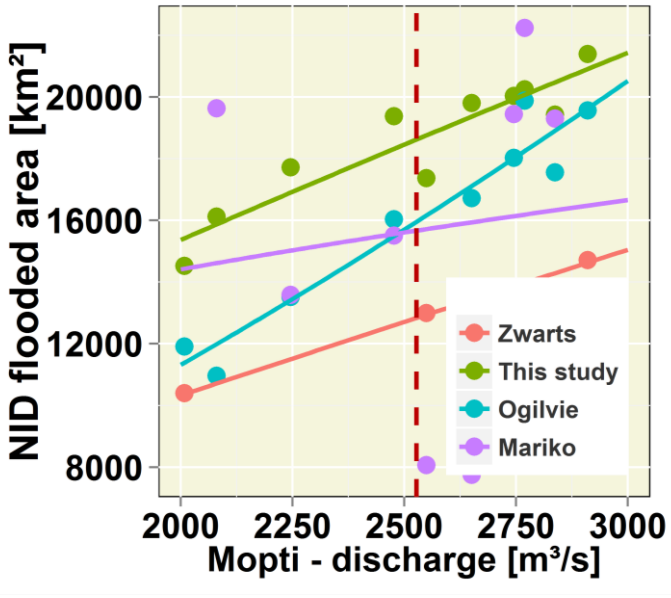

(**a**)

Figure5. 10: *Comparison with other results on the area flood extent.*

The Mopti gauging station is usually used to model the annual floods in the NID (Zwarts et al., 2005; Mahé et al., 2009), as its central location allows study of flow variations in both the Niger river and, indirectly, the Bani river, a major tributary. Changes in rainfall in the Niger and Bani upper catchments are known to be main drivers of fluctuations in the total flood area (Mahé et al., 2009). The annual flood dynamic observed through remote sensing is consistent with the NID flow regime, providing a correct representation of the flooding. Interannual variations in the max flooded areas are also strongly correlated (~R^2 = 085), with the max monthly flows in October at Mopti confirming the data's capacity to represent the variations in the peak amplitude of the flooding (Ibrahim et al., 2017). This appears legitimate, the range of values obtained and their variation according to peak flow in October are consistent with previous remotely sensed estimates (Mariko, 2003; Ogilvie et al., 2015; Zwarts et al., 2005). The difference in the remote sensing area estimates discloses the difficulty in assessing wetland flood area extent accurately and may be due to micro wave data type and source in their reflectance of the indexes, as well as modifications in the delineation of the NID boundaries. Moreover Mariko, (2003), was limited with number of suitable images of NOAA AVHRR products, to characterize the flooded area relationship with flow. Zwarts et al., (2005) used 24 Landsat images spread over several years derive a correlation between flooded areas and the Akka stage level. Ogilvie et al., (2015) used MODIS images

and was limited in the accuracy in of the rise of the flood due to the presence of cloud interference. While our study, uses imagery with Radar information which usefully improves accuracy during the increase of the flood extent.

5.2.2. Comparing assessed water balance components with the previous

The average annual rainfall contribution (varying from 3.26 to 8.402 km^3/year) of to NID's water budget is in line with the recent estimated direct precipitation over the wetland by Ogilvie et al., (2015) over the MODIS flooded areas which varied between 2.6 km^3/year and 8.5 km^3/year. Despite the neglecting of groundwater in line with previous studies (Mahé et al., 2002; Ogilvie et al., 2015; Olivry, 1994; Zwarts et. al, 2005), this study uses storage changes and the remaining flows parameters to assess the balance. Despite too the neglecting of infiltration loss; result like rainfall contributions is fairly similar to the recent calculated water budget residual terms (infiltration + rainfall runoff) in between -0.7 and 5 km^3 (Ogilvie et al., 2015). Monthly average storage changes of 0.329 km^3 was estimated. This is in line with previous studies who suggested that its contribution is minimal (Mahé et al., 2009; Mahé et al., 2002; Olivry, 1994). Storage also decreased during the wet season (April-September) and slightly increased during the JFM and OND obviously in concordance with seasonal rainfall pattern (Oguntunde & Abiodun, 2012; Zwarts et al., 2005).

Regarding the ET component, understanding concerns of local water losses will contribute to the analysis of relevant hydrological processes and improvement of NID's water budget (Ogilvie et al., 2015). Reported ET losses for 1980 to 2004 was calculated from remote sensing estimated flooded areas, and evapotranspiration data rates across the NID from ET model. Over the period of 1980 - 2010, annual potential ET values from north to south ranging between 1481 mm and 2468 mm, and the mean annual PET across the NID is estimated at 2314 mm. This value is slightly higher than previous estimates of 2300 mm by Olivry, (1994) which only considered evaporation. Measuring ET also takes soil moisture and vegetation across the wetland into account, which would increase overall evaporation loss.

Potential ET rates in the NID's wetland from 1980 to 2009 are 2.61 to 9.56 mm/day, which compares slightly higher with the values of 3 to 7 mm/day in Dadson et al., (2010). The annual cumulative ET loss over the entire NID ranges approximately between 12.71 to 21.78 km^3, which equates averagely to 196.3 mm/month (1.443 km^3 per month), close to the range of values modelled by recent studies from the period 1980 - 2002, notably 140 to 240 mm/month

in Zwarts,et al., (2005). However, evaporation from flooded areas may have been overestimated slightly, as evaporation rates from the NID, which is open water covered by vegetation, can be less than those of open water. The transpiration process was not considered explicitly because no vegetation cover data were available. However, uncertain data from remotely sensed flooded areas are expected to become more accurate. Though ET loss per flooded area is highest during the dry season, total ET from the NID is higher during September, October and November due to the large surface area flooded. In addition, spatial variations in actual evaporation (Dadson et al., 2015) were significant, due to higher PET values in the northern areas and the longer flood durations along river stretches and lakes.

The water budget return flow term is the non-consumptive water used drained to the NID and generated by the irrigation schemes. Observed significant increase in flooded area at NID from 2000 was the result of an upward shift in the river discharge which resulted into rainfall increase all over West Africa from 2000s decades compared to 1970-1990 (Thierry Lebel & Ali, 2009). The flooded area change witnessed in the NID is attributed to changes in land use or irrigated agriculture, and or the accuracy in the remote sensing data over the wetland; which led to ~10% increase of flood extent from the month of October to that of September in comparison with reference period of 2000-2009. Observed increasing discharge since 1994 in Mopti and Douna increases the flooding extent and in combination with increasing population pressure led to greater irrigation implications in the study area. This is in line with the observations of Andrew (Ogilvie et al., 2015) who reported that the peak flooded area in the NID was 45% lower than in 2008.

From a water availability point of view, it is important to look beyond abstracted water from rivers (Niger and Bani) for irrigation. The range in monthly variability is ~0.013 km^3 to ~0.559 km^3 as the average for water volume of return flow from irrigation dataset (Table 5.3). This is very smaller than the average water depth arising from abstracted water for irrigated areas. Zwarts et al., (2006) also noted the importance of inter-annual variability in irrigation water used impacting on the NID's flood area extent. Our computed relative average annual return flow from irrigation is lowest (~ 4.5%) over the NID, but significant to the water balance and often impact on downstream wetland benefits. NID's floodplains are being modified as the result of water management activities, in particular large-scale irrigation schemes; which, irrigation water increase with higher crop evapotranspiration and high intake

of water abstracted from rivers (Niger & Bani)can be explained due to a lack of adequate efficient irrigation system (Zwarts et al., 2006). Some studies conducted, since the early developments of the "Office du Niger" until now have confirmed this hypothesis. The level of the water table is increasing after many years under the influence of irrigation in areas of "Office du Niger", this rise is linked not only to the return of irrigation water in delta, but also to the permanent retention of water in irrigation channels (Marlet & N'Diaye, 2002). With use of surface water for irrigation, e.g., in large River valleys, drainage and net groundwater recharge may have increased (Kurtzman et al., 2011). Our analysis suggests that the return flow from irrigation can only partially replace the lost water abstracted from reducing floodplain inundation. Thus, further extension of irrigation schemes within the rivers basin should also be avoided.

5.2.3. Water balance analysis

The water balance cannot be closed by the data available. Figure 5.9 shows the Sankey diagram of the water budget over the NID's surface flooded area which shows an error of 1.9%. Our simulated mean annual evaporation loss of 17.31 km^3 is superior to that of the discharge differences (11.18 km^3). The average of evaporation losses is in accordance with the previous result based on the hydrological balance.

The water balance was performed from observed hydro-climatic and optical & microwave remote sensing data adapted from the NIDWat modelling approach providing input and output fluxes across the NID's wetland (Figure 5.9). This NIDWat model also provides the main features that leads to the explanation of the overall hydrological functioning of NID's reservoir. However, NIDWat in the present situation differed on approaches compared to models of above mentioned publications in which the natural variations as well as the impact of human activities (e.g., irrigation aspect) on NID's floodplain are not well captured. Hence, for this article, the output of NIDWat is mostly compared with the recent model results by Ogilvie et al. (2015), as mentioned in the introduction of this paper because the two approaches can be used in a complementary manner.

The calculated amount of water reduction in discharge difference (inflow minus outflow) for the inlet and outlet gauging stations is compared with the results of NIDWat. The annual

mean evapotranspiration's are overestimated as compared to the discharge differences between inflow and outflow over the NID, which is confirmed by Ogilvie et al.'s (2015) results. This implies that other hydrological component over the wetland must be accounted for; and also, the actual ET losses would be considered. Our simulated mean annual evaporation loss of 17.31 km^3 (i.e., 43% of the total input) was found consistent with a mean value of 17.2 km3 in Ogilvie et al. (2015); and moderately superior to a value of 11. 4 km^3 (i.e., 33%) in Zwarts et al. (2005). Values for the contribution of rainfall, and values on the return of water withdrawal for irrigation are found coherent with the references mentioned above. The water budget's difference is 1.9% between the input fluxes and output fluxes confirms that our model provides an adequate representation of the potential evaporation losses (Figure 5.9). The interpretation of this error is difficult since no local studies are known that confirmed the water budget modeled in the present study. However, Ogilvie et al. (2015) assumed that his water budget residual term corresponds the difference between infiltration and runoff generated by rainfall falling upon non-flooded areas of the NID. Hence, the good performance of the NIDWat model confirms that, SeaWinds data and the WCI estimates may therefore be used to provide additional insights and refine the water balance of the NID (Ibrahim et al., 2017). Nonetheless, the trends generally remain good, even if some parameters are not considered; the limitations with respect to data availability and uncertainties in the significance of the estimated parameters, however, remain.

5.2.4. Uncertainty and Outlook

Input data used in the estimates of the available energy for ET are source of uncertainty since measured solar radiation is not available at meteorological stations in or near the study area. In addition, we used only Mopti pan recorded data pan for the whole study area due to the lack of other local pan recordings for our study area based on the assumption that the climate classification is the same (Oguntunde & Abiodun, 2012). The uncertainty of the single ET models in percentage deviation from the mean ET of 17.67 km^3/year is in the range of -15.31% to +15.54%. PMO has the smallest differences to this mean value (-2%) resulting in a water balance error of 0.79 km^3/year. The water balance error is calculated by summing all in and outflows. The uncertainty in ET results in a water balance error in the range of -2.31 to +3.14 km^3/year. This error is the smallest (0.435 km^3/year) when the ET losses are calculated as the mean over the eight models is used and only slightly higher when the PMO model is applied.

Our water balance modeling approach, like previous studies to assess water losses under hydro-climatic conditions (Olivry, 1994; Mariko, 2003; Zwarts et al., 2005; Ogilvie et al., 2015) is limited by some assumptions and some processes that are not represented in the model. Although infiltration is the dominant process of groundwater movement in portions of the wetland (Mahé et al., 2009); and could become more important in a water balance. Therefore, infiltration process in NID's wetland can potentially lead to the error in balancing the water fluxes over the NID. Constraints in our water balance are not only caused by constraints in the characterization of hydrological processes but also by uncertainties arising from the data. Moreover, the possible changes in the NID hydraulic pathways due to dams or land use changes as discussed in Ogilvie, et al., (2015) were not considered.

5.5. Partial Conclusion

Flooded area assessment was carried out and it was primary based on the microwave remote sensing data classification and the quantitative estimation of flood extent. The best represented potential evaporation model was selected through a process based on combined statistical indicators. These techniques helped selection a number some of ET methods having as input the available weather parameters. It was obtained that the PMO model was the best method among the group in representing the potential ET in our study area.

The water balance model for the NID was developed and tested using the obtained flooded area extent and the computed evaporative losses.

The use of Sankey diagram and graphs of the water balance of calculated WB terms enable to find that water balance model using PMO for water losses estimation performs better. Thus, water balance model with such parameters could be the best for water budget in the NID. Indeed, fluctuations in the inflow-flood extent relationship according to discharge amplitude, combined with the with microwave remote sensing procedure, appear to be a good skill for water balance model in the wetland.

In conclusion, this water balance model helped understanding that nonlinear methods could also be used instead of the common linear methods. The specificity of this work is the comparison of some ET models for best representation of the potential evaporation rather than using directly one method to compute the water losses. Despite uncertainties at each stage of the calculation of the water budget (flooded area extent, evaporation losses, direct and indirect rainfall, and return flow from irrigation schemes), the results presented here were

coherent with the limited information available for the NID's hydrological functioning. Significantly, it highlighted that annual evaporation losses being higher to the discharge-difference between inflow and outflow, further rainfall and return flow from irrigation over the floodplain must be considered.

However, the limit of the approach resides on the short number of pan evaporation data used for the whole wetland. Consequently, to improve the results for other researchers, it is suggested that combination of Radar information during the flood area extent estimate might neatly reduce cloud interference and improve the flood map result

Chapter 6. Impact of climate change on the NID

This chapter presents estimates of the influence of climatic change on the hydrological functioning of the NID and water availability in the basin using the developed hydrological model driven with output from regional climate models.

6.1. Climate Future Projections

The CORDEX model performs reasonably well in estimating the mean daily precipitation over in the NID. The result for the near future projection of the ensemble mean for the 16 scenarios is shown in the figure 6.1 below.

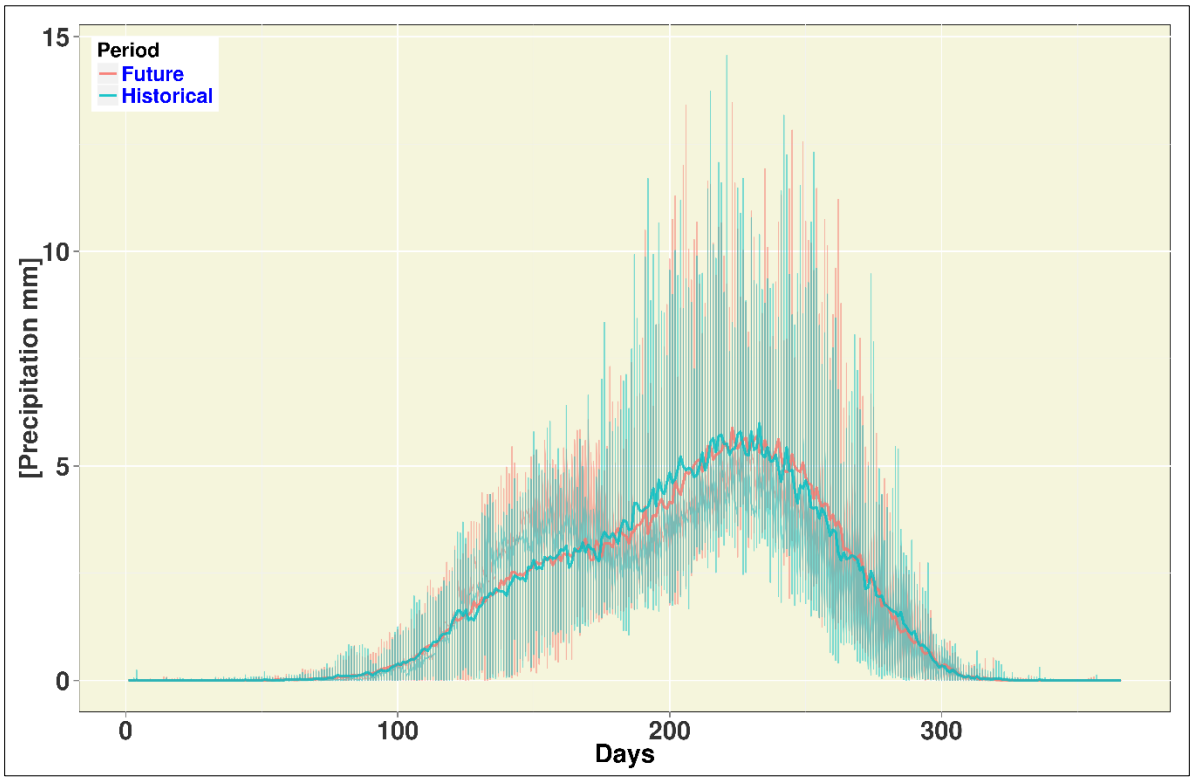

Figure6. 1: *Average daily precipitation over the NID for near future RCP 8.5 2035-2065.*

An increase of precipitation is predicted by the ensemble mean of relative changes in daily precipitation compared to 1951-2005 shows about 3 - 5% increase in the Niger Inland Delta (Fig.6.2). The increase in average daily precipitation might be higher especially during August, September and October.

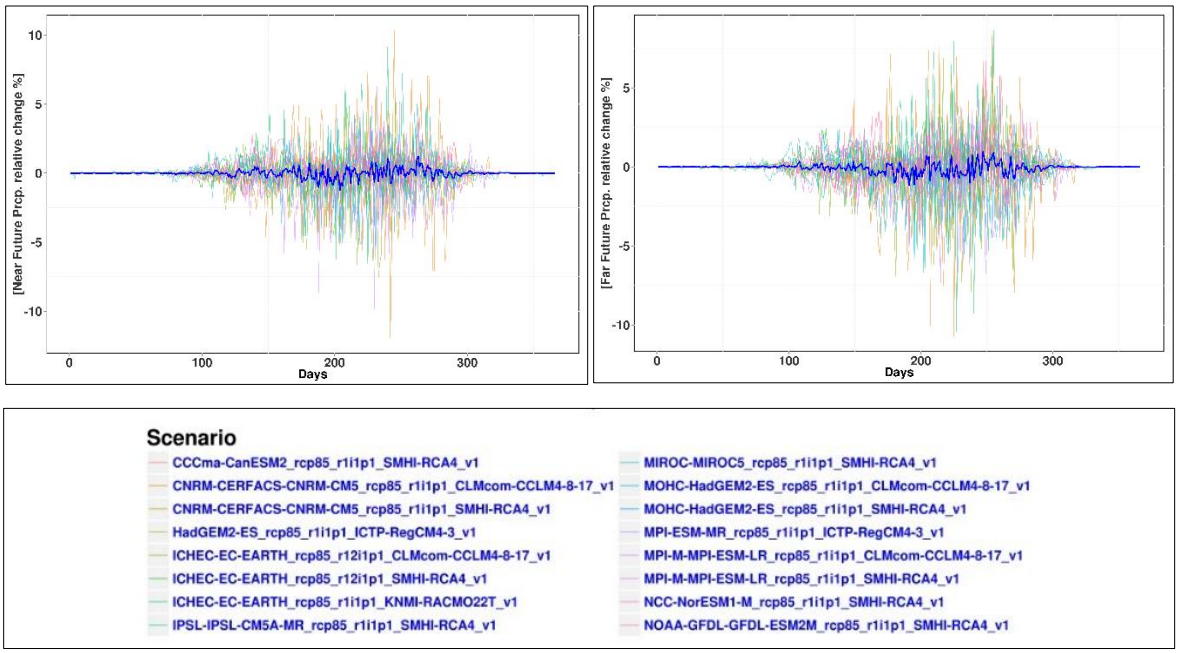

Figure6. 2: *Percentage change in average projected precipitation from the near and far future period.*

Based on the scenarios developed for the future period, the temperature over the NID, slightly show an increase (Fig. 6.3).

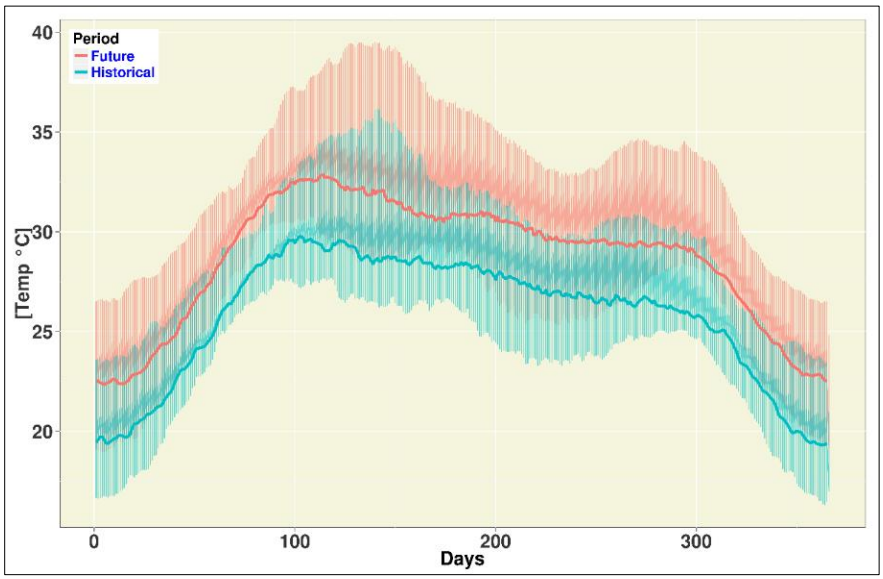

Figure6. 3: *Average daily Temperature over the NID catchment by near future RCP 8.5 2035-2065.*

The change in simulated potential evaporation over the NID according to the three processed scenarios (CCma-CanESM2_r1i1p1_SMHI-RCA4, MPI-M-MPI-ESM-

LR_r1i1p1_CLMcom-CCLM4-8-17, and NOAA-GFDL- ESM2M_r1i1p1_SMHI-RCA4) for the near future period (2035-2065) shows a slight increase with respect to the temperature (Fig. 6.4).

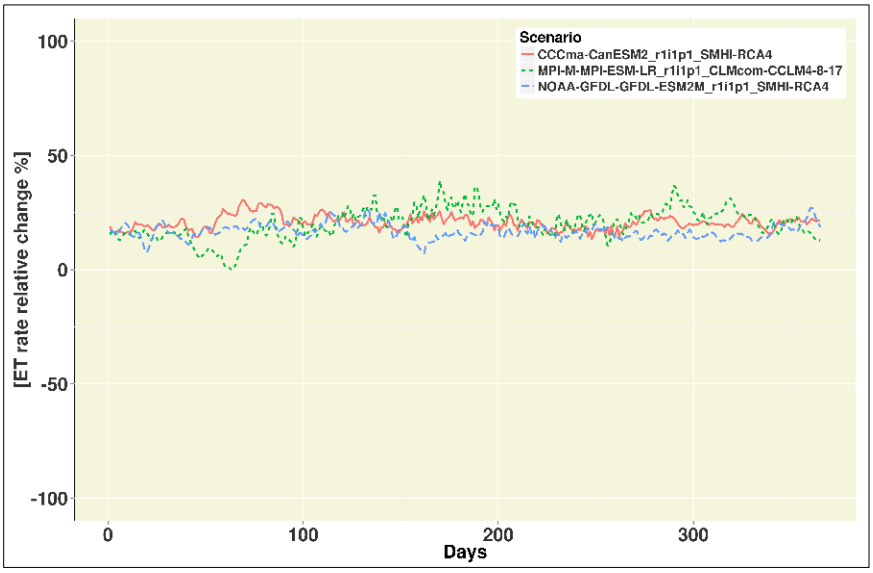

Figure6. 4: *Change in average potential evaporation rate in the future from the base period.*

6.2. Streamflow and Flooded area for the future period

From the three processed scenarios CCma-CanESM2_r1i1p1_SMHI-RCA4, MPI-M-MPI-ESM-LR_r1i1p1_CLMcom-CCLM4-8-17, and NOAA-GFDL-ESM2M_r1i1p1_SMHI-RCA4), the results of modelling are presented in two modes for analysis: change in river flow discharge (Projected runoff at Mopti station), and change in flooded area (surface flood area extent over the NID) (Fig. 6.5).

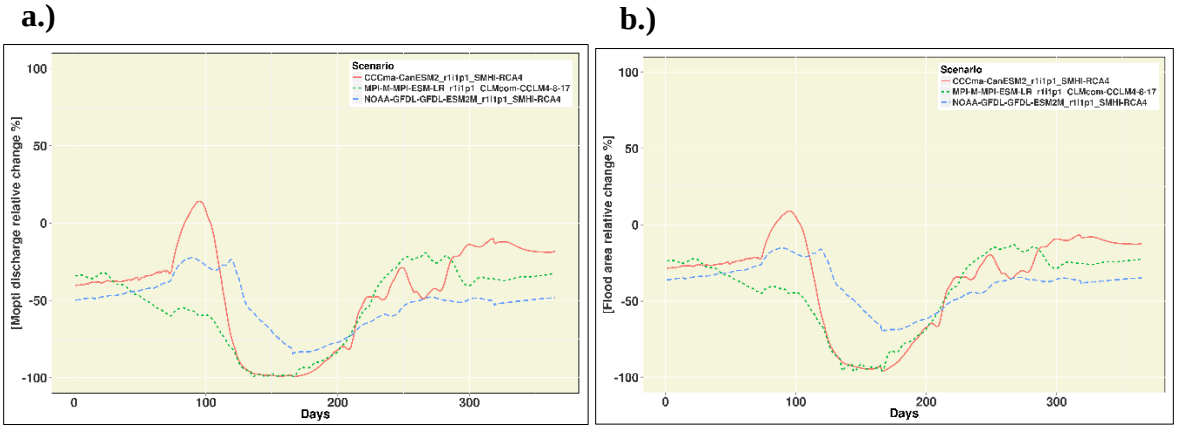

Figure6. 5: *Hydrological projected relative change over the NID for the near future (2035-2065)*
a.)-Relative change of the river flow discharge at Mopti station, and b.) relative change in flooded area extent over the NID

6.3. Discussion

A likely increase of precipitation is predicted by the CORDEX output. The seasonal rainfall distribution is showing wetter period during August-September-October. This fact follows the changes in spatial distribution of seasonal rainfall by Oguntunde and Abiodun, (2012). With respect to temperature over the NID, this ensemble mean of models from CORDEX output, also predicts an intensive rise of air temperature for the same period over the NID as well as the highest evaporation rate. This is in line with the general warmer climate over NRB in all months and seasons pointed out by Oguntunde and Abiodun, (2012).

As regards, to scenarios streamflow over for the future period extracted for the station of Mopti in the NID, the mean relative change of the river discharge was determined for all the 16 scenes by comparing the prediction changes with the long-term averages from the base period. The mean river discharge is decreasing to about 70% at the station of Mopti according to different climate change scenarios for the near future period. More significant changes of decrease in mean runoff in the river basins are forecasted on the basis of CCma-CanESM2_r1i1p1_SMHI-RCA4, and MPI-M-MPI-ESM-LR_r1i1p1_CLMcom-CCLM4-8-17 (RCP8.5) rather than on NOAA-GFDL- ESM2M_r1i1p1_SMHI-RCA4. This climate change scenario predicts the lowest flood area extent over the NID, while the highest surface flood extent is forecasted by NOAA-GFDL- ESM2M_r1i1p1_SMHI-RCA4 for near future (2035-2065) (Fig. 6.5b). These changes are not correlated with increase changes in precipita-

tion for CCma-CanESM2_r1i1p1_SMHI-RCA4, and MPI-M-MPI-ESM-LR_r1i1p1_CLM-com-CCLM4-8-17. In contrast, evaporation showed opposing changes as well as the temperature.

The decrease of mean discharge over the NID can be linked with the relative lowering of the groundwater table as the contribution of groundwater to the surface runoff is highly variable (Mahé, et al., 2013). The predicted values of evaporation and the forecasted rise in air temperature throughout NID will result in decreased possibility of permanent flood surface extent in NID's wetland.

6.4. Partial Conclusion

Climate change will induce changes of streamflow discharge over the NID with a year. These changes will be determined by both climate model and basin location. The warming of the climate considerably modifies the discharge pattern. According 3 scenarios processing, the average relative change of river flow value is approximately 70%. The shift is observed almost in all the scenarios studied. Therefore, a higher decrease in streamflow will result in important reduction of flooded area extent over the NID.

Chapter 7. Conclusion and Perspectives

The problem statement and the contributions, with their limitations are summarized in this chapter. This chapter speaks of to the preceding chapters where details are provided. According to perspectives resulting from this thesis work, the future works are proposed.

7.1. Conclusion

The development and assessment of water balance model over the NID will help local rural population who mainly rely on irrigation to for their survival by changing their agricultural system through a water resource management system. This thesis study endeavors to a water balance model over the NID system which could be potentially integrated into hydrological models to improve the NID representation in models.

This water balance model was first based on the development of a method to find the flooded area extent over the NID which are indispensable conditions for obtaining good estimates of water losses. The physical hydrological system over the NID as a set input and output fluxes were considered based on the previous studies and knowledge on the area. Hydrological processes were conceptualized using a water budget approach with flood area extent as the system of change of storage over NID region. A spatial-temporal characterization of the inundated area extent was done by means of optical and microwave remote sensing data. These approaches included the use of (i) combined of two remote sensing data namely the SeaWinds data from QuikSCAT, and the Landsat7 ETM+ due to their overlapping timeseries. (ii) Then preprocessing method was applied to reduce the effect of cloud cover; before using the land cover classification. (iii) At the last step, quantitative assessment of the land cover classes obtained over the NID. The result performance was assessed using the MODIS NDVI estimates over the same period, and with the previous surface flooded area estimation. At the end of the process, the calculated flood area timeseries were retained and, then a non-linear relationship with the inflow (combination of station KéMacina and Douna) was established. Flooded can then be predicted with discharge as inputs for non-linear model.

To assess the water losses over the NID, potential evaporation models were evaluated to represent potential evaporative water losses using the required climate inputs. The Models performances were assessed using the Nash-Sutcliffe coefficient, percent bias, correlation and Root Mean Square Error - Standard Deviation Ratio. the Penman - Monteith equation was the best represented model to compute potential ET over the study area. It was found that the best represented potential evaporation model is the PMO method. Later, the values of the components (rainfall contributions, change of storage, and return flow from irrigation) of NID water balance were also determined. NID Water balance model appear to be a good in representing the hydrological processes over the region.

NIDwat performances were evaluated using the Sankey diagram. Results showed that non-linear model performed well. The limit of this model could reside on the short length of data used because such model need long length of data. Many factors such as climate change and variability impacts induced changes in streamflow which directly affect water availability for all activities particularly agriculture which is the main survival issue of NID population. Thereby, it can be concluded that that NIDWat model approach could be a good way to represent NID hydrological processes in hydrological models. We then used the model as a module in representing NID hydrological processes WBMplus hydrological model in analyzing water availability under changing conditions. Multi model approach using regional climate data from the CORDEX initiative was used as inputs to the calibrated hydrological model (WBMplus) on Niger River Basin (NRB). According to the Climate Change scenarios and modelling results, the discharge of the Niger river at Mopti station inside the NID will decrease in the 21st century.

In conclusion, this work showed the importance of developing a reliable method water losses estimation over the NID flooded area rather assigning them subjectively as done in many studies in the region. Moreover, the results achieved demonstrated that other potential water balance components such as indirect and direct rainfall, and return flow from irrigation, could refine the water budget over the NID. The study helped understanding the hydrological processes over the NID, and assessing the water resources availability over the NID under changing condition. Therefore, any hydrological model for Niger river basin should consider the hydrological processes of the NID in order to make good predictions.

7.2. Contributions

This thesis has contributed to the understanding of hydrological processes in the NID. This was done, through the development of new water balance model for the NID. One interesting finding in this work is that different characteristics of the flooded area were best predicted by different microwave remote sensing data, suggesting that a combined approach to estimate the flood extent may be an interesting solution to surface flooded area estimate in the NID. The study also highlighted that there was strong non-linearity between flooded area extent and streamflow in the study area.

A large contribution of this work was the evaluation of the best represented potential evaporation method to quantify the water losses over the NID. This assessment result of this work also helps to better quantify the losses in the models which are important in the NID region undergoing the impacts of climate change and variability. So, this is a big advantage over previous models in the NID.

Another contribution is the assessment of climate change impacts on the water availability in the NID. This will serve policy makers and the NID population to better adapt to reduction in surface flooded area in the region.

7.3. Future work

This work has developed and tested water balance model on the NID floodplain. Therefore, as a perspective there is need to continue developing and testing water balance model over the NID by considering the surface water and groundwater interaction in the region.

From the flood area results, a multi-approach using Radar data to estimate the extent of the flood area may be an interesting solution to improve land cover maps in the NID. Thus, this work will continue to test other flooded area estimates in order to confirm its skills.

As a future step of this work, a dynamic-model approach will be used to compare the resulting skills to that of the previous water balance models in the region.

References

Adams, E. A., Boateng, G. O., Amoyaw, J. A., Contents, T. O. F., Profileinformation, C., Statement, M., … WRC. (2014). General Guidelines for Calculating a Water Budget Land and Water Management Division (LWMD) March 2010 ISSUES : DISCUSSION : *Journal of Chemical Information and Modeling*, *23*(March), 99. http://doi.org/10.1017/CBO9781107415324.004

Alazard, M., Leduc, C., Travi, Y., Boulet, G., & Ben Salem, A. (2015). Estimating evaporation in semi-arid areas facing data scarcity: Example of the El Haouareb dam (Merguellil catchment, Central Tunisia). *Journal of Hydrology: Regional Studies*, *3*, 265–284. http://doi.org/10.1016/j.ejrh.2014.11.007

Ali, A., Lebel, T., & Amani, A. (2005). Rainfall Estimation in the Sahel. Part I: Error Function. *Journal of Applied Meteorology*, *44*(11), 1691–1706. http://doi.org/10.1175/JAM2304.1

Allen, R. G., Pereira, L. S., Raes, D., Smith, M., & Ab, W. (1998). Allen_FAO1998, 1–15.

Ashcraft, I. S., & Long, D. G. (2003). The spatial response function of SeaWinds backscatter measurements. *Proceedings of SPIE*, *5151*, 609–618. http://doi.org/10.1117/12.506255

Ball, J. E., & Luk, K. C. (1998). Modeling spatial variability of rainfall over a catchment. *Journal of Hydrologic Engineering*, *3*(2), 122–130.

Brouwer, R., & Hofkes, M. (2008). Integrated hydro-economic modelling: Approaches, key issues and future research directions. *Ecological Economics*, *66*(1), 16–22. http://doi.org/10.1016/j.ecolecon.2008.02.009

Brown, J. D., & Heuvelink, G. B. M. (2005). 79 : Assessing Uncertainty Propagation Through Physically based Models of Soil Water Flow and, (i).

Carter, R. C., & Parker, A. (2009). Climate change, population trends and groundwater in Africa. *Hydrological Sciences Journal-Journal Des Sciences Hydrologiques*, *54*(4 Special Issue: Groundwater and Climate in Africa), 676–689. http://doi.org/10.1623/hysj.54.4.676

Chelton, D. B., & Freilich, M. H. (2005). Scatterometer-Based Assessment of 10-m Wind Analyses from the Operational ECMWF and NCEP Numerical Weather Prediction Models. *American Meteorological Society*, *134*(2), 737–742.

http://doi.org/10.1175/MWR3111.1

Chen, H., Guo, S., Xu, C. yu, & Singh, V. P. (2007). Historical temporal trends of hydro-climatic variables and runoff response to climate variability and their relevance in water resource management in the Hanjiang basin. *Journal of Hydrology*, *344*(3–4), 171–184. http://doi.org/10.1016/j.jhydrol.2007.06.034

Cohen, S., Kettner, A. J., Syvitski, J. P. M., & Fekete, B. M. (2013). WBMsed, a distributed global-scale riverine sediment flux model: Model description and validation. *Computers & Geosciences*, *53*, 80–93. http://doi.org/10.1016/j.cageo.2011.08.011

Communities, C. of the E. (2009). White Paper: Adapting to climate change: Towards a European framework for action. *Impact Assesment*. http://doi.org/10.1017/CBO9781107415324.004

Csaplovics, E. (1996). SAR-Based Monitoring of Flood-Induced Land Cover and Landuse Change in the Region of tha Inland Delta of the the River Niger (Mali).

Dadson, S. J., Ashpole, I., Harris, P., Davies, H. N., Clark, D. B., Blyth, E., & Taylor, C. M. (2010). Wetland inundation dynamics in a model of land surface climate: Evaluation in the Niger inland delta region. *Journal of Geophysical Research*, *115*(D23), 1–7. http://doi.org/10.1029/2010JD014474

De Bruin, H. a. R., & Holtslag, a. a. M. (1982). A Simple Parameterization of the Surface Fluxes of Sensible and Latent Heat During Daytime Compared with the Penman-Monteith Concept. *Journal of Applied Meteorology*, *21*, 1610–1621. http://doi.org/10.1175/1520-0450(1982)021<1610:ASPOTS>2.0.CO;2

De Bruin, H. a R. (1983). Evapotranspiration in humid tropical regions. *Hydrology of Humid Tropical Regions with Particular Reference to the Hydrological Effects of Agriculture and Forestry Practice (Proceedings of the Hamburg Symposium, August 1983). IAHS Publ. No. 140.*, *140*(140), 1–14.

Descroix, L., Mahé, G., Lebel, T., Favreau, G., Galle, S., Gautier, E., Sighomnou, D. (2009). Spatio-temporal variability of hydrological regimes around the boundaries between Sahelian and Sudanian areas of West Africa: A synthesis. *Journal of Hydrology*, *375*(1–2), 90–102. http://doi.org/10.1016/j.jhydrol.2008.12.012

Descroix, L., Niang, A. D., Panthou, G., Bodian, A., Sane, Y., Dacosta, H., Quantin, G. (2015). Évolution récente de la pluviométrie en Afrique de l'Ouest à travaers deux régions: La sénégambie et le bassin du Niger moyen. *Climatologie*, *12*, 25–43.

Ding, X. Y., Jia, Y. W., Jia, J. S., Zhou, H. D., & Wang, Y. C. (2011). Variability, change

and prediction of hydro-climatic elements in the Hai River basin, China. *Hydro-Climatology: Variability and Change*, *344*(July), 45–51. Retrieved from <Go to ISI>://WOS:000297611800008

Drexler, J. Z., Snyder, R. L., Spano, D., & Paw U, K. T. (2004). A review of models and micrometeorological methods used to estimate wetland evapotranspiration. *Hydrological Processes*, *18*(May), 2071–2101. http://doi.org/10.1002/hyp.1462

Druyan, L. M. (2011). Studies of 21st-century precipitation trends over West Africa. *International Journal of Climatology*, *31*(10), 1415–1424. http://doi.org/10.1002/joc.2180

Eastham, J., Mpelasoka, F., Ticehurst, C., Dyce, P., Ali, R., & Kirby, M. (2008). Mekong River Basin Water Resources Assessment : Impacts of Climate Change. *Water for a Healthy Country Flagship Report Series ISSN: 1835-095X Australia*, (August).

Fathian, F., & Aliyari, H. (2016). Temporal trends in precipitation using spatial techniques in GIS over Urmia Lake Basin , Iran Farshad Fathian * and Hamed Aliyari Ercan Kahya Zohreh Dehghan. *Int. J. Hydrology Science and Technology*, *6*(1), 62–81.

Frappart, F., Hiernaux, P., Guichard, F., Mougin, E., Kergoat, L., Arjounin, M., Lebel, T. (2009). Rainfall regime across the Sahel band in the Gourma region, Mali. *Journal of Hydrology*, *375*(1–2), 128–142. http://doi.org/10.1016/j.jhydrol.2009.03.007

Frenken, K. (2005). *Irrigation in Africa in figures, FAO WATER REPORTS 29, AQUASTAT Survey, FAO Land and Water Development Division*. (K. Frenken, Ed.). Rome.

Frolking, S., Milliman, T., Palace, M., Wisser, D., Lammers, R., & Fahnestock, M. (2011). Tropical forest backscatter anomaly evident in SeaWinds scatterometer morning overpass data during 2005 drought in Amazonia. *Remote Sensing of Environment*, *115*(3), 897–907. article. http://doi.org/http://dx.doi.org/10.1016/j.rse.2010.11.017

Fung, F. A. I., Lopez, A. N. A., & New, M. (2009). *1 Introduction*.

Glover, J., & McCulloch, J. S. G. (1958). The empirical relation between solar radiation and hours of sunshine. *Quarterly Journal of the Royal Meteorological Society*, *84*, 172–175. http://doi.org/10.1002/qj.49708436011

Hiernaux, P., Ayantunde, A., Kalilou, A., Mougin, E., Gérard, B., Baup, F., Djaby, B. (2009). Trends in productivity of crops, fallow and rangelands in Southwest Niger: Impact of land use, management and variable rainfall. *Journal of Hydrology*, *375*(1–2), 65–77. http://doi.org/10.1016/j.jhydrol.2009.01.032

HIERNAUX, P., & DIARRA, L. (1986). La végétation et les ressources pastorales du Delta

intérieur du Niger. Etat des connaissances, perspectives d'applications et de recherches complémentaires. In M. BERTHOD & B. TEME (Eds.), *Gestion des Ressources et Aménagement du Fleuve Niger des Connaissances Scientifiques pour la Décision Publique* (pp. 77–82). Bamako, 14-16 janvier 2002.

Hiernaux, P., Diarra, L., Trichon, V., Mougin, E., Soumaguel, N., & Baup, F. (2009). Woody plant population dynamics in response to climate changes from 1984 to 2006 in Sahel (Gourma, Mali). *Journal of Hydrology*, *375*(1–2), 103–113. http://doi.org/10.1016/j.jhydrol.2009.01.043

Hoogeveen, J., Faurès, J.-M., Peiser, L., Burke, J., & van de Giesen, N. (2015). GlobWat – a global water balance model to assess water use in irrigated agriculture. *Hydrology and Earth System Sciences Discussions*, *12*(1), 801–838. http://doi.org/10.5194/hessd-12-801-2015

Howard, K., & Griffith, A. (2009). Can the impacts of climate change on groundwater resources be studied without the use of transient models? *Hydrological Sciences Journal-Journal Des Sciences Hydrologiques*, *54*(4), 754–764. http://doi.org/DOI 10.1623/hysj.54.4.754

Hubert P., Carbonnel, J. P. (1987). Approche statistique de l'aridification de l'Afrique de l'Ouest. *Journal of Hydrology*, *95*, 165–183.

Hughes, D. a., Tshimanga, R. M., Tirivarombo, S., & Tanner, J. (2014). Simulating wetland impacts on stream flow in southern Africa using a monthly hydrological model. *Hydrological Processes*, *28*(4), 1775–1786. http://doi.org/10.1002/hyp.9725

Ibrahim, M., Djibo, A. G., & Afouda, A. (2016). Recent trend analysis of hydro-climatic data in the upper and Niger Inland Delta of the Niger River basin (West Africa). *International Journal of Current Engineering and Technology*, *Vol.6*(6), 2167–2177. http://doi.org/10.14741

Ibrahim, M., Wisser, D., Ali, A., Diekkrüger, B., Seidou, O., Mariko, A., & Afouda, A. (2017). Water Balance Analysis over the Niger Inland Delta-Mali: Spatio-Temporal Dynamics of the Flooded Area and Water Losses. *Hydrology*, *4*(3), 40. http://doi.org/10.3390/hydrology4030040

IPCC. (2007). Climate change 2007: the physical science basis. *Intergovernmental Panel on Climate Change*, *446*(7137), 727–8. http://doi.org/10.1038/446727a

IPCC. (2014). *Summary for Policy Makers. Climate Change 2014: Impacts, Adaptation and Vulnerability - Contributions of the Working Group II to the Fifth Assessment Report*.

KFW. (2010). Adaptation to Climate Change in the Upper and Middle Niger River Basin, (May).

Kim, J., Waliser, D. E., Mattmann, A., Goodale, C. E., Hart, A. F., Zimdars, P. A., & Crichton, J. (2013). Evaluation of the CORDEX-Africa multi- RCM hindcast: systematic model errors. *Climate Dynamics Observational, Theoretical and Computational Research on the Climate System*. http://doi.org/10.1007/s00382-013-1751-7

Knowles, N., Dettinger, M. D., & Cayan, D. R. (2006). Trends in snowfall versus rainfall in the western United States. *Journal of Climate*, *19*(18), 4545–4559. http://doi.org/10.1175/JCLI3850.1

Kuper, M., Mullon, C., Poncet, Y., & Benga, E. (2003). Integrated modelling of the ecosystem of the Niger river inland delta in Mali. *Ecological Modelling*, *164*(1), 83–102. http://doi.org/10.1016/S0304-3800(03)00006-1

Kurtzman, D., & Scanlon, B. R. (2011). Groundwater Recharge through Vertisols: Irrigated Cropland vs. Natural Land, Israel. *Vadose Zone Journal*, *10*(2), 662. http://doi.org/10.2136/vzj2010.0109

L'Hôte, Y., Mahé, G., Somé, B., & Triboulet, J. P. (2002). Analysis of a Sahelian annual rainfall index from 1896 to 2000; the drought continues. *Hydrological Sciences Journal*, *47*(4), 563–572. http://doi.org/10.1080/02626660209492960

Landmann, T., Schramm, M., Colditz, R. R., Dietz, A., & Dech, S. (2010). Wide area wetland mapping in semi-arid Africa using 250-meter MODIS metrics and topographic variables. *Remote Sensing*, *2*(7), 1751–1766. http://doi.org/10.3390/rs2071751

Le Barbé, L., & Lebel, T. (1997). Rainfall climatology of the HAPEX-Sahel region during the years 1950-1990. *Journal of Hydrology*, *188–189*(1–4), 43–73. http://doi.org/10.1016/S0022-1694(96)03154-X

Le Lay, M., Galle, S., Saulnier, G. M., & Braud, I. (2007). Exploring the relationship between hydroclimatic stationarity and rainfall-runoff model parameter stability: A case study in West Africa. *Water Resources Research*, *43*(7), n/a-n/a. http://doi.org/10.1029/2006WR005257

Lebel, T., & Ali, A. (2009). Recent trends in the Central and Western Sahel rainfall regime (1990–2007). *Journal of Hydrology*, *375*(1–2), 52–64. http://doi.org/10.1016/j.jhydrol.2008.11.030

Lebel, T., Amani, A., Cazenave, F., Lecocq, J., Taupin, J.-D., Elguero, E., … Robin, J. (1996). La distribution spatio-temporelle des pluies au Sahel : apports de l'expérience EPSAT-

Niger. In *L'hydrologie tropicale : géoscience et outil pour le développement* (pp. 77–98).

Lehner, B., Verdin, K., & Jarvis, A. (2006). HydroSHEDS, 1–27.

Leroux, M. (1997). Climat local, climat global / Local cfimate, global climate. *Revue de Géographie de Lyon, 72*, 339–345. http://doi.org/10.3406/geoca.1997.4715

Li, K. Y., Coe, M. T., & Ramankutty, N. (2005). Investigation of Hydrological Variability in West Africa Using Land Surface Models. *Journal of Climate*, *18*(16), 3173–3188. http://doi.org/10.1175/JCLI3452.1

Lopez, A. (2011). Modelling the Impact of Climate Change on Water Resources.

MacDonald, a M., Bonsor, H. C., Dochartaigh, B. É. Ó., & Taylor, R. G. (2012). Quantitative maps of groundwater resources in Africa. *Environmental Research Letters*, *7*(2), 24009. http://doi.org/10.1088/1748-9326/7/2/024009

Mahe G., Olivry J.-C, Dessouassi R., Orange D., Bamba F., Servat E., 2000 - Relations eaux de surface-eaux souterraines d'une rivière tropicale au Mali. C. R >Acad. Se, Paris, série 11a, 330 : 689-692.

Mahe, G., Bamba, F., Orange, D., Fofana, L., Kuper, M., Marieu, B., Cissé, N. (2002). Dynamique hydrologique du delta intérieur du Niger (Mali). *In : Séminaire International. Gestion Intégrée Des Ressources Naturelles En Zones Inondabless Tropicales Bamako (Mali) 20-23 Juin 2000.*, 179–195.

Mahe, G., Bamba, F., Soumaguel, A., Orange, D., & Olivry, J. C. (2009). Water losses in the inner delta of the River Niger : water balance and flooded area. *Hydrological Processes 23, 3157–3160 August 2009 in Wiley InterScience*, *3160*(August), 3157–3160. http://doi.org/10.1002/hyp.7389

Mahe, G., Lienou, G., Descroix, L., Bamba, F., Paturel, J. E., Laraque, A., Khomsi, K. (2013). The rivers of Africa : witness of climate change and human impact on the environment. http://doi.org/10.1002/hyp

Mahe, G., Mariko, A., & Orange, D. (2013). Relationships between water level at hydrological stations and inundated area in the River Niger Inner Delta, Mali. In *Deltas: Landforms, Ecosystems and Human Activities* (Vol. 358, pp. 110–115).

Mahe, G., Orange, D., Mariko, A., & Bricquet, J. P. (2011). Estimation of the flooded area of the Inner Delta of the River Niger in Mali by hydrological balance and satellite data. In *In: Hydro-climatology (ed. by S.W. Franks et al.). Proceedings of symposium J-H02 held during IUGG2011 in Melbourne, Australia, July 2011, 138–143. IAHS Pub. 344. IAHS*

Press, Wallingford, UK (pp. 138–143).

Mahe, L'Hote, Y., Olivry, J. C., & Wotling, G. (2001). Trends and discontinuities in regional rainfall of West and Central Africa: 1951–1989. *Hydrological Sciences Journal*, *46*(March 2015), 211–226. http://doi.org/10.1080/02626660109492817

Marie, J. (2002). DELMASIG : Un SIG d'aide à la décision pour une gestion régionale et locale. In M. BERTHOD & B. TEME (Eds.), *Gestion des Ressources et Aménagement du Fleuve Niger des Connaissances Scientifiques pour la Décision Publique* (pp. 94–98). Bamako, 14 -16 janvier 2002.

Mariko, A. (2003). *Caractérisation et suivi de la dynamique de l ' inondation et du couvert végétal dans le Delta intérieur du Niger (Mali) par télédétection* . (École doct). Université Montpellier II, Paris.

Mariko, A., Mahe, G. I. L., & Orange, D. (2013). Monitoring flood propagation in the Niger River Inner Delta in Mali : prospects with the low resolution NOAA / AVHRR data. *IAHS-IAPSO-IASPEI Assembly, Gothenburg, Sweden, July 2013 (IAHS Publ. 358, 2013)*, *2013*(July), 101–109.

Marlet, S., & N'Diaye, M. K. (2002). Impacts environnementaux de la mise en valeur d'une zone inondable par irrigation Evolution des sols et des eaux à l'Office du Niger (Mali). *In : Séminaire International. Gestion Intégrée Des Ressources Naturelles En Zones Inondabless Tropicales Bamako (Mali) 20-23 Juin 2000.*, 364–374.

Moret, B., Chaperon, P., Lamagat, J. P., & Molinier, M. (1986). *Monographie Hydrologique du fleuve Niger. Tome II – Cuvette Lacustre et Niger Moyen* (Ed. ORSTOM). Paris.

Moriasi, D. N., & Arnold, J. G. (2007). Model evaluation guidelines for systematic quantification of accuracy in watershed simulations. *Transactions of the American Society of Agricultural and Biological Engineers 2007*, *50*(3), 885–900. http://doi.org/10.13031/2013.23153

Neumann, R., Jung, G., Laux, P., Kunstmann, H., & Karlsruhe, F. (2007). International Journal of River Basin Management Climate trends of temperature, precipitation and river discharge in the Volta Basin of West Africa Climate trends of temperature, precipitation and river discharge in the Volta Basin of West Africa. *International Journal of River Basin Management Intl. J. River Basin Management*, *5*(1), 17–30. http://doi.org/10.1080/15715124.2007.9635302

Nicholson, S. E. (1981). Rainfall and Atmospheric Circulation during Drought Periods and Wetter Years in West Africa. *American Meteorological Society*, 18. http://doi.org/0027-

0644/81/102191-18$08.50

Nicholson, S. E. (2000). Land Surface Processes and Land Use Change Land. *Reviews of Geophysics, 38, 1 / February 2000*, *38*(1999), 117–139. Retrieved from http://www.peer.eu/fileadmin/user_upload/opportunities/metier/course3/c3_land_surface_processes.pdf

Nicholson, S. E. (2001). Climatic and environmental change in Africa during the last two centuries. *Climate Research*, *17*, 123–144.

Nicholson, S. E., & Palao, I. M. (1993). A RE-Evaluation of rainfall variability in the sahel. Part I. Characteristics of rainfall fluctuations. *International Journal of Climatology, Vol.13, 371-389*, 371–389. http://doi.org/0899-8418/93/0403371-19$14.50

Nygaard, I., Rasmussen, K., Badger, J., Nielsen, T. T., Hansen, L. B., Stisen, S., Togola, I. (2010). Using modeling, satellite images and existing global datasets for rapid preliminary assessments of renewable energy resources: The case of Mali. *Renewable and Sustainable Energy Reviews*, *14*(8), 2359–2371. http://doi.org/10.1016/j.rser.2010.04.001

Ogilvie, A., Belaud, G., Delenne, C., Bailly, J.-S., Bader, J.-C., Oleksiak, A., Martin, D. (2015). Decadal monitoring of the Niger Inner Delta flood dynamics using MODIS optical data. *Journal of Hydrology*, *523*, 368–383. http://doi.org/10.1016/j.jhydrol.2015.01.036

Oguntunde, P. G., & Abiodun, B. J. (2012). The impact of climate change on the Niger River Basin hydroclimatology, West Africa. *Climate Dynamics*, *40*(1–2), 81–94. http://doi.org/10.1007/s00382-012-1498-6

Oguntunde, P. G., Friesen, J., van de Giesen, N., & Savenije, H. H. G. (2006). Hydroclimatology of the Volta River Basin in West Africa: Trends and variability from 1901 to 2002. *Physics and Chemistry of the Earth, Parts A/B/C*, *31*(18), 1180–1188. http://doi.org/10.1016/j.pce.2006.02.062

Olago, D., Opere, A., & Barongo, J. (2009). Holocene palaeohydrology, groundwater and climate change in the lake basins of the Central Kenya Rift. *Hydrological Sciences Journal*, *54*(4), 765–780. http://doi.org/10.1623/hysj.54.4.765

Olivry, J. C. (1994). Fonctionnement hydrologique de la cuvette lacustre du Niger et essai de la modélisation de l'inondation du delta intérieur. *Grands Bassins Fluviaux (Olivry, J.C. et Boulegue, J., Ed. Sci.), Actes Du Colloque PEGI, INSU- CNRS-ORSTOM Paris, Colloque et Séminaire ORSTOM*, (1994), 267–280.

Orange, D., Mahe, G., Dembélé, L., Diakité, C. H., Kuper, M., & Olivry, J.-C. (2002). Hydrologie, agro-écologie et superficies d'inondation dans le delta intérieur du Niger. *Séminaire International. Gestion Intégrée Des Ressources Naturelles En Zones Inondabless Tropicales Bamako (Mali) 20-23 Juin 2000*, 208–228.

Oudin, L., Hervieu, F., Michel, C., Perrin, C., Andréassian, V., Anctil, F., & Loumagne, C. (2005). Which potential evapotranspiration input for a lumped rainfall–runoff model? *Journal of Hydrology*, *303*(1–4), 290–306. http://doi.org/10.1016/j.jhydrol.2004.08.026

Oyebande, L., & Odunuga, S. (2010). Climate change impact on water resources at the transboundary level in West Africa: the cases of the Senegal, Niger and Volta basins. (A. J. Adeloye & C. S. P. Ojha, Eds.)*Special Issue Analysis of Climate Change Impacts on Water Resources for Developing Economies Successes and Challenges*.

Ozer, P., Erpicum, M., Demaree, G., & Vandiepenbeeck, M. (2003). DISCUSSION of "Analysis of a Sahelian annual rainfall index from 1896 to 2000; the drought continues" The Sahelian drought may have ended during the 1990s. *Hydrological Sciences Journal-Journal Des Sciences Hydrologiques*, *48*(3), 489–492. http://doi.org/10.1623/hysj.48.3.489.45285

Paturel, J. E., Servat, E., Kouamé, B., Lubès, H., Ouedraogo, M., & Masson, J. M. (1997). Climatic variability in humid Africa along the Gulf of Guinea. Part II: An integrated regional approach. *Journal of Hydrology*, *191*(1–4), 16–36. http://doi.org/10.1016/S0022-1694(96)03069-7

Paturel, J.-E., Ouedraogo, M., Servat, E., Mahe, G., Dezetter, A., & Boyer, J.-F. (2003). The concept of rainfall and streamflow normals in West and Central Africa in a context of climatic variability. *Hydrological Sciences Journal*, *48*(August), 125–137. http://doi.org/10.1623/hysj.48.1.125.43479

Pedinotti, V., Boone, a., Decharme, B., Crétaux, J. F., Mognard, N., Panthou, G., Tanimoun, B. a. (2012). Evaluation of the ISBA-TRIP continental hydrologic system over the Niger basin using in situ and satellite derived datasets. *Hydrology and Earth System Sciences*, *16*(6), 1745–1773. http://doi.org/10.5194/hess-16-1745-2012

Pellerin, B. A., Wollheim, W. M., Feng, X., & Charles, J. V. (2007). The application of electrical conductivity as a tracer for hydrograph separation in urban catchments. http://doi.org/10.1002/hyp

Rebelo, L., Johnston, R., Hein, T., Weigelhofer, G., Dhaeyer, T., Kone, B., & Cools, J. (2012). Challenges to the integration of wetlands into IWRM : The case of the Inner

Niger Delta (Mali) and the Lobau Floodplain. *Environmental Science and Policy*, 1–11. http://doi.org/10.1016/j.envsci.2012.11.002

Sarr, B. (2012). Present and future climate change in the semi-arid region of West Africa: a crucial input for practical adaptation in agriculture. *Atmospheric Science Letters*, *13*(2), 108–112. http://doi.org/10.1002/asl.368

Schmidli, J., Goodess, C. M., Frei, C., Haylock, M. R., Hundecha, Y., Ribalaygua, J., & Schmith, T. (2007). Statistical and dynamical downscaling of precipitation: An evaluation and comparison of scenarios for the European Alps. *Journal of Geophysical Research*, *112*(D4), D04105. http://doi.org/10.1029/2005JD007026

Schwerdtfeger, J., Johnson, M. S., Couto, E. G., Amorim, R. S. S., Sanches, L., Campelo Júnior, J. H., & Weiler, M. (2014). Inundation and groundwater dynamics for quantification of evaporative water loss in tropical wetlands. *Hydrology and Earth System Sciences Discussions*, *11*(4), 4017–4062. http://doi.org/10.5194/hessd-11-4017-2014

Seiler, R., & Csaplovics, E. (2005). Monitoring landcover changes of the Niger inland delta (Mali) by means of Envisat-MERIS data, *2003*(May), 10–13. Retrieved from https://earth.esa.int/envisat/workshops/meris03/participants/89/paper_34_seiler.pdf

Seiler, R., Schmidt, J., Diallo, O., & Csaplovics, E. (2009). Flood monitoring in a semi-arid environment using spatially high resolution radar and optical data. *Journal of Environmental Management*, *90*(7), 2121–2129. http://doi.org/10.1016/j.jenvman.2007.07.035

Servat, E., Paturel, J. E., Lubès, H., Kouamé, B., Ouedraogo, M., & Masson, J. M. (1997). Climatic variability in humid Africa along the Gulf of Guinea. Part I: Detailed analysis of the phenomenon in Cote d'Ivoire. *Journal of Hydrology*, *191*(1–4), 1–15. http://doi.org/10.1016/S0022-1694(96)03068-5

Shepard, D. (1968). A two-dimensional interpolation function for irregularly-spaced data. *23rd ACM National Conference*, 517–524. http://doi.org/10.1145/800186.810616

Sircoulon. (1976). Les données hydro-pluviométriques de la sécheresse récente en Afrique inter-tropicale. Comparaison avec les sécheresses de 1913 et 1940. *Cahier ORSTOM, Hydrol.*, *13*(2).

Sircoulon, J. H. A. (1987). Variation des débits des cours d'eau et des niveaux des lacs en Afrique de l'Ouest depuis le début du 20ème siècle. *The Linflence of Clirnate Cllange Arid Cliiiratic Variability on the Hydrologic Regime and Water Resources; IAHS Publ.*,

(168).

Steve Tanessong, R. (2012). Evaluation of Eta Weather Forecast Model over Central Africa. *Atmospheric and Climate Sciences*, *2*(4), 532–537. http://doi.org/10.4236/acs.2012.24048

Sylla, M. B., Giorgi, F., Coppola, E., & Mariotti, L. (2013). Uncertainties in daily rainfall over Africa: assessment of gridded observation products and evaluation of a regional climate model simulation. *International Journal of Climatology*, *33*(7), 1805–1817. http://doi.org/10.1002/joc.3551

Tardy, Y., Bustillo, V., & Boeglin, J.-L. (2004). Geochemistry applied to the watershed survey. *Applied Geochemistry*, *19*(4), 469–518. http://doi.org/10.1016/j.apgeochem.2003.07.003

Taupin, J. D., Amani, A., & Lebel, T. (1998). Variabilite spatiale des pluies au Sahel : une question d ' echelles. *Waler Resources Variabiliry in Africa during Ihe XXlh Cen/ury (Proceedings of !.he Abidjan'98 Conference 143 Held at AbidJan, Cote D'lvoire, November 1998). I,\HS Pub!. No. 252.1998.*, (252), 143–158.

Termeer, C., Biesbroek, R., & van den Brink, M. (2012). Institutions for Adaptation to Climate Change: Comparing National Adaptation Strategies in Europe. *European Political Science*, *11*(1), 41–53. http://doi.org/10.1057/eps.2011.7

Testa, G., Gresta, F., & Cosentino, S. L. (2011). Dry matter and qualitative characteristics of alfalfa as affected by harvest times and soil water content. *European Journal of Agronomy*, *34*(3), 144–152. http://doi.org/10.1016/j.eja.2010.12.001

Vandersypen, K., Keita, A. C. T., Coulibaly, Y., Raes, D., & Jamin, J. Y. (2007). Formal and informal decision making on water management at the village level: A case study from the Office du Niger irrigation scheme (Mali). *Water Resources Research*, *43*, 1–10. http://doi.org/10.1029/2006WR005132

Vegas, L. (2002). Modeling and Prediction, 1–8. http://doi.org/10.1006/rwas.2002.0172

Vittek, M., Brink, A., Donnay, F., Simonetti, D., & Descl??e, B. (2013). Land cover change monitoring using landsat MSS/TM satellite image data over west Africa between 1975 and 1990. *Remote Sensing*, *6*(1), 658–676. http://doi.org/10.3390/rs6010658

Wada, Y., Beek, L. P. H. Van, & Bierkens, M. F. P. (2011). Supplementary material to " Modelling global water stress of the recent past : on the relative importance of trends in water demand and climate variability ," (December), 1–12.

Wei, J., Dirmeyer, P. a., Wisser, D., Bosilovich, M. G., & Mocko, D. M. (2013). Where Does

the Irrigation Water Go? An Estimate of the Contribution of Irrigation to Precipitation Using MERRA. *Journal of Hydrometeorology*, *14*(1), 275–289. http://doi.org/10.1175/JHM-D-12-079.1

Weissman, D. E., Bourassa, M. A., O'Brien, J. J., & Tongue, J. S. (2003). Calibrating the Quikscat/SeaWinds radar for measuring rainrate over the oceans. *IEEE Transactions on Geoscience and Remote Sensing*, *41*(12 PART I), 2814–2820. http://doi.org/10.1109/TGRS.2003.817975

Wilby, R. L., Charles, S. P., Zorita, E., Timbal, B., Whetton, P., & Mearns, L. O. (2004). Guidelines for Use of Climate Scenarios Developed from Statistical Downscaling Methods, (August), 1–27.

Wisser, D., Frolking, S., Douglas, E. M., Fekete, B. M., Schumann, A. H., & Vörösmarty, C. J. (2010). The significance of local water resources captured in small reservoirs for crop production – A global-scale analysis. *Journal of Hydrology*, *384*(3–4), 264–275. http://doi.org/10.1016/j.jhydrol.2009.07.032

Wolski, P., Savenije, H. H. G., Murray-Hudson, M., & Gumbricht, T. (2006). Modelling of the flooding in the Okavango Delta, Botswana, using a hybrid reservoir-GIS model. *Journal of Hydrology*, *331*(1–2), 58–72. http://doi.org/10.1016/j.jhydrol.2006.04.040

Wu, Y. H., Key, R., Sander, S., Blavier, J. F., & Rider, D. (2011). A Panchromatic Imaging Fourier Transform Spectrometer for the NASA Geostationary Coastal and Air Pollution Events Mission. *Cryogenic Optical Systems and Instruments Xiii*, *8150*(818), 1–12. http://doi.org/81500o\n10.1117/12.892437

Xu, C. Y., & Singh, V. P. (2002). Cross comparison of empirical equations for calculating potential evapotranspiration with data from Switzerland. *Water Resources Management*, *16*(1), 197–219. http://doi.org/10.1023/A:1020282515975

Yue, S., Pilon, P., & Cavadias, G. (2002). Power of the Mann-Kendall and Spearman's rho tests for detecting monotonic trends in hydrological series. *Journal of Hydrology*, *259*(1–4), 254–271. http://doi.org/10.1016/S0022-1694(01)00594-7

Zhang, Q., Xu, C. Y., Tao, H., Jiang, T., & Chen, Y. D. (2010). Climate changes and their impacts on water resources in semiarid regions: A case study of the wei river basin, China. *Stochastic Environmental Research and Risk Assessment*, *24*(3), 349–358. http://doi.org/10.1007/s00477-009-0324-0

Zwarts, L., Beukering, P. Van, Koné, B., Wymenga, E., & Taylor, D. (2006). The Economic and Ecological Effects of Water Management Choices in the Upper Niger River:

Development of Decision Support Methods. *International Journal of Water Resources Development*, *22*(1), 135–156. http://doi.org/10.1080/07900620500405874

Zwarts, L., Van Beukering, P., Kone, B., & Wymenga, E. (2005). The Niger, a lifeline Effective water management in the Upper Niger Basin. *RIZA, Lelystad / Wetlands 989 International, Sévaré / Institute for Environmental Studies (IVM), Amsterdam / A&W 990 Ecological Consultants, Veenwouden. Mali / the Netherlands*, *169*(Ivm), 169.

Appendixes

Appendix A

Supplementary information:

Table3. 4: *Data availability and periods of records for the main climatic variables and evaporation at Mopti synoptic station (longitude = -4.1, latitude=14.52, Elevation=272m)*

Source: National Meteorological service Mali

Data	Units	Periods of records	Time scale
Air Temperature minimum & maximum	°C	1980 - 2010	daily observed
Mopti Pan evaporation	mm	1970 - 2009	monthly
Relative humidity minimum & maximum	%	1980 - 2010	daily observed
Wind speed	m/s	1980 - 2010	daily observed

Table3. 5: *Inputs data of all potential ET methods used in this study*

ET Methods	Data requirements	Variables description
Hargreaves method (HARG)	T_a and R_s (mean daily air temperature and solar radiation respectively)	Air temperature measured at height of 1.2 m above the ground, (°C); Solar radiation estimated for clear sky (no clouds) condition as the total incoming short-wave radiation.
Hamon method (HAM)	T_a and DL (mean daily air temperature and day length)	Day length the maximum possible daylight hours for a given day calculated from the sunset hour angle.
Oudin method (OUD)	T_a, R_e, λ, and ρ (mean daily air temperature, extraterrestrial radiation, latent heat flux and density of water)	The extraterrestrial radiation, R_e, is expressed in equivalent evaporation units for a given latitude and day;

		The latent heat is the energy used for phase change from liquid to vapor during the ET process; The water density is at 20°C.
Modified Turc method (TUR)	T_{max} and S_t (daily maximum air temperature, solar radiation)	S_t is the total incoming shortwave Radiation
Penman – Monteith combination equation (PMO)	R_n, G, ϒ, ʎ, Δ, C_p, e_s, e (net solar radiation, soil heat flux, psychrometric constant, latent heat flux, slope of vapor pressure, specific heat, saturation vapour pressure and actual vapour pressure)	The net radiation is the difference between incoming and outgoing radiation; Soil heat flux is the sensible heat conducting into or out of the soil; Psychrometric constant is derived from the measured the atmospheric pressure in the area; Slope of vapor pressure is the gradient of the function de_s/dT_a; C_p is the specific heat of the air at constant pressure; $Θ_s$ & Θ are the maximum and actual partial pressure of water vapor in the air; Surface albedo is the proportion of incident solar radiation reflected by the surface

Appendix B

a.) Potential PET estimation methods

1) Edited potential evapotranspiration (PE) model published by Oudin (2005)

$$PE = \frac{R_e}{\lambda\rho} \frac{T_a+5}{100} \quad \text{if } T_a + 5 > 0$$

$$PE = 0 \qquad \text{(Eq.a.1)}$$

where: PE = rate of potential evapotranspiration in mm per day;

Re = extraterrestrial radiation in MJ per m^2 per day;

λ = latent heat flux for the vaporization (as 2.45 Mj per kg);

ρ = value of the density of water (ρ =995.6502 kg per m^3); and

T_a = air temperature (°C) which correspond to the mean daily air temperature.

2) Penman - Monteith combination equation (PMO)

The Penman - Monteith equation is the most physically based model and corresponds to the Penman equation which is the updated equation recommended by FAO (Allen et. al, 1998) known as the FAO-56 Penman-Monteith. It is expressed as (Allen et. al, 1998).

$$PMO = \frac{1}{\lambda} \frac{\Delta(R_n+G)+\rho_a c_{p(\theta_s-\theta)}}{\Delta+\gamma\left(1+\frac{r_s}{r_a}\right)} \qquad \text{(Eq.a.2)}$$

where PMO is the ET rate (mm d-1), Ta is mean air temperature (°C), v is wind speed (m s-1) at 2 m above the ground, G is the soil heat flux, which can usually be neglected in the tropics (De Bruin, 1983), Δ is the slope of the saturation vapor pressure curve, γ is the psy-chrometric constant (see calculation under radiation), θ and θ_s is the actual and saturated vapor pressure at given RH in kPa (see calculation under radiation), ρ_a is the mean air density at constant pressure in kgm^{-3}, c_p is the specific heat of the air in MJkg-1°C pressure in kPa (see calculation under radiation), r_s is the surface resistance in s m^{-1},and r_a is the aerodynamic resistance in s m^{-1}. r_s in the case of open water is 0 and r_a can be calculated from Thom and Oliver (1977) (as cited in Schwerdtfeger et al., (2014):

3) Priestley - Taylor equation (PRT)

Xu & Singh, (2002), highlighted that the Priestley - Taylor model derived after Priestley and Taylor, (1972); is a simplified version of the combination equation of Penman (1948). It is generally used when surface areas were wet and therefore the atmosphere is saturated. Thus,

the Priestley - Taylor coefficient α_{PRT} is introduced, which is multiplied by the energy component:

$$PRT = \alpha_{PRT} \frac{\Delta}{\Delta+\gamma} \frac{R_n}{\lambda} \qquad \text{(Eq.a.4)}$$

where α_{PRT} can be set to 1.18 (Schwerdtfeger et al., 2014).

4) Hargreaves equation (HAG)

The combined form of Hargreaves equation (HAG) is the Hargreaves and Samni (1982, 1985) formula after Hargreaves, 1975 (as in Schwerdtfeger et al., 2014). The equation can be expressed as:

$$HAG = 0.0135(T_a + 17.8)R_s \qquad \text{(Eq.a.5)}$$

Where: T_a is the average temperature, R_s is the global solar radiation which can be calculated from formula for estimating R_s from the temperature range (TR), the extraterrestrial radiation (R_a); and an empirical coefficient (k_r) depending on the station location: $R_s = k_r * R_a * TR^{0.5}$

5) Modified Makkink equation (MAK)

Makkink (1957) estimated ET in millimeters per day over 10 - day periods for grassed lands under cool climatic conditions of the Netherlands. After Makkink, 1957; Abtew and Melesse, 2013 (as cited in Schwerdtfeger et al., 2014) , calibrated the Makkink equation to the simple Abtew method (Eq. a.6) for tropical South Florida and has the following form:

$$MAK = 0.743 \frac{\Delta S_t}{(\Delta+\gamma)\lambda} \qquad \text{(Eq.a.6)}$$

where: S_t is the solar radiation in $MJm^{-2}\ day^{-1}$ (see Eq.b.14 below).

6) Simple Abtew equation (ABT)

The simple Abtew equation was developed for tropical South Florida by Abtew and Melesse, (2013) from open water evaporation and wetland lysimeter studies (work cited in Schwerdtfeger et al., 2014). It can be expressed as:

$$ABT = K_1 \frac{S_t}{\lambda} \qquad \text{(Eq.a.7)}$$

where K_1 is a dimensionless coefficient given with 0.53 (Schwerdtfeger et al., 2014).

7) Modified Turc equation (TUR)

We use the empirical Turc equation modified for a humid subtropical region. Tmax is used instead of Ta since it showed a better fit with observed data (Schwerdtfeger et al., 2014). The modified Turc equation is written as:

$$\mathrm{TUR} = \mathrm{K}_2 \frac{(23.89\mathrm{S_t} + 50)\mathrm{T_{max}}}{\mathrm{T_{max}} + 15} \qquad \text{(Eq.a.8)}$$

where the coefficient K_2 has the value 0.013 derived from the original Turc equation by Abtew and Melesse, (2013) (as in Schwerdtfeger et al., 2014)

8) Hamon equation (HAM)

Hamon (1961) (as in Oudin et al., 2005)derived a potential evapotranspiration method based on the mean air temperature and is expressed as:

$$\mathrm{HAM} = 2 * \mathrm{DL}^2 * \theta_s * \mathrm{e}^{\left(\mathrm{T_a}/_{16}\right)} \qquad \text{(Eq.a.9)}$$

Where:

HAM = evapotranspiration, [mm day^{-1}]

DL = average number of daylight hours per day during the month

θ_s = saturated vapor pressure at temperature T

T_a= mean daily air temperature [° C]

b.) Calculation of short and long-wave radiation

The relative distance between the earth and the sun (dimensionless) dr is given by the following equation:

$$\mathrm{d_r} = 1 + 0.033\ \cos\left(\frac{2\pi}{365}\ \mathrm{j}\right) \qquad \text{(Eq.b.1)}$$

where: j is the Julian Day Number.

The solar declination δ in radians is calculated by:

$$\delta = 0.4093 \sin\left(\frac{2\pi}{365}\mathrm{j} - 1.405\right) \qquad \text{(Eq.b.2)}$$

The sunset hour angle ω_s in radians is given by:

$$\omega_s = \arccos(-\tan \emptyset \tan \delta) \qquad \text{(Eq.b.3)}$$

where: $\emptyset$ is the latitude of the study site (negative for the Southern Hemisphere).

The sunset hour angle is used to calculate the maximum possible daylight hours N(h):

$$N(h) = \frac{24}{\pi}\omega_s \qquad \text{(Eq.b.4)}$$

Then, the extra-terrestrial solar radiation S_0 in MJ $m^{-2}d^{-1}$ is:

$$S_0 = \frac{G_{sc} * d_r}{\pi}(\omega_s \sin\emptyset \sin\delta + \cos\emptyset \cos\delta \sin\omega_s) \qquad \text{(Eq.b.5)}$$

where: G_{sc} is the solar constant being 118.11 MJ $m^{-2}d^{-1}$.

The saturated vapor pressure θ_s in kPa can be calculated by:

$$\theta_s = 0l6108\exp\left(\frac{17.27T_a}{237.3T_a}\right) \qquad \text{(Eq.b.6)}$$

where: T_a is the daily mean air temperature in °C. For a physically based model of evaporation calculation the gradient of the function $d\theta_s/dT$ in kPa°C^{-1} is calculated by:

$$\Delta = \frac{4098\theta_s}{(237.3+T_a)^2} \qquad \text{(Eq.b.7)}$$

The vapor pressure θ in kPa at a given RH can then be derived from:

$$\theta = \theta_s\left(\frac{RH}{100}\right) \qquad \text{(Eq.b.8)}$$

where RH is relative humidity in %, which is not available at the study area.

The energy used for phase change from liquid to vapor during the process of evaporation is the latent heat of vaporization in $MJkg^{-1}$. This is the required for separating the molecules can be set as 2.45, MJ kg^{-1}.

$$\lambda = 2.45 \qquad \text{(Eq.b.9)}$$

where: T_s is the surface temperature of the water in °C. The psychrometric constant γ in kPa°C^{-1} is derived from:

$$\gamma = 0.0016286\frac{P}{\lambda} \qquad \text{(Eq.b.10)}$$

where: P is the atmospheric pressure in kPa, and can be derived from:

$$P = 101.3\left[\frac{293-0.0065z}{293}\right]^{5.26} \qquad \text{(Eq.b.11)}$$

where: z elevation above sea level, m.

Martínez-Lozano et al., (1984) (cited in Schwerdtfeger et al., 2014), stated that the Angstrom coefficients a, and b vary with a change in latitude, height of the station, albedo, mean solar altitude, vapor and pollution concentration in the air. Many approaches to derive the Angstrom coefficients have been undertaken. In this study a, and b were derived from the approach in the previous paper (Glover & McCulloch, 1958) due to restriction in data availability. This approach depends only on the latitude of the study site and can be formulated with:

$$a = 0.29\cos\emptyset \qquad \text{(Eq.b.12)}$$

which result in a value of a = 0.28 in our case. b was set to 0.52 since it was practically constant (Schwerdtfeger et al., 2014). These correspond well with the values given in Shuttleworth (1993) (as in Schwerdtfeger et al., 2014) (a = 0.25 and b = 0.5) for average climates, when there is not enough information available for calculating the Angstrom coefficients.

The Angstrom coefficients are used to calculate the clear sky radiation S_{t0} in $MJm^{-2}d^{-1}$ according to:

$$S_{t0} = (a + b) * S_0 \qquad \text{(Eq.b.13)}$$

where: S_t is the solar radiation or total incoming short-wave radiation in $MJm^{-2}d^{-1}$ derived from:

$$S_t = \left(a + b\frac{n}{N}\right) * S_0 \qquad \text{(Eq.b.14)}$$

with nN^{-1} as the cloudiness factor. n are the bright sunshine hours of a day and N is the total day length already explained above. With the solar radiation S_t the net shortwave radiation S_n in $MJm^{-2}d^{-1}$ is calculated by:

$$S_n = (1 - \alpha)S_t \qquad \text{(Eq.b.15)}$$

where: the albedo for open water α was set to 0.08. It is the part of short-wave radiation, where losses due to reflections are taken into account. The long-wave net radiation Ln in $MJm^{-2}d^{-1}$ is the net long-wave surface emission and can be expressed as:

$$L_n = \sigma\left[\frac{(T_{max}+273.16)^4+(T_{min}+273.16)\hat{}4}{2}\right]\left(0.34-0.14\sqrt{\theta}\right)\left[1.35\frac{S_t}{f}-0.35\right] \qquad \text{(Eq.b.16)}$$

where: σ is the Stefan Boltzmann constant (4.903×10^{-9} $MJm^{-2}K^{-4}$) and f is the adjustment for cloud cover, derived from:

$$f = (0.75 + 2^{-5} * z)S_o \qquad \text{(Eq.b.17)}$$

And the net radiation Rn in $MJm^{-2}d^{-1}$ finally is:

$$R_n = S_n + L_n \qquad \text{(Eq.b.18).}$$

Appendix C

International Journal of Current Engineering and Technology
E-ISSN 2277 – 4106, P-ISSN 2347 – 5161

Available at http://inpressco.com/category/ijcet

Research Article

Recent trend analysis of hydro-climatic data in the upper and Niger Inland Delta of the Niger River basin (West Africa)

Moussa Ibrahim*, Abdouramane Gado Djibo and Abel Afouda

*GRP Climate Change and Water Resources, West African Science Service Center on Climate Change and Adapted Land Use, University of Abomey Calavi, Benin
International Institute for Water and Environmental Engineering (2iE), 01 BP 594, Ouagadougou 01, Burkina Faso

Accepted 04 Dec 2016, Available online 10 Dec 2016, **Vol.6, No.6 (Dec 2016)**

Abstract

The fresh water resources of the West Africa stressed due to the increasing population. The climate change has also affected the water resource availability due to the occurrence of recurrent and uneven extreme events such as drought and flood. In the context of Niger river basin, Niger Inland Delta (NID) water resource availability is a concern for water management over the basin. In this study, we evaluate the recent hydro-climatic trends in the upper basin and Niger inland delta of the Niger River basin in order to assess the potential climate change. Trend of Niger inland delta pan-evaporation were also analysed. An overall decrease of precipitation (1950-2010) and runoff (1950-2010) and an increase of temperature (1980-2010) and pan-evaporation (1970-2009) were observed (1950-2010); however, when a long study period is considered, all the trends are not statistically significant. In the same way, when IPCC standard period (1981-2010) is considered; all the climatic data show a significantly increasing trend in the NID except the evaporation whose trend is not significantly decreasing over the area. In this period, Significant decreasing trends are found for mean annual discharge at a 0.05 significance level. Therefore, it cannot be concluded that the climate has changed in the Niger basin with regards to trend analysis. But, it should be noted that the water resource availability will decrease in the NID if the current trend in the hydro-climatic data remains. Moreover, a spatial analysis shows that, the increase in precipitation is higher in the western part of the NID compared to eastern and inland part of the wetland. However, the results presented here shows a general idea about the water resource conditions in time and space, and should be taken as a basic skill for water resource management instead of models in order to reduce uncertainties.

Keywords: *Niger inland delta, hydro-climatic data, trend analysis, climate change, water resources availability*

1. Introduction

Studies of regional and global climatic changes and variabilities and their impacts on the water resources have received considerable attention in recent years. Intergovernmental Panel on Climate Change (IPCC) revealed that, the historical climate record for Africa shows warming of approximately 0.7°C over most of the continent during the 20th century, and a decrease in rainfall over large portions of the Sahel (IPCC, 2007). The surface water resources of the major river basins of West Africa in general and in particular the Sahel region show very sensitive inter-annual fluctuations due to climate changes facing this vast region for over thirty years (Le Lay *et al.*, 2007; Lebel & Ali, 2009). The identification and characterization of the variability of water resources in order to better guide the mitigation approaches of potential impacts have generated much more interest among the scientific world.

Water resource management is a major issue in Niger Inland Delta (Mariko 2003; Zwarts *et al.*, 2005). The past and current trend of the Hydro-climatic data is of very high importance for a more sustainable evaluation and characterization of the past and present status of water resource (Descroix *et al.*, 2009). Therefore, the hydro-climatic data can be the major source of information for the analysis of the water resource availability. In arid and semi-arid areas of West Africa rainfall is a concern for both people and the scientific world; with its important role in the successful development of the agriculture, irrigation, water supply, reservoir operation and hydro-power generation. These latter, are strongly penalized by declining resources (Mariko *et al.*, 2013). Therefore, to improve understanding about the water budget for developing strategies on water resources management over the Niger River Basin (NBR); identification of the temporal and spatial patterns of rainfall that influence the hydrological processes is a must (Oguntunde and Abiodun, 2012) . To know the recent status of water

*Corresponding author **Moussa Ibrahim**'s Tel.: +227-904-456-02

resources downstream the NID in the future and to develop water balance model for satisfying hydrological functioning; understanding the spatial assessment of rainfall volume upstream is a key factor. Assessment of the overall quality of the climate information from the available data particularly precipitation trend analysis showing the degree of temporal and spatial variability which is key tools impacting on a number of concerns such as population growth, economy, society, environment and water resources (Hiernaux *et al.*, 2009; Frappart *et al.*, 2009; Mahe *et al.*, 2013).

In this study the potential temporal and spatial trends of hydro-climatic data are considered for the upper and middle basins of the Niger river. Using the available meteorological data and the statistical methods, the major components of the water resource namely, temperature, evapotranspiration and the precipitation are analyzed.

To assess the overall quality of the climate information it is necessary to analyze trends in the hydro-climatic data. So, statistical approach is proposed to investigate consistency in the recent trends on climate with observations of hydro-climatic variables. Furthermore, the main discharge stations on the Niger basin are used to assess the runoff trend. This allows an assessment of the overall quality of the climate information from the available data in the Niger River Basin. This study focuses on the hydro-climatology of the Upper Niger River and The Niger Inland Delta (NID). The Upper Niger is defined as the Niger basin up to and not including the NID.

2. Review of the previous studies on the sahelian hydro-climatic variability

Many studies related to rainfall time series fluctuations were done across West Africa that include the NID or different parts in NRB; and show a noticeable decline trend from the 70 particularly in the Sahel region (Descroix *et al.*, 2009; Druyan, 2011; Hubert P., Carbonnel, 1987; Le Barbé & Lebel, 1997; Li, Coe, & Ramankutty, 2005; Mahe *et al.*, 2001; Sharon E. Nicholson & Palao, 1993; Sharon E. Nicholson, 2000; Sircoulon, 1987). The study done by Oguntunde *et al.* (2012) has included the whole NRB but the study was related to climate change. They used the climate models to assess the potential change of different climatic feature within NRB using meteorological data. The average seasonal temperature of NRB was studied using data from 6-hourly sea surface temperature data for present-day and future; and the temperature changes were plotted (Oguntunde & Abiodun, 2012). Generally, the mean baseline and future mean surface temperatures for this region show increases over a 20-year period.

New approaches to improve the estimate of one-time parameters at different time steps (decadal, yearly, etc.) were tested (Le Barbé & Lebel, 1997; T. Lebel *et al.*, 1996; Taupin, Amani, & Lebel, 1998) to improve visualization of rainfall variability in the Sahel. Similarly in the past, some authors have studied the evolution of rainfall in the Sahel (L'Hôte, Mahé, Somé, & Triboulet, 2002; J. E. Paturel *et al.*, 1997; J.-E. Paturel *et al.*, 2003; Servat *et al.*, 1997). According to their results, since the beginning of the century, four periods of droughts 1907-1916, 1940-1949, 1968-1974 and 1980-1984 affected the Sahelian zone with transboundary rigorousness (Sircoulon, 1976). Among which it has been noticed some dramatic drought's years like the 1973-1974 and 1983-1984 ones; for their considerable extension beyond the Sahel and their persistence over several years.

Many authors have studied the rainfall variability in the Sahel which has strongly affected the discharge evolutions over the past decades in West Africa (WA) (L'Hôte *et al.*, 2002; J.-E. Paturel *et al.*, 2003). However, after the wet periods 1950s and 1960s, and the strong rainfall deficit since 1970; some studies have highlighted that the rainy seasons are becoming wetter and wetter in some parts of WA (Thierry Lebel & Ali, 2009; Ozer, Erpicum, Demaree, & Vandiepenbeeck, 2003). Therefore, it is important to assess this affirmation from those authors in the NID's local condition. Recently, Descroix *et al.*, (2015), based on the variation of rainfall, pointed out a strong fluctuations in river discharge with a generally decreased trend from 1960 to 2010. While (Mahe *et al.*, 2013) emphasized on the nonlinear effect of the negative rainfall variation over WA resulting in a decrease runoff.

Therefore, this study seeks to analyze the recent spatiotemporal change of annual rainfall in the Niger river basin in general and the NID in particular during 1981 - 2010; including analysis of discharge trends by using Man-Kendall test as non-parametric approach and a simple linear regression method, known as a parametric approach. Also a nonlinear trend analysis was performed by means of polynomial regression method. In order to have good understanding of the hydro-climatic change, analyses are not only based on rainfall and runoff time series but include temperature and, evaporation.

3. Materials and Methods

3.1. Study Area

The Niger River Basin (NRB) is a transnational catchment shared by ten riparian countries: Algeria, Benin, Burkina Faso, Cameroon, Chad, Guinea, Ivory Coast, Mali, Niger and Nigeria. NRB lies between latitudes 5°N and 24°N and longitudes 17°E to 12°W and covers a huge area of land of the order of 2.27 million km². The source of the Niger is located close to the Fouta Djallon Mountains in the South of Guinea at an altitude about 800 m. With a length of 4,200 km, NRB is the third longest river in Africa after the Nile and the Congo River. The watershed is 8.5% in Algeria, 2.0% in Benin, 3.4% in Burkina Faso, 3.9% in Cameroun, 0.9% in Chad, 4.3% in Guinea, 1.0% in Ivory Coast, 25.5% in Mali, 24.8% in Niger, and 25.7% in Nigeria.

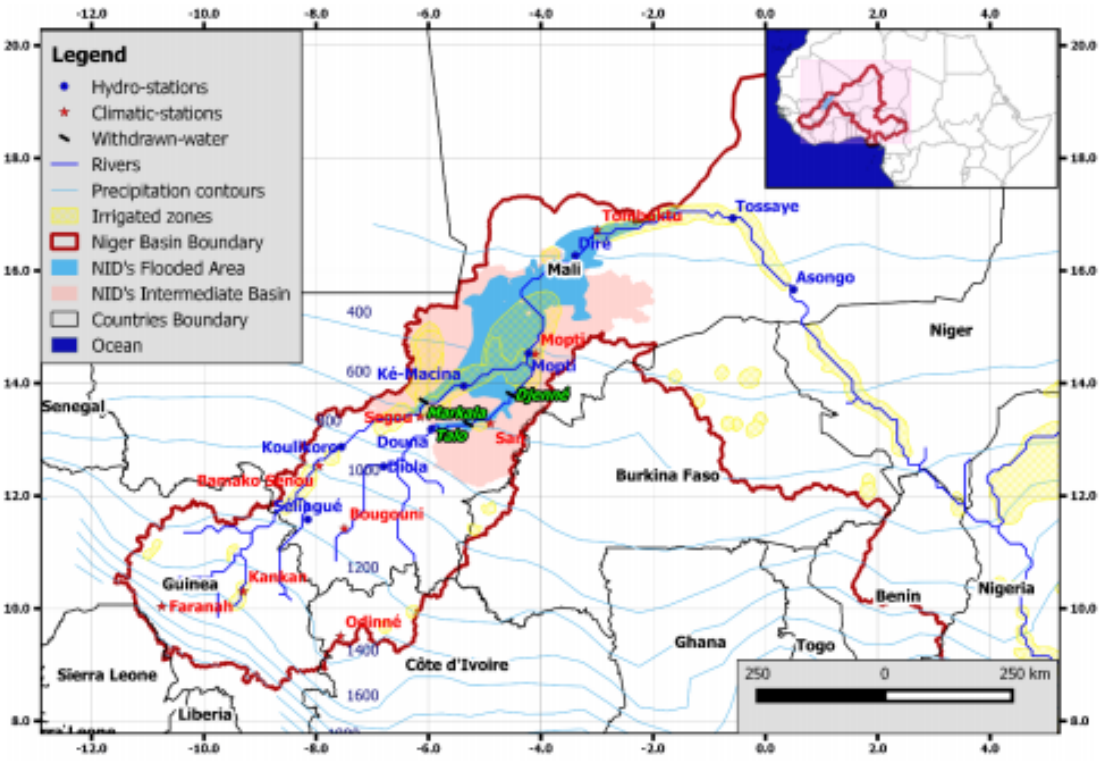

Fig.1: Location Map of the study area

The coverage of the Niger basin is shown in Figure 1. The Niger Inland Delta (NID) has a maximum submerged area of 73000 km² (Mahe *et al.*, 2009) and is one of the most important wetland in Mali. Major tributaries to the NID include the Niger river, and the Bani river (both rivers flow from Guinea and Ivory Coast respectively). Average annual river flows in the Niger Basin, observations since 1907, at the inlet monitoring station of delta (Koulikoro, Mali) has been as high as 2308 m³/s (1925)and as low as 637 m³/s (1989) (Zwarts *et al.*, 2005). A large part of the water is lost in the NID due to evaporation and seepage. Temperatures vary between approximately 10°C and 45°C depending on season, time of day, and elevation. Highest rainfall levels occur in the south west and can be as high as 2000 mm/year, where levels in the north-eastern regions can be as low as 250 mm/year. Throughout the region, main land cover types include savanna, grassland, rain forest, water bodies, shrubs and croplands (Oguntunde, *et al.*, 2012).

3.2. Data source and quality control

The data used in this study include climate, hydrological, and topographical data. To analysis the long-term hydroclimatic trends in the NRB the following available hydro-meteorological datasets were used. Daily precipitation and temperature data (1950 - 2010) from 5 National Meteorological Observatory (NMO) stations were provided by the countries National Meteorology Agency and the AGHRYMET regional Centre of Niamey. The monthly and annual precipitation & temperature used in this study were compiled from the 5 rain gauge stations, whose records started from 1950s, 1960s, and 1980s and ended in 2006 & 2010 (each station having a 30-year long record at least). The location of the stations in the basin is shown in Figure 1, and their longitudes latitudes are listed in Table 1. In addition, the daily streamflow data (Table 2) of the NRB used in this study, was sourced from the Bureau of Niger Authority Basin (NBA) of the Niger river.

Besides, to view the long-term climatic trends in the NID the historical available remote sensing precipitation: Modern-Era Retrospective Analysis for Research and Applications (MERRA), MERRA precipitation with the observation-based Global Precipitation Climatology Project (GPCP) pentad product 1-degree daily data set were used. The data cells that cover the study area were sorted out from the daily climate data of the world. The range of the spatial coverage was taken between 10°W to 10°E and 5°N to ~20°N. The annual aver-age and the average of the cells were calculated for year 1996 to 2013.

Table 1: List of the stations and available climate data

No.	Station name	Latitude (°decimal)	Longitude (°decimal)	Country	Climatic Data	Range
1	Faranah	10.03	-10.75	Guinea	Precipitation	1950-2006
					Temperature	-
2	Kankan	10.30	-9.30	Guinea	Precipitation	1950-2006
					Temperature	-
3	Sikasso	11.35	-5.68	Mali	Precipitation	1950-2010
					Temperature	-
4	Bamako-Senou	12.53	-7.95	Mali	Precipitation	1950-2010
					Temperature	1980-2010
5	Bougouni	11.42	-7.50	Mali	Precipitation	1950-2010
					Temperature	1980-2010
6	Segou	13.40	-6.15	Mali	Precipitation	1950-2010
					Temperature	1980-2010
7	Mopti	14.52	-4.10	Mali	Precipitation	1950-2009
					Temperature	1980-2010
					Pan ET	1970-2009
8	Tombuktu	16.72	-3.00	Mali	Precipitation	1950-2010
					Temperature	-
9	San	13.28	-4.90	Mali	Precipitation	1950-2010
					Temperature	-

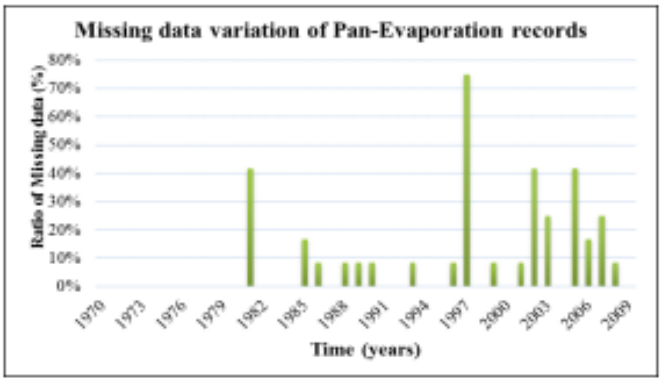

Figure 2: Gap ratios in monthly Pan evaporation records at Mopti (1970-2009)

Table 2: Hydrometric stations on the Niger Basin and available data

Serial No	Longitude	Latitude	River	Station Name	Observation period	Country
1	-7.56	12.86	Niger	Koulikoro	1921-2013	Mali
2	-5.39	13.96	Niger	Ké-Macina	1954-2013	Mali
3	-5.9	13.21	Bani	Douna	1923-2004	Mali
4	-3.38	16.28	Niger	Diré	1950-2013	Mali
5	-4.22	14.53	Niger	Mopti	1952-2013	Mali
6	-8.66	11.68	Niger	Banankoro	1968-2013	Niger

Data quality control was conducted for all variables since there is a lack of good climate data throughout African Sahel. For each station, rain gauges' time series have less than 10% missing data as this ratio varies from 0 to 6% for all 9 stations over the period. Also, only a few gaps were found in the other climate data records, and they do not alter the quality. For the Mopti pan evaporation records, figure 3 shows that the annual missing data ratios are significant (>10%) at the beginning of the series, and more pronounced in 1997 (75%). We have an average rate of missing data of 9% per year for the period 1970-2009. Interpolation process was used to approximately fill the gaps. Then, annual values were by summing up for a year all the monthly values.

For runoff, the data are characterized by missing data ratios of 0 to 46% over the period. Runoff analyses were done with the raw data and periods of non-negligible discharge flow found. Mean runoff of a given month is considered insignificant if it is less than 25% of the mean monthly discharge of the entire period. Time series with more than one month of missing data within the hydrological year of non-negligible discharge were omitted.

3.3. Data Analyses

3.3.1. Trend analysis for considered time series

From literature review, moving average method is not a relevant test for trend analysis. We have two types of trend: a linear and nonlinear. Classically in literature we can find the linear trend as linear regression that fits data with straight lines in selected time intervals (e.g., linear test, Mann-Kendal, etc.). Such a trend is frequently sensitive to the selected time series intervals. Therefore, based on our data, to evaluate the trend and variability of hydro-climatic elements including precipitation, temperature, Pan-evaporation and river discharge in the basin during the recent years, we employed some trend analysis methods, such as the moving-average method, non-linear regression method and Mann-Kendall method. A trend is considered to be present if it has been detected by at least 2 tests. The trend analysis tests were applied on stations for available climatic data on the upper and Niger Inland Delta regions. Using Thiessen polygon method, mean annual catchment temperature and precipitation were calculated for the upper Niger and NID for the year 1950 - 2006 and 1950 - 2010 respectively, from the stations where data was available (Table 1). Stations that do not have data of temperature during the period of collection were not considered (Table 1).

3.3.2. Breakpoints analyses of runoff

Another approach was to assess change points. The breakpoint analysis in the annual maximal discharge using Cross-Entropy method (Priyadarshana and Sofronov, 2014) embedded in the R-software. The Cross-Entropy method seems the most appropriate techniques providing multiple breaks and offering the possibility for the user to choose the number of breaks desired; as compared to other widely used statistical methods such as the non-parametric Pettitt test (Pettitt, 1979), and Hubert's Segmentation (Hubert, 1989). Also, this method is more suitable to the context of high inter-annual rainfall and runoff variability in West Africa.

3.3.3. Precipitation spatial analysis

In this study, we use the interpolated technique, explicitly, Ordinary Kriging (OK) to spatial analysis of annual precipitation trends in the basin. The OK is a stochastic model that incorporate autocorrelation, referring to the statistical connections among the measured sites in order to provide estimates for accuracy in predictions (Ali, Lebel, and Amani, 2005). Furthermore, the performance technique of the OK is better; compared to other interpolation techniques such as Inverse Distance Weighted (IDW) and Spline interpolation (Fathian & Aliyari, 2016).

4. Results

4.1. Climatic and hydrologic data trend

4.1.1. Temperature

The meteorological station data shows a general increasing trend of the temperature in the Niger basin. The increase is not significant for the period of the IPCC standard period (1981-2010). On the other hand, the trend seen over the NID and at upstream NID for the study period of 1980 to 2010, the rise is slightly less and not statistically significant as compared to IPCC standard period (Fig. 3 (a) & (b)). The average temperature for IPCC standard period for the upper and inside the NID is respectively 27.9°C & 29.4°C. However, the 10 years moving average over the NID shows that the temperature decreased by 0.2°C by the year 1990 and increased by 0.3°C up to 2005. While, the 10 years moving average at NID's upstream shows that the temperature decreased by 0.1°C by the year 1994 and increased by 0.1°C at 2007 (Fig. 3 (c) & (d)). Then, the temperature showed an increasing trend by 0.5°C by the year 2010 with reference to the average temperature at IPCC standard period (Fig. 3 (c)).

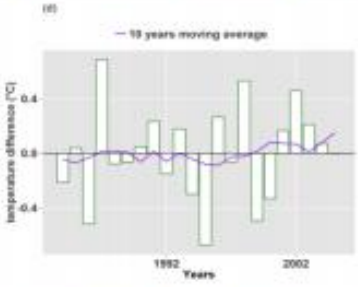

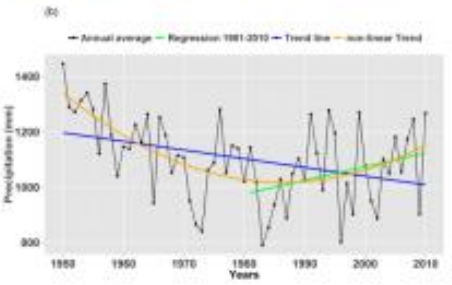

(a) annual average temperature trend of the meteorological stations (Segou & Mopti) data over the NID, b. annual average temperature trend of the meteorological stations (Bougouni & Bamako Senou) data at upper the NID, (c) Annual average temperature trend over the NID minus the mean IPCC standard period average temperature for meteorological stations data, (d) Annual average temperature trend upstream the NID minus the mean IPCC standard period average temperature for meteorological stations data

Fig. 3: The average temperature trend

4.1.2. Precipitation

In case of precipitation, the trend is opposite to the temperature. For the period of 1950 2010, it is decreasing. In contrast, during the IPCC standard period it is increasing and is statistically significant. The average precipitation over the NID, Mali-upstream NID, and Guinea-upstream NID, for the IPCC standard period according to the meteorological stations records is 475, 1051, and 1481 mm/year respectively (Fig. 4 (a)).

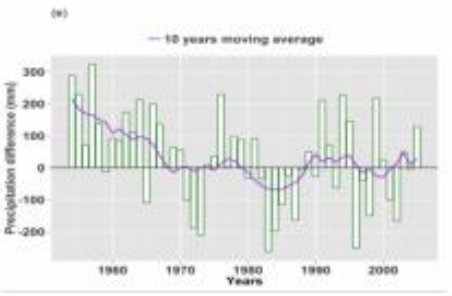

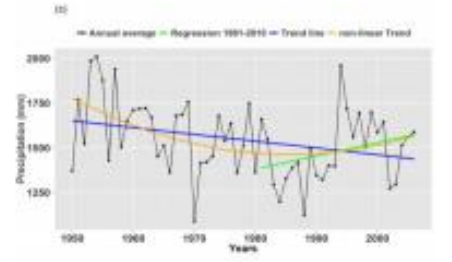

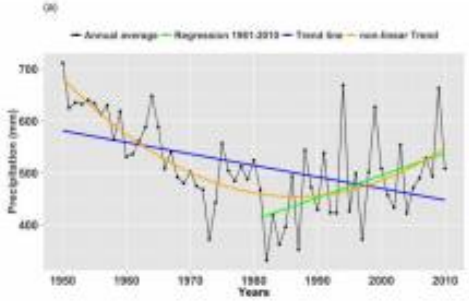

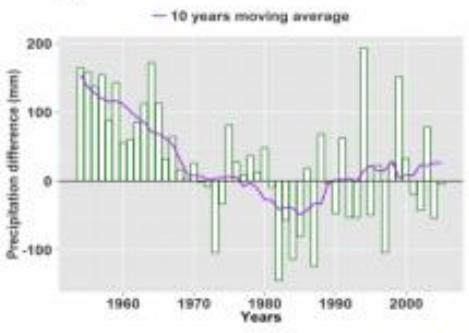

(a) annual average precipitation trend of the meteorological stations (Segou, San, Mopti & TombuKtu) data over the NID, (b) annual average precipitation trend of the meteorological stations (Sikasso, Bougouni & Bamako Senou) data at upper the NID in Mali, (c) annual average precipitation trend of the meteorological stations (Kankan & Faranah) data at upper the Niger Basin in Guinea, (d) Annual average precipitation trend over the NID minus the mean IPCC standard period average precipitation for meteorological stations data, (e) Annual average precipitation trend at Mali upstream the NID minus the mean IPCC standard period average precipitation for meteorological stations data, (f) Annual average precipitation trend at Guinea upstream the NID minus the mean IPCC standard period average precipitation for meteorological stations data

Fig.4: The average precipitation trend

The 10 years moving average for the period of 1950-2010 show a decreasing trend of precipitation in the NID wetland. The precipitation was lowest from 1981 to 1985. The precipitation decreased by 125mm compared to the average precipitation at IPCC standard period. If the 10 years moving average is considered there is a slight increase not significant in the precipitation over the NID in the year 1990 to 2010 whereas, there is a decreasing trend in the periods 1950-1970 (Fig. 4 (d)).

4.1.3 Evaporation trend

The Mopti pan evaporation data show a slightly increasing trend in the NID. The evapotranspiration is increasing at the rate of 5 mm per year and the trend is not statistically significant. However, the decrease is at higher rate and not statistically significant at the IPCC standard period (Fig. 5 (a)). The average Mopti evaporation is approximately 2500 mm/year considering the study period 1970-2009; and The average evapotranspiration is 2485 mm/year if IPCC standard period is only considered. Similarly, the 10 years moving average of evapotranspiration has slightly increasing trend for 10 mm per year considering the period of 1981-2009 (Fig. 5 (b)).

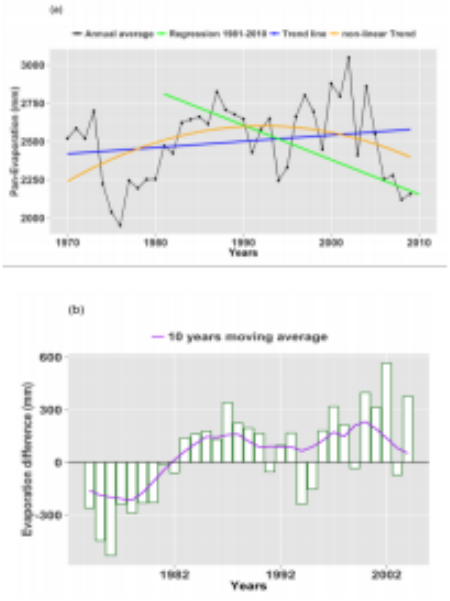

(a) annual average evaporation trend of the Mopti pan recorded data over the NID, (b) Annual average evaporation trend over the NID minus the mean IPCC standard period average evaporation for Mopti Pan Evaporation data records.

Fig. 5: The average evaporation trend

4.1.3. Streamflow trend

These results were plotted in Fig. 6. It observes that: (1) For the upper basin a wet period (1920-1930; 1945-1970) and a dry (1971-2010) period are clearly seen which have a mean annual discharge of 700 m^3/s (450 m^3/s) higher (lower) and (2) for the NID a mean annual discharge of 450 m^3/s higher (350 m^3/s) higher (lower) than the long-term mean, respectively. This variation in the discharge shows the idea of how dry or wet the part of Niger Basin are in the upstream of NID and the wetland. The discharge runoff is higher in the upper basin at the Niger basin part of Mali (for e.g. Koulikoro); whereas, the streamflow values are lower in the NID cathment at the outlet of the delta. The changepoints (breaks red dotted lines) plot for runoff timeseries (Fig. 6 (a.) & (c.) shows that there are 3 distinct changes of the specific runoff with regards test statistic for the analysis of the data. The linear fit (Fig. 6 (a.) & (c)) shows that the flow discharge decreases with the increase in area but it is not statistically significant. Furthermore, the streamflow varies according to moving average plot rather than the trend line.

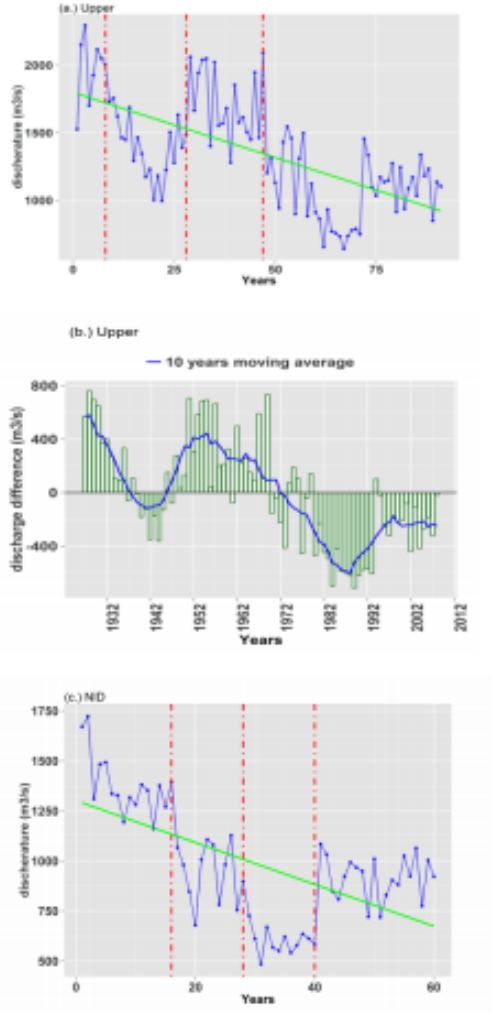

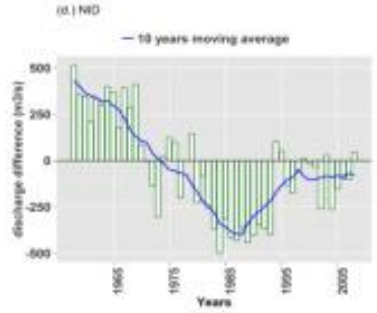

(a.) annual average streamflow of the upper gage stations of Mali with green line = trend line and red dotted lines= changepoints for the timeseries; (b.) Annual average discharge difference trend minus the long term mean period of discharge data over the upper stations of Mali; (c.) annual average streamflow of gage stations inside the NID of Mali with green line = trend line and red dotted lines= changepoints for the timeseries; (d.) Annual average discharge difference trend minus the long term mean period of discharge data over the NID stations of Mali

Fig. 6: The average discharge trend

4.2 Spatial analysis

The GCPC data which is the average calculated from 1996 - 2013 shows that the precipitation varies from 200 to 1400mm/year in the study region (Fig. 7 (a.)). The statistical analysis for the region shows that the mean precipitation is 773mm. The precipitation value is alike to the satellite climate data (Fig. 7 (b.)).

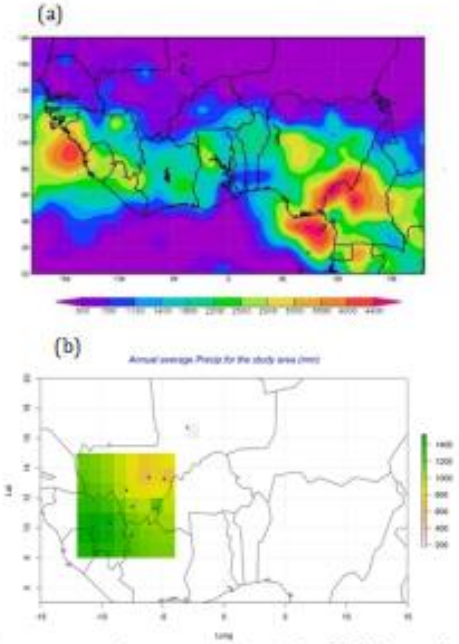

(a.) Long term annual average precipitation for GCPC dataset of study area stations of; (b.) the OK spatial variation of the of the recorded data of gage stations within the basin

Fig.7: The spatial distribution of precipitation

In this study, we use the interpolated technique, explicitly, Ordinary Kriging (OK) to spatial analysis of annual precipitation trends in the basin. In this section, the interpolated trend results are shown in Figure 8 using the method at significance levels between minimum and maximum range of Mann-Kendall statistics.

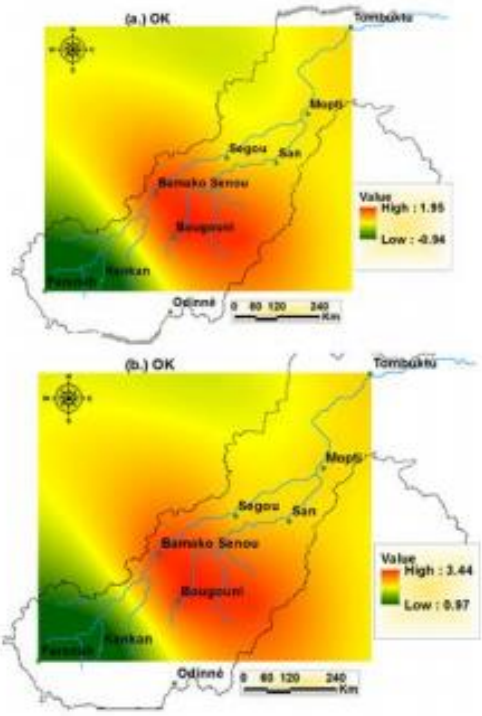

Fig. 8: Spatial distribution of the statistics Z of the Mann–Kendall test for the annual rainfall (a.) Period 1950-2010 (b.) Period 1981 - 2010

5. Discussion

5.1. Hydro-climatic data trend analysis

To study the variation of historical annual and seasonal precipitation, temperature, evaporation, and discharge, the mean annual and seasonal values for the entire study period (1950 – 2010, and 1980 -2010) and for each the IPCC period (1981 - 2010) are assessed and compared. During these periods, the climate variables in the region as regards the temperature and precipitation, show variation similar for the upper region and the NID wetland zone. The general trend of the temperature is increasing and the precipitation shows decrease in line with the previous studies in West Africa (Paturel *et al.*, 1997; Servat *et al.*, 1997; Paturel *et al.*, 2003; L'Hôte *et al.*, 2002). The period (1981-2010) is slightly warmer than the long-term average. The results demonstrate that the seasonal variations of the 10 years moving values are much

larger than those of mean annual differences, especially for temperature. The climatic trend in NID's floodplain is in line with this fact (Fig. 3 & Fig. 4). The temperature and precipitation are increasing in the IPCC standard analysis (from 1981-2010). The precipitation trend is not in line with these facts for the overall study period of 1950-2010; however, the trend is not statistically significant. Henceforward, in summary the long term trend analysis demonstrate that the temperature and precipitation has increasing and decreasing trend respectively in the study area. Although it should also be noted that the current trend (after 1990s) of the precipitation is increasing but it is not statistically significant. Subsequently, the increasing trend might be linked randomly to that of the temperature for some decades.

According to many studies (Descroix *et al.*, 2009; Druyan, 2011; Hubert P., Carbonnel, 1987; Le Barbé & Lebel, 1997; Li *et al.*, 2005; Mahe *et al.*, 2001; Sharon E. Nicholson, 2000; Sharon E. Nicholson & Palao, 1993; Sircoulon, 1987) there was a decline in rainfall from the 70 in the Sahel region. In similarity, to this study, the lowest rainfall occurred within that period (331 mm/year in 1982 for NID, 840 mm/year in 1984 for upper NID in Mali, and 1087 mm/year in 1970) and showed likely return period of some 15 to 20 years (Fig. 4 (d), Fig. 4(e), and Fig.4 (f)).

The effect of increasing temperature and decreasing precipitation can be seen over the evaporation trend of the NID. In general, an increasing trend of the evaporation is seen in the NID (Fig. 5 (a) & Fig. 5 (b)). However, the trend is decreasing and not statistically significant considering the period 1981-2009 (Fig. 5 (a)). This result can be justified with the overall decreasing trend of precipitation. Nevertheless, the evaporation is increasing with temperature for the study period, the decrease in the precipitation decreases the discharge runoff. The observed streamflow based analyses shows decrease of river runoff in their long-term average for the study region. Therefore, the decreasing trend in the discharge runoff may be a major problem in the water resource management.

For each considered region (either upper or the NID), the years of break marked in dotted red lines as the significant breakpoints. For the whole area, the application of the changepoint method resulted in approximately 1972 and 1992 as the most significant breakpoints (1st break and 2nd break respectively). The year of 1st break reveals the period of significant low flow mainly observed in the West African rivers (Descroix *et al.*, 2009) during the drought of the 1980s. As regards to the 2nd break (1992), it almost in line with the rising of the nonlinear trend line in rainfall data (1990).

The above discussion shows that when entering the 1970s there is a very dry period in the Niger basin. More essentially, this decrease in streamflow will have a direct impact on the very sustainability of the ecosystem's services in the NID. Though, some authors (Ozer *et al.*, 2003; Pedinotti *et al.*, 2012; Descroix *et al.*, 2015) suggested a return of a wetted period meanwhile the 1990s. If this situation does not change in this 21st century it will have positive impact for water availability in the Niger basin region.

The trend analysis illustrates that the long term trend is not statistically significant as compared to IPCC standard period trend. This result suggests that hydro-climatic data trend is decreasing except temperature and evaporation trend. Yet, it might not be concluded that the climate has changed in the study region, because all variables are not statistically significant for the same study period. In addition, the trend analysis also shows the importance of considering the region in three features (upper Guinea, Upper Mali, and NID) of the catchment and two parts of the study period. The schematic representation of the hydro-climatic data shows that, with regards to the length of the study period, the trends look to be significant or else not significant. The decrease or increase seems to be regular for a certain period whereas, it appears to be affected by some random variation of the extreme values within the study period when range of the analysis period is changed. This fact is in accordance with Druyan, (2011) who stated that, no clear trend for either decreasing or increasing precipitation from global climate model (GCM) products. With such context, while, it could not be assumed that the climate has not changed in the Niger Basin whereas looking at the trends of the climatic data, it must be noted that there will be decrease in the water resource availability in the future if the trends in the hydro-climatic data remains. With this regards, the water resource management should be done considering the plausible decrease of the water resource availability in the Niger basin.

5.2. Spatial interpolation of precipitation

The spatial analysis of precipitation data shows different variation of change in annual rainfall. Decreasing change in mean annual rainfall is not significant for the period 1950 - 2010. For the IPCC standard (recent years 1981-2010), the increasing change in mean annual rainfall is seen to positively significant. This fact is in line with the study by Oyebande and Odunuga, (2010) that for the past 4 decades, 10 to 30% drop in mean annual rainfall was observed in the region. This decrease can be related to changes in the sea surface temperature afterward 1960s (Lebel and Ali, 2009). For the period 1981-2010, the maximum positive significant change is observed in the regions showing lower yearly rainfall (Fig. 8 (b.)). Therefore, the precipitation excess for the period 1981-2010 is increased compared to overall trend values in the basin. The potential evapotranspiration is high in the Niger Inland Delta area; this variation can be justified by the variation of the temperature and precipitation. In this context, a special focus is required to the NID zones because they are the zones with high water use. This has pointed out

that evapotranspiration is most important factor compared to the precipitation.

The dominant trend in precipitation is clearly positive in southern and northern NID, while there is an apparent negative trend in western part of NID. The interpolated maps exhibit that negative trends are few and located in the west region of NID's wetland and upper region of the basin in Guinea (Fig. 8 (a.)).

Conclusion

Hydroclimatic data trend analysis is found to be with high importance for the study region. The assessment of the water resource availability from past and the probable future condition is a paramount tool for management of the water resource. For the evaluation of the water resource condition, the hydroclimatic data trend can be a reliable skill. This fact made the statistical approach of the hydroclimatic data trend to be widely used to show whether the climate change has happened in the area or if the tendency seen is just climate variation. In this research, the hydroclimatic data trend does not exhibited a consistent trend when considered overall period of the data for the study. The trend and its statistical significance differ according to the range of the study period considered. Regarding this trend analysis, it cannot be concluded that, the climate change has occurred in the upstream and NID's wetland areas. However, considering the period 1981-2010, it would be noted that all the climatic data show an increasing trend in the NID except the evaporation whose trend is not significantly decreasing over the area. The temporal trends of stream flow discharge are the result of the combined effect of precipitation and temperature. Significant decreasing trends are found for mean annual discharge at a 0.05 significance level.
The spatial variation of the hydroclimatic data shows that the precipitation is higher at the inland part of the study region. Historical data show no trend for precipitation in considering the study period while, the trend for the 1981-2010 has positive significant trend especially for the NID areas of the Niger basin at the 0.05 significance level. Hence, results in this study from the trend analysis can provide a general idea about the water resource availability in the basin.

The key findings of the study can be summarized in following points:

- The general trend of the hydroclimatic data analysis shows a decreasing trend in the basin except for the evaporation; however, all trends are not statistically significant when considering the full study period. Hence, it cannot be concluded that climate has changed in the basin.
- The long term trend shows decreasing water resource availability in the NID.
- Spatially, the increase in precipitation is higher in the western part of the NID compared to eastern and inland part of the wetland.
- The results presented here shows a general idea about the water resource conditions in time and space, this should be taken as a basic skill for water resource management instead of models in order to reduce uncertainties.

Acknowledgments

This study was funded by the German Ministry of Education and research (BMBF) through the West African Science Service Center on Climate Change and Adapted Land Use (WASCAL; www.wascal.org), that supports the Graduate Research Program Climate Change and Water Resources at the University of Abomey Calavi). We thank AGHRYMET regional center, Niger Basin Authority, and Niger & Mali Meteorological and Hydrological service for providing the hydro-meteorological data for Niger Basin.

Conflicts of Interest

The authors declare no conflict of interest.

References

Ali, A., Lebel, T., & Amani, A. (2005). Rainfall Estimation in the Sahel. Part I: Error Function. *Journal of Applied Meteorology*, *44*(11), 1691–1706. http://doi.org/10.1175/JAM2304.1

Descroix, L., Mahé, G., Lebel, T., Favreau, G., Galle, S., Gautier, E., ... Sighomnou, D. (2009). Spatio-temporal variability of hydrological regimes around the boundaries between Sahelian and Sudanian areas of West Africa: A synthesis. *Journal of Hydrology*, *375*(1–2), 90–102. http://doi.org/10.1016/j.jhydrol.2008.12.012

Descroix, L., Niang, A. D., Panthou, G., Bodian, A., Sane, Y., Dacosta, H., ... Quantin, G. (2015). Évolution récente de la pluviométrie en Afrique de l'Ouest à travaers deux régions: La sénégambie et le bassin du Niger moyen. *Climatologie*, *12*, 25–43.

Druyan, L. M. (2011). Studies of 21st-century precipitation trends over West Africa. *International Journal of Climatology*, *31*(10), 1415–1424. http://doi.org/10.1002/joc.2180

Fathian, F., & Aliyari, H. (2016). Temporal trends in precipitation using spatial techniques in GIS over Urmia Lake Basin , Iran Farshad Fathian * and Hamed Aliyari Ercan Kahya Zohreh Dehghan. *Int. J. Hydrology Science and Technology*, *6*(1), 62–81.

Frappart, F., Hiernaux, P., Guichard, F., Mougin, E., Kergoat, L., Arjounin, M., ... Lebel, T. (2009). Rainfall regime across the Sahel band in the Gourma region, Mali. *Journal of Hydrology*, *375*(1–2), 128–142. http://doi.org/10.1016/ j.jhydrol. 2009.03.007

Hiernaux, P., Ayantunde, A., Kalilou, A., Mougin, E., Gérard, B., Baup, F., ... Djaby, B. (2009). Trends in productivity of crops, fallow and rangelands in Southwest Niger: Impact of land use, management and variable rainfall. *Journal of Hydrology*, *375*(1–2), 65–77. http://doi.org/ 10.1016/j.jhydrol.2009.01. 032

Hubert, P., Carbonnel, J. P., & Chaouche, A. (1989). Segmentation des séries hydrométéorologiques. Application à des séries de précipitations et de débits de Afrique de l'Ouest. *Journal of Hydrology*, *110*, 349–367.

Hubert P., Carbonnel, J. P. (1987). Approche statistique de l'aridification de l'Afrique de l'Ouest. *Journal of Hydrology*, *95*, 165–183.

IPCC. (2007). Climate change 2007: the physical science basis. *Intergovernmental Panel on Climate Change*, *446*(7137), 727–8. http://doi.org/10.1038/446727a

L'Hôte, Y., Mahé, G., Somé, B., & Triboulet, J. P. (2002). Analysis of a Sahelian annual rainfall index from 1896 to 2000; the drought continues. *Hydrological Sciences Journal*, *47*(4), 563–572. http://doi.org/10.1080/02626660209492960

Le Barbé, L., & Lebel, T. (1997). Rainfall climatology of the HAPEX-Sahel region during the years 1950-1990. *Journal of Hydrology*, *188–189*(1–4), 43–73. http://doi.org/10.1016/S0022-1694(96)03154-X

Le Lay, M., Galle, S., Saulnier, G. M., & Braud, I. (2007). Exploring the relationship between hydroclimatic stationarity and rainfall-runoff model parameter stability: A case study in West Africa. *Water Resources Research*, *43*(7), n/a-n/a. http://doi.org/10.1029/2006WR005257

Lebel, T., & Ali, A. (2009). Recent trends in the Central and Western Sahel rainfall regime (1990–2007). *Journal of Hydrology*, *375*(1–2), 52–64. http://doi.org/10.1016/j.jhydrol.2008.11.030

Lebel, T., Amani, A., Cazenave, F., Lecocq, J., Taupin, J.-D., Elguero, E., … Robin, J. (1996). La distribution spatio-temporelle des pluies au Sahel : apports de l'expérience EPSAT-Niger. In *L'hydrologie tropicale : géoscience et outil pour le développement* (pp. 77–98).

Li, K. Y., Coe, M. T., & Ramankutty, N. (2005). Investigation of Hydrological Variability in West Africa Using Land Surface Models. *Journal of Climate*, *18*(16), 3173–3188. http://doi.org/10.1175/JCLI3452.1

Mahe, G., Bamba, F., Soumaguel, A., Orange, D., & Olivry, J. C. (2009). Water losses in the inner delta of the River Niger : water balance and flooded area. *Hydrological Processes 23, 3157–3160 August 2009 in Wiley InterScience*, *3160*(August), 3157–3160. http://doi.org/10.1002/hyp.7389

Mahe, G., Lienou, G., Descroix, L., Bamba, F., Paturel, J. E., Laraque, A., … Khomsi, K. (2013). The rivers of Africa : witness of climate change and human impact on the environment. http://doi.org/10.1002/hyp

Mahe, L'Hote, Y., Olivry, J. C., & Wotling, G. (2001). Trends and discontinuities in regional rainfall of West and Central Africa: 1951–1989. *Hydrological Sciences Journal*, *46*(March 2015), 211–226. http://doi.org/10.1080/02626660109492817

Mariko, A. (2003). *Caractérisation et suivi de la dynamique de l ' inondation et du couvert végétal dans le Delta intérieur du Niger (Mali) par télédétection* . (École doct). Université Montpellier II, Paris.

Mariko, A., Mahe, G. I. L., & Orange, D. (2013). Monitoring flood propagation in the Niger River Inner Delta in Mali : prospects with the low resolution NOAA / AVHRR data. *IAHS-IAPSO-IASPEI Assembly, Gothenburg, Sweden, July 2013 (IAHS Publ. 358, 2013)*, *2013*(July), 101–109.

Nicholson, S. E. (2000). Land Surface Processes and Land Use Change Land. *Reviews of Geophysics*, *38*, *1 / February 2000*, *38*(1999), 117–139. Retrieved from http://www.peer.eu/fileadmin/user_upload/opportunities/metier/course3/c3_land_surface_processes.pdf

Nicholson, S. E., & Palao, I. M. (1993). A RE-Evaluation of rainfall variability in the sahel. Part I. Characteristics of rainfall fluctuations. *International Journal of Climatology*, *Vol.13*, *371–389*, 371–389. http://doi.org/0899-8418/93/040337I-19$14.50

Oguntunde, P. G., & Abiodun, B. J. (2012). The impact of climate change on the Niger River Basin hydroclimatology, West Africa. *Climate Dynamics*, *40*(1–2), 81–94. http://doi.org/10.1007/s00382-012-1498-6

Oguntunde, P. G., Friesen, J., van de Giesen, N., & Savenije, H. H. G. (2006). Hydroclimatology of the Volta River Basin in West Africa: Trends and variability from 1901 to 2002. *Physics and Chemistry of the Earth, Parts A/B/C*, *31*(18), 1180–1188. http://doi.org/10.1016/j.pce.2006.02.062

Oyebande, L., & Odunuga, S. (2010). Climate change impact on water resources at the transboundary level in West Africa: the cases of the Senegal, Niger and Volta basins. (A. J. Adeloye & C. S. P. Ojha, Eds.).*Special Issue Analysis of Climate Change Impacts on Water Resources for Developing Economies Successes and Challenges*.

Ozer, P., Erpicum, M., Demaree, G., & Vandiepenbeeck, M. (2003). DISCUSSION of "Analysis of a Sahelian annual rainfall index from 1896 to 2000; the drought continues" The Sahelian drought may have ended during the 1990s. *Hydrological Sciences Journal-Journal Des Sciences Hydrologiques*, *48*(3), 489–492. http://doi.org/10.1623/hysj.48.3.489.45285

Paturel, J. E., Servat, E., Kouamé, B., Lubès, H., Ouedraogo, M., & Masson, J. M. (1997). Climatic variability in humid Africa along the Gulf of Guinea. Part II: An integrated regional approach. *Journal of Hydrology*, *191*(1–4), 16–36. http://doi.org/10.1016/ S0022-1694(96)03069-7

Paturel, J.-E., Ouedraogo, M., Servat, E., Mahe, G., Dezetter, A., & Boyer, J.-F. (2003). The concept of rainfall and streamflow normals in West and Central Africa in a context of climatic variability. *Hydrological Sciences Journal*, *48*(August), 125–137. http://doi.org/10.1623/hysj.48.1.125.43479

Pedinotti, V., Boone, a., Decharme, B., Crétaux, J. F., Mognard, N., Panthou, G.,Tanimoun, B. a. (2012). Evaluation of the ISBA-TRIP continental hydrologic system over the Niger basin using in situ and satellite derived datasets. *Hydrology and Earth System Sciences*, *16*(6), 1745–1773. http://doi.org/10.5194/hess-16-1745-2012

Pettitt, A. N. (1979). A Non-Parametric Approach to the Change-Point Problem. *Journal of the Royal Statistical Society. Series C (Applied Statistics)*, *28*(2), 126–135. JOUR. http://doi.org/10.2307/ 2346729

Priyadarshana, W. J. R. M., & Sofronov, G. (2014). Multiple Break-Points Detection in array CGH Data via the Cross-Entropy Method. *Computational Biology and Bioinformatics*, *12*(2), 1–13. http://doi.org/10.1109/TCBB.2014.2361639

Servat, E., Paturel, J. E., Lubès, H., Kouamé, B., Ouedraogo, M., & Masson, J. M. (1997). Climatic variability in humid Africa along the Gulf of Guinea. Part I: Detailed analysis of the phenomenon in Cote d'Ivoire. *Journal of Hydrology*, *191*(1–4), 1–15. http://doi.org/10.1016/S0022-1694(96)03068-5

Sircoulon. (1976). Les données hydro-pluviométriques de la sécheresse récente en Afrique inter-tropicale. Comparaison avec les sécheresses de 1913 et 1940. *Cahier ORSTOM, Hydrol.*, *13*(2).

Sircoulon, J. H. A. (1987). Variation des débits des cours d'eau et des niveaux des lacs en Afrique de l'Ouest depuis le début du 20ème siècle. *The Linfience of Clirnate Cilange Arid Cliiiratic Variability on the Hydrologic Regime and Water Resources; IAHS Publ.*, (168).

Taupin, J. D., Amani, A., & Lebel, T. (1998). Variabilite spatiale des pluies au Sahel : une question d ' echelles. *Waler Resources Variabiliry in Africa during lhe XXth Cen/ury (Proceedings of!.he Abidjan'98 Conference 143 Held at Abidjan, Cote D'Ivoire, November 1998). I,\IHS Pub!. No. 252.1998.*, (252), 143–158.

Zwarts, L., Van Beukering, P., Kone, B., & Wymenga, E. (2005). The Niger, a lifeline Effective water management in the Upper Niger Basin. *RIZA, Lelystad / Wetlands 989 International, Sévaré / Institute for Environmental Studies (IVM), Amsterdam / A&W 990 Ecological Consultants, Veenwouden. Mali / the Netherlands*, *169*(lvm), 169.

hydrology

MDPI

Article

Water Balance Analysis over the Niger Inland Delta-Mali: Spatio-Temporal Dynamics of the Flooded Area and Water Losses

Moussa Ibrahim [1,*], Dominik Wisser [2], Abdou Ali [3], Bernd Diekkrüger [4], Ousmane Seidou [5,6], Adama Mariko [7] and Abel Afouda [1]

1 GRP Climate Change and Water Resources, West African Science Service Center on Climate Change and Adapted Land Use (WASCAL), University of Abomey Calavi, Cotonou BP 526, Benin; aafouda@yahoo.fr
2 Center for Development Research (ZEF), University of Bonn, Bonn 53113, Germany; dwisser@uni-bonn.de
3 Regional Center AGRHYMET, Niamey BP 11011, Niger; a.ali@agrhymet.ne
4 Department of Geography, University of Bonn, Meckenheimer Allee 166, Bonn 53115, Germany; b.diekkrueger@uni-bonn.de
5 Department of Civil Engineering, University of Ottawa, 161 Louis Pasteur office A113, Ottawa, ON K1N6N5, Canada; Ousmane.Seidou@uottawa.ca
6 United Nations University Institute for Water, Environment and Health (UNU-INWEH), 204-175 Longwood Road South, Hamilton, ON L8P 0A1, Canada
7 Ecole Nationale d'Ingénieurs Abderhamane Baba Touré (ENI-ABT), Bamako BP 242, Mali; adama.mariko@ird.fr
* Correspondence: imoussa47@yahoo.fr; Tel.: +227-90-44-56-02

Received: 2 July 2017; Accepted: 15 August 2017; Published: 18 August 2017

Abstract: The Niger Inland Delta (NID) wetland comprises a large flooded area that plays an important role in the ecosystem services. This study provides a comprehensive understanding of the NID's hydro-climatological functioning using water balance approach. After a clear description of the water budget's elements specific to the NID catchment, a spatial and temporal dynamics of the annual flood across the NID over the period 2000–2009 was performed using data from satellite QuickSCAT and its associated sensor SeaWinds. The estimated areas were used along with observed discharge and remotely-sensed climatic data to quantitatively evaluate each water balance component. The results indicate: (i) a clear spatiotemporal of the flooded areas varied between 25,000 km^2 in wet periods and 2000 km^2 in dry periods; (ii) an average evapotranspiration loss of 17.31 km^3 (43% of the total inflow) was assessed in the catchment; (iii) precipitation's contribution to the NID's budget totals 5.16 km^3 (12.8% of the total inflow); and (iv) the contribution of return flow from irrigated fields totals 1.8 km^3 (4.5% of the total inflow, among which 1.2 km^3 are from Office du Niger) to the flooded areas, refined the NID's water balance estimates. Knowledge gained on NID's water balance analysis will be used to develop and calibrate hydrological models in the Niger Inland Delta of the basin.

Keywords: remote sensing flooded area extent; evapotranspiration models; water losses; return flow; water balance

1. Introduction

The Niger River Basin (NRB), West Africa's largest river basin, covers about 2.2×10^6 km^2 (shared over ten countries) and is populated by more than 100 million people. The Niger River has a total length of 4200 km [1], flowing from its source high on the Fouta Djallon Mountains in the South of Guinea at an altitude about 800 m, through Guinea, Mali, Niger, and Nigeria, before discharging approximately 175 km^3 annually into the Atlantic Ocean through an extensive delta [2]. The river flows Northeast through the Upper Niger basin and enters the Niger Inland Delta (NID) in Mali; a

Article

Water Balance Analysis over the Niger Inland Delta-Mali: Spatio-Temporal Dynamics of the Flooded Area and Water Losses

Moussa Ibrahim [1,*], Dominik Wisser [2], Abdou Ali [3], Bernd Diekkrüger [4], Ousmane Seidou [5], Adama Mariko [6] and Abel Afouda [1]

[1] GRP Climate Change and Water Resources, West African Science Service Center on Climate Change and Adapted Land Use (WASCAL), University of Abomey Calavi, Cotonou BP 526, Benin; aafouda@yahoo.fr
[2] Center for Development Research (ZEF), University of Bonn, Bonn 53113, Germany; dwisser@uni-bonn.de
[3] Regional Center AGRHYMET, Niamey BP 11011, Niger; a.ali@agrhymet.ne
[4] Department of Geography, University of Bonn, Meckenheimer Allee 166, Bonn 53115, Germany; b.diekkrueger@uni-bonn.de
[5] Department of Civil Engineering, University of Ottawa, 161 Louis Pasteur office A113, Ottawa (ON) K1N6N5, Canada; adjunct professor, United Nations University Institute for Water, Environment and Health (UNU-INWEH) , 204-175 Longwood Road South, Hamilton, Ontario L8P 0A1, Canada; Ousmane.Seidou@uottawa.ca
[6] Ecole Nationale d'Ingénieurs Abderhamane Baba Touré (ENI-ABT), BP 242 Bamako, Mali; adama.mariko@ird.fr
* Correspondence: imoussa47@yahoo.fr; Tel.: +227-90-44-56-02

Received: 2 July 2017; Accepted: 15 August 2017; Published: date

Abstract: The Niger Inland Delta (NID) wetland comprises a large flooded area that plays an important role in the ecosystem services. This study provides a comprehensive understanding of the NID's hydro-climatological functioning using water balance approach. After a clear description of the water budget's elements specific to the NID catchment, a spatial and temporal dynamics of the annual flood across the NID over the period 2000–2009 was performed using data from satellite QuickSCAT and its associated sensor SeaWinds. The estimated areas were used along with observed discharge and remotely-sensed climatic data to quantitatively evaluate each water balance component. The results indicate: (i) a clear spatiotemporal of the flooded areas varied between 25,000 km^2 in wet periods and 2000 km^2 in dry periods; (ii) an average evapotranspiration loss of 17.31 km^3 (43% of the total inflow) was assessed in the catchment; (iii) precipitation's contribution to the NID's budget totals 5.16 km^3 (12.8% of the total inflow); and (iv) the contribution of return flow from irrigated fields totals 1.8 km^3 (4.5% of the total inflow, among which 1.2 km^3 are from Office du Niger) to the flooded areas, refined the NID's water balance estimates. Knowledge gained on NID's water balance analysis will be used to develop and calibrate hydrological models in the Niger Inland Delta of the basin.

Keywords: remote sensing flooded area extent; evapotranspiration models; water losses; return flow; water balance

1. Introduction

The Niger River Basin (NRB), West Africa's largest river basin, covers about 2.2 × 10^6 km^2 (shared over ten countries) and is populated by more than 100 million people. The Niger River has a total length of 4200 km [1], flowing from its source high on the Fouta Djallon Mountains in the South of Guinea at an altitude about 800 m, through Guinea, Mali, Niger, and Nigeria, before discharging approximately 175 km^3 annually into the Atlantic Ocean through an extensive delta [2]. The river flows

Northeast through the Upper Niger basin and enters the Niger Inland Delta (NID) in Mali; a large floodplain ranging from 30,000 to 40,000 km^2 along the Niger River in Mali [3]. The annual flooding of large alluvial plains is a vital resource for many ecosystem services, including agriculture, livestock, groundwater recharge, and biodiversity. The NID plays an important role in sustaining the livelihood of one million people, and is an important component affecting the water availability of the basin downstream [1]. Food production in the NID is very important; for example, yields can go up to 6–7 tons/ha for irrigated rice. In addition, fisheries constitute an important source of revenue for the inhabitants of the NID with annual production between 70,000 to 120,000 tons [1].

Climate change impacts on water resources have been reported in the assessment reports of the Intergovernmental Panel on Climate Change [4]. In particular, changing climate conditions are expected to modify the availability of water resources in the NID and the timing and availability of water resources downstream of the NID [1,3,5–8,9]. Therefore, detailed information on the processes that control NID's role in the hydrological cycle of the basin is of notable interest for ensuring rational management of water resources under current and future climate and environmental conditions [10].

Several models of the NID have been developed previously [1,3,7,11]. These were hydrological and/or reservoir versions, hydraulic and agro-ecological models that simulated either a part of or the entire system, while the dynamics of the inland delta have been largely neglected in basin scale hydrological models. Modelling approaches differ in complexity, physical basis, and data requirements, so the choice of a model depends on the specific purpose of the modelling exercise [8]. Past studies revealed difficulties in estimate the various components of hydrological processes, or to create hydrologic simulations over extended time periods [12,13], arising from the complexity of these processes in the NID. These are partly due to the low topography of the area which existing Digital Elevation Models (DEMs) cannot sufficiently capture.

Starting with the study of Gallais 1967 (cited by Olivry [11]), a number of studies have been conducted regarding the water balance of NID and its flood extent. Olivry et al. [11] conducted a thorough evaluation of the water losses of NID system based on 38 years of available data and deduced the flooded area from the hydrological balance of the NID without considering the natural physical flood processes and the dynamics of the flooded area in terms of duration and flood frequency.

Further studies on the water balance of the NID by Orange et al. [3] revealed information on the maximum flooded area extent that can occur over the NID at maximum surface water levels. Orange's approach was quite different to that of Olivry [11]. Surface flood area analysis of the behavior of the NID by Orange et al. [3] has revealed that there is high variability of the inundated area based on the discharge inflow from upstream. Similar studies on water balance by Zwarts et al. [1] attempted to represent the effects of upstream abstractions on an inundation area, by estimating average reduction in outflow and flooded area. Similar indices were used by Mahé et al. [14] in their spatial-temporal model, aimed at forecasting surface flood areas using the water balance. On the other hand, Dadson et al. [12] modeled the evaporative losses that occur over the NID by adding an overbank flow parameterization to the Joint UK Land-Environment Simulator (JULES) land surface model. Although it consistently overestimated outflows from the NID by 40%, it performed well for reproduction of the timing of observed flows. The study of Dadson et al. [12] seriously underestimates the influence of the key regions, and has revealed that the model's over-prediction of discharge in the system could have been caused by ignoring losses due to the abstraction of water from the river, groundwater recharge in the NID, or by underestimating evaporation from the land surface and the river channel. This reasoning was plausible, since all the three processes could possibly affect the water balance of the NID [15].

The most recent work on the water balance of NID is the study done by Ogilvie et al. [16] who studied the remotely sensed flooded areas at high temporal and spatial resolution, and refined evaporation estimates as well as precipitation across the NID wetland using a water balance model. This result is consistent with the previously explored correlation between the NID flood area extent and

surface water inflow. However, the model's simulated evaporation losses were underestimated by 12% for the period 2001–2011, when compared to the previous study of Olivry [11], or in situ pan evaporation measurements. Ogilvie et al. [16] have recognized that the lower evaporation losses could have been caused either by evapotranspiration (ET) from non-flooded areas of the wetland (soil moisture, vegetation) which was not assessed; and would have increased the overall evaporation losses, or by uncertainties related to the remote sensing approach.

While most previous studies have underestimated water losses in the basin resulting from evaporation, the main component of water loss in wetlands [17], very few studies have considered additional water losses through water withdrawal for irrigation purposes, that are estimated to amount to 2.69 $km^3\ yr^{-1}$ of water on average [1].

The aim of this study is first to assess the spatiotemporal dynamics of the flooded area using optical and microwave remote sensing data and second to calculate the water losses over the inland delta, taking into account the impact of water abstraction for irrigation, return flows, and the flooded area. An evaluation of methods to calculate potential was also performed. In addition, we assess return flows from irrigated areas that were ignored in previous studies.

2. Materials and Methods

2.1. Study Area

The Niger Inland Delta, located in Mali between the cities of Segou and Tombouctou, spans an area of about 100 km width and 350 km length (Figure 1). The NID receives flow from the Niger and the Bani basins, whose rivers confluence inside the NID near the Mopti discharge station. The NID is extremely flat, and contains many lakes and streams of varying morphology. The altitude of the river bed decreases only by approximately 10 m over the 350 km between the entry and exit of the delta [18].

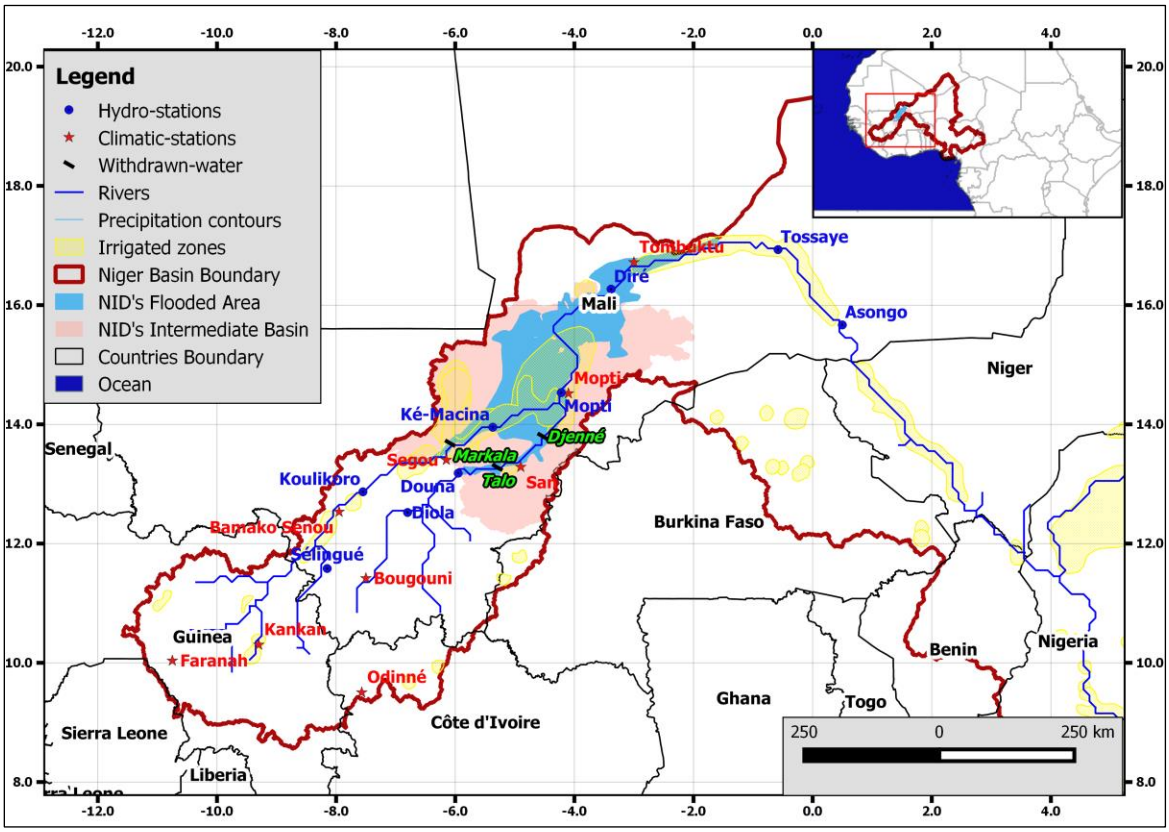

Figure 1. Location of the Niger Inland Delta (NID) within the Niger River basin and hydro-meteorological stations.

Flooding in the NID is primarily caused by the annual flood wave arriving from the Guinea part of the Niger River basin [14]. Due to the flood wave, the inundated area of the NID increases and decreases as the flooding varies within the system. The NID, primarily the southern part, functions like a transit plain where the flow is simply delayed, while in the Northern Delta the flooding recharges many lateral depressions and the water is trapped.

Precipitation over the NID is limited to the rainy season from March to October and varies between 350 mm in the north and 700 mm in the south [5]. The rainy season peaks between July and October, but since the flood in the NID is generated by rainfall 900 km upstream rather than locally, peak flow values occur between September and December due to propagation lag times.

2.2. Data

2.2.1. Remote Sensing (RS) Data

To analyze the spatial and temporal variations of the floodplain extent, we used optical and microwave remote sensing data (Satellite-borne measurements of the ETM+ sensor on-board of Landsat 7 and the SeaWinds sensor on-board of QuikSCAT). We acquired Landsat 7 8-Day Raw Composite 7 with a spatial resolution of 30 m, with a thermal band with a resolution of 60 m and a panchromatic band with a resolution of 15 m for the period 1999–2009 from the Landsat archives (http://earthexplorer.usgs.gov). For each month between October 1999 and 2009, we selected the most cloud free scenes from the Landsat archive and applied a Brovey pan sharpening algorithm of the I.pansharpen tool (http://grass.osgeo.org/grass70/-manuals/i.pansharpen.html) to achieve the spatial resolution of the spectral bands of 15 m.

Microwave remote sensing data was taken from the SeaWinds scatterometer instrument onboard the QuikSCAT instrument (available from http://podaac.jpl.nasa.gov/QuikSCAT).

SeaWinds is an active radar scatterometer with the primary mission to be able to get high-resolution measurements of near-surface winds over ice-free global oceans (http://podaac.jpl.nasa.gov/QuikSCAT) and was used for climatological studies, weather forecasting, general meteorology, and other applications, including land use classifications [19].

SeaWinds has a spatial resolution of approximately 25 km and has been in operation for more than ten years from 19 June 1999 to 23 November 2009 [19].

We used the 25 × 25 km version, from Jet Propulsion Laboratory (JPL) (http://podaac.jpl.nasa.gov/OceanWind). We reprojected both satellite data sets to UTM 29 (EPSG 32629).

To validate the classification results from the Landsat 7 images we used NDVI maps created from MODIS satellite land cover data MCD12Q1 (Land Cover Type Yearly L3 Global 500 m SIN Grid "MCD12Q1") [20].

2.2.2. Hydro-Meteorological Data

To analyze the water balance of the NID, we collected historical records of precipitation, temperature, river discharge, wind-speed, relative-humidity (RH), and evaporation. Meteorological data were acquired at two meteorological stations in Mali situated within the NID, close to Segou and Mopti (Figure 1). Daily precipitation data were available for the period 1950 to 2010; daily air temperature, wind speed, and RH for the stations of Segou and Mopti from 1980 to 2010; and monthly pan evaporation for the station of Mopti from 1970 to 2010.

For stations in Mali, daily hydrological records (daily water level and discharge data) for Ké-Macina, Douna, Diré and Mopti were obtained from Mali's "Direction Nationale de l'Hydraulique" for a 50-year period (the maximum length of records that was made available) from 1960–2013.

2.2.3. Field Irrigation Data

There are many irrigation schemes along the Niger River in Mali. While part of the irrigation schemes from "Office-Riz-Mopti (ORM)" are partly traditional irrigation (free flooding & recession flooding). The "Office du Niger (ON)" irrigation scheme (14°18′ N, 5°59′ W) is destined chiefly for small-holder irrigation and cultivation of flooded rice. Irrigation for ON water is drawn from the Niger River at Markala dam and is conveyed by gravity to a hierarchic irrigation network composed of primary, secondary, and tertiary canals. From the tertiary canals, field canals convey water to the rice basins and evacuate it to a drainage network. This gravity-fed scheme is considered highly successful, independent of rainfall and flood performance [1].

Monthly water withdrawals for the period 2000 to 2010 were available for the two major irrigation schemes. The first irrigation scheme covers an area of about 36,000 ha and is supplied by water abstracted from the Bani River at Mopti (responsible Office-Riz-Mopti (ORM). The second irrigation scheme is supplied by water from the Markala dam along the Niger River and has about 100,000 ha of cropland (mostly rice) under irrigation (responsible "Office du Niger" (ON)). At such big irrigation schemes located in the study area, part of the non-consumptive water previously unevaluated over large hydraulic system is drained back to the Niger River [21].

2.3. Methods

2.3.1. Land Cover Mapping and Flooded Areas Assessment

Initially, we carried out a literature review on image classifications employed in NID land cover mapping [1,14,16,22,23]. Of the different methods used, unsupervised classification was by far the most popular [1,17], but with different techniques. With the exception of color composite image analysis, which showed poor performance in previous comparative studies [14,23], we included the supervised classification with different training data from unsupervised classifiers applied in the previous publications [1,16].

We performed supervised classification and unsupervised classification of Landsat 7 and images and to a SeaWinds onboard QuikSCAT data respectively, and compared the results of these two methods. In addition, this study performed the unsupervised classification of Landsat 7 to use its result to help defining the training areas for the supervised classification. To characterize the landscape and to account for these flooded areas extents, we used a both classification methods to identify major land cover classes and flooded areas using a combination of SeaWinds and Landsat 7 images.

Supervised Classification of Landsat 7 Images

Landsat 7 images from 2000 to 2009 were used for classifying land cover using training areas. However, to find homogeneous zones, the distinction of the training areas was done by the help of an unsupervised classification performed with the ISODATA unsupervised algorithm whose results also used as training samples. Thus, the creation of training areas was improved with the help of unsupervised classification, and existing knowledge on land-cover classification features of the area (Land use map for the West Africa version 2000, collected from AGRHYMET (Agronmeteorology and Operational Hydrology and Their Applications) regional center [24]). Finally, we classified the image mosaic with Maximum Likelihood (ML) and sequential maximum a posteriori (SMAP) algorithm and estimated thresholds and kappa values to distinguish between vegetation and water. The highest Kappa accuracy of 80.37% and 64.36% was achieved from all seven bands both SMAP and ML classifications algorithm respectively.

SeaWinds Classification

SeaWinds data is not typically used to classify land cover but several methods were published for land cover mapping from SeaWinds data [25,26]. In this paper, we compare the results of the classification with the results of supervised and unsupervised classification of Landsat 7 images and by using the MODIS NDVI datasets for the same time period.

To distinguish flooded and non-flooded areas using the SeaWinds data for each month between January 2000 and December 2009, we performed an unsupervised classification with the "I.maxlik" module of the GRASS toolbox and defined the thresholds by comparing the classification results with the maps created using the Landsat classification.

2.3.2. Water Balance of the NID

We conceptualized the hydrological system of the NID as a set of storage terms, and inflow and outflow terms (Figure 2).

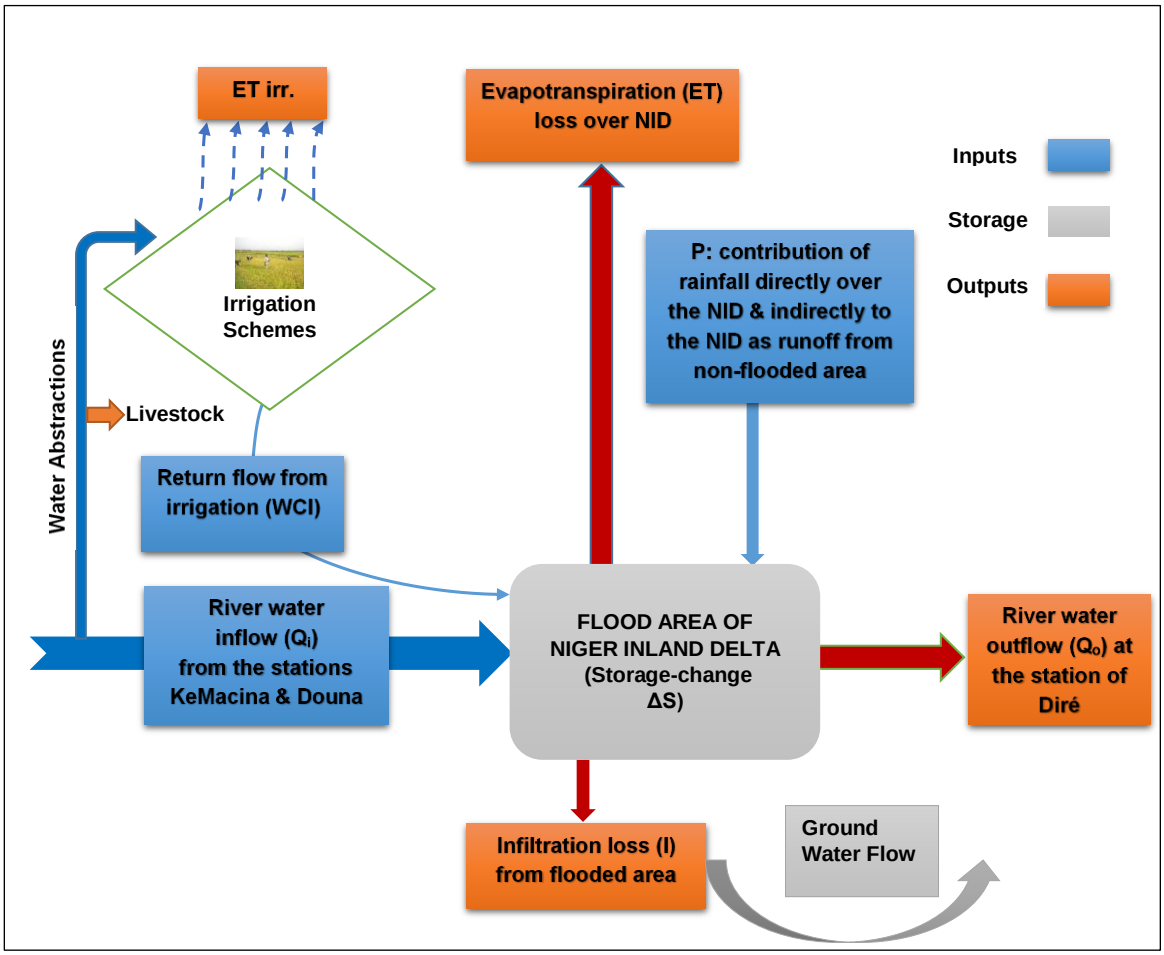

Figure 2. Schematic diagram showing stores and fluxes of water in the NID.

The surface water inflow component into the NID is a combination of the discharge records from all major catchments in the upstream basins of the Niger and Bani rivers, as shown in Figure 1, and surface runoff generated within the NID and rainfall over the flooded areas.

The water balance of the NID can be expressed as:

$$\Delta S = Q_i(t) + P(t) - ET(t) - I(t) + WCI(t) - Q_o(t) \quad (1)$$

where:

ΔS = change of storage,
Q_i = river water inflow, calculated as the sum of discharge measured at the stations KeMacina and Douna,

P = Rainfall contribution (directly on the flooded area and indirectly as runoff from areas in the NID's catchment that drain to the flooded areas),

ET = evapotranspiration loss over the NID,

I = infiltration loss from flooded area,

WCI = return flow from irrigation to the NID's water balance,

Q_o = river water outflow at the station of Diré, and

t = time.

All units are in ($km^3 \cdot month^{-1}$).

Although there is some evidence of groundwater movement in parts of the wetland, there is a highly impermeable clay layer under much of the system [12] which minimizes the influences of infiltration loss. We therefore did not consider infiltration.

2.3.3. Estimation of Water Balance Terms

Evaporation (ET) Loss Computation

Radiation is the principal weather parameters that determines evapotranspiration in the tropics [27]. We tested eight different methods to calculate PET (potential evapotranspiration) models (see supplementary information in Table S1 & Table S2) that differ with respect to complexity and input data requirements.

We computed PET for each of those methods for the climate data available for the station Mopti and compared those results with measured Class A pan evaporation at Mopti, that was obtained from the "Division de la Climatologie" at the "Bureau Alerte Précoce, Agence Nationale de la Météo" in Bamako, Mali. We multiplied pan observations with a pan coefficient of 0.75, the mean of reported pan coefficients in the Sahel that typically range from 0.70 to 0.80 [28]. Monthly values of ET losses in the NID were calculated by multiplying the remotely sensed area with the calculated PET depth.

Precipitation (P) Contribution to the NID

We interpolated average areal precipitation [29] with the Thiessen polygon method and calculated the direct monthly contribution of precipitation over the remotely sensed are and for the non-flooded areas draining to the NID assuming a runoff coefficient of 5% [5].

Return Flow from Irrigated Fields (WCI)

To estimate the amount of water returning to the NID from irrigated areas as return flow, we subtracted estimated consumptive water use in irrigation schemes from the reported water abstraction data from the Bani and Niger rivers. Consumptive use was calculated as potential crop evapotranspiration, ET_{irr}, by multiplying a crop coefficient, kc with the reference potential evapotranspiration (ET_0) computed with the Penman-Monteith equation according to FAO [30].

Net Irrigation water requirement is expressed as (derived from Allen et al. [30]):

$$I_{net} = ET_{irr} + S + I_n - P_e \quad (2)$$

where:

I_{net} = net irrigation water requirement,
ET_{irr} = water requirement ($ET_{irr} = K_c \times ET_0$),

S = depth of water for soil condition (data collected from the "Office du Niger"),

I_n = Infiltration rate (refers to percolation losses) within the irrigation scheme (Data collected at "Office du Niger); and

P_e = effective rainfall ($P_e = P \times e_r$, with P as rainfall over the area and e_r as coefficient for effective rainfall).

Gross water requirement (consumptive water use (CW)):

$$CW = I_{gross} = I_{net}/e_p \quad (3)$$

where: e_p is the irrigation scheme efficiency coefficient (0.65, this efficiency is not already considered in the percolation losses), taken from available "Office du Niger" statistics.

Change of Storage (ΔS) Assessment

Data surface water level (h) collected from the National Hydraulic Headquarters of Mali, were used for assessment of the storage changes in the NID.

$$\Delta S = \overline{A_f} \times \overline{\Delta h} \quad (4)$$

$\overline{A_f}$ = Average flooded area (km²) between two time intervals,

$\overline{\Delta h}$ = average variation of surface water level (in km) between two time intervals, calculated from the mean water height at the gauging stations (Mopti, Diré & Ké-Macina) between two time intervals.

2.3.4. Analyzing the Water Balance

The closing of the water balance over the NID (NIDWat) at monthly time steps was carried out in two steps. First, we assessed the water budget terms over the NID described above independently of the terms of the water balance equation (Equation 1) using input datasets derived from the observed and satellite data time series. Then, simulated water losses were compared to discharge differences obtained from the inflow-outflow for annual time steps.

3. Results

3.1. Assessment of Flooded Area

The maximum monthly flooded surface area in the NID obtained from SeaWinds data varies between a maximum of 25,054 km² in 2009, and a minimum of 14,525 km² in 2002 (Figure 3a). The 2000 to 2009 mean of the maximum flooded surface area was 14,977 km² with a standard deviation of 7227 km², highlighting the significant inter-annual variability. During the dry season, the flooded surface area receded progressively to a minimum of 317 km² (2000 to 2009 inter-annual mean) then following April, they increased in June and rose rapidly in August. Minimum values, measured between March and April, vary between 300 km² and 4000 km².

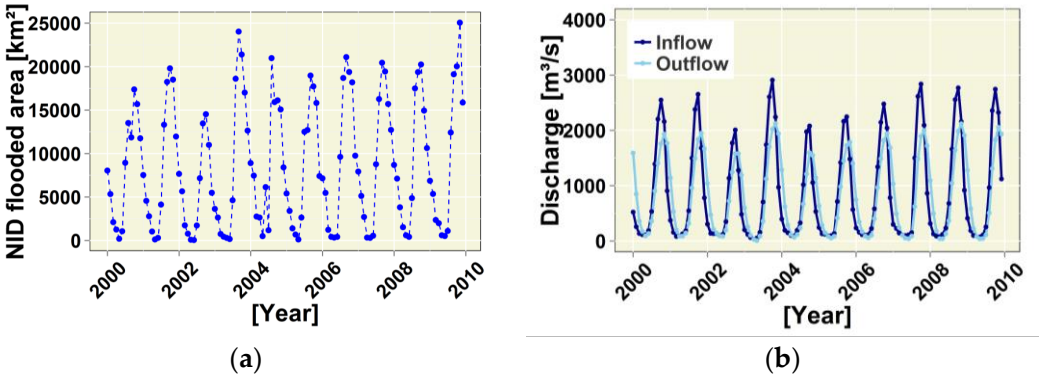

(**a**) (**b**)

Figure 3. (**a**) Monthly flooded surface area estimated using SeaWinds data in the NID over the period 2000–2009; (**b**) Inflow and outflow discharge values over the period 2000–2009.

Remotely Sensed Flooded Area Comparison-Discharge and Area Relationship

Following other studies [1,16,31], we analyzed the relationship between the maximum discharge at Mopti and the extent of the flooded area in the NID. This relationship can best be expressed by a non-linear regression model:

$$A_f = 129 \times (Q_i)^{0.64} \quad (5)$$

$$(R^2 = 0.92)$$

where: A_f is the flooded area in km²; and Q_i is the mean monthly inflow data in m^3s^{-1} at the Mopti gauging station (Figure 4a).

This relationship between inflow and flooded area is plotted in Figure 4a for the last 10 years; implying that the behavior as the flood rises in Figure 4b led to a greater surface area during maximum October flow discharge at Mopti. The positive slope of the regression line in Figure 4b indicates a positive relationship between the maximum inflow discharge and the peak flood extent.

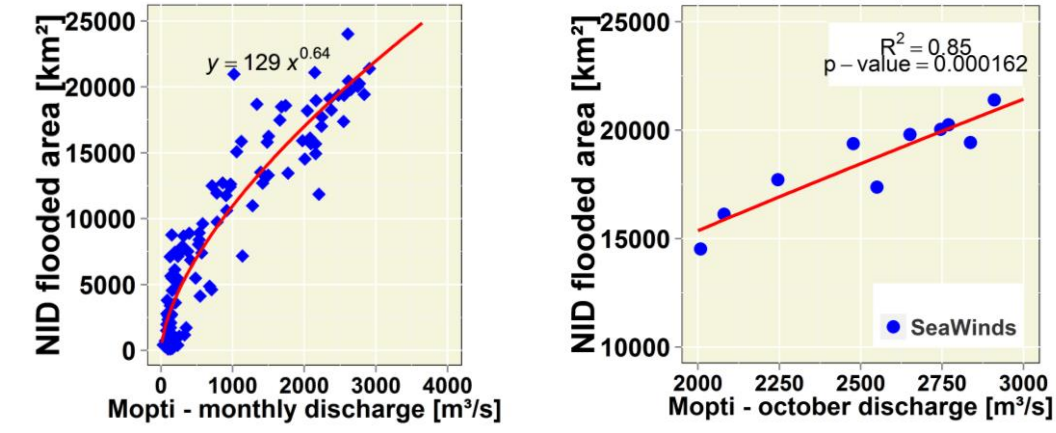

(**a**) (**b**)

Figure 4. (**a**) Non-linear regression relationship between inflow discharge and remote sensing area estimates (SeaWinds data), relative to the gauge of Mopti (Monthly discharge m^3/s), (**b**) correlation between Mopti October mean maximum monthly flows and SeaWinds monthly peak flood extent estimates.

3.2. Water Balance Hydrological Variables Estimations

3.2.1. Water Losses (Evaporation (ET)) Estimations over the NID

Comparing the results from the eight PET models with the Mopti class A pan records over 360 months (January 1980 to December 2009), we found that the modeled data adequately represented the dynamics observed. The simulated mean annual evapotranspiration rate computed using the eight PET models showed significant differences ranging from −500 and 500 mm per year. Comparing the recorded pan evaporation data at Mopti and using performance criteria recommended by Moriasi & Arnold [32], we found that the Penman-Monteith model is best suited to calculate PET in the NID. The comparisons of the methods are first made on an annual basis. The observed yearly evapotranspiration and the relative errors of the calculated evapotranspiration to the observed pan values are presented in Table 3. It is seen that on a mean annual basis the Modified Turc model (2549 mm) gives the smallest error & the lowest bias compared with measured pan evaporation (2558 mm), followed by the Hamon (2409 mm), and Penman-Monteith (2370 mm) models.

Regarding the Pearson coefficient of correlation, it is seen that the PMO (Penman-Monteith) model and the Priestley-Taylor model have the highest coefficient's values, with $r = 0.73$ and $r = 0.72$, respectively. The Modified Turc method has the lowest value, with $r = 0.01$ as shown in Table 3.

Table 3. Evapotranspiration Models comparison results from based on the statistical indicators (Where: OUD = Oudin evapotranspiration equation, HAM = Hamon method; TUR = Modified Turc method; HARG = Hargreaves method; PMO = Penman-Monteith combination equation; ABT = Simple Abtew equation; PRT = Priestley-Taylor method; MAK = Modified Makkink equation).

Model Performance Tools	OUD	HAM	TUR	HARG	PMO	ABT	PRT	MAK
ET Mean values estimates (mm)	2153	2409	2549	2059	2370	2760	2795	2087
Percent Bias (%)	−15.8	−5.8	−0.4	−19.5	−7.4	7.9	9.3	−18.4
RMSE-RSR	1.98	1.11	1.04	2.34	1.23	1.30	1.38	2.24
Pearson coefficient of correlation with observation	0.30	0.27	0.01	0.60	0.73	0.68	0.72	0.64
Average rank	6	3.25	2.75	7.25	2.5	3.75	4.25	6.25
Rank	6	3	2	8	1	4	5	7

The calculated water loss due to evapotranspiration is shown in Figure 5. The percentage of ET loss calculated for each annual inflow in selected hydrological years (Figure 6b) was compared with corresponding available discharge data inflow (KeMacina + Douna). Time series of input water volumes in the Niger Inland delta and of the water losses through the NID show that the average percentage of water losses, due to the high evapotranspiration, is approximately 50% (Figure 6b). Observations reveal that the Niger River at NID experienced a downward shift in discharge in 1982 and 1992 is proportional to the decrease in ET loss; and is also coherent as observed rise from 1994 till 2004 (Figure 6a). However, a large volume of inflow in the NID at Mopti led to greater floods in the area and hence larger ET loss (Figure 6b).

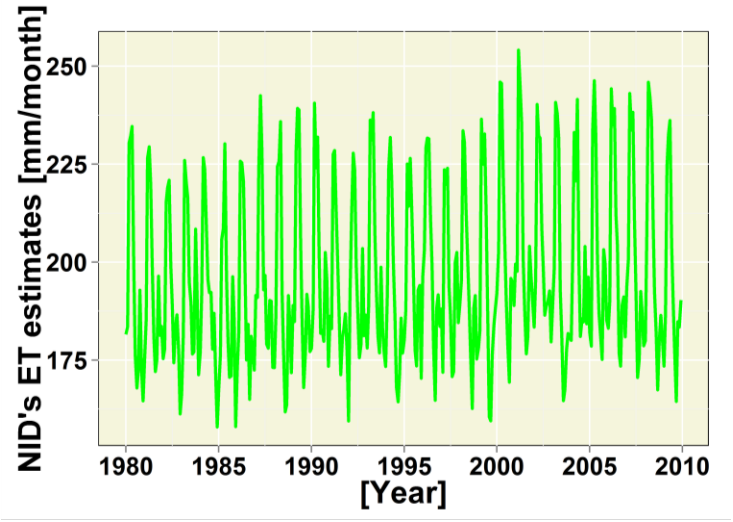

Figure 5. Monthly Potential Evapotranspiration (PET) computed using the Penman-Monteith model for the period of 1980 to 2010 in the NID.

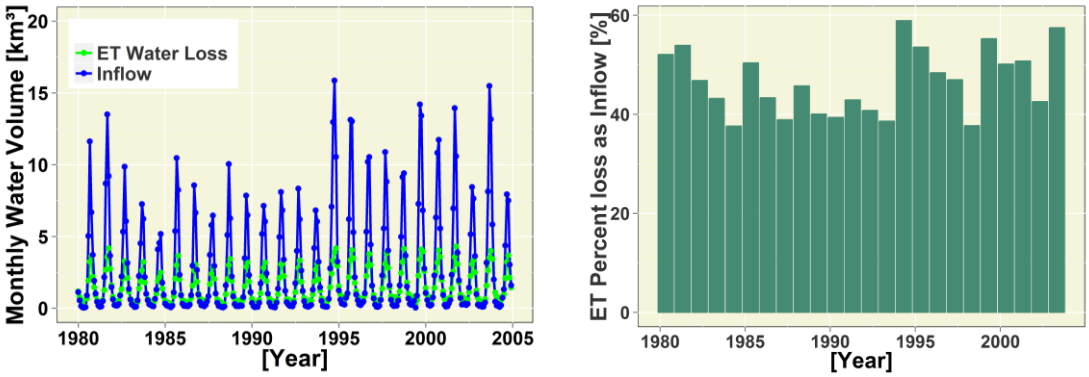

Figure 6. (**a**) Calculated evaporation (ET) losses in the Niger Inner Delta and combined river flows in KeMacina + Douna with values over the period 1980–2004; (**b**) Annual ET loss as a percent of the inflow in the NID.

3.2.2. Accounting for Rainfall and Estimating Return Flow from Irrigation

The annual total contribution of precipitation & runoff over the wetland, calculated from the observed average rainfall data over the estimated flooded areas and runoff from non-flooded areas draining to the NID, varies between 3.10 to 9.12 km^3. Precipitation draining to the NID from non-flooded areas is around 2.6 km^3 per year indicating a non-negligible contribution to the overall water balance of the wetland.

The volume of the abstracted water needed for irrigation based on the available irrigation details from the ON amounts to 0.223 km^3 per month. "Office du Niger" takes approximately 2.5 km^3 water per year; this becomes more important, when irrigating more areas. For the "Office Riz Mopti" (ORM) we consider data on the Bani River only. Before the Bani enters the Niger Inland Delta, 0.291 km^3 per month (Table 4) is taken for irrigation at Djenné and Talo dams. This represent an average flow reduction from Bani River to the NID expected at Mopti (Table 5).

Table 4. Average monthly amount of water abstraction (km^3/month) over the Niger Inland Delta for irrigation (Where ON is "Office du Niger" irrigation schemes, Djenné & Talo are reservoirs for the ORM's ("Office-Riz-Mopti") irrigation schemes).

	J	F	M	A	M	J	J	A	S	O	N	D	Sum
ON	0.150	0.168	0.181	0.207	0.226	0.254	0.264	0.264	0.314	0.337	0.194	0.117	2.677
Djenné	0.000	0.000	0.000	0.000	0.000	0.000	0.039	0.156	0.236	0.290	0.218	0.000	0.938
Talo	0.000	0.000	0.000	0.000	0.000	0.000	0.008	0.129	0.040	0.077	0.155	0.000	0.408
Total	0.150	0.168	0.181	0.207	0.226	0.254	0.311	0.549	0.589	0.704	0.567	0.117	4.024

Table 5. Monthly water contribution from irrigated fields (WCI) (km^3 $month^{-1}$) (WU is defined as the total withdrawn water, CW is the consumptive water used and WCI is water contribution from irrigation refers to return flow from irrigated fields).

Months	WU (10^{-3} km^3 $month^{-1}$)	CW (10^{-3} km^3 $month^{-1}$)	WCI (10^{-3} km^3 $month^{-1}$)
January	151	138	13
February	168	153	15
March	182	163	19
April	207	184	23
May	225	206	19
June	254	224	30
July	312	260	52
August	512	226	286
September	566	236	330
October	833	273	560
Novenber	605	141	464
December	118	102	16

4. Discussion

4.1. Comparing Remotely Sensed Flooded Areas with Previous Estimates

Estimates of the flooded area in the NID using remotely sensed data were carried out by a number of studies [1,16,31]. Generally, our estimates of the monthly extent compare well with these studies (Figure 7b). This is an important result, as all previous studies were optical based and therefore limited by clouds during the flood rise (Figure 7a). However, the first impression shows that the SeaWinds classification results in higher wetland area extents than the Landsat 7 classification, when considering all 77 scenes, where the Landsat images as well as the SeaWinds images are available.

This high difference is to be expected for two reasons. First, the grid size of the SeaWinds raster has an average area of 3014.3 km^2 per pixel, while Landsat 7 has a pixel size of 225 m^2. Secondly, SeaWinds reacts much more sensibly to the availability of moisture, while Landsat 7 is more sensitive to vegetation growth, at least in the bands five and seven, and the vegetation needs some reaction time to the change between drought and abundance of water. Also, by analyzing the created SeaWinds time series no dominant trend is recognizable. The main reason for this could either be the short time span of the observation or just because no real general shift exists. Comparing the dry season and the rainy season separately, no further evidence of extern influence like through the global climate change can be found. Only the maximum spread of the wetland seems to have a weak tendency to an increasing value, as visible in the Figure 7a.

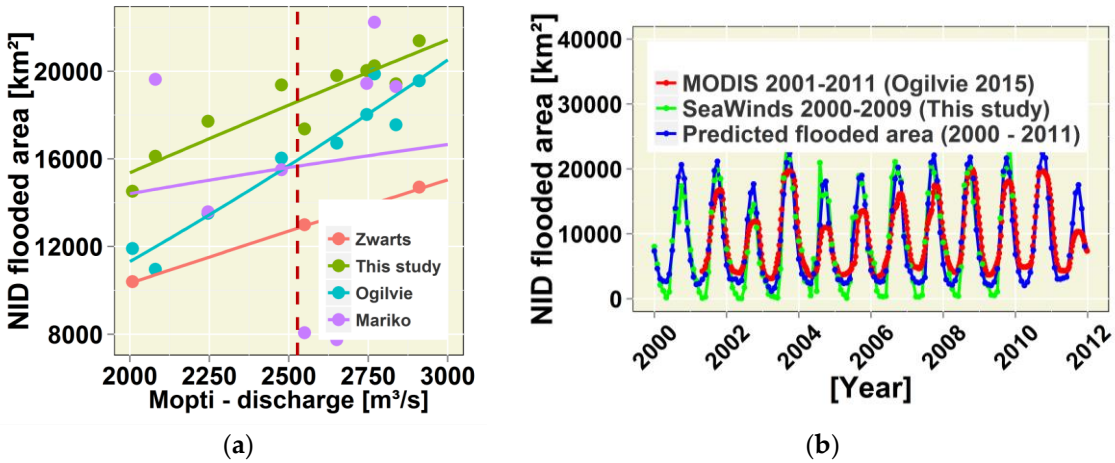

Figure 7. (**a**) Comparison with other results on the area flood extent; (**b**) Monthly flooded surface area.

The Mopti gauging station is usually used to model the annual floods in the NID [1,5], as its central location allows study of flow variations in both the Niger river and, indirectly, the Bani River, a major tributary. Changes in rainfall in the Niger and Bani upper catchments are known to be main drivers of fluctuations in the total flooded area [5]. The annual flood dynamic observed through remote sensing is consistent with the NID flow regime (Figure 3b), providing a correct representation of the flooding. Interannual variations in the max flooded areas are also strongly correlated (about R^2 = 0.90), with the maximum monthly flows in October at Mopti, suggesting a strong dependence of the area on the peak amplitude of the flooding. The range of values obtained and their variation according to peak flow in October are consistent with previous remotely sensed estimates [1,16,31]. The difference in estimates by different methods used for the remote sensing area estimates reveals the difficulties in assessing the spatio-temporal dynamic of the flood area extent. Mariko [31] was limited in his study with the number of suitable images of NOAA AVHRR products to characterize the flooded area relationship with discharge. Zwarts et al. [1] used 24 Landsat images spread over several years to derive a correlation between flooded areas and the Akka stage level. Ogilvie et al. [16] used MODIS images and was limited in the accuracy in determining the rise of the flood due to the presence of clouds. Our area estimates based on SeaWinds demonstrate the potential of radar remote sensing to overcome these limitations.

The predicted extent based on Mopti discharge which is the annual flood dynamic observed through nonlinear model, appeared coherent with MODIS's estimates by Ogilvie et al. [16] (Figure 7b); providing confirmation of the method's ability to correctly represent the variation of the flood. Therefore, the flooded surface area extent in the previous years could be predicted and, this partly explains the variation along the non-linear regression line shown in Figure 4a. However, the microwave remote sensing data based on which the nonlinear model was established, overestimates the minimum flood extent area (Figure 7b). This is in line with the explanation by Aich et al. [33] and Liersch et al. [34] with regards to the substantial uncertainty on the surface flooded area modeling in the NID. The reason they mention it is likely the effects of land use changes, and lack of detailed regional studies in this regards for the NRB. Besides, observed increasing discharge since 1994 in Mopti and Douna increases the flooding extent and in combination with increasing population pressure led to greater irrigation water use in the study area. This is in contrast with the observations of Ogilvie et al. [16] who reported that in 2004, the peak flooded area in the NID was 45% lower than in 2008. Still, between 2004 and 2009, a non-linear decline in this area is recognizable

Furthermore, the most recent decade (2000–2009) display higher flooded area compared to decades 1990s and 2000s. Figure 8 illustrated the 2000–2009 of relative mean area change at NID over sample period of our analysis of maximum in the extent of flood with maximum peak flow. Observed percentage change in flooded area trends highlights slightly its response with increase in flow (Figure

8). The flooded area change witnessed in the NID is attributed in general to changes in peak flows, and in particular to land use or irrigated agriculture; which led to ~10% increase of flood extent from the month of October under the reference period of 2000–2009 (Figure 8). The interpretation of this result is difficult since no local studies are known that confirmed the changes in the October's flood area extent. However, Zwarts et al. [1] and Orange et al. [3] explained that this result might be an effect of the delay of the high-water wave through the Niger Inland Delta which varies between 1 to 2 months.

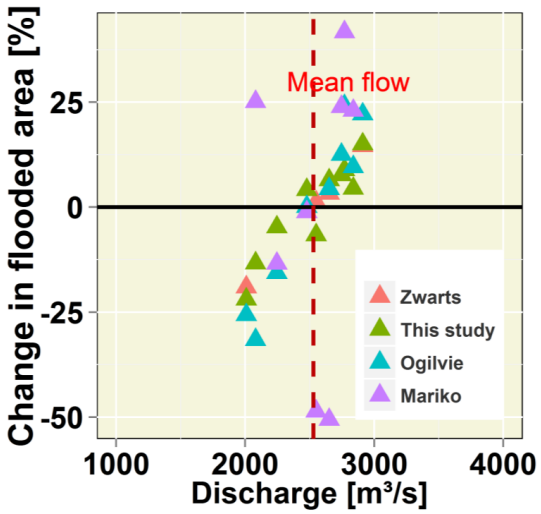

Figure 8. Remote sensing estimates of the flooded surface areas and peak flow discharge at Mopti perceptions of relative mean flooded area change at NID; Points show percentage of change in flooded area response with increase in flow.

4.2. Comparing Water Balance Components with the Previous Studies

The average annual rainfall contribution (varying from 3.26 to 8.4 km³/year) to the water budget of the NID is in line with the recent estimated direct precipitation over the wetland by Ogilvie et al. [16] over the MODIS flooded areas which varied between 2.6 km³/year and 8.5 km³/year. Despite neglecting of groundwater in line with previous studies [1,11,16,35], this study uses storage changes and the remaining flows parameters to assess the balance. Our estimate of the rainfall contribution to the NID's flooded area is fairly similar to the recent calculated water budget residual terms (infiltration (which we neglected) and rainfall runoff) in between −0.7 and 5 km³ [16]. Monthly average NID's flooded area storage changes of 0.329 km³ was estimated. This is in line with previous studies who suggested that its contribution to the NID floodplain is minimal [5,11,35]. Storage also decreased during the wet season (April–September) and slightly increased during October to March in concordance with seasonal rainfall pattern [1,36].

Regarding the ET component, understanding concerns of local water losses will contribute to the analysis of relevant hydrological processes and improvement of NID's water budget [16]. ET losses were calculated from remote sensing estimated flooded areas and evapotranspiration data rates across the NID from ET models for 1980 to 2004. Over the period of 1980–2010, monthly potential ET values from north to south ranging between 157 and 255 mm/month, and the mean monthly PET across the NID is estimated at 196 mm/month. This value is slightly higher than previous evaporation estimates of 192 mm/month by Olivry [11] who used the proportionality between flooded areas and total evaporation to assess the flood surface areas variation in the NID. Measuring ET also takes soil moisture and vegetation across the wetland into account, which would increase overall evaporation loss.

Potential ET rates in the NID's wetland from 1980 to 2009 are 2.61 to 9.56 mm/day, which are slightly higher than the values of 3 to 7 mm/day in Dadson et al. [12]. The annual cumulative ET loss over the entire NID ranges approximately between 12.71 to 21.78 km^3, which is 196.3 mm/month (1.443 km^3 per month), close to the range of values modelled by recent studies from the period 1980–2002, notably 140 to 240 mm/month in Zwarts, et al. [1]. However, evaporation from flooded areas may have been overestimated slightly, as evaporation rates from the NID, for submerged vegetation area, can be less than those of open water (McMahon et al., 2013 as cited by Ogilvie et al. [16]). However, uncertainties from remotely sensed flooded areas are expected to be more determinant with regards to wetland's evapotranspiration estimates. Though, potential ET is highest during the dry season, total ET from the NID is higher during September, October, and November due to the large surface area flooded. In addition, spatial variations in actual evaporation [12] were significant, due to higher PET values in the northern areas and the longer flood durations along river stretches and lakes.

To enhance the water budget of the NID to distinguish the water availability, it is important to look beyond abstracted water from rivers (Niger and Bani) for irrigation. The return flow which referred to the non-consumptive water used drained to the NID and generated by the irrigation schemes, was computed. The average water volume of return flow from irrigation dataset (Table 5) is ranging from 0.013 km^3 to 0.559 km^3 per month. This is lower than the values between 2.50 km^3 in 1994 to 2.85 km^3 in 1999, with an average of 2.69 km^3 per year of the total annual intake for irrigation (at ON). It is important to highlight that this is before the KéMacina station, and therefore the abstraction is not relevant in the water balance, it is indeed the WCI which is of interest here, and this totals 1.8 km^3. Some of this is from Office Riz Mopti and the total balance of these may be null (as withdrawals, PET and return occur within the NID), hence it's really the return flow from Office du Niger, which was not previously estimated, and this is in the order of 1.2 km^3 per year in line with previous findings [1]. Zwarts et al. [1] also noted the importance of inter-annual variability in irrigation water use impacting on the NID's flood area extent. Our computed relative average annual return flow from irrigation is lowest (about 4.5%) over the NID, but significant for the water balance and on downstream wetland benefits (Figure 9). The range of values obtained were consistent with previous value of 3.7 km^3 estimated by Zwarts et al. [1] (less than 10% of total inflow) of annual water intake for irrigation, though the value was moderately superior and met our expectation.

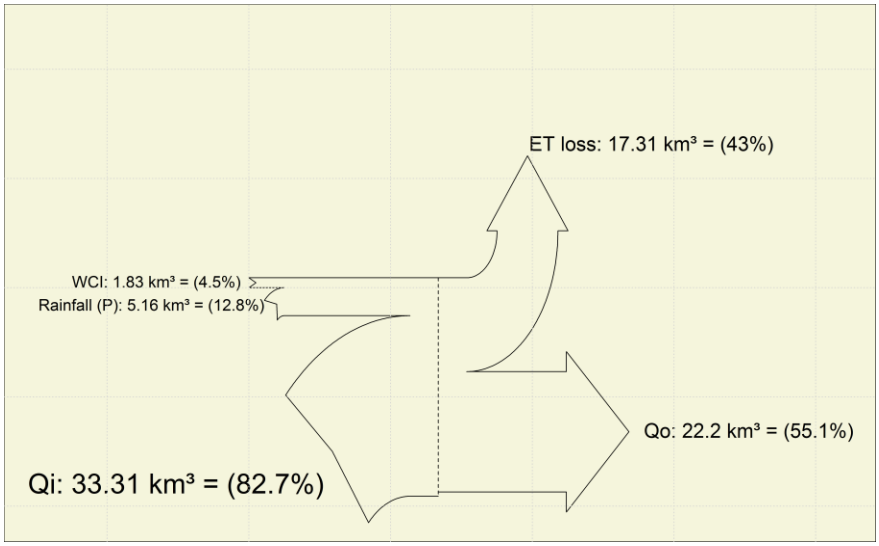

Figure 9. Sankey plot showing the annual average water fluxes of the water balance terms over the NID's floodplain for the period 1980–2004. (With: Q_i = river water inflow, calculated as the sum of discharge measured at the stations KeMacina and Douna, P = contribution (direct and indirect) of rainfall over the NID, ET = evapotranspiration loss over the NID calculated by PMO, WCI = return

flow from irrigation to the NID's water balance, Q_o = river water outflow at the station of Diré, and % refer to the percent of the total annual flux).

NID's floodplains are being modified as the result of water management activities, in particular large-scale irrigation schemes; which, irrigation water increases with higher crop evapotranspiration and high intake of water abstracted from rivers (Niger & Bani) can be explained due to a lack of an adequate efficient irrigation system [1,15,37]. Some studies were conducted, since the early developments of the "Office du Niger" and have confirmed this hypothesis. The level of the water table is increasing after many years under the influence of irrigation in areas of "Office du Niger", this rise is linked not only to the return of irrigation water in delta, but also to the permanent retention of water in irrigation channels [38]. With use of surface water for irrigation, e.g., in large River valleys, drainage and net groundwater recharge may have increased [39]. Our analysis suggests that the return flow from irrigation can only partially replace the lost water abstracted from reducing floodplain inundation. Thus, further extension of irrigation schemes within the rivers basin should also be avoided, because of the expanding demand for irrigation which will increase the water losses.

4.3. Water Balance (NIDWat) Analysis

The water balance cannot be closed by the data available. Figure 9 shows the Sankey diagram of the water budget over the NID's surface flooded area which shows an error of 1.9%. Our simulated mean annual evaporation loss of 17.31 km^3 is superior to that of the discharge differences (11.18 km^3). The average of evaporation losses is in accordance with the previous result based on the hydrological balance.

The water balance was performed from observed hydro-climatic and optical & microwave remote sensing data adapted from the NIDWat modelling approach providing input and output fluxes across the NID's wetland (Figure 9). This NIDWat model also provides the main features that leads to the explanation of the overall hydrological functioning of NID's reservoir. However, NIDWat in the present situation differed on approaches compared to models of above mentioned publications in which the natural variations as well as the impact of human activities (e.g., irrigation aspect) on NID's floodplain are not well captured. Hence, for this article, the output of NIDWat is mostly compared with the recent model results by Ogilvie et al. [16], as mentioned in the introduction of this paper because the two approaches can be used in a complementary manner.

The calculated amount of water reduction in discharge difference (inflow minus outflow) for the inlet and outlet gauging stations is compared with the results of NIDWat. The annual mean evapotranspiration's are overestimated as compared to the discharge differences between inflow and outflow over the NID, which is confirmed by Ogilvie et al.'s [16] results. This implies that other hydrological component over the wetland must be accounted for; and also, the actual ET losses would be considered. Our simulated mean annual evaporation loss of 17.31 km^3 (i.e., 43% of the total input) was found consistent with a mean value of 17.2 km^3 in Ogilvie et al. [16]; and moderately superior to a value of 11. 4 km^3 (i.e., 33%) in Zwarts et al. [1]. Values for the contribution of rainfall, and values on the return of water withdrawal for irrigation are found coherent with the references mentioned above. The water budget's difference is 1.9% between the input fluxes and output fluxes confirms that our model provides an adequate representation of the potential evaporation losses (Figure 9). The interpretation of this error is difficult since no local studies are known that confirmed the water budget modeled in the present study. However, Ogilvie et al. [16] assumed that his water budget residual term corresponds the difference between infiltration and runoff generated by rainfall falling upon non-flooded areas of the NID. Hence, the good performance of the NIDWat model confirms that, SeaWinds data and the WCI estimates may therefore be used to provide additional insights and refine the water balance of the NID. Nonetheless, the trends generally remain good, even if some

parameters are not considered; the limitations with respect to data availability and uncertainties in the significance of the estimated parameters, however, remain.

4.4. Uncertainty and Outlook

Input data used in the estimates of the available energy for ET are source of uncertainty since measured solar radiation is not available at meteorological stations in or near the study area. In addition, we used only Mopti pan recorded data pan for the whole study area due to the lack of other local pan recordings for our study area based on the assumption that the climate classification is the same [40]. The uncertainty of the single ET models in percentage deviation from the mean ET of 17.67 km^3/year is in the range of −15.31% to + 15.54%. PMO has the smallest differences to this mean value (−2%) resulting in a water balance error of 0.79 km^3/year. The water balance error is calculated by summing all in and outflows. The uncertainty in ET results in a water balance error in the range of −2.31 to + 3.14 km^3/year. This error is the smallest (0.435 km^3/year) when the ET losses are calculated as the mean over the eight models is used and only slightly higher when the PMO model is applied.

Our water balance modeling approach, like previous studies to assess water losses under hydroclimatic conditions [1,11,16,31] is limited by some assumptions and some processes that are not represented in the model. One of these limitations is the neglect of infiltration from flooded areas and rainfall. Although infiltration is the dominant process of groundwater movement in portions of the wetland [5]; and could become more important in a water balance. Therefore, infiltration process in NID's wetland can potentially lead to the error in balancing the water fluxes over the NID. Constraints in our water balance are not only caused by constraints in the characterization of hydrological processes but also by uncertainties arising from the data.

Moreover, the possible changes in the NID hydraulic pathways due to dams or land use changes as discussed in Ogilvie, et al. [16] were not considered.

5. Conclusions

This study demonstrates how remote sensing data can be used to help conducting hydrological process analysis at high temporal and spatial resolution across large wetlands. Understanding surface flooded area processes for the Niger Inland Delta are crucial for water balance purposes. The advantage of effectively mapping wetland using microwave SeaWinds data have been illustrated and allows describing the flooding dynamic in the delta in terms of inundation extent. We have shown a clear correlation between maximum October flow at Mopti and peak flooded area in NID. The results are in good agreements between the estimated flooded area data and the remotely observed surface flooded area from past studies.

We present the Penman Monteith model as best in representing the potential ET in our study area. In addition, this study shows how knowledge from the flood characteristics was used to significantly improve our understanding of hydrological processes in the NID's floodplains and their interaction with hydrological observations. Thus, NIDWat was developed to understand the hydrological functioning at play in NID's flooded area. Estimated flooded areas were used to refine evaporation estimates as well as precipitation over the wetland. Additionally, actions from irrigation schemes on a large scale (e.g., ON & ORM) have implications for water balance in the system. Despite often neglected infiltration and ground water fluxes, annual differences in annual rainfall, discharge and evaporation over the wetland are essential to explain inter-annual variations in the water balance. The water balance model NIDWat was shown to be suited for assessing the hydrologic characteristics of NID's wetland. Its information can be used into existing hydrological models on the basin to improve runoff simulation downstream the NID.

Supplementary Materials: The following are available online, Table S1: Data availability and periods of records for the main climatic variables and evaporation at Mopti synoptic station (longitude = −4.1, latitude = 14.52, Elevation = 272 m); Table S2: Inputs data of all potential ET methods used in this study.

Acknowledgments: This study was funded by the German Ministry of Education and Research (BMBF) through the West African Science Service Center on Climate Change and Adapted Land Use (WASCAL; www.wascal.org), that supports the Graduate Research Program Climate Change and Water Resources at the University of Abomey Calavi). We thank AGHRYMET regional center, Niger Basin Authority, and Niger & Mali Meteorological and Hydrological Service for providing the hydro-meteorological data for the Niger Basin.

Author Contributions: Moussa Ibrahim, Dominik Wisser, Abdou Ali, Bernd Diekkrüger, and Abel A. Afouda conceived the study, developed the methodology. Moussa Ibrahim performed the field work, collected the data, and conducted the analysis with Dominik Wisser and Abdou Ali. Manuscript was drafted by Moussa Ibrahim, with input from Dominik Wisser, Ali Abdou, Ousmane Seidou, and Adama Mariko; while Abel A. Afouda and Bernd Diekkrüger supervised this part of the work.

Conflicts of Interest: The authors declare no conflict of interest.

Abbreviations

The following abbreviations are used in this manuscript:

ABT	Simple Abtew equation
AGRHYMET	Agrometeorology and Operational Hydrology and Their Applications
CW	Consumptive Water used
DEM	Digital Elevation Models
HAM	Hamon evaporation model
HARG	Hargreaves evapotranspiration model
JULES	Joint UK Land-Environment Simulator
MAK	Modified Makkink equation
NID	Niger Inland Delta
NIDWat	Niger Inland Delta Water balance model
NRB	Niger River Basin
ON	"Office du Niger"
ORM	"Office Riz Mopti"
OUD	Oudin evapotranspiration model
PET	Potential Evapotranspiration
PMO	Penman-Monteith combination equation
PRT	Priestley-Taylor method
RMSE	Root Mean Square Error
RSR	Ratio of RMSE to the standard deviation of the observations
TUR	Modified Turc evapotranspiration method
WASCAL	West African Science Service Center on Climate Change and Adapted Land Use
WU	Withdrawn water
WCI	Return flow from irrigated fields
ZEF	Center for Development Research

Appendix A

(a) Potential PET Estimation Methods

(1) Edited Potential Evapotranspiration (PE) Model Published by Oudin et al. [40]

$$PE = \frac{R_e}{\lambda\rho}\frac{T_a+5}{100} \text{ if } T_a + 5 > 0$$

$$PE = 0 \quad \text{(A1)}$$

where:

PE = rate of potential evapotranspiration in mm per day;

Re = extraterrestrial radiation in MJ per m^2 per day;

λ = latent heat flux for the vaporization (as 2.45 MJ per kg);

ϱ = density of water (ϱ = 995.6502 kg per m^3); and

T_a = air temperature (°C) which correspond to the mean daily air temperature.

(2) Penman-Monteith Combination Equation (PMO)

The Penman-Monteith equation is the most physically based model and corresponds to the Penman equation which is the updated equation recommended by FAO [41] known as the FAO-56 Penman-Monteith. It is expressed as [30].

$$\mathrm{PMO} = \frac{1}{\lambda}\frac{\Delta(R_n + G) + \rho_a c_{p(\theta_s - \theta)}}{\Delta + \gamma\left(1 + \frac{r_s}{r_a}\right)} \quad (A2)$$

where PMO is the ET rate (mm d^{-1}), Ta is mean air temperature (°C), v is wind speed (m s^{-1}) at 2 m above the ground, G is the soil heat flux, which can usually be neglected in the tropics [41], Δ is the slope of the saturation vapor pressure curve, γ is the psychrometric constant (see calculation under radiation), θ and θ_s is the actual and saturated vapor pressure at given RH in kPa (see calculation under radiation), ϱ_a is the mean air density at constant pressure in kg m^{-3}, c_p is the specific heat of the air in MJ kg^{-1} °C pressure in kPa (see calculation under radiation), r_s is the surface resistance in s m^{-1},and r_a is the aerodynamic resistance in s m^{-1}. r_s in the case of open water is 0 and r_a can be calculated from Thom and Oliver (1977) (as cited in Schwerdtfeger et al., [17]):

$$r_a = \frac{4.72\left(ln\left(\frac{2}{z_0}\right)\right)}{1 + 0.54\,v} \quad (A3)$$

where z_0 is the roughness length, which can be set to z_0 = 1.37 mm [41].

(3) Priestley-Taylor Equation (PRT)

Xu & Singh [42], highlighted that the Priestley-Taylor model derived after Priestley and Taylor, (1972); is a simplified version of the combination equation of Penman (1948). It is generally used when surface areas are wet. Thus, the Priestley-Taylor coefficient α_{PRT} is introduced, which is multiplied by the energy component:

$$\mathrm{PRT} = \alpha_{PRT}\frac{\Delta}{\Delta + \gamma}\frac{R_n}{\lambda} \quad (A4)$$

where α_{PRT} can be set to 1.18 [17].

(4) Hargreaves Equation (HAG)

The combined form of Hargreaves equation (HAG) is the Hargreaves and Samni (1982, 1985) formula after Hargreaves, 1975 (as in Schwerdtfeger et al. [17]). The equation can be expressed as:

$$\mathrm{HAG} = 0.0135(T_a + 17.8)R_s \quad (A5)$$

where: T_a is the average temperature, R_s is the global solar radiation which can be calculated from formula for estimating R_s from the temperature range (TR), the extraterrestrial radiation (R_a); and an empirical coefficient (k_r) depending on the station location: $R_s = k_r x R_a x TR^{0.5}$.

(5) Modified Makkink Equation (MAK)

Makkink (1957) estimated ET in millimeters per day over 10-day periods for grassed lands under cool climatic conditions of the Netherlands. After Makkink, 1957; Abtew and Melesse, 2013 (as cited in Schwerdtfeger et al. [17]), calibrated the Makkink equation to the simple Abtew method (Equation A6) for tropical South Florida and has the following form:

$$MAK = 0.743 \frac{\Delta S_t}{(\Delta + \gamma)\lambda} \quad (A6)$$

where: S_t is the solar radiation in MJ m^{-2} day^{-1} (see Equation A23 below).

(6) Simple Abtew Equation (ABT)

The simple Abtew equation was developed for tropical South Florida by Abtew and Melesse, (2013) from open water evaporation and wetland lysimeter studies (work cited in Schwerdtfeger et al. [17]). It can be expressed as:

$$ABT = K_1 \frac{S_t}{\lambda} \quad (A7)$$

Where: K_1 is a dimensionless coefficient given with 0.53 [17].

(7) Modified Turc Equation (TUR)

We use the empirical Turc equation modified for a humid subtropical region. Tmax is used instead of Ta since it showed a better fit with observed data [17]. The modified Turc equation is written as:

$$TUR = K_2 \frac{(23.89 S_t + 50) T_{max}}{T_{max} + 15} \quad (A8)$$

where the coefficient K_2 has the value 0.013 derived from the original Turc equation by Abtew and Melesse, (2013) (as in Schwerdtfeger et al., [17]).

(8) Hamon Equation (HAM)

Hamon (1961) (as cited in Oudin et al., [40]) derived a potential evapotranspiration method based on the mean air temperature and is expressed as:

$$HAM = 2 x DL^2 x \theta_s x e^{\left(T_a/16\right)} \quad (A9)$$

where:

HAM = evapotranspiration, (mm day^{-1})

DL = average number of daylight hours per day during the month

θ_s = saturated vapor pressure at temperature T

T_a = mean daily air temperature (°C)

(b) Calculation of Short and Long-Wave Radiation

The relative distance between the earth and the sun (dimensionless) d_r is given by the following equation:

$$d_r = 1 + 0.033 \cos\left(\frac{2\pi}{365} j\right) \quad \text{(A10)}$$

where: j is the Julian Day Number.

The solar declination δ in radians is calculated by:

$$\delta = 0.4093 \sin\left(\frac{2\pi}{365} j - 1.405\right). \quad \text{(A11)}$$

The sunset hour angle ω_s in radians is given by:

$$\omega_s = \arccos(-\tan \emptyset \tan \delta) \quad \text{(A12)}$$

where: $\emptyset$ is the latitude of the study site (negative for the Southern Hemisphere).

The sunset hour angle is used to calculate the maximum possible daylight hours N(h):

$$N(h) = \frac{24}{\pi}\omega_s. \quad \text{(A13)}$$

Then, the extra-terrestrial solar radiation S_0 in $MJ\,m^{-2}d^{-1}$ is:

$$S_0 = \frac{G_{sc} x d_r}{\pi}(\omega_s \sin\emptyset \sin\delta + \cos\emptyset \cos\delta \sin\omega_s) \quad \text{(A14)}$$

where: G_{sc} is the solar constant being 118.11 $MJ\,m^{-2}d^{-1}$.

The saturated vapor pressure θ_s in kPa can be calculated by:

$$\theta_s = 0.l6108 \exp\left(\frac{17.27T_a}{237.3T_a}\right) \quad \text{(A15)}$$

where: T_a is the daily mean air temperature in °C. For a physically based model of evaporation calculation the gradient of the function $d\theta_s/dT$ in kPa $°C^{-1}$ is calculated by:

$$\Delta = \frac{4098\theta_s}{(237.3+T_a)^2}. \quad \text{(A16)}$$

The vapor pressure θ in kPa at a given RH can then be derived from:

$$\theta = \theta_s\left(\frac{RH}{100}\right) \quad \text{(A17)}$$

where RH is relative humidity in %, which is not available at the study area.

The energy used for phase change from liquid to vapor during the process of evaporation is the latent heat of vaporization in MJ kg^{-1}. This is the required for separating the molecules can be set as 2.45, MJ kg^{-1}.

$$\lambda = 2.45 \quad \text{(A18)}$$

where: T_s is the surface temperature of the water in °C. The psychrometric constant γ in kPa $°C^{-1}$ is derived from:

$$\gamma = 0.0016286\frac{P}{\lambda} \quad \text{(A19)}$$

where: P is the atmospheric pressure in kPa, and can be derived from:

$$P = 101.3\left[\frac{293 - 0.0065z}{293}\right]^{5.26} \quad \text{(A20)}$$

where: z elevation above sea level, m.

Martínez-Lozano et al., (1984) (cited in Schwerdtfeger et al. [17]), stated that the Angstrom coefficients a and b vary with a change in latitude, height of the station, albedo, mean solar altitude, vapor and pollution concentration in the air. Many approaches to derive the Angstrom coefficients have been undertaken. In this study a and b were derived from the approach in the previous paper [43], due to restriction in data availability. This approach depends only on the latitude of the study site and can be formulated with:

$$a = 0.29 \cos \emptyset \tag{A21}$$

which result in a value of a = 0.28 in our case, b was set to 0.52 since it was practically constant [17]. These correspond well with the values given in Shuttleworth (1993) (as in Schwerdtfeger et al. [17]) (a = 0.25 and b = 0.5) for average climates, when there is not enough information available for calculating the Angstrom coefficients.

The Angstrom coefficients are used to calculate the clear sky radiation S_{t0} in MJ $m^{-2}d^{-1}$ according to:

$$S_{t0} = (a + b) \times S_0 \tag{A22}$$

where: S_t is the solar radiation or total incoming short-wave radiation in $MJm^{-2}d^{-1}$ derived from:

$$S_t = \left(a + b\frac{n}{N}\right) \times S_0 \tag{A23}$$

with nN^{-1} as the cloudiness factor. n are the bright sunshine hours of a day and N is the total day length already explained above. With the solar radiation S_t the net shortwave radiation S_n in MJ $m^{-2}d^{-1}$ is calculated by:

$$S_n = (1 - \alpha)S_t \tag{A24}$$

where: the albedo for open water α was set to 0.08. It is the part of short-wave radiation, where losses due to reflections are taken into account. The long-wave net radiation Ln in $MJm^{-2}d^{-1}$ is the net long-wave surface emission and can be expressed as:

$$L_n = \sigma\left[\frac{(T_{max} + 273.16)^4 + (T_{min} + 273.16)\text{^}4}{2}\right]\left(0.34 - 0.14\sqrt{\theta}\right)\left[1.35\frac{S_t}{f} - 0.35\right] \tag{A25}$$

where: σ is the Stefan Boltzmann constant (4.903×10^{-9} MJ $m^{-2}K^{-4}$) and f is the adjustment for cloud cover, derived from:

$$f = (0.75 + 2^{-5} \times z)S_o. \tag{A26}$$

And the net radiation Rn in MJ $m^{-2}d^{-1}$ finally is:

$$R_n = S_n + L_n. \tag{A27}$$

References

1. Zwarts, L.; Van Beukering, P.; Kone, B.; Wymenga, E. *The Niger, a Lifeline. Effective Water Management in the Upper Niger Basin*; RIZA/Wetlands International/Institute for Environmental Studies (IVM)/A&W Ecological Consultants, Lelystad/Sevare/Amsterdam/Veenwouden, Netherlands. 2005; p. 169.
2. Hoogeveen, J.; Faurès, J.-M.; Peiser, L.; Burke, J.; van de Giesen, N. GlobWat—A global water balance model to assess water use in irrigated agriculture. *Hydrol. Earth Syst. Sci. Discuss.* **2015**, *12*, 801–838, doi:10.5194/hessd-12-801-2015.
3. Orange, D.; Mahe, G.; Dembélé, L.; Diakité, C.H.; Kuper, M.; Olivry, J.-C. Hydrologie, agro-écologie et superficies d'inondation dans le delta intérieur du Niger. In *Gestion Intégrée des Ressources Naturelles en Zones Inondables Tropicales*; Séminaire International: Bamako, Mali, 2002; pp. 208–228.
4. IPCC. Climate change 2007: The physical science basis. *Intergov. Panel Clim. Chang.* **2007**, *446*, 727–728, doi:10.1038/446727a.

5. Mahe, G.; Bamba, F.; Soumaguel, A.; Orange, D.; Olivry, J.C. Water losses in the inner delta of the River Niger: Water balance and flooded area. *Hydrol. Process.* **2009**, *23*, 3157–3160, doi:10.1002/hyp.7389.
6. Mahé, G.; Lienou, G.; Descroix, L.; Bamba, F.; Paturel, J.E.; Laraque, A.; Khomsi, K. The rivers of Africa: Witness of climate change and human impact on the environment. *Hydrol. Process.* **2013**, *27*, 2105–2114.
7. Descroix, L.; Mahé, G.; Lebel, T.; Favreau, G.; Galle, S.; Gautier, E.; Sighomnou, D. Spatio-temporal variability of hydrological regimes around the boundaries between Sahelian and Sudanian areas of West Africa: A synthesis. *J. Hydrol.* **2009**, *375*, 90–102, doi:10.1016/j.jhydrol.2008.12.012.
8. Kuper, M.; Mullon, C.; Poncet, Y.; Benga, E. Integrated modelling of the ecosystem of the Niger river inland delta in Mali. *Ecol. Model.* **2003**, *164*, 83–102, doi:10.1016/S0304-3800(03)00006-1.
9. Lebel, T.; Ali, A. Recent trends in the Central and Western Sahel rainfall regime (1990–2007). *J. Hydrol.* **2009**, *375*, 52–64, doi:10.1016/j.jhydrol.2008.11.030.s.
10. Wolski, P.; Savenije, H.H.G.; Murray-Hudson, M.; Gumbricht, T. Modelling of the flooding in the Okavango Delta, Botswana, using a hybrid reservoir-GIS model. *J. Hydrol.* **2006**, *331*, 58–72, doi:10.1016/j.jhydrol.2006.04.040.
11. Olivry, J.C. Fonctionnement hydrologique de la cuvette lacustre du Niger et essai de la modélisation de l'inondation du delta intérieur. In *Grands Bassins Fluviaux*; Olivry, J.C., Boulegue, J., Ed.; Actes Du Colloque PEGI, INSU-CNRS-ORSTOM Paris; Colloque et Séminaire: Paris, France, 1994; pp. 267–280.
12. Dadson, S.J.; Ashpole, I.; Harris, P.; Davies, H.N.; Clark, D.B.; Blyth, E.; Taylor, C.M. Wetland inundation dynamics in a model of land surface climate: Evaluation in the Niger inland delta region. *J. Geophys. Res.* **2010**, *115*, 1–7, doi:10.1029/2010JD014474.
13. Hughes, D.A.; Tshimanga, R.M.; Tirivarombo, S.; Tanner, J. Simulating wetland impacts on stream flow in southern Africa using a monthly hydrological model. *Hydrol. Process.* **2014**, *28*, 1775–1786, doi:10.1002/hyp.9725.
14. Mahe, G.; Orange, D.; Mariko, A.; Bricquet, J.P. Estimation of the flooded area of the Inner Delta of the River Niger in Mali by hydrological balance and satellite data. In *Hydro-Climatology, Proceedings of Symposium J-H02 Held during IUGG2011 in Melbourne, Australia, July 2011*; Franks, S.W., Ed.; IAHS Pub. 344; IAHS Press: Wallingford, UK, 2011; pp. 138–143.
15. Zwarts, L.; Beukering, P.; Van Koné, B.; Wymenga, E.; Taylor, D. The economic and ecological effects of water management choices in the Upper Niger River: Development of decision support methods. *Int. J. Water Resour. Dev.* **2006**, *22*, 135–156, doi:10.1080/07900620500405874.
16. Ogilvie, A.; Belaud, G.; Delenne, C.; Bailly, J.-S.; Bader, J.-C.; Oleksiak, A.; Martin, D. Decadal monitoring of the Niger Inner Delta flood dynamics using MODIS optical data. *J. Hydrol.* **2015**, *523*, 368–383, doi:10.1016/j.jhydrol.2015.01.036.
17. Schwerdtfeger, J.; Johnson, M.S.; Couto, E.G.; Amorim, R.S.S.; Sanches, L.; Campelo Júnior, J.H.; Weiler, M. Inundation and groundwater dynamics for quantification of evaporative water loss in tropical wetlands. *Hydrol. Earth Syst. Sci. Discuss.* **2014**, *11*, 4017–4062, doi:10.5194/hessd-11-4017-2014.
18. Moret, B.; Chaperon, P.; Lamagat, J.P.; Molinier, M. *Monographie Hydrologique du fleuve Niger*; ORSTOM, Ed.; Tome II—Cuvette Lacustre et Niger Moyen; Monographies Hydrologiques: Paris, France, 1986.
19. Chelton, D.B.; Freilich, M.H. Scatterometer-based assessment of 10-m wind analyses from the operational ECMWF and NCEP numerical weather prediction models. *Am. Meteorol. Soc.* **2005**, *134*, 737–742, doi:10.1175/MWR3111.1.
20. NASA LP DAAC. Land Cover Type Yearly L3 Global 500 m SIN Grid (MCD12Q1). Version 051. NASA EOSDIS Land Processes DAAC, USGS Earth Resources Observation and Science (EROS) Center, Sioux Falls, South Dakota, 2005. Available online: https://lpdaac.usgs.gov/dataset_discovery/modis/modis_products_table/mcd12q1 (accessed on 1 January 2014).
21. Vandersypen, K.; Keita, A.C.T.; Coulibaly, Y.; Raes, D.; Jamin, J.Y. Formal and informal decision making on water management at the village level: A case study from the Office du Niger irrigation scheme (Mali). *Water Resour. Res.* **2007**, *43*, 1–10, doi:10.1029/2006WR005132.
22. Vittek, M.; Brink, A.; Donnay, F.; Simonetti, D.; Desclée, B. Land cover change monitoring using landsat MSS/TM satellite image data over west Africa between 1975 and 1990. *Remote Sens.* **2013**, *6*, 658–676, doi:10.3390/rs6010658.
23. Mariko, A.; Mahe, G.I.L.; Orange, D. Monitoring flood propagation in the Niger River Inner Delta in Mali:

Prospects with the low resolution NOAA/AVHRR data. In Proceedings of the IAHS-IAPSO-IASPEI Assembly, Gothenburg, Sweden, 22–26 July 2013; pp. 101–109, IAHS Publ. 358.
24. Mayaux, P.; Bartholome, E.; Fritz, S.; Belward, A. A New Land Cover Map of Africa for the Year 2000. *J. Biogeogr.* **2004**, *31*, 861–877, doi:10.1111/j.1365-2699.2004.01073.x.
25. Ashcraft, I.S.; Long, D.G. The spatial response function of SeaWinds backscatter measurements. *Proc. SPIE* **2003**, *5151*, 609–618, doi:10.1117/12.506255.
26. Weissman, D.E.; Bourassa, M.A.; O'Brien, J.J.; Tongue, J.S. Calibrating the Quikscat/SeaWinds radar for measuring rainrate over the oceans. *IEEE Trans. Geosci. Remote Sens.* **2003**, *41*, 2814–2820, doi:10.1109/TGRS.2003.817975.
27. De Bruin, H.A.R.; Holtslag, A.A.M. A Simple parameterization of the surface fluxes of sensible and latent heat during daytime compared with the penman-monteith concept. *J. Appl. Meteorol.* **1982**, *21*, 1610–1621, doi:10.1175/1520-0450(1982)021<1610:ASPOTS>2.0.CO;2.
28. Alazard, M.; Leduc, C.; Travi, Y.; Boulet, G.; Ben Salem, A. Estimating evaporation in semi-arid areas facing data scarcity: Example of the El Haouareb dam (Merguellil catchment, Central Tunisia). *J. Hydrol. Reg. Stud.* **2015**, *3*, 265–284, doi:10.1016/j.ejrh.2014.11.007.
29. Ball, J.E.; Luk, K.C. Modeling spatial variability of rainfall over a catchment. *J. Hydrol. Eng.* **1998**, *3*, 122–130.
30. Allen, R.; Pereira, L.S.; Raes, D.; Smith, M. *Crop Evapotranspiration: Guidelines for Computing Crop Requirements*; Irrigation and Drainage Paper No. 56; FAO: Rome, Italy, 1998; p. 300.
31. Mariko, A. *Caractérisation et Suivi de la Dynamique de L'inondation et du Couvert Végétal dans le Delta intérieur du Niger (Mali) par Télédétection.* PhD Thesis, Université Montpellier II: Paris, France, 2003.
32. Moriasi, D.N.; Arnold, J.G. Model evaluation guidelines for systematic quantification of accuracy in watershed simulations. *Trans. Am. Soc. Agric. Biol. Eng.* **2007**, *50*, 885–900, doi:10.13031/2013.23153.
33. Aich, V.; Liersch, S.; Vetter, T.; Fournet, S.; Andersson, J.C.M.; Calmanti, S.; Paton, E.N. Flood projections within the Niger River Basin under future land use and climate change. *Sci. Total Environ.* **2016**, *562*, 666–677, doi:10.1016/j.scitotenv.2016.04.021.
34. Liersch, S.; Cools, J.; Kone, B.; Koch, H.; Diallo, M.; Reinhardt, J.; Hattermann, F.F. Vulnerability of rice production in the Inner Niger Delta to water resources management under climate variability and change. *Environ. Sci. Policy* **2013**, *34*, 18–33, doi:10.1016/j.envsci.2012.10.014.
35. Mahé, G.; Bamba, F.; Orange, D.; Fofana, L.; Kuper, M.; Marieu, B.; Cissé, N. Dynamique hydrologique du delta intérieur du Niger (Mali). In *Gestion Intégrée des Ressources Naturelles en Zones Inondabless Tropicales*; Séminaire International: Bamako, Mali, 2002; pp. 179–195. Available online: http://www.documentation.ird.fr/hor/fdi:010030365 (accesssed on 10 March 2015).
36. Oguntunde, P.G.; Abiodun, B.J. The impact of climate change on the Niger River Basin hydroclimatology, West Africa. *Clim. Dyn.* **2012**, *40*, 81–94, doi:10.1007/s00382-012-1498-6.
37. Frenken, K. *Irrigation in Africa in Figures, FAO WATER REPORTS 29, AQUASTAT Survey, FAO Land and Water Development Division*; Frenken, K., Ed.; FAO: Rome, Italy, 2005.
38. Marlet, S.; N'Diaye, M.K. Impacts environnementaux de la mise en valeur d'une zone inondable par irrigation Evolution des sols et des eaux à l'Office du Niger (Mali). In *Gestion Intégrée des Ressources Naturelles en Zones Inondabless Tropicales*; Séminaire International: Bamako, Mali, 2002; pp. 364–374.
39. Kurtzman, D.; Scanlon, B.R. Groundwater recharge through vertisols: Irrigated cropland vs. natural land, Israel. *Vadose Zone J.* **2011**, *10*, 662, doi:10.2136/vzj2010.0109.
40. Oudin, L.; Hervieu, F.; Michel, C.; Perrin, C.; Andréassian, V.; Anctil, F.; Loumagne, C. Which potential evapotranspiration input for a lumped rainfall-runoff model? *J. Hydrol.* **2005**, *303*, 290–306, doi:10.1016/j.jhydrol.2004.08.026.
41. De Bruin, H.A.R. Evapotranspiration in humid tropical regions. In *Hydrology of Humid Tropical Regions with Particular Reference to the Hydrological Effects of Agriculture and Forestry Practice, Proceedings of the Hamburg Symposium, Hambury, Germany, 15–27 August 1983*; IAHS Publ. No. 140; Hamburg; pp. 1–14.
42. Xu, C.Y.; Singh, V.P. Cross comparison of empirical equations for calculating potential evapotranspiration with data from Switzerland. *Water Resour. Manag.* **2002**, *16*, 197–219, doi:10.1023/A:1020282515975.
43. Glover, J.; McCulloch, J.S.G. The empirical relation between solar radiation and hours of sunshine. *Q. J. R. Meteorol. Soc.* **1958**, *84*, 172–175, doi:10.1002/qj.49708436011.